FLINDERS UNIVERSITY
ADELAIDE • AUSTRALIA

Silica Immobilised Metal Ion Activated Molecular Receptors

A Thesis Presented for the Degree of

Doctor of Philosophy

by

Jozef Andrew Zbigniew Hodyl BSc.(Hons.)

at

Flinders University

School of Chemistry, Physics and Earth Sciences

Faculty of Science and Engineering

August, 2008

TABLE OF CONTENTS

Abstract		ii
Declaration		iv
Acknowledgements		v
Abbreviations		vi
Chapter 1	Introduction	1
Chapter 2	Synthesis of macrocyclic receptor precursors	35
Chapter 3	Guest molecule inclusion studies with the receptor model	52
Chapter 4	Modification of the silica surface	70
Chapter 5	Metal ion uptake studies with silica immobilised receptor ligands	87
Chapter 6	Guest molecule inclusion studies with silica immobilised receptors	94
Chapter 7	Experimental	121
Appendices		
Appendix A	Binding constant determination procedure	154
Appendix B	Determination of stoichiometry by the method of continuous variations	157
Appendix C	Solid state ^{13}C CPMAS NMR spectra of some silica immobilised host-guest complexes	160
References		164

ABSTRACT

Immobilisation of functional entities, such as, enzymes, onto solid supports, as a means of facilitating their removal from the surrounding environment and subsequent regeneration has been in practice for many decades. This work focuses on the immobilisation and analysis of three-walled (pendant armed), cyclen based receptor complexes immobilised onto a silica surface for the purpose of sequestering aromatic anions from aqueous solution: Si-GPS-[Cd(Trac)]$(ClO_4)_2$, Si-GPS-[Cd(DiPTrac)]$(ClO_4)_2$, and Si-GPS-[Cd(TriPTrac)]$(ClO_4)_2$ were the immobilised receptors used.

Initially, synthesis of a three-walled model receptor, [Cd(TracHP12)]$(ClO_4)_2$, that is not bound to silica yet mimics the properties of the silica anchored receptor complexes with a hydroxypropyl pendant arm was effected. Aromatic anion binding constant measurements were made on the model receptor using ^{1}H NMR monitored titrations in DMSO-d_6 which showed that, in comparison to the first generation four-walled receptors, the removal of one of the pendant arms did not affect the binding capability of the receptor's cavity significantly. It was shown that the binding strength correlated well with the pK_a of the particular anion with, for example, *p*-hydroxybenzoate > *m*-hydroxybenzoate > *o*-hydroxybenzoate. The precursor to this receptor was then immobilised onto a silica surface and subjected to metal ion uptake studies to gauge its coordination properties with a number of divalent metal(II) ions: Cd(II), Pb(II), Zn(II), Cu(II) and Ca(II). The three Cd(II) coordinated receptor complexes mentioned above were then subjected to inclusion studies with a number of aromatic anions in aqueous conditions whereupon a reversal of the previously mentioned trend, *i.e.* *o*-hydroxybenzoate > *m*-hydroxybenzoate > *p*-hydroxybenzoate was observed. This indicated that the presence of water in the system changes the

hydrogen bonding mode of the host-guest complexes, and was a major discovery arising from this work.

DECLARATION

I certify that this thesis does not incorporate, without acknowledgement, any material previously submitted for any degree or diploma in any university; and that to the best of my knowledge and belief it does not contain any material previously published or written by another person except where due reference is made in the text.

signed.....

Jozef Andrew Zbigniew Hodyl

ACKNOWLEDGEMENTS

I would like to begin by thanking my supervisor Prof. Kevin P. Wainwright, firstly, for allowing me to conduct these studies and, secondly, for his undivided assistance, support and enduring patience. Many thanks also to Dr. Martin Johnston for his help and wealth of expertise with regard to NMR spectroscopy. I would also like to thank Dr. Ron Smernik of the Waite Institute for acquiring the initial solid state NMR spectra for me and for his advice when I acquired the spectra myself.

I would also like to express my gratitude to the many souls who have at one time or another resided in room 337: Dr. Adam Bradbury, Dr. Akhmad Damsyik, Professor Xu Xing You, Dr. Yakub Baran, Tim Robinson, La Ode Kadidae, Saprizal Hadisaputra, Lachlan Cavell, Blake Tooth, Rachel King, Kim Salvatore, Zihan Poh and Thomas Carter. Also I would like to thank the countless individuals catacombed throughout Physical Sciences for their entertaining and informative discussions.

In finality, but definitely not with the least of my thanks I am eternally grateful to my "long suffering" wife Debbie who has had to endure my many absences and without whose encouragement and love, survival of the "long haul" of these PhD studies would have been tough.

ABBREVIATIONS

Å	Ångstrom (10^{-10} m)
APT	attached proton test
b	broad
c	g ml^{-1}
cbz	carboxybenzyl
CD	cyclodextrin
CP	cross polarisation
CTAB	cetyltrimethylammonium bromide
cyclam	1,4,8,11-tetraazacyclotetradecane
cyclen	1,4,7,10-tetraazacyclododecane
δ	chemical shift
DiPTrac	1,4,7-*tris*(*S*)-2-hydroxy-3-[4-((2-(2-hydroxyethoxy)ethoxy)phenoxypropyl]-1,4,7,10-tetraazacyclododecane
DMF	dimethylformamide
DMSO	dimethylsulfoxide
DNA	deoxyribonucleic acid
DOTA	1,4,7,10-tetraazacyclododecane-1,4,7,10-tetraacetic acid
DOTAM	1,4,7,10-tetrakis(acetamido)cyclen
DOTEP	1,4,7,10-tetraazacyclododecane-1,4,7,10-tetrakis(methyleneethylphosphinate)
DRIFT	Diffuse Reflectance Infrared Fourier Transform spectroscopy
EC	endcapped

EtOH	ethanol
GPDMS	glycidoxypropyldimethylsilane
GPDMES	3-(glycidoxypropyl)dimethylethoxysilane
GPS	glycidoxypropylsilane
GPTS	3-(glycidoxypropyl)trimethoxysilane
$\{^1H\}$	proton decoupled
HTPE	hydroxy terminated polyether
J	coupling constant
K	apparent stability constant
K	Kelvin
kHz	kilohertz (10^3 s^{-1})
kJ	kilo Joule
m	multiplet
M^{2+}	unspecified divalent metal ion
MAS	magic angle spinning
MCM-41	Mobil catalytic or crystalline material - batch 41
MeCN	acetonitrile
MeOH	methanol
MHz	megahertz (10^6 s^{-1})
NMR	nuclear magnetic resonance
OTs	tosylate
PEG	polyethylene glycol
pK_a	$-\log_{10}K_a$
pm	picometre
ppm	parts per million
r	radius
s	singlet

SBP	sulfate binding protein
t	triplet
tert	tertiary
tlc	thin layer chromatography
TMCS	trimethylchlorosilane
TOSS	TOtal Suppression of Spinning Side-bands
Trac	1,4,7-*tris*-((*S*)-2-hydroxy-3-phenoxypropyl)-1,4,7,10-tetraazacyclododecane
TracHP12	1-(2-hydroxypropyl)-4,7,10-*tris*-((*S*)-2-hydroxy-3-phenoxypropyl)-1,4,7,10-tetraazacyclododecane
TriPTrac	1,4,7-*tris*(*S*)-2-hydroxy-3-[4-(2-(2-(2-hydroxyethoxy)ethoxy)-ethoxy)phenoxypropyl]-1,4,7,10-tetraazacyclododecane
UV-vis	ultraviolet-visible spectroscopy
VOC	volatile organic compound

CHAPTER ONE

INTRODUCTION

CHAPTER 1 INTRODUCTION

1.1 Genesis: Supramolecular Chemistry

The rationale behind the development of supramolecular chemistry stems from studies involving biological systems. For example, the study of enzymatic processes whereby a suitably configured enzyme (host molecule) is able to non-covalently and reversibly bind a substrate (guest species), thus catalysing a particular biological process.[1-5] This in essence, provides, economically, a definition for "supramolecular" and, its often used synonym, "host-guest, chemistry", which is generally described as "chemistry beyond the molecule" or the chemistry of "non-covalent interactions between molecules".[2, 6-9] Enzymes in biological systems tend to be specific or, more precisely, selective for a particular substrate, which can be a neutral, cationic or anionic molecule that is "recognised" at a supramolecular level and thence secured by the enzyme's chemical or geometrical character, forming a stable enzyme-substrate complex. An example of an enzyme-substrate complex is the sulfate binding protein SBP responsible for sulfate transport by *Salmonella typhimurium*. Here sulfate is bound by an array of seven hydrogen bonds between the NH groups of the protein backbone and the oxygen atoms of the substrate as shown in **Figure 1.1**.[2, 10, 11] This host molecule consists of two globular domains separated by a flexible pivot. The crystal structure of this complex has also revealed that the sulfate anion is bound in a cleft between the two globular domains and is 7Å below the surface of the protein.[5] The active site of SBP does not contain a guanidinium or other positively charged amino acid and, hence binding of the anion is essentially through hydrogen bonds.[5, 10, 11]

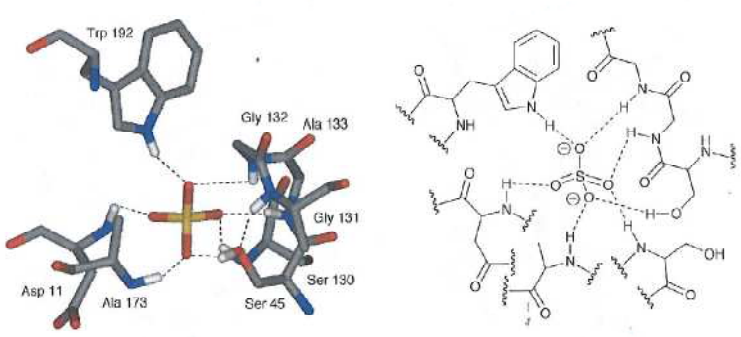

Figure 1.1 X-ray determined crystal structure and diagrammatic depiction of the hydrogen bonding pattern within the active centre of a sulfate binding protein, SBP, bound with SO_4^{2-}.[5]

Applications utilising supramolecular chemical concepts are now possible in a variety of fields including, catalysis,[12] drug delivery and design,[13, 14] host-guest chemistry,[15] and molecular electronics.[16] Many of these applications, such as, catalysis, or sequestration of molecules from solution by receptors, suffer from an inherent deficiency in that the catalyst or the receptor is difficult to recycle due to its solubility in the reaction medium. To overcome this complication, immobilisation of the catalyst or receptor onto a solid support results in an insoluble material that is easy to isolate and can be reused. Immobilisation in this manner must, however, preserve the functionality of the original free system. This idea has long been popular, with the immobilisation of enzymes both prolonging their longevity and reducing their production costs.[17] There exist a number of methods by which enzymes are immobilised including, covalent bonding to a modified water-insoluble matrix such as silica,[18, 19] which is of interest in this work; adsorption onto a water-insoluble matrix;[20] and, entrapment within a water-insoluble polymer lattice.[21, 22]

Considering that water is regarded as a "green" solvent, being able to control, regulate and mediate many natural processes, an objective of supramolecular chemistry is the synthesis and design of receptor systems that can operate with high affinity and selectivity in binding guest molecules in an aqueous environment.[10, 23]

The focus of this work was to prepare and explore a silica immobilised metal-ion activated receptor system that would successfully bind aromatic, anionic guest molecules, ideally, in aqueous media.

1.2 Molecular Recognition

Generally, molecular recognition is associated with intermolecular non-covalent interactions involving a large organic host molecule that preorganises by assuming a conformation whose framework is chemically and geometrically complementary to acceptance of a smaller organic or inorganic guest molecule.[7, 24-27] Inclusion of the guest molecule can be either by metal-ligand coordination,[28] hydrogen bonding, hydrophobic interactions, charge-transfer interactions, electrostatic van der Waals forces, and, recently the introduction of reversible covalent bonds such as, ester, imine or disulfide linkages.[2, 7, 29, 30] Inclusion through utilisation of these non-covalent forces fulfils a number of potential objectives such as enhancing solubility, thermodynamic and kinetic stabilisation as a defence against decomposition, and the development of molecular sensors.[29] The scope of research connected with molecular recognition has now achieved a level of sophistication whereby design and synthesis of receptors with predictable selectivity for a range of guest species allows for their preparation with a high degree of confidence.[24, 31-33]

Many of the early host-guest studies concerned receptors capable of capturing cationic guest molecules for example, coordination chemistry with group 1 and 2 metal ions or ammonium cations and therefore this area of supramolecular chemistry is now well developed. [34-40] An example is the complex formed between a methylammonium cation and a crown ether host, **1**, which is held together by hydrogen bonds between ethereal oxygens and ammonium hydrogen atoms.[34, 35] Synthesis and design of receptors for the capture of neutral species is also well

documented throughout the literature.[41-47]

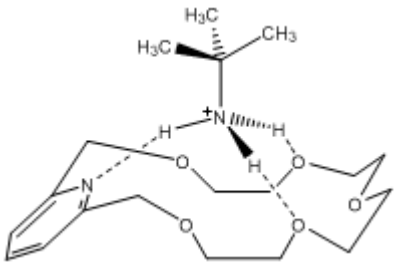

1

An example of a neutral guest species captured by a polarised chiral calix[6]aza-cryptand, **2**, is shown below as the host-guest complex.[47] Garrier *et al*. have demonstrated from inclusion studies with racemic guests that this enantiopure tetra-ammonium host is also capable of behaving as an enantioselective molecular receptor.[47]

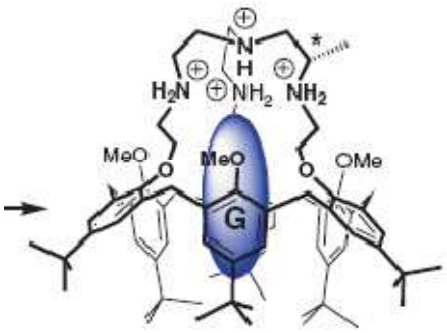

2

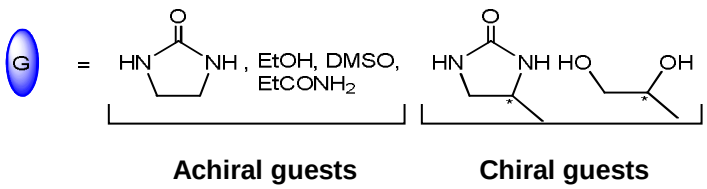

Design, synthesis and exploration of receptor complexes that selectively capture anionic guest species has only become prominent in recent years.[2, 36, 48-50] This interest originates from the ubiquity of anionic species throughout biological systems. For example, DNA is a polyanion and many substrates and co-factors for enzymes are also anionic.[36, 51-53] However, synthesis of artificial receptors for

sequestering anions has proved to be more demanding than the preparation of receptors for neutral or cationic species.[10, 36] Part of the difficulty in this area comes from the larger size of anions with respect to isoelectronic cations and, accordingly, a lower charge to radius ratio as shown in **Table 1.1**.[36, 48]

Table 1.1 Radii (r) of isoelectronic cations and anions compared.[36]

Cation[a]	r(pm)	Anion[a]	r(pm)
Na^+	116	F^-	119
K^+	152	Cl^-	167
Rb^+	166	Br^-	182
Cs^+	181	I^-	206

[a]In an octahedral environment.

Adding to the problem is the even larger size and variation in topology of poly-atomic anions, for example: linear, CN^- (300 pm) and SCN^- (350 pm); tetrahedral, ClO_4^- (240 pm) and SO_4^{2-} (230 pm); and, trigonal planar, NO_3^- (179 pm) and CO_3^{2-} (178 pm).[10, 54, 55] As a result, the effectiveness of electrostatic binding interactions with a host species is reduced in comparison with the smaller cation.[36] Furthermore, there is the sensitivity of anions to changes in pH, *i.e.* being prone to protonation and losing their negative charge at low pH puts limitations on their receptors as they are only functional within the target anion's pH range.[36, 54] This may restrict anion binding events to media where the guest's negative charge and the efficacy of the host is maintained. This is also evident in the vast differences in free energies of solvation for cations and anions. Simple cations such as Rb^+ and K^+ have solvation free energies of -281 and -304 kJ mol^{-1}, respectively, whereas SO_4^{2-} and CO_3^{2-} have -1090 and -1315 kJ mol^{-1}, respectively. This shows that binding anionic species in water is not as facile as in organic solvents due also to relatively small overall

enthalpy changes, resulting from competition with water molecules that might arise upon inclusion. Biological anion receptor processes operate within highly defined environments where selectivity depends on an unusually high free energy loss for the preferred substrate, upon inclusion, compared to the free energy increase associated with dehydrating it.[10]

1.3 Evolution of Synthetic Anion Receptors

Studies involving the specific recognition of anionic species by synthetically designed hosts have their beginnings in the late 1960s when there was a report by Park and Simmons concerning encapsulation of a halide ion into the cavity of macrobicyclic ammonium cage compounds **3** and **4**. An example is shown below of the capture of a chloride ion by **3** or **4** demonstrating that coordination of the anion is both by hydrogen bonding and electrostatic interactions with the ammonium ion. [10, 56]

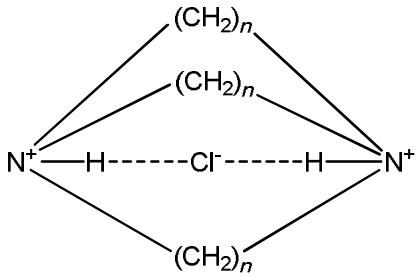

3, *n* = 9
4, *n* = 10

Analysis by NMR and X-ray crystallography of these complexes showed that the halide ions are spaced between the protonated nitrogen atoms rather than simply acting as counter ions to the protonated amine host.[10, 57]

Since Park and Simmon's report of their seminal anion receptor many studies have also been conducted using positively charged anion receptors based on the guanidinium moiety, which has the benefit of being able to operate under a wide

range of pH due to its high basicity.[5] Examples of guanidinium derived receptors are the foldable bis-guanidinium receptors **5** and **6** synthesised by Schiessl and Schmidtchen.[58] It was discovered that receptor **5** was good at binding dicarboxylate guest anions such as oxylate, malonate, isophthalate and *p*-nitroisophthalate giving log*K* values of 3.4, 4.2, 3.8 and 4.2, respectively.

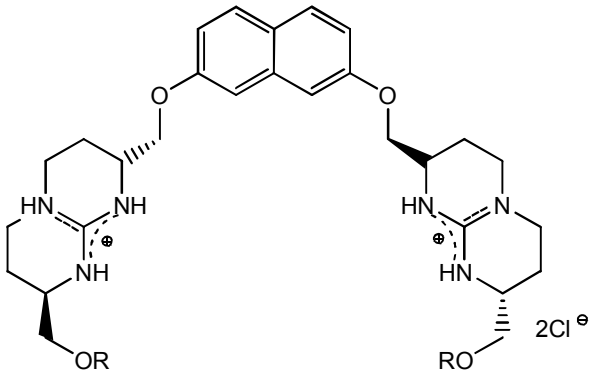

5, R = SiPh$_2$*t*Bu
6, R = H

Each of the complexes formed displayed 1:1 H:G (host:guest) binding by analysis using ^{1}H NMR monitored titrations in CD_3OD. Both receptor **5** and **6** also showed affinity for nucleotide phosphates in polar solvents. For example ^{1}H NMR monitored titration studies with **5** gave log*K* values of between 4.3 and 4.6 in CD_3OD while **6** bound $H_2PO_4^-$ with a log*K* of 3.0 in D_2O. Receptor **6** is also capable of binding biological materials, for example 5'-adenosine monophosphate (5'AMP) with a log*K* of 4.0.[58, 59]

Exploration and synthesis of receptors for anionic guest species has since broadened beyond straightforward predisposition of positively charged regions within a host species, which, by their electronic status, are inclined toward binding anions. Later receptors included architectures based on calixarenes, cryptands, cyclodextrins, steroids and crown ethers that use singly, or in combination, neutral hydrogen bond donor groups, hydrophobic binding, electrostatic van der Waals

forces and essentially the whole gamut of intermolecular interactions, previously mentioned, as part of their anion retention mechanism.[5] Some of these receptor types will be discussed in the following pages.

1.3.1 Cyclodextrins

Since their discovery in 1891 by Villiers[60] the exploitation and development of cyclodextrins has extended into many areas of research.[61] In more recent times cyclodextrins have been the focus of considerable studies with regard to their ability to act as synthetic hosts for guest molecule inclusion using hydrophobic binding.[62-67]

Cyclodextrins are a class of naturally occurring, toroid-shaped cyclic oligosaccharides the best known of which comprise 6, 7 or 8 D-glucopyranoside subunits assigned as α-, β- and γ-CD (with internal diameters of 4.7 - 5.3 Å, 6.0 - 6.5 Å and 7.5 - 8.3 Å, respectively); and, connected by α-(1,4) linkages, for example β-CD, **7**.[62]

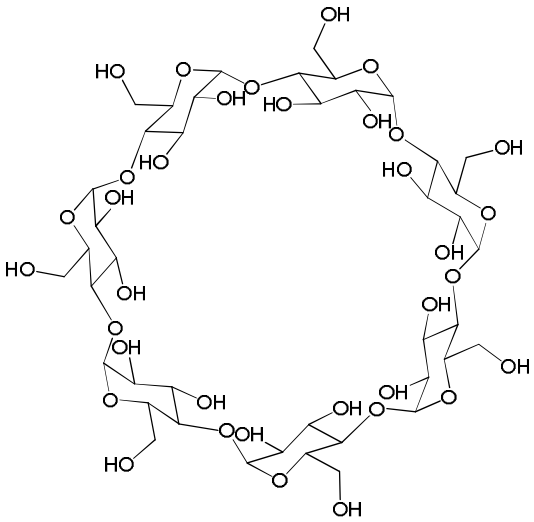

7

Cyclodextrins have an exceptional ability to form stable 1:1 complexes with a wide variety of appropriately sized hydrophobic guest species in aqueous media.[5, 62] In 1977 Bergeron and co-workers reported the inclusion of a molecule of either *p*-

nitrophenol or *p*-nitrophenolate within the cavity of an α-CD placing great importance on the orientation of the phenolic moiety. They pointed out that *p*-nitrophenolate is able to position itself with either the nitro end or phenolate end first, as shown in **Figure 1.2**.[68] It was found that the guest species normally bound nitro group first, but that various positional substitutions on the aromatic ring by methyl groups tended to prevent this orientation and then a decrease in binding strength was observed.[68]

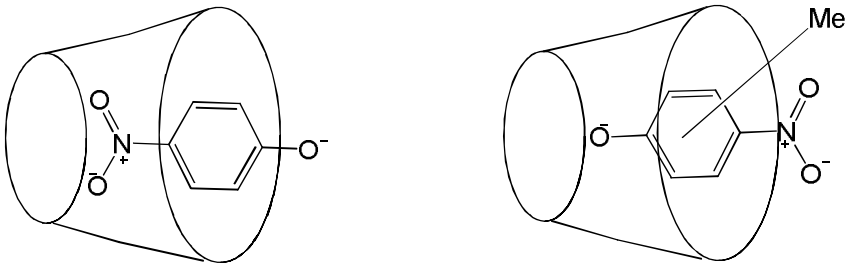

Figure 1.2 Possible orientation of *p*-nitrophenolate and methyl substituted phenolate within the cavity of α-cyclodextrin.

They were also curious as to why sodium *p*-nitrophenolate bound 13 times tighter than *p*-nitrophenol whereas studies with sodium-benzoate showed that it bound 82 times less effectively than benzoic acid.[69] Further investigation revealed that, like sodium *p*-nitrophenolate, *p*-nitrophenol binds with its nitro group first and the hydroxy group protruding out of the cavity into the solution with binding to the CD mediated by an induced dipole-dipole interaction with the water.[69] Therefore, due to the resonance delocalisation of the negative charge on the phenolate, which promotes binding, but impedes hydration, the phenolate was inclined to bind much stronger than the phenol.[68-70] It was found that benzoate and benzoic acid bound within the cavity carboxy group first as this orientation is more effective at filling the cavity. Since it is more difficult for the partially solvated charged carboxylate to move from a high dielectric environment to one of low dielectric *i.e.* from the aqueous

environment to the hydrophobic interior of the CD, the binding strength is lowered accordingly, compared to benzoic acid.[69] Moreover, studies with *p*-nitrobenzoate guests conducted by Davies and Savage revealed that guest species derived from *p*-nitrobenzoic acid bound more weakly than those from benzoic acid. They concluded that the charged species bound as Bergeron *et al*. proposed, but that binding in both charged and uncharged species was also mediated by the electron withdrawing or donating ability of the substituents. They ascertained that substituents with higher electron withdrawing ability penetrated the cavity first. As the nitro group has higher electron withdrawing ability than the carboxy moiety the carboxy group was likely to protrude into the aqueous environment and hence the lower binding observed for *p*-nitrobenzoic acid derivatives.[71]

1.3.2 Calixarenes

The calixarenes exhibit some similarity with cyclodextrins as both have recurring structural subunits containing peripheral functional groups arranged around a hydrophobic core.[72] Since their discovery they have become the subject of many studies as receptors due to the ease of modifying their backbones and their well-defined upper and lower rims surrounding a central annulus, as shown for **8**, a typical calixarene.[59, 73, 74]

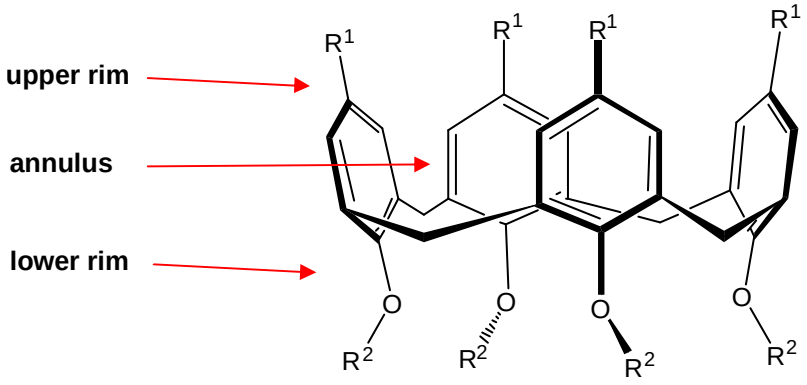

8

It has been shown by NMR and crystallographic data that due to the flexibility of the methylene linkage between the phenolic moieties, calix[4]arenes, such as, **8**, may adopt four rotational conformers, namely: cone, where all the phenyl rings align in the same direction to form a "basket-like" cavity; partial cone, where one of the phenyl rings aligns in a downward direction while the other three orient upwards; 1,2-alternate, where two of the phenyl rings align downward and two upward in a *cis* arrangement; 1.3-alternate as previous, but with a *trans* arrangement, as shown in **Figure 1.3**.

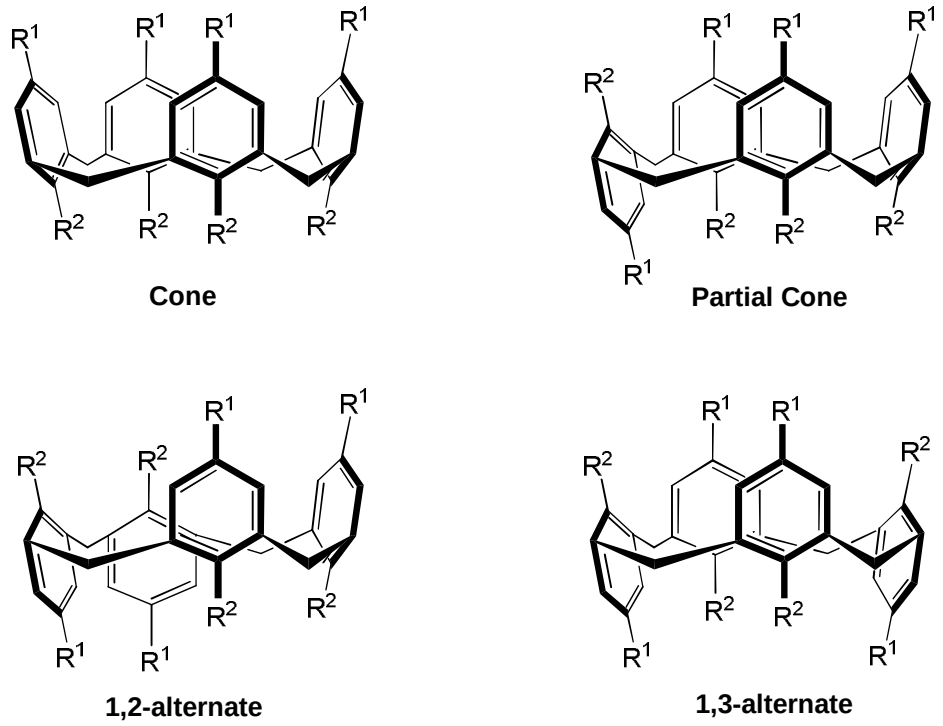

Figure 1.3 The four possible conformers of calix[4]arenes.

Of these four conformations the most common is the cone conformation. It can be seen that in the cone conformation the calix[4]arene molecule forms a hydrophobic "basket-like" cavity that can be used for molecular recognition of guest molecules, and hence as a receptor.

To preserve the cone conformation and prevent interconversion between the four conformations, flipping of the rings can be restricted by bridging between two opposite *p*-positions with, for example, either aliphatic[75] or ethereal chains[76] as shown for **9** and **10**, respectively.[72]

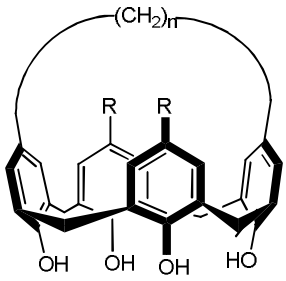

9, R = CH_3, n = 5

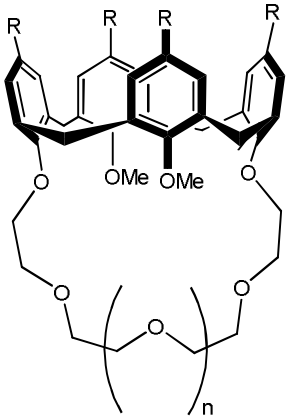

10, R = H, n = 2

The first conclusive report of the inclusion of a small neutral guest molecule (toluene) within the cavity of a calixarene-based receptor was by Andreetti and co-workers in 1979.[77] X-ray structures showed a 1:1 H:G complex of *p-tert*-butylcalix[4]arene with an included toluene molecule as shown in **Figure 1.4**.[77]

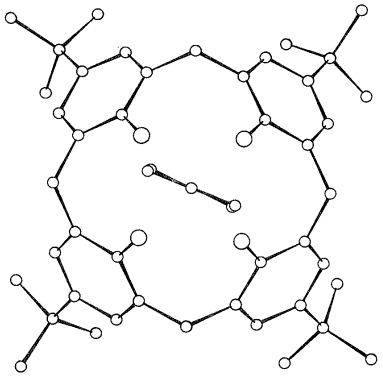

Figure 1.4 Crystal structure of *p-tert*-butylcalix[4]arene toluene (1:1) clathrate, looking down onto the O_4 plane of the complex, and the *p*-carbon.[77]

Bott and co-workers reported in 1986 their observation of toluene inclusion

within the cavity of a *p-tert*-butylcalix[4]arene complexed with sodium through its phenolic lower rim.[78] This demonstrated that the potential for inclusion of a guest molecule was retained after complexation with metal ions, as shown in **Figure 1.5**.[78]

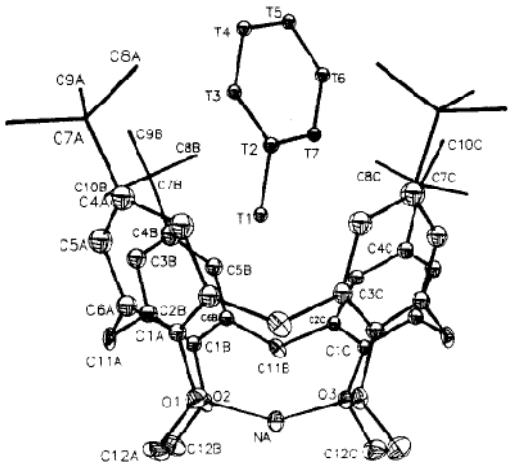

Figure 1.5 Structure of the [*p-tert*-butylmethoxycalix[4]arene-sodiumtoluene]$^+$ cation. The toluene molecule is seen at the core of the cavity.[78]

These early studies have provided the basis from which calixarene-based receptor synthesis and design has grown. They have led to more complex and chemically selective receptor systems, for example, the strapped C-linked 1,3-dialanyl-calix[4]arenes **11** and **12** synthesised by Sansone and co-workers.[79]

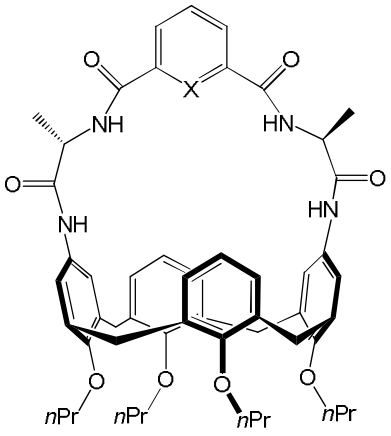

11, X = CH
12, X=N

Receptors **11** and **12** both displayed a high affinity for carboxylate anions in

acetone-d_6. For instance, the log*K* for benzoate was 4.6 whereas chloride and nitrate anions gave log*K* values of 3.4 and 2.3, respectively.

1.3.3 Amide based anion receptors

It is well known that anion binding to proteins is not solely the domain of positively charged side groups, but that neutral amide linkages are also involved. The ability of the amide subunits to function as both hydrogen bond donors (NH group) and hydrogen bond acceptors (oxygen lone pairs on carbonyl) makes these versatile groups for anion sequestration. Since amide based binding motifs have such significance in biological systems, development of synthetic anion receptors with comparable capabilities has been given substantial attention. [5, 7, 80, 81]

Kondo *et al*. synthesised anion receptors containing an isophthalamide core with terminal amide groups bearing pyridyl moieties at their periphery. For example **13**, as shown in **Figure 1.6**.[82]

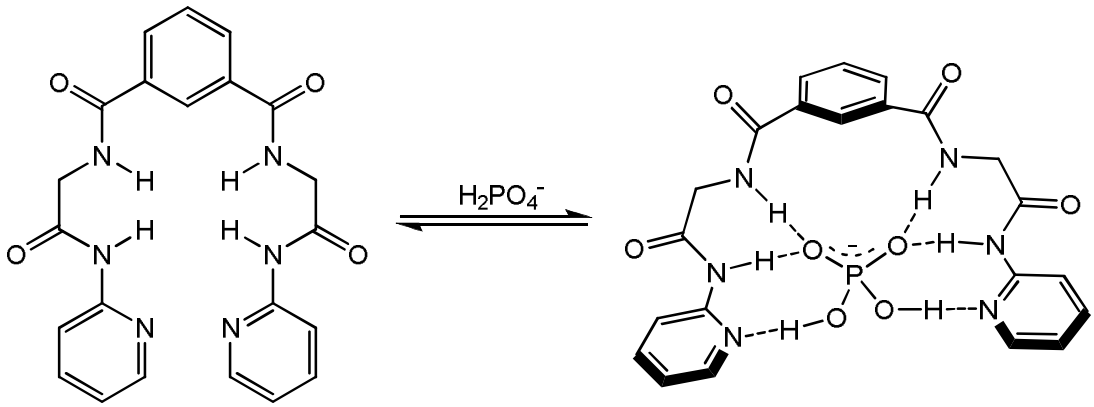

13

Figure 1.6 Complexation of dihydrogen phosphate by receptor **13**.[82]

Receptor **13** forms complexes with dihydrogen phosphate and Y-shaped anions such as acetate by forming hydrogen bonds with the four amide NH groups. Studies have shown that receptor **13** is selective towards $H_2PO_4^-$ with $K(H_2PO_4^-)/K(AcO^-)$ >

60 in 0.5% DMSO-MeCN (v/v).[82] The terminal pyridyl groups are presumed also to accept hydrogen bonds from dihydrogen phosphate adding to the binding strength and hence selectivity.

A set of cyclic anion receptors **14** and **15** containing amide and amine moieties as part of their backbone was reported by Hossain *et al*. in 2003.[83] These receptors were designed to bind tetrahedral anions, for instance sulfate and phosphate, selectively. [83]

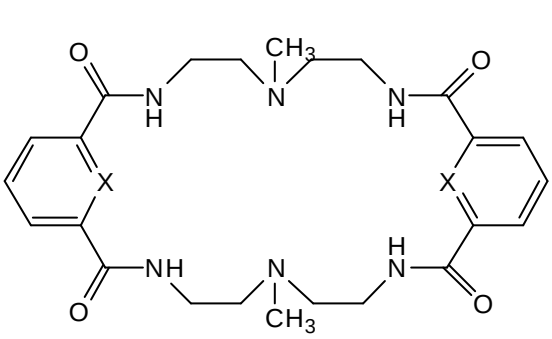

14, X = CH
15, X = N

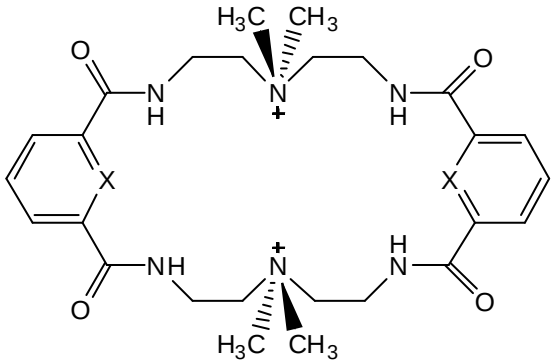

16, X = CH
17, X = N

These receptors contain four amide NH hydrogen bond donor groups and two tertiary amine moieties that can be methylated to give quaternarised ammonium receptors **16** and **17**, in effect furnishing the receptor with two additional sites for binding anions.[83] Binding of anions such as $H_2PO_4^-$ is strengthened in receptors **16** and **17** where the log*K* values are 4.06 and 5.32, respectively, whereas receptors **14** and **15** give log*K* values of 2.92 and 4.04, respectively, as determined from ^{1}H NMR monitored titration experiments in CD_3OD.

The "catalogue" for anion receptors bearing the amide moiety is vast due to the efficacy of the amide group in binding anionic species in a range of both polar and non-polar solvents.[84-88]

1.3.4 Alcohol based anion receptors

Considering that hydroxy groups are excellent hydrogen bonding donor groups it can

be appreciated that many biological processes are reliant on specific recognition between hydroxy subunits and anionic substrates. An example from nature is the interaction between carbohydrate moieties and anionic proteins.[89]

Due to the efficiency of the hydroxy group in participating in hydrogen bonding interactions in natural systems a great deal of investigation has gone into synthesis and design of synthetic anion binding receptors with hydroxy groups as part of their framework.[90]

An anion receptor **18** for selectively binding fluoride ions, based on a bile acid derived cyclic dimer, was synthesised by Ghosh and Choudhury.[91] This receptor was designed to bind through OH···F^- and CH···F^- interactions and it was determined from ^{1}H NMR Job's Plot analysis that the stoichiometry of the complex formed was 1:2 H:G. They found that receptor **18** bound F^- in $CDCl_3$ with binding constants of logK_1 = 3.3 and logK_2 = 2.4 whereas, the log$K$ for Cl^- in the same solvent was 2.0. Job's Plot analysis for the Cl^- ion showed that only the 1:1 H:G complex was formed. It was deduced from ^{1}H NMR monitored titration experiments that each F^- is held by two OH···F^- and one CH···F^- hydrogen bonds.

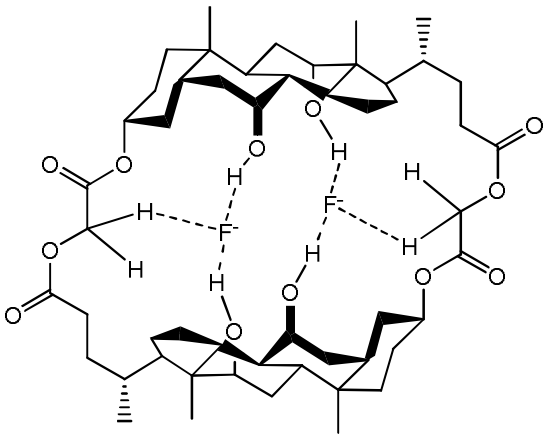

18

A number of studies have also been involved in investigating the guest anion recognition properties of calixarene hydroxy groups. Staffilani and co-workers

synthesised bi- tri- and tetra - π-metalated macrocyclic complexes using, for example, *p-tert*-butylcalix[5]arene.[92]

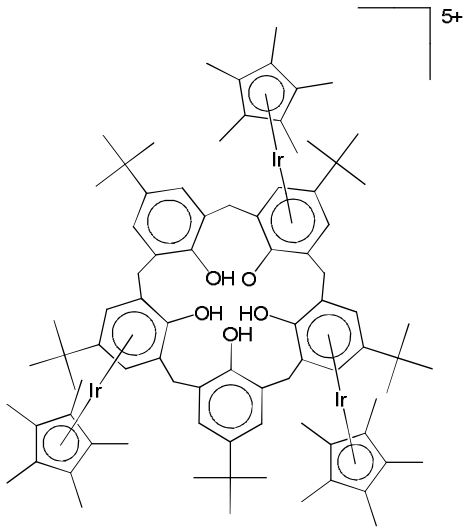

19

They found that the presence of transition metal ions (Ir(III) in these complexes considerably amplifies the acidity of the hydroxy functionalities at the calixarene lower rim such that monodeprotonated **19** is able to include anionic species, such as BF_4^-, HSO_4^- and SO_4^{2-}.[92] A crystal structure was obtained for the host-guest complex formed with **19** and BF_4^- that showed one of the five tetrafluoroborate anions was included within the cavity, **Figure 1.7**.

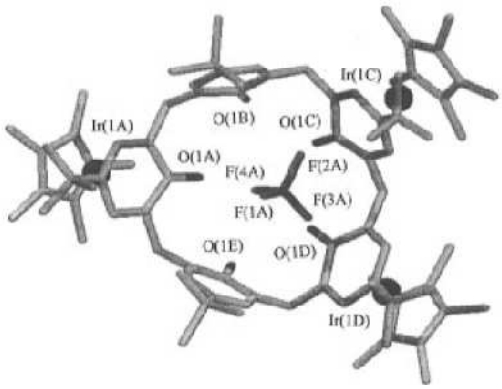

Figure 1.7 Crystal structure of tri-iridium complexed *p-tert*-butylcalix[5]arene, **19**, with a tetrafluoroborate anion included within its cavity.[92]

It was determined that the distance of the nearest included BF_4^- fluorine atom to

an aromatic ring centroid, F(2A)···C(3C) was 2.93Å, whereas the BF_4^-···Cp* and BF_4^- ···arene distances for the anions outside the calixarene cavity were more than 3.10Å. It was found that the metal ions were essential for inclusion of BF_4^- to occur.[92]

1.3.5 Tetraaza based Molecular Receptors

The number of studies involving tetraazamacrocycles has steadily increased over the last few decades as these molecules show considerable ability in complexing metal ions and also because their functionality can be diversified through their reactive nitrogen atoms.

Undeveloped tetraazamacrocycles suffer one drawback, which is their inability to enclose metal ions with coordination numbers greater than four. Nevertheless, by incorporating pendant donor groups capable of metal ion coordination within their framework this obstacle can be overcome. The chemistry of tetraazamacrocycles appended with pendant donor groups has been extensively explored in recent times and instances within the scientific literature are abundant.[90, 93-103]

It is well known that appending pendant donor groups at the periphery of tetraazamacrocycles leads to the retention of the chemical properties inherent in both the macrocycle and the pendant arms.[104] As tetraazamacrocycles can be modified at either their carbon skeletons or their secondary amines the chemistry of both has been widely investigated.[105-107] However, *N*-substitution has proven to be much more facile and therefore studies in this area predominate.[108-111]

Many of these studies have focussed on the chemistry of 1,4,8,11-tetraazacyclotetradecane (cyclam), **20**, first synthesised by van Alphen,[112, 113] which, for the purpose of this work, is unsuitable in that substitution with four pendant arms and subsequent metal coordination will generally cause the cyclam complex to

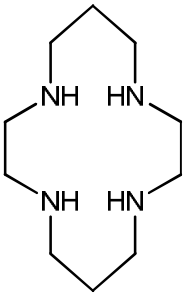

20

adopt a *trans*-III conformation, where two of the pendant arms project above the plane of the metal ion and two below, **Figure 1.8**.[111, 114]

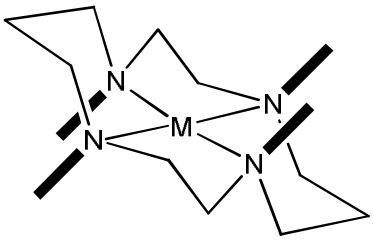

Figure 1.8 Representation of the *trans*-III conformation for 1,4,8,11-tetraazacyclotetradecane (cyclam), **20**.

This problem does not occur with 1,4,7,10-tetraazacyclododecane (cyclen), **21**, as the pendant arms are inclined to project in the same direction and upon metal coordination to form a molecular cavity above the plane of the aza groups.[94]

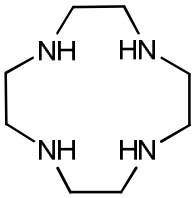

21

Cyclen, **21**, was first synthesised in 1976 by Stetter[115], and has since featured in numerous literature reports in a diversity of fields, for example contrast imaging agents in magnetic resonance imaging,[116-118] models for enzymatic complexes[119, 120]

and chelation therapy.[111, 121]

The exploration of eight coordinate metal complexes of cyclen derivatives containing four pendant arms has been of interest for some time using, for example, DOTAM, **22**, which was synthesised by Hancock *et al*. in 1995.[122]

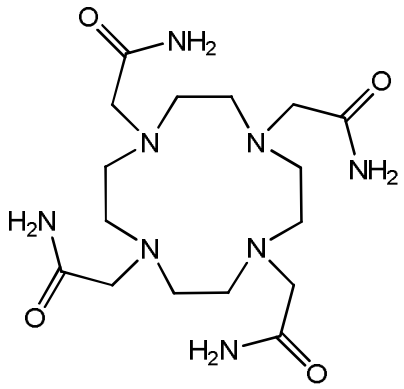

22

It has been demonstrated with X-ray determined crystal structures; for example of the Cd^{2+} complex with DOTAM, **22**, shown in **Figure 1.9**, that this ligand readily forms eight coordinate complexes with metal ions such as Pb^{2+}, Cd^{2+} and Ca^{2+} and six coordinate complexes with metal ions such as Zn^{2+}.[122, 123]

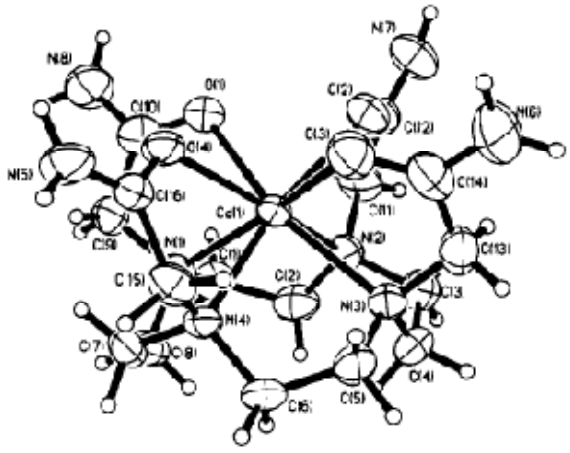

Figure 1.9 A view of the crystal structure of $[Cd(DOTAM)]^{2+}$ showing the two planes of donor atoms enclosing Cd^{2+} due to the outward projection of all the pendant arms away from the same face of the macrocycle.[122]

Complexation occurs through the four *N*-atoms on the cyclen scaffold and the four

amide oxygen atoms on the pendant arms, with the metal ion situated between the two planes. In all cases this causes the pendant arms to juxtapose away from the cyclen skeleton in a *pseudoaxial* conformation.[122]

The outward projection of the pendant arms in **22** suggests that if the pendant arms were increased in length, or broadened, or both, a partially or fully enclosed cavity could result. Hence, the arrival of studies concerned with producing a functionalised cavity. Cadmium(II) complexes **23** to **26** were all prepared from ligands obtained by reacting cyclen with an appropriate epoxide: ethylene oxide for **23**, (*S*)-propylene oxide for **24**, (*S*)-styrene oxide for **25** and (2*S*)-(+)-3-phenoxy-1,2-epoxypropane for **26**. Quantitative yields are common when functionalising cyclen in this way, as is the formation of the complex as its diperchlorate salt.

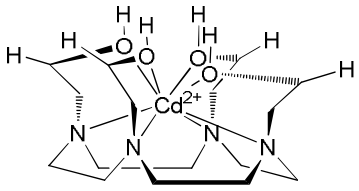

23

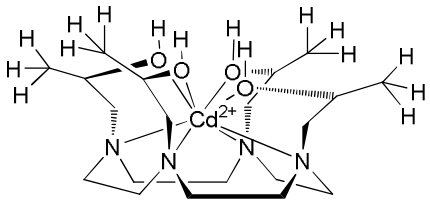

24

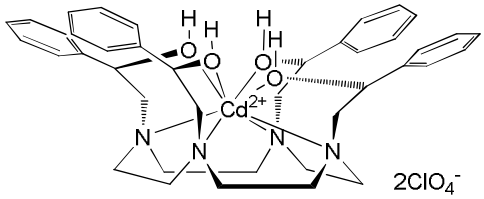

25

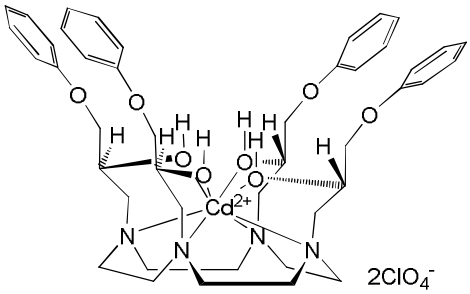

26

The size of the cavity above the O_4 plane in these receptor complexes may vary from negligible in **23** and **24** to shallow and saucer-shaped in **25** to quite substantial in **26**, depending on the length and positioning of the pendant arms.[124] The (*S*)-propylene oxide appended structure **24** was first synthesised in 1988 by Hancock and

co-workers in their investigations relating to neutral oxygen donors as regulators of selectivity for Pb(II) ions.[100] Kimura *et al.*[125] utilised (*S*)-styrene oxide to attach a benzyl alcohol pendant arm to cyclen. This mono-*N* substituted cyclen derivative was then complexed with zinc(II) to yield a model biocatalyst for cleavage of phosphodiester bonds.[125] In an investigation of full cavity development by tetra-*N*-substitution with benzyl alcohol pendant arms, Whitbread *et al.*, found through *ab initio* modelling work that the phenyl groups of a ligand formed in this way would juxtapose to give a shallow cavity.[99, 100, 126] However, although these studies of this complex showed its suitability as a potential receptor, exploration of guest inclusion with **25** was not pursued due to the low yields (*ca.* 40%) obtained when producing the ligand.[96, 126]

In 1999 Smith synthesised **26**, which has come to be known, within the Wainwright group, as one of the first generation metal-ion activated aromatic anion receptors.[90, 93-97] It is possible to alter the size of the cavity within these receptors in correspondence with the ionic radius of the coordinating metal.[126, 127] Thus the Pb(II) complexes appear to have slightly larger cavities than the Cd(II) complexes. These studies by Smith proved to be the advent of investigation into receptor complexes of this class. They operate with considerable efficacy by including aromatic anions, such as phenolates, sulfonates and benzoates and, aromatic amino acids.

Smith obtained crystal structures for many of the inclusion complexes formed with his first generation receptor, **26**, two of which are shown in **Figures 1.10** and **1.11**. These crystal structures reveal the mode of bonding between the aromatic anionic guest species and the first generation receptor as primarily being hydrogen bonding between the guest oxoanion and the host pendant hydroxy groups. Although π-π interactions between the host aromatic rings and that of the guest are not

apparent there is, nonetheless, evidence from guest binding constant data that suggests preferential stabilisation of these guest species that are aromatic in nature.[124]

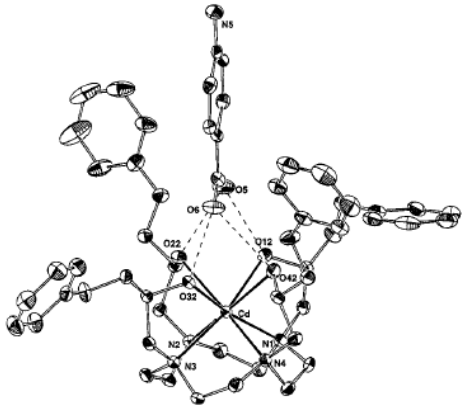

Figure 1.10 X-ray determined structure of the inclusion complex formed between *p*-aminobenzoate and $[Cd(\mathbf{26})]^{2+}$.[93]

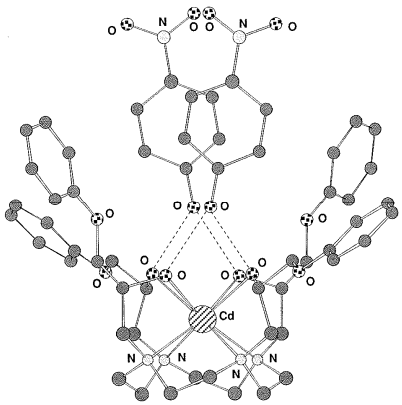

Figure 1.11 X-ray determined structure of the inclusion complex formed between two *p*-nitrophenolate molecules and $[Cd(\mathbf{26})]^{2+}$.[124]

Moreover, electrostatic interaction between the Cd^{2+} ion and the anion is minimal and therefore is not a great contributor to the stability of the complex as the closest point of approach between them is greater than 3.9 Å.[124]

As the properties of the pendant arms and the macrocycle are retained upon *N*-substitution the chemical properties of the receptor could be diversified to include for example groups that would increase its solubility in aqueous media. Examples of

first generation water soluble ionic receptor ligands are the trimethylammonium appended (*S*)-tmappc12, **27** and sulfonated (*S*)-stmppc12, **28**.[128]

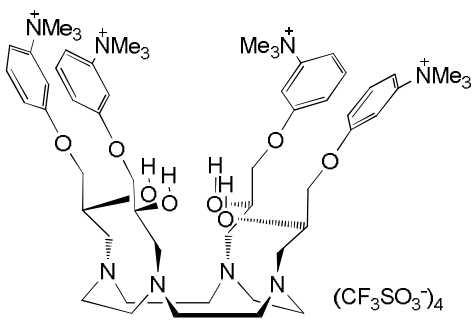

27

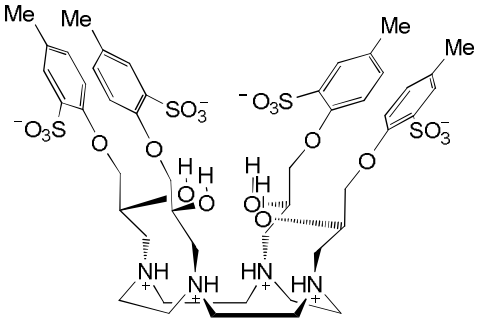

28

It was demonstrated that anion binding properties for the cationic receptor $[Cd(\mathbf{27})]^{6+}$ firstly investigated in DMSO were retained in water. Anionic, hydrophilic sulfonated $[Cd(\mathbf{28})]^{2-}$ exhibited greater water solubility, but, predictably, its anion binding capability was much weaker due to charge repulsion effects.[128]

The success gained with the first generation, four-walled receptors, as host compounds for inclusion of aromatic anionic species such as benzoates, phenolates and amino acids has prefaced design and synthesis of hetero-*N*-substituted cyclen derivatives, for example **29**, which has as one of the pendant arms an anthracene moiety capable of signalling the entry of a guest molecule through changes in its fluorescence. This allows the host to act as a sensor.[129]

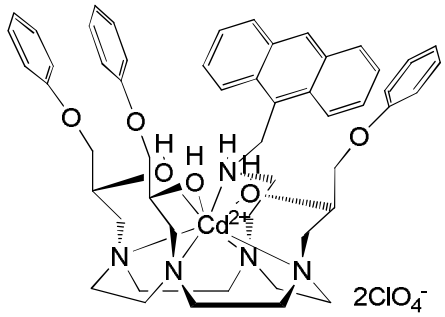

29

However, hetero-*N*-substitution on the cyclen skeleton is not as easy as homo-*N*-substitution and there are relatively few instances within the literature.[109, 130, 131] The methodology behind hetero-*N*-substitution requires that the macrocycle is incompletely substituted with a particular moiety and that the remaining unsubstituted *N*-atoms are subsequently substituted with a different group. For instance, to acquire a tri-*N*-substituted adduct necessitates a stepwise development with initial protection of three nitrogen atoms followed by protection, with a different protecting group, of the fourth. Removal of the three initial protecting groups, derivatisation of the deprotected nitrogen atoms with the required moiety followed by deprotection of the second protecting group provides a homo-tri-*N*-substituted macrocycle. This allows for substitution of the fourth nitrogen atom with a different functionality, for example the fluorophore on **29**, or immobilisation onto a solid surface via a linker molecule.[109]

1.4 Immobilised Receptor Complexes

1.4.1 The silica surface

It is well known that immobilisation of chelating groups on a silica surface via a linker group not only allows better contact of the functional group with its environment, but also provides for regeneration of the material after use.[132] For this reason the investigation of silica immobilised chelating groups for pre-concentration of metal ions has generated a great deal of interest.[133-138]

As noted on page 3, the primary focus of this work was to immobilise aromatic anion binders on a silica surface. In particular, it was to be the cyclen derived aromatic, anion binders similar to **26** that were to be immobilised. Silica gel is a very effective agent for immobilisation of chelating ligands and has therefore been at the forefront of many investigations concerning the preparation of materials for

preconcentration of metal ions from aqueous media.[139-144] Certain advantages can be gained by using an inorganic solid support, such as silica gel, instead of polymeric resins or beads.[136, 145, 146] Some of these advantages are: good selectivity, no swelling, and good mechanical stability.[136] It is, therefore, essential to understand the nature of silica surface chemistry, specifically, the properties and reactivity of its surface silanol groups.[136, 147]

The surface of untreated silica has three layers of physi-adsorbed water hydrogen bonded to silanol groups.[148] Activated silica *i.e.* silica that has been heated to 423 K *in vacuo* to remove most of the physi-adsorbed water from its surface, is structured such that at the surface either a siloxane group (ΞSi-O-SiΞ) forming part of the bulk matrix or a silanol group (ΞSi-OH) can be found. Concentrations of surface silanol groups generally range from 4.5 to 8.0 groups per square nanometre after activation of the silica surface.[148]

Surface silanol groups may exist in more than one form as shown in **Figure 1.12**.

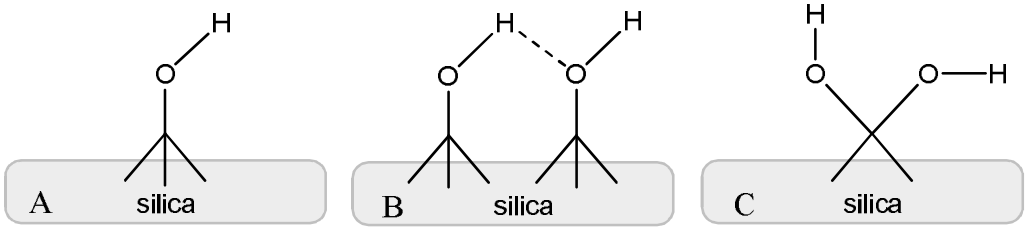

Figure 1.12 Schematic depiction of (A) isolated, (B) vicinal and (C) geminal silanol groups that can be found on the surface of silica.[136]

Hydrogen bonded, silanol groups have a lower pK_a than non hydrogen bonded silanols with values of ~4.9 and ~8.5, respectively.[136] Thus silanol groups remain protonated under acidic conditions, but are susceptible to hydrolysis if their environment becomes too basic by the following process.[149, 150]

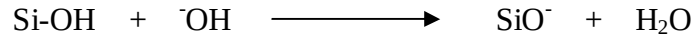

For surface immobilisation of a substrate it is imperative that the number of available silanol groups on the silica surface is maximised as they are the reactive species utilised in surface modification processes.[132, 136, 149, 151] This is commonly done by heating the silica to 423 K under vacuum. Immobilising the functional group directly onto the silanol groups on the silica surface has disadvantages and hence it is desirable to append a linkage between the surface and the functional group.[136] Linker molecules are generally silane coupling agents that contain reactive moieties at each terminus.[152] They are able to attach to the surface of silica by reacting with the surface silanol groups. Once attached to silica they are able to retain some form of functionality at their periphery, such as an aminopropysilane which uses the terminal amino group as the reactive centre for further functionalisation. The terminus that reacts with the surface silanol groups tends to be composed of hydrolysable groups such as chloro or alkoxy moieties.[152] Three examples of silane coupling agents are 3-(aminopropyl)trimethoxysilane, **30**, vinyltrichlorosilane, **31**, and, 3-(glycidoxypropyl)trimethoxysilane, **32**.

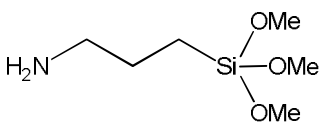

30

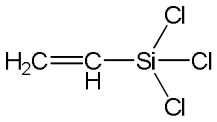

31

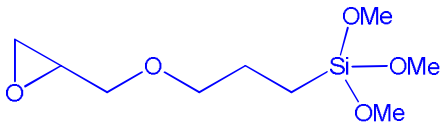

32

These coupling reagents readily react with a silica surface to produce an array of linkers capable of covalently binding to a molecule of interest, as shown in **Figure 1.13**, for a single molecule of **32** covalently attached to silica to form Si-GPS, **33**.

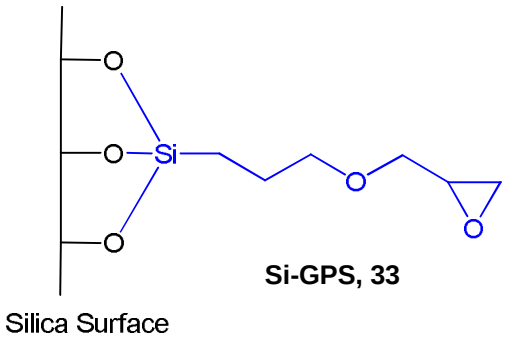

Figure 1.13 Silica attached glycidoxypropylsilane (GPS) linker material, Si-GPS, **33**, derived from the reaction of 3-(glycidoxypropyl)trimethoxysilane (GPTS), **32**, with a silica surface.

A fully developed example of a 2-mercaptobenzothiazole modified silica material **34** has been used for the pre-concentration and separation of silver in aqueous solutions.[137]

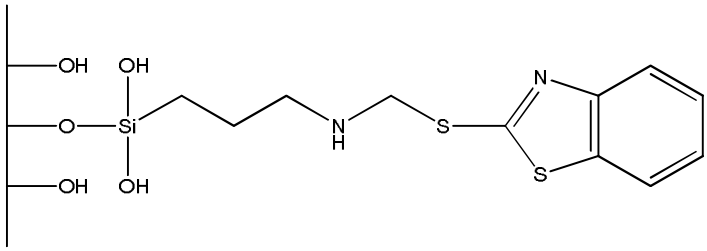

34

This material was synthesised by the Mannich reaction between 2-mercaptobenzothiazole and 3-aminopropyl modified silica gel.[137] The linker moiety immobilises the 2-mercaptobenzothiazole functionality of the material while allowing it to project into the solvent.[136]

This type of methodology for linking chelating groups to a silica surface via an organic silane coupling agent has been used to anchor mixed donor macrocyclic ligands by Dudler and co-workers in 1987.[153] They linked an O_2N_3 donor macrocycle to a silica surface that they had first derivatised with 3-(chloropropyl)trimethoxysilane, to obtain **35**.

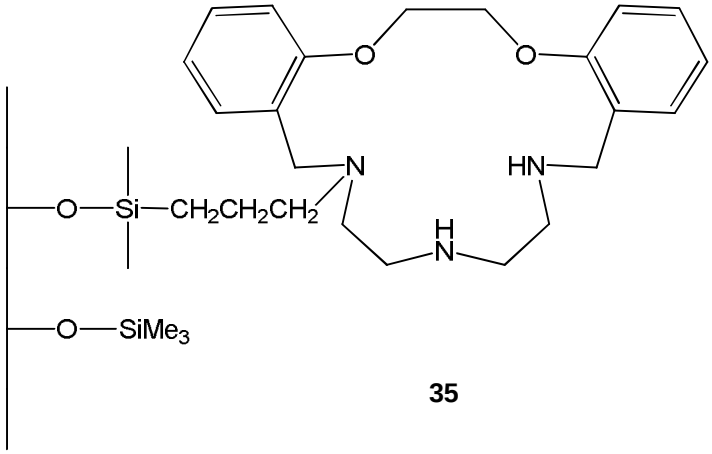

35

This material was obtained with a loading of 0.41 mmol of macrocycle per gram of functionalised silica. It was used to investigate the attached macrocycles selectivity toward Co^{2+}, Ni^{2+}, Cu^{2+}, Zn^{2+} and Cd^{2+} in aqueous solution by atomic absorption spectrometry.[153] They found, not unexpectedly, that **35** demonstrated selectivity toward Cu^{2+} when confronted with a mixture of all the metal ions mentioned.[153]

An example of silica tethered tetraazamacrocycles being used for extraction of uranyl ions from aqueous solution comes from Barbette *et al*. in 2004.[132] They prepared functionalised silica materials with either a derivatised cyclen, **36**, or cyclam, **37**, moiety attached via a linker arm.[132] This was done by two different methods. Method one required firstly functionalising a silica surface with a linker molecule using 3-chloropropyltriethoxysilane then attaching the macrocycle.[132] Method two involved firstly attaching a linker molecule with 3-iodopropyltriethoxysilane to the one of the macrocycle's nitrogen atoms and then functionalising the three remaining nitrogen atoms with propionate pendant arms followed by anchorage on silica.[132]

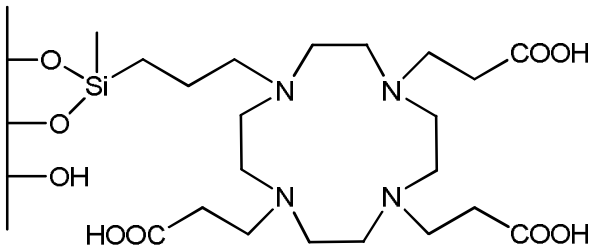

36

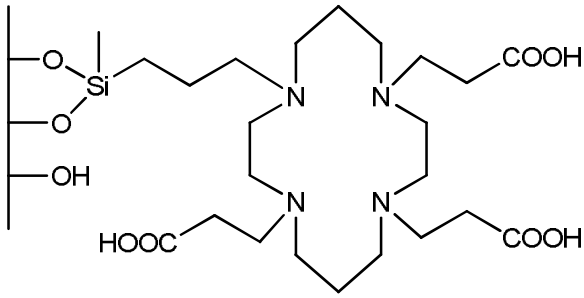

37

The loading of macrocycle obtained for these materials was 0.28 mmol of macrocycle per gram of functionalised silica for **36** and 0.32 mmol of macrocycle per gram of functionalised silica for **37**. Immobilisation of macrocycles in materials **35**, **36** and **37** demonstrates that it is possible to graft bulky molecules onto linker functionalised silica with good results.

1.4.2 Receptor complexes tethered to solid supports

Many studies involving immobilisation of a receptor onto a silica surface concern the tethering of either calixarene or cyclodextrin moieties.[154, 155] An example is from an account published in 2002 by Katz and co-workers.[156] They reported the tethering of *p-tert*-butyl-calix[4]arene to a silica surface initially modified with $SiCl_4$ (tetrachlorosilane) to obtain **38** with a coverage of calixarene per gram of silica material of 0.27 mmol g^{-1}.

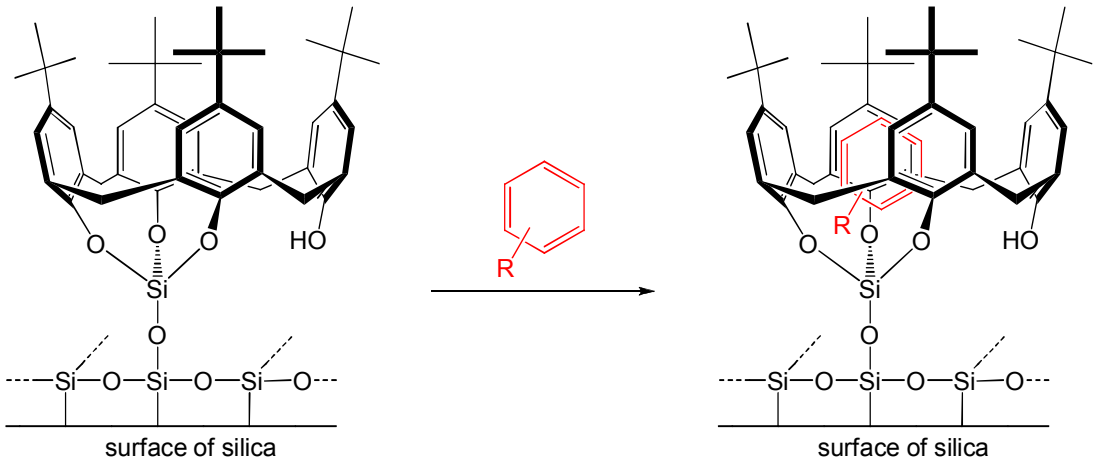

Scheme 1.1 Depiction of the inclusion of a small neutral aromatic guest molecule (R = H, OH, CH_3 or NO_2) within the cavity of silica immobilised receptor **38** to give the host-guest complex **39**. The guest molecule is seen to be held between the aromatic moieties of the calixarene host.[156]

The inclusion capability of **38** was tested with volatile organic molecules (VOCs) such as toluene, benzene, phenol and nitrobenzene in aqueous conditions by determining tentative binding constants for the host-guest complexes formed between these guests and **38**. These are tabulated in **Table 1.2**. [156]

Table 1.2 Binding constants for various VOCs with silica immobilised *p-tert*-butyl-calix[4]arene, **38**, in aqueous solution.[156]

Guest Species	Structure	Binding Constant $K(M^{-1})$
phenol	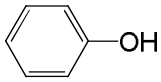	35 ±15
benzene		275 ±15
toluene	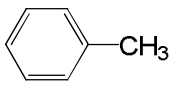	560 ±20
nitrobenzene	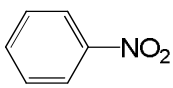	715 ±30

In the host-guest complex **39**, formed as shown in **Scheme 1.1**, it is believed that the guest molecule is positioned between the π-rich calixarene aromatic rings which is indicative of the suitability of **38** for guest inclusion.[157]

An example of an immobilised receptor for anionic species is the glycidoxypropylsilane tethered β-cyclodextrin moiety **40** synthesised by Ponchel *et al*.[158]

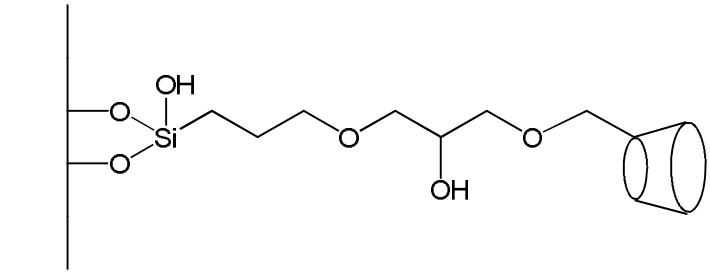

40

Loading of β-cyclodextrin on the functionalised silica was found by thermogravimetric analysis to be 0.067 mmol per gram of the SiO_2 material. The loading of cyclodextrin was also confirmed by titration where reduction of the tetrazolium blue molecule (TB^{2+}) occurs in the presence of reducing sugars.[159]

The guest inclusion capability and guest molecule accessibility to the cyclodextrin moiety of this material was tested with the basic form of methyl orange, **41**, using UV Vis spectroscopy.[158, 160, 161] Studies by Clarke *et al*. have shown that methyl orange forms a 1:1 complex with β-cyclodextrins.[161]

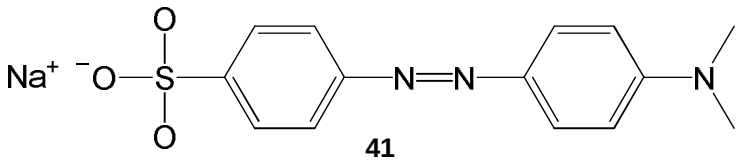

41

At the time of publication Ponchel *et al*. stated that they were working on using the silica immobilised β-cyclodextrin materials as mass transfer promoters in aqueous organometallic catalysis.[158]

Tetraaza metal complexes immobilised on solid supports have been utilised as biomimetic catalysts in the hydrolysis of plasmid DNA,[162] phosphodiesters,[163] and proteins.[164] These artificial enzyme systems all consist of a metal complexed cyclen derivative attached to an organic polymeric backbone. An example is the polymer immobilised Zn^{2+} cyclen complex **42** synthesised as an artificial enzyme for cleavage of phosphodiesters.[163]

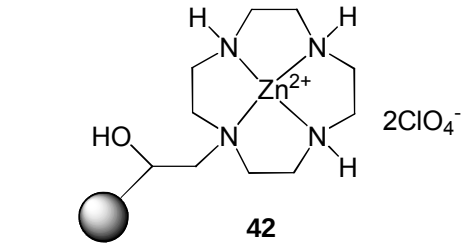

42

polymeric support

1.5 Aims of the Project

The objectives of this project were to explore the inclusion properties, in aqueous conditions, of three-walled, cyclen-based, receptor complexes immobilised on a silica surface. It was thought that this system, shown as **94** would extend the capabilities of the previously studied four-walled, first generation receptor complexes, **26**, synthesised by Smith.[94, 95]

This would entail initial synthesis and exploration of the aromatic anion retention capabilities of a non silica attached, three-walled model system which, if successful, would then be anchored onto chromatographic silica gel. Various derivatives with different properties such as wettability in water, **95** and **96** would also be synthesised and characterised.

These silica attached receptor materials would then be subjected to metal ion complexation with subsequent inclusion studies involving a range of aromatic

anionic guest species in aqueous conditions.

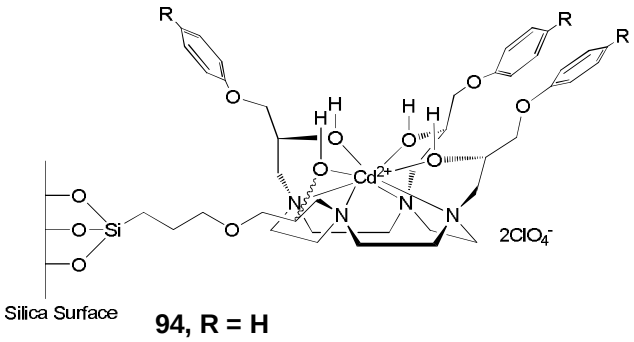

94, R = H
95, R = $(OCH_2CH_2)_2OH$
96, R = $(OCH_2CH_2)_3OH$

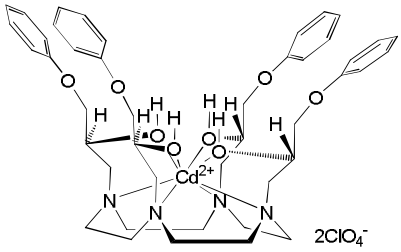

26

CHAPTER TWO

SYNTHESIS OF MACROCYCLIC RECEPTOR PRECURSORS

CHAPTER 2 SYNTHESIS OF MACROCYCLIC RECEPTOR PRECURSORS

2.1 Synthetic design strategy

As indicated in the Introduction, the synthetic protocol formulated for the first generation of tetra-*N*-substituted, phenoxy derived, cyclen-based receptors, exemplified by **26**, is quite straightforward.

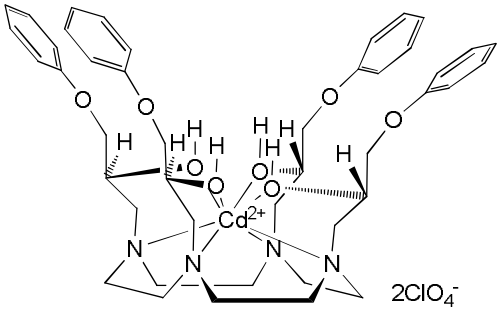

26

Finding a synthetic protocol for the silica immobilised receptors **94** - **96**, shown below, that are the objects of this investigation is necessarily more complex since there are two types of pendant arm to be attached to the macrocycle; the linker arm, to connect the receptor to the silica surface, and the three arms that ultimately constitute the walls of the anion binding cavity.

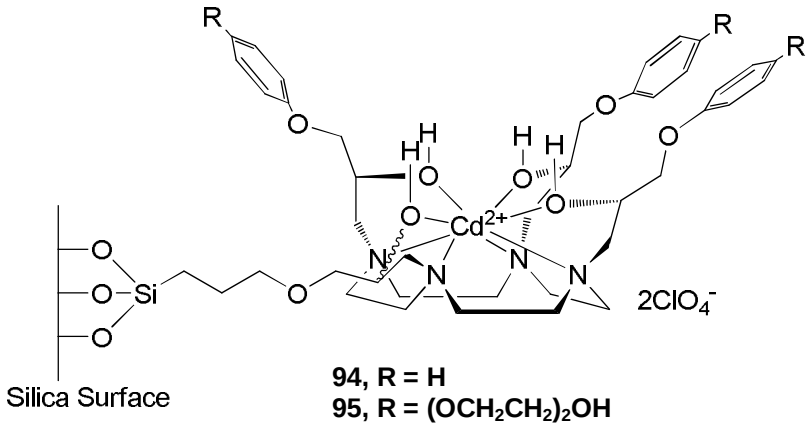

94, R = H
95, R = $(OCH_2CH_2)_2OH$
96, R = $(OCH_2CH_2)_3OH$

In addition, successful immobilisation of these receptors on a silica surface complicates the characterisation of the guest uptake process.[136] In particular, the silica immobilised receptor materials cannot be quantitated to obtain binding constants as this requires dissolution of both the host and the guest to set up conditions for a rapidly established equilibrium between the bound and free guest.[165] Taking this point into account, it was decided firstly to synthesise a structurally and chemically similar model receptor, **49**, that could be used to test the suitability of a three-walled binding cavity. In this molecular receptor model the place of the linker group would be taken by an (*S*)-hydroxypropyl pendant arm, as shown in **Figure 2.1**, and because of its solubility anion binding constants could be measured and compared with those found for a comparable first generation receptor such as **26**.

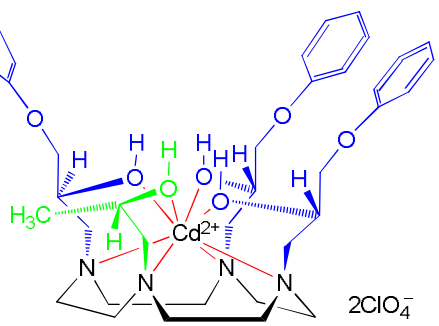

49

Figure 2.1 Schematic depiction of the structural features of the molecular receptor model, **49**, highlighting its correspondence with silica attached receptor **94**: blue, three phenoxy derived pendant arms, red, octa-coordination with cadmium(II) and green, (*S*)-hydroxypropyl pendant arm, simulating the linker group.

Conceptually, the three-walled cavity appears to have an "open gate" through which included species are likely to escape through increased contact with the solvent. Furthermore, the reduction in the number of aromatic species forming the walls of the cavity may result in a proportional loss of possible π-π interactions, presupposing, of course, that hydrogen bonding interactions between the host O-H

groups and guest species are augmented by some level of π-π interaction. Therefore, synthesising the molecular receptor model, **49**, was essential in examining whether three pendant arms would adequately provide a binding cavity capable of including aromatic anionic species, as well as in developing a synthetic strategy that could also be used for silica attached receptors.

2.2 Synthetic strategy

The strategy to accomplish the synthesis of both the silica attached receptors **94**, **95** and **96** and the model receptor, **49**, requires preparation of tri-*N*-substituted cyclen precursor ligands **46**, **47** and **48**, **Figure 2.2**. This necessitates attachment of the pendant arms, to a mono-*N*-protected cyclen synthon. Literature precedent suggested that the mono-carbamate, **50**, would be useful for this purpose, **Figure 2.2**.[109]

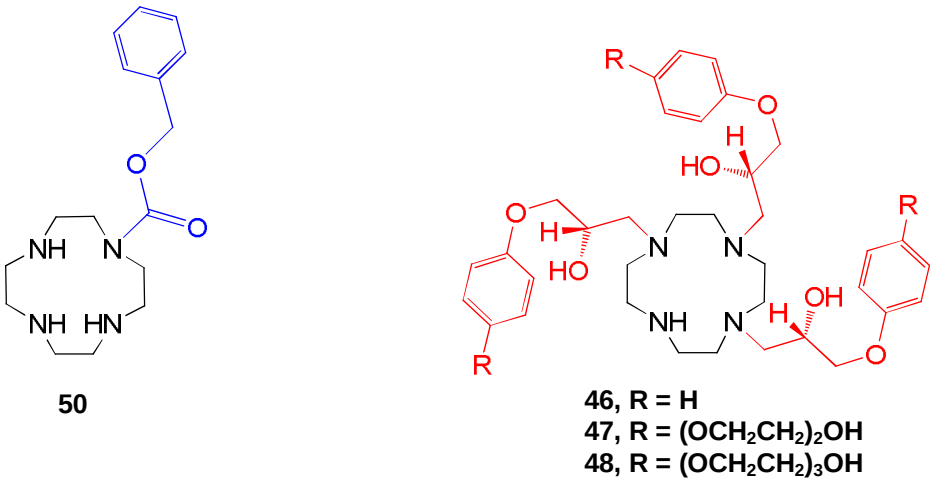

Figure 2.2 Mono-protected cyclen synthon, **50**, and tri-*N*-substituted cyclen derivatives, **46**, **47** and **48**.

Anchorage of **46** - **48** to silica could then be effected by reaction with a silica surface silanised with an appropriate alkoxysilane linker. In this work racemic 3-(glycidoxypropyl)trimethoxysilane, **32**, (hereafter GPTS) was used to attach a suitably reactive linker to the silica surface, as shown in **Figure 2.3**.

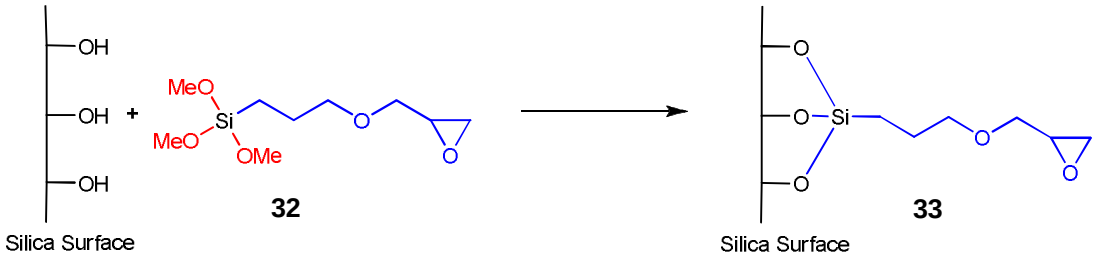

Figure 2.3 Reaction of 3-(glycidoxypropyl)trimethoxysilane, **32**, with silica to provide the silanised surface capable of subsequently reacting with **46** - **48** to immobilise the receptor on the surface.

Preparation of model receptor, **49**, requires attachment of a 2-hydroxyalkyl pendant arm to the unsubstituted fourth aza group on the tri-*N*-substituted cyclen derivative **46**. For this work the (*S*)-2-hydroxypropyl group was chosen. The optical purity of this group is essential if only a single diastereomer of the product, **51**, is to be formed.

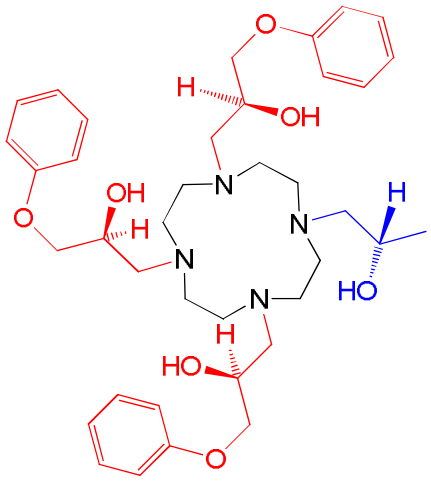

51

2.3 Synthesis of mono-protected cyclen synthon

In accord with the aims of this project a synthetic strategy was devised to prepare a mono-protected cyclen synthon to facilitate tri-*N*-alkylation of cyclen with appropriately functionalised pendant arms. This is shown in Scheme **2.1**

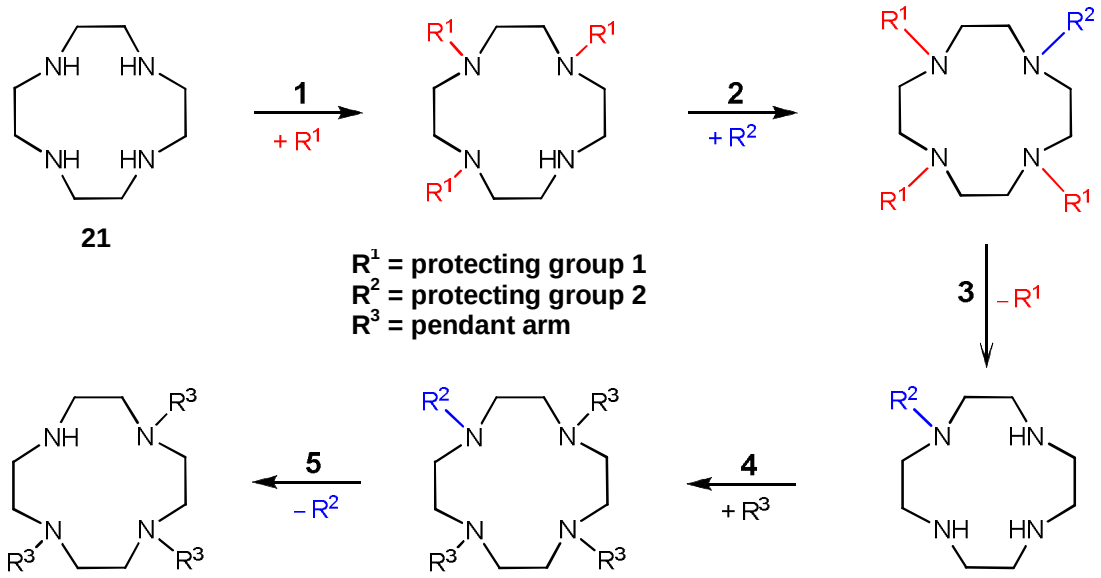

Scheme 2.1: Five step synthetic strategy for tri-*N*-alkylation of cyclen, **21**.

It can be seen conceptually in **Scheme 2.1** that synthesis of a tri-*N*-alkylated cyclen derivative requires five steps involving protection with two different protecting groups and subsequent deprotection to achieve the desired alkylation pattern on the cyclen skeleton.

2.3.1 Synthesis of tri-formyl protected cyclen

Synthesis of the mono-*N*-protected cyclen used in this work commenced with preparation of a cyclen derivative with three of the four available *N*-positions protected with formyl groups as depicted in **Scheme 2.2**.

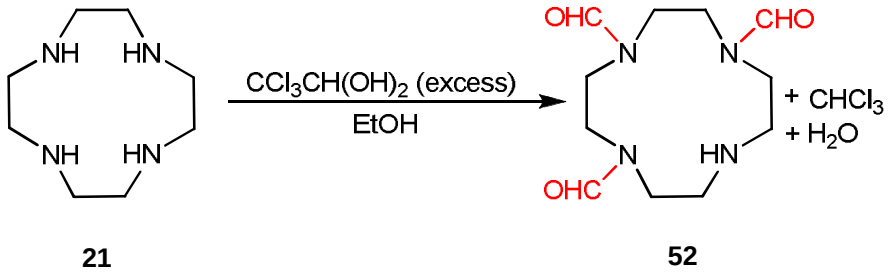

Scheme 2.2 Synthesis of the tri-*N*-formylated cyclen, **52**.

The methodology chosen was adapted from relatively recent developments established by Boldrini,[131] and Yoo.[109]

Synthesis of the tri-formyl protected cyclen derivative **52** proceeded by the reaction of cyclen, **21**, with an excess of chloral hydrate at 60° C in anhydrous ethanol. This adduct was attained in quantitative yield and a high degree of purity as the residual chloral hydrate and reaction by-products, chloroform and water were readily removed *in vacuo*.[131]

Due to restricted rotation around the *N*-CHO bonds both ^{1}H NMR and ^{13}C NMR spectra for **52** show broad peaks due to superimposition of the slightly separated resonances from the four geometrical isomers illustrated in **Figure 2.4**.[166]

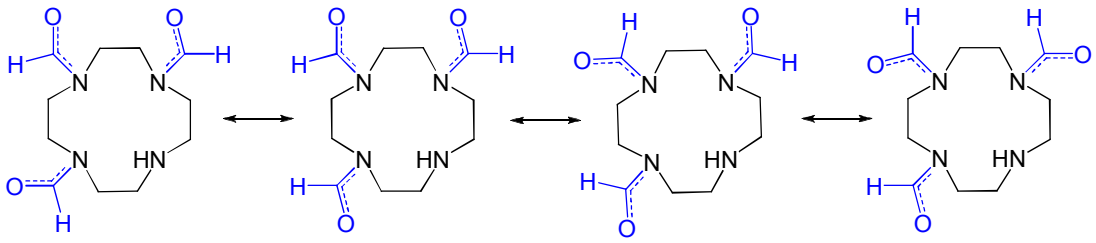

Figure 2.4 Schematic illustration of the four geometrical isomers originating from restricted rotation around the amidic C-N bond.

Remarkably this synthetic procedure gives, exclusively, the triformyl protected cyclen derivative **52** as shown in **Scheme 2.2**, even in the presence of excess chloral hydrate. Boldrini *et al*. explain this phenomenon as arising from intramolecular base catalysis of the formylation reaction by the cyclen nitrogen atoms. This implies that for substitution to occur at one of the nitrogen atoms a second unsubstituted nitrogen atom is required. Therefore, after three of the nitrogen atoms have been reacted the fourth nitrogen atom is bereft of a basic nitrogen atom able to provide the necessary catalytic cooperation for substitution to occur.[131] Another twist on this interpretation

is that the electron withdrawing capability of the formyl groups causes the fourth nitrogen atom to become less basic thus augmenting its inability to act as an effective nucleophile.

2.3.2 Preparation of mono-carboxybenzyl (cbz) protected cyclen

Protection of the fourth nitrogen atom of tri-formylated cyclen, **52**, to obtain tri-formyl-cbz-protected cyclen, **53**, was achieved by treatment of **52** with an excess of benzyl chloroformate, **54**, in de-ionised water at room temperature overnight, **Scheme 2.3**.

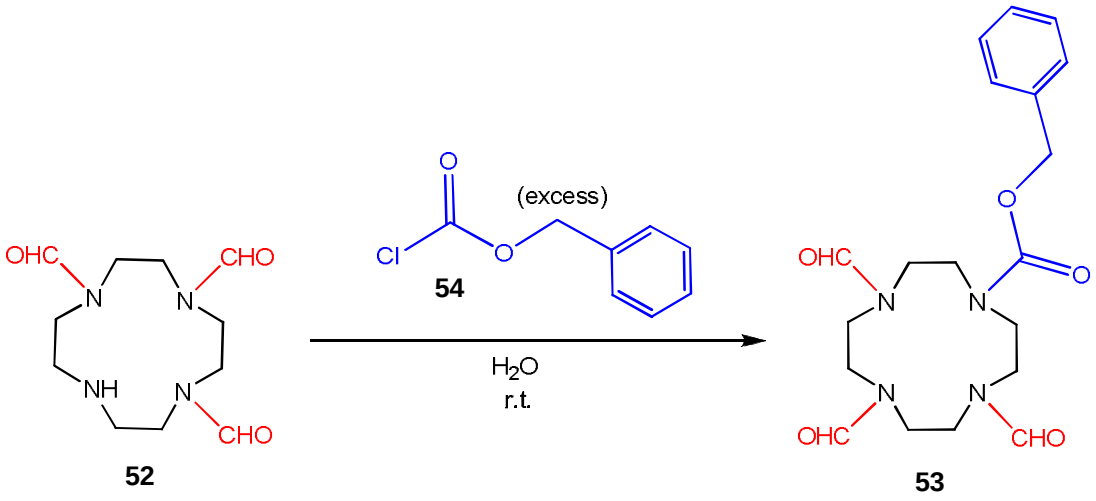

Scheme 2.3 Protection of the fourth *N*-position with a carboxybenzyl group.

Since the HCl generated during the reaction may hydrolytically remove some or all of the formyl protecting groups and also cleave the cbz protecting group the pH of the reaction was maintained between 4 and 10 with the addition of saturated sodium carbonate solution.[131, 166, 167] The tetra-*N*-protected product **53** was extracted into dichloromethane and following evaporation of the solvent was used without added purification.[109] For the purpose of characterisation, a pure sample of the tri-formyl-cbz-protected cyclen derivative was obtained by trituration with diethyl ether over a one week period and used to obtain ^{1}H NMR and ^{13}C NMR spectral data which

agreed with literature values.[109]

Removal of the formyl groups was performed by stirring compound **53** in solution with 1 M HCl at 50° C for five hours. The reaction mixture was then concentrated *in vacuo* to complete dryness and subsequently dissolved in EtOH, which was boiled for one hour. After cooling this solution, filtration (1st crop) and precipitation by addition of diethyl ether (2nd crop) gave the trihydrochloride salt of mono-cbz-protected cyclen, **50**, in 96% yield, **Scheme 2.4**.

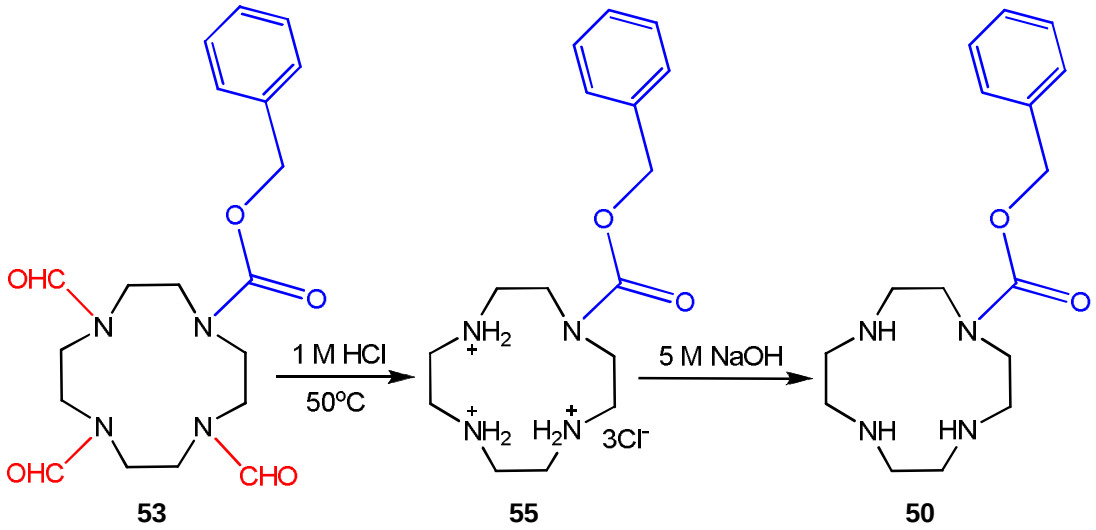

Scheme 2.4 Preparation of the mono-*N*-protected cyclen synthon **50**.

The pH of an aqueous solution of **55** was then adjusted to ~13 by the drop-wise addition of ice-cooled 1M NaOH to give the basic form, **50**, in 98% yield. The ^{1}H NMR and ^{13}C NMR spectra for both **55** and **50** show the disappearance of the broad peaks for the three formyl groups and are in good agreement with literature values.[109]

2.4 Synthesis of the pendant arms

Having successfully prepared mono-protected cyclen, **50**, with high purity and in good yield, the next element in the sequential progression towards tri-*N*-alkylation was to synthesise the epoxides that would be used to form the pendant arms.

The chiral phenolic epoxide **56** was prepared by an established method, first formulated by Klunder,[168, 169] and subsequently modified by Smith,[94] in 74% yield from the reaction of phenol, **57**, with enantiomerically pure (*2S*)-(+)-glycidyl tosylate, **58**, **Scheme 2.5.** ^{1}H NMR and ^{13}C NMR spectral data agreed with literature values.[94]

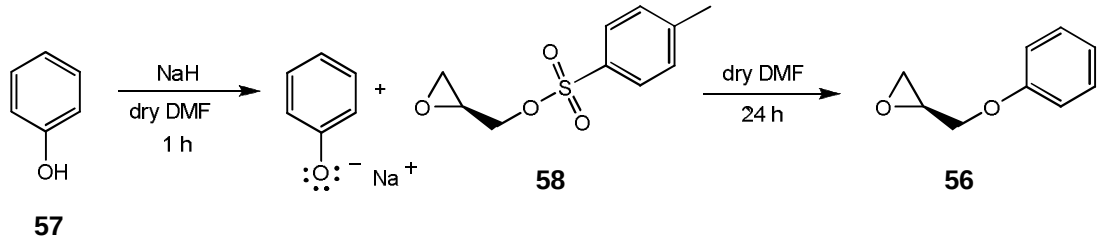

57 **58** **56**

Scheme 2.5 Synthesis of chiral phenolic epoxide **56**.

2.4.1 Preparation of hydroxy terminated polyether (HTPE) appended pendant arm epoxides with enhanced hydrophilicity

To impart and improve wettability in aqueous solution to the silica immobilised macrocyclic receptor materials, functional groups that increase their hydrophilic character seemed appropriate. Reasoning that the elements of the receptors displaying most contact with the ambient solution are the upwardly projecting pendant arms, it was determined that, modification of these pendant arms to augment their contact with the aqueous environment and, confer hydrophilicity at the periphery of the receptors would satisfy the objective for increased receptor wettability in aqueous solution.

The choice of adding a "dendritic" hydroxy terminated polyether chain to each pendant arm developed from other studies pursuing the same objective of instilling hydrophilic properties to their synthetic targets.[170-173] Synthesis of the pendant arm HTPE epoxides **59** and **60** does not reflect the ease of producing phenolic epoxide, **56**, and requires a four step process as shown in **Scheme 2.6**.

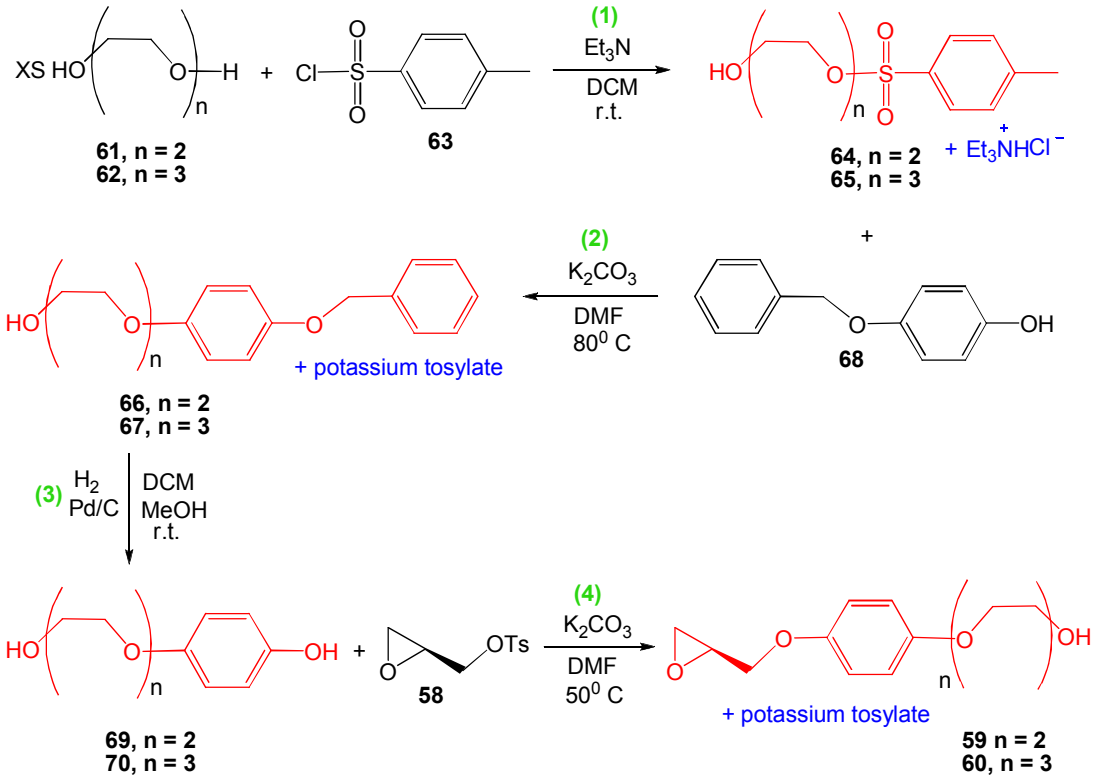

Scheme 2.6 Preparation of the hydroxy terminated polyether appended pendant arm epoxides **59** and **60** with synthetic steps numbered in green.

In step one it is apparent from the generic structure of parent polyethylene glycol (PEG) that substitution is possible at each hydroxy terminus. This is avoided[174] by providing an excess of the appropriate PEG to optimise the formation of the mono-substituted products in 81% yield for **64** and 76% yield for **65**.

It is well established that tosylates provide superior leaving ability to hydroxyl groups ensuring that nucleophilic attack from the deprotonated phenolic oxygen of 4-(benzyloxy)phenol, **68**, would, in the following step, occur at the *alpha* carbon of the mono-tosylated HTPEs **64** or **65**. Thus the mono-benzyl-protected, hydroxy terminated di- or tri-ethylene glycol ether substituted hydroquinone derivatives, **66** and **67**, were obtained in four days with 68% yield for **66** and 72% yield for **67**.

Cleavage of the benzyl protecting group, Step 3, to gain *p*-HTPE substituted phenols **69** and **70** was accomplished by hydrogenation of the benzyl protected

phenolic oxygen of **66** or **67** over Pd/C catalyst under an atmosphere of hydrogen in 2 days. Both were formed in quantitative yield. ^{1}H and ^{13}C spectral properties correspond with literature values.[174, 175]

Step 4, of the *p*-HTPE substituted phenoxy epoxide synthesis gave **59** in 63% yield and **60** in 70% yield. This was achieved by initial deprotonation of the phenolic oxygen of **69** or **70**. The resulting phenoxides then engage in a nucleophilic substitution reaction involving enantiomerically pure glycidyl tosylate, **58**, giving the required products. This reaction was conducted at a temperature of 50^{o} C to safeguard the glycidyl functionality. Higher temperatures can affect kinetic stability adversely and contribute to ring opening of the oxirane moiety generating an unwanted vicinal diol.[176 177]

The HTPE epoxides **59** and **60** are new compounds. ^{1}H HMR and ^{13}C NMR spectra for both **59** and **60** exhibit the appearance of resonances for the 1,2-epoxypropane moiety that are consistent with literature values for epoxide **56**.[94] Chemical shifts for the HTPE appendages are in agreement with those found for the precursors of these compounds. Optical rotation studies were conducted on **59** and **60** to ensure that racemisation had not occurred. For **59**: $[\alpha]^{25}_{D} = +4.21^{o}$ (c 2.19, MeOH); and, for **60** $[\alpha]^{25}_{D} = +2.35^{o}$ (c 2.13, MeOH). Whilst the presence of a non-zero $[\alpha]^{25}_{D}$ value does not guarantee that full optical purity has been preserved later reaction of three equivalents of each epoxide with monoprotected cyclen and the observation of the product as a single diastereomer, in each case, proves that it has.

2.5 Preparation of tri-*N*-alkylated cyclen receptor precursors

To obtain the cbz-protected, tri-*N*-alkylated-cbz-protected cyclen derivatives **71**, **72** and **73**, three molar equivalents of the previously synthesised chiral epoxides **56**, **59** or **60** were introduced into a stirring solution of mono-cbz-protected cyclen, **50**, in

anhydrous ethanol, **Scheme 2.7**. The reactions were conducted under reflux for seven to 14 days dependent on the rate of consumption of the epoxide monitored by thin layer chromatography. Subsequent removal of the solvent *in vacuo* provided **71**, **72** and **73** in quantitative yield.

The homochirality of these products was confirmed from ^{13}C NMR and APT spectral data, which showed no evidence of multiple diastereomers.

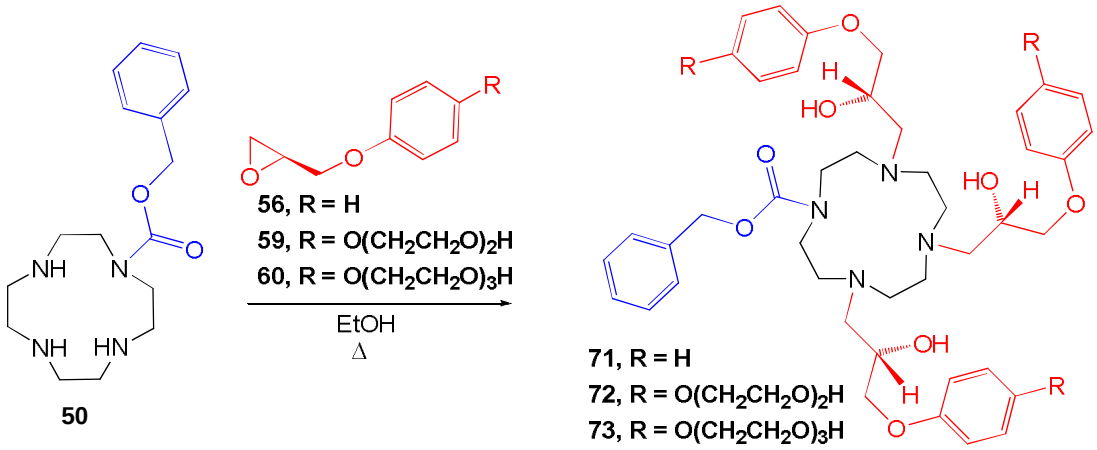

Scheme 2.7 Synthesis of the monoprotected tri-*N*-alkylated cyclen receptor precursors.

All of the products **71**, **72** and **73** displayed the characteristic chemical shifts for the pendant arms with the outer pendant arms giving resonances twice as intense as the corresponding resonance from the central arm. Compounds **72** and **73** also exhibit the appropriate number of resonances for the HTPE appendages.

The next step in the preparation of the receptor precursor ligands was to cleave the cbz protecting group to furnish the tri-*N*-alkylated derivatives. The initial deprotection method was adapted from protein studies where acid hydrolysis of cbz protecting groups with 45% HBr in glacial acetic acid has been used.[178, 179] This proved to be low yielding and was subsequently abandoned when a more recent, cleaner and higher yielding alternative was found in the literature: catalytic transfer hydrogenation, **Scheme 2.8**.[167]

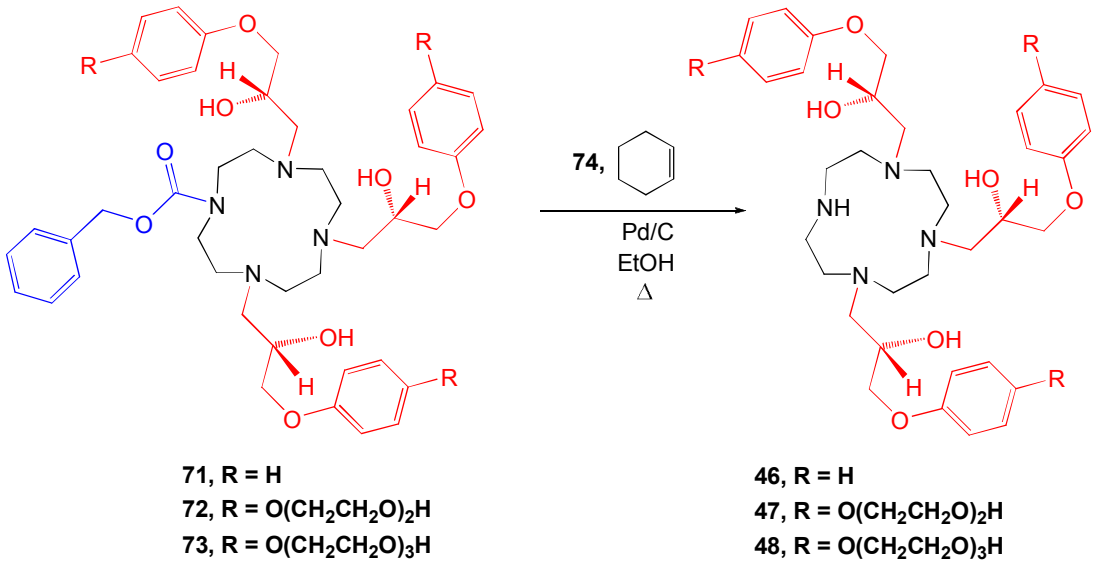

Scheme 2.8 Deprotection of monoprotected tri-N-alkylated cyclen derivatives by catalytic transfer hydrogenation.

This deprotection process progresses with fragmentation of the cbz group into a benzyl and a carboxy group which are hydrogenated to form toluene and formic acid.[180] This was effected by gentle reflux of a solution of **71**, **72** or **73** in anhydrous ethanol with a fivefold excess of cyclohexene, **74**, as the hydrogen donor, over Pd/C catalyst to give **46** in 98% yield, **47** in 83% yield and, **48** in 85% yield. ^{13}C NMR spectroscopy showed the loss of the cbz group resonances with conservation of the pendant arms at resonances approximating those of the parent cbz-protected compounds.

2.6 Synthesis of the silica attached molecular receptor model

To conserve the overall *S* configuration at the stereogenic carbon atoms in each of the four pendant arms it was decided that the chiral epoxide (*S*)-(-)-propylene oxide, **75**, would provide an appropriate alkylating reagent to introduce the pendant arm intended to simulate a linker to a silica surface, **Figure 2.5**.

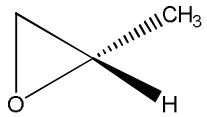

75

Figure 2.5 Structure of (*S*)-(-)-propylene oxide, **75**.

Studies relating to N-alkylation of cyclen with propylene oxide are few in number[100, 118, 181-183] and most relate to substitution on all four nitrogen atoms of the cyclen framework.[181-183] The only recorded procedure leading to hetero-*N*-alkylation of cyclen specifically at one nitrogen atom alkylates the fourth nitrogen atom of the tri-*N*-substituted cyclen adducts DOTA and DOTEP, which are water soluble.[118, 181] However, this method could not be used here as, the tri-*N*-alkylated cyclen adduct **46** is not water soluble. In the absence of catalysis, direct reaction of (*S*)-(-)-propylene oxide with **46** was prohibitively slow. Lithium bromide was chosen to catalyse the epoxide ring-opening reaction as there are examples of successful synthetic procedures in the literature for the aforesaid reaction with amines.[184, 185] Previous studies have discovered that Li^+ has the ability to activate oxygen-bearing electrophiles, due to its high oxophilic capacity, enabling attack by a nucleophile at the α carbon, **Figure 2.6**.[184, 185] Successful regioselective ring-opening reactions adhering exclusively to S_N2 nucleophilic attack at the terminal carbon of propylene oxide by aliphatic amines, utilising lithium bromide as catalyst have been reported with good yields.[185]

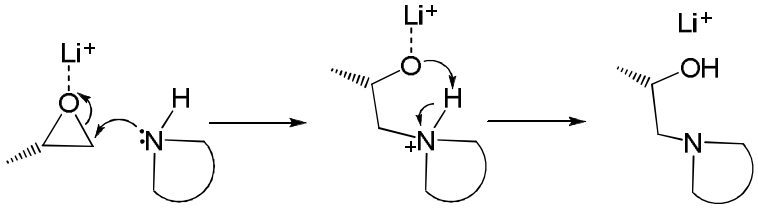

Figure 2.6 Proposed mechanism for the LiBr catalysed ring-opening reaction of (*S*)-(-)-propylene oxide, **75**, by cyclen.

The model receptor ligand **51** was prepared by heating a stirred acetonitrile solution of **46** with a 100% excess of (*S*)-(-)-propylene oxide, **75**, and lithium bromide, in a sealed pressure vessel at 80^{o} C for 72 hours, **Scheme 2.9**.

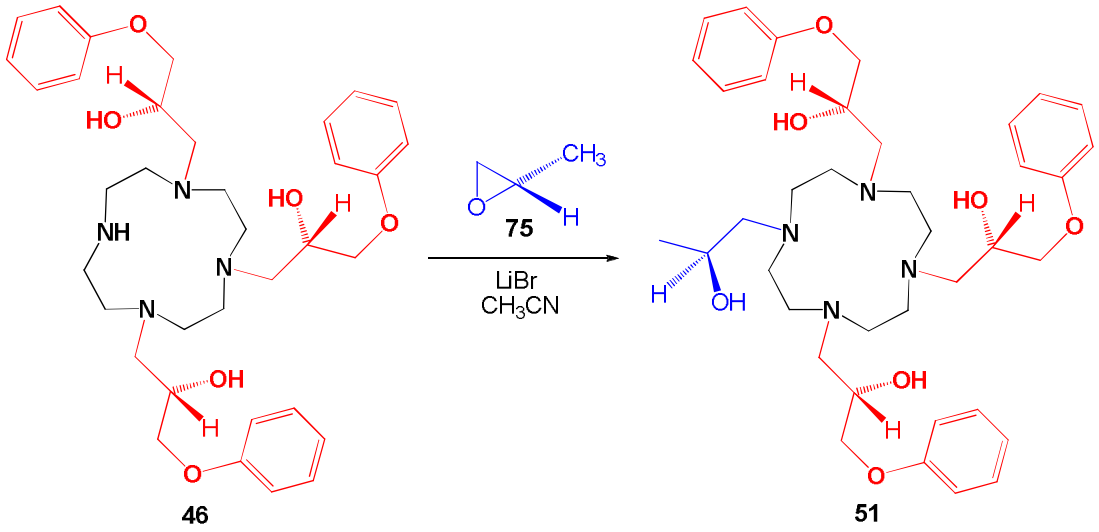

Scheme 2.9 Synthesis of the silica attached molecular receptor model precursor, **51**.

Following the reaction, the desired product, **51**, was extracted with chloroform, after the addition of water to the reaction mixture to remove the lithium bromide. The resulting extract was concentrated *in vacuo* to give **51** in 97% yield and high purity. Analysis of the ^{13}C and ^{13}C APT spectra of compound **51** revealed the appearance of three distinct peaks for the methyl, methylene and methine carbons of the appended hydroxypropyl pendant arm. The chemical shifts of the resonances due to the three phenoxy and the hydroxypropyl pendant arms were at positions normally found for these moieties.[94, 174]

2.7 Metal ion complexation with the silica attached receptor model

2.7.1 Molecular receptors activated by metal ion coordination: Background

Previous studies of cyclen based receptor complexes have demonstrated that upon

metal ion coordination the pendant arms of the ligand project away from the same face of the cyclen framework forming a cavity large enough to include small molecules.[93-96, 166, 186] It is also well established by these studies that, with the ligands examined, cadmium(II) forms decidedly stable eight-coordinate complexes with a high level of rigidity. Therefore, the metal ion selected to form the receptor model complex was cadmium(II).

2.7.2 Synthesis of the cadmium complex of the receptor model

The model macrocyclic receptor cadmium(II) complex, **49**, was synthesised by an established method as reported by Smith, **Scheme 2.10**.[94, 186]

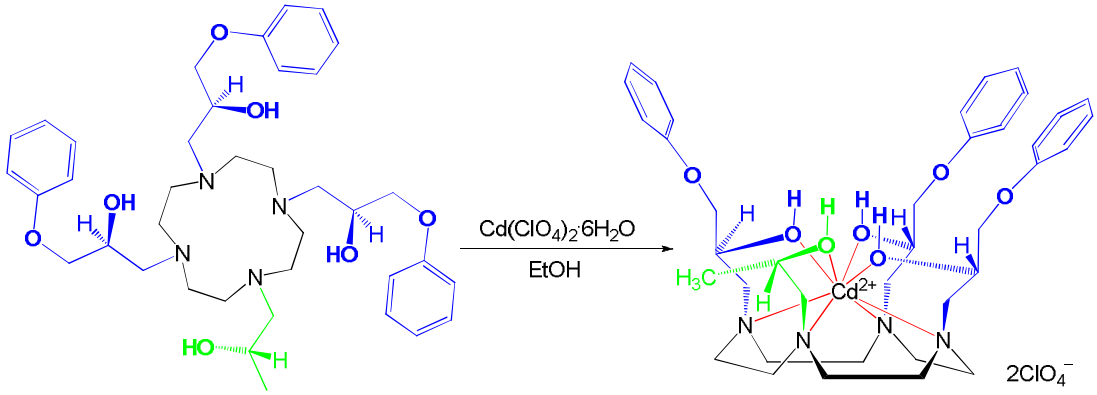

51 **49**

Scheme 2.10 Synthesis of the molecular analogue cadmium(II) diperchlorate complex **49**.

An ethanolic solution of cadmium perchlorate hexahydrate, in excess, was added to a refluxing solution of the receptor precursor **51** also in ethanol causing an initial precipitate that redissolved upon refluxing for a further hour. After cooling the solution a fine off-white solid formed that was filtered and washed with cold ethanol to give **49** in 91% yield. Characterisation of **49** was by microanalysis and ^{13}C NMR spectroscopy, which revealed resonances in the spectrum shifted slightly downfield compared to those observed with the free ligand.

Before proceeding with anion inclusion studies (Chapter 3) with receptor **49**,

hereafter referred to as [Cd(TracHP12)]$(ClO_4)_2$, it was crucial to determine its solubility. The complex was found to be soluble in a range of solvents encompassing primarily those with some degree of polarity, such as, DMF, acetone, acetonitrile and DMSO. The solubility parameters for this compound correlate well with prior experimental findings for the tetra phenoxy pendant armed adduct [Cd((*S*)-thphpc12] $(ClO_4)_2$, **26**.[94]

Isolating complex **49** as its di-perchlorate salt was desirable as it is well established that when perchlorate ions hydrogen bond or ligate with metal cations the interactions are quite weak. Therefore, these ions are potentially ideal for displacement in guest inclusion studies as there is no competition for the metal ion or the anion binding cavity with potential guest species.[187, 188] The nature of the interactions between the perchlorate ions and the complex cation was confirmed as being essentially ionic through molar electrical conductivity studies in DMF, which gave a value of 128 Ω^{-1} cm^2 mol^{-1}, demonstrating that in this medium, receptor **49** behaves as a 2:1 electrolyte and is thus fully dissociated.[166, 189]

CHAPTER THREE

GUEST MOLECULE INCLUSION STUDIES WITH THE RECEPTOR MODEL

CHAPTER 3 GUEST MOLECULE INCLUSION STUDIES WITH THE RECEPTOR MODEL

3.1 Background

Earlier it was mentioned that prior to immobilisation of molecular receptor precursor **46** onto a silica surface, guest uptake studies would be undertaken on a tri-phenoxy pendant-armed, molecular receptor, to ascertain the ability of a receptor equipped with only three aromatic groups to function as a satisfactory host species. These studies were required as the silica immobilised host species would lack one aromatic group compared to hosts such as **26**. To do this a series of guest inclusion experiments was performed with [Cd(TracHP12)]$(ClO_4)_2$, **49**, with a view to acquiring guest molecule binding constant data that could be used to gauge whether the loss of stability of the host-guest complex, associated with the loss of one aromatic group, would be prohibitively large or not.

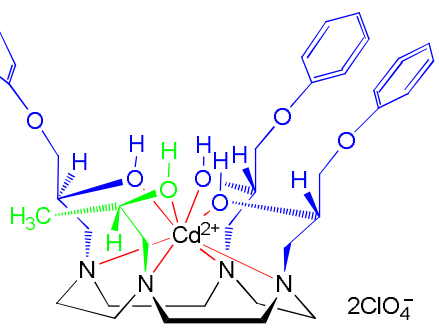

49

3.2 Measurement of Host-Guest Binding Constants

3.2.1 Binding constant measurements using the ^{1}H NMR monitored titration method

Titrations in which NMR chemical shift values are monitored are routinely used as a means of obtaining binding constant data.[190-194] It is well established that upon dissolution, host-guest complexes will establish the equilibrium shown in equation

3.1 where K_A is the association, or guest binding constant that is sought.

$$HG \underset{K_A}{\overset{K_D}{\rightleftharpoons}} H + G \qquad \textbf{(3.1)}$$

K_A = association constant

K_D = dissociation constant

If the system undergoes slow exchange of the guest between the free and bound states the resonances of the host, the guest and the host-guest complex are observed as separate entities allowing the equilibrium constant to be evaluated, directly, from the integration of the resonances' intensity.[7] More commonly, though, the rate of exchange between the associated and dissociated forms of the host-guest complex is rapid on an NMR timescale and only a single set of resonances for the host and guest are seen where the chemical shift values are the average of the values for the associated and dissociated species, weighted by the prevailing mole fraction of each. Thus, for example,

$$\delta_G = \delta_G\chi_G + \delta_{HG}\chi_{HG}$$

It is then the case that when the chemical shift values associated with the monitored species, which in this work was the guest, are plotted against the increasing concentration of the host, a titration curve is produced, the curvature of which diminishes with increasing magnitude of K_A. Cursory inspection of the physical appearance of the titration curve, which may vary from virtually a flat line, to a steep climb with an angular bend at its zenith, plateauing into linearity, gives, to the experienced eye, a rough estimate of the strength of the host-guest interaction. An accurate, quantitative determination of the host-guest binding constant can be calculated by a curve fitting program that displays the experimental data in comparison with the theoretical curve for calculated values of K and δ_{HG}. A

comprehensive description of the methodology used in this work for determining guest molecule binding constants has been provided in **Appendix A**.

Before commencing ^{1}H NMR monitored titration experiments it was decided, that, due to the difference in the architectural framework of molecular receptor **49** and, previously studied hosts, such as **26**, the previously established 1:1 stoichiometry between the host and the guest should be checked. This was achieved by subjecting some of the intended host-guest inclusion partners to examination by the method of continuous variations (Job's Method) using ^{1}H NMR spectroscopy. A detailed description of the method of continuous variation can be found in **Appendix B**.[195, 196]

3.2.2 Determining the stoichiometry of the host-guest complexes

Job's Method entails the preparation of a series of solutions each consisting of a constant total number of moles of H and G but, with variation in the molar ratio of H to G where $0 \leq [G]/([H] + [G]) \leq 1$. A measurable parameter such as a change in the chemical shift ($\Delta\delta$) in the normalised form $\chi\Delta\delta$, in the resonances of either the host or the guest species is then followed and plotted as a function of its mole fraction (χ) to give what is known as a Job's Plot. The plot should reach a peak at the point where the maximum amount of product, HG, is obtained. This apical point is located at the stoichiometric ratio of G to H characteristic of the composition of the product. For a 1:1 H:G complex the stoichiometric ratio is maximised at $\chi_G = 0.5$ giving a parabolic curve on the Job's Plot, as depicted in **Figure 3.1**.[197]

It can also be seen in, **Figure 3.1**, that the magnitude of the binding constant (K) influences the appearance of the curve with larger binding constants tending to give it a triangular form.[165, 195, 197, 198]

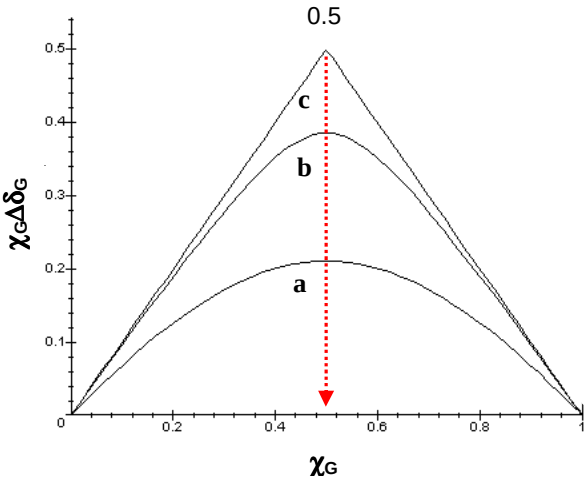

Figure 3.1 Simulated Job's Plot for 1:1 stoichiometry generated with Maple V,[199] from **Equation 1.1** in **Appendix B**. The data plotted in this figure are for a model system where $\Delta\delta_{HG}$ = 1.0 ppm and $\Delta\delta_{HGmax}$ = 0.5 ppm, with *K* ranging from (a), 3 x 10^2 M^{-1} through (b), 3 x 10^3 M^{-1} to (c), 10^6 M^{-1}.

For a system where the composition of the host-guest complex has stoichiometry of 1:2, H:G, for example, **76**, the Job's Plot loses its symmetry and reaches a maximum where χ_G = 0.67 or χ_H = 0.33 depending on which species is monitored, as depicted in, **Figure 3.2**.

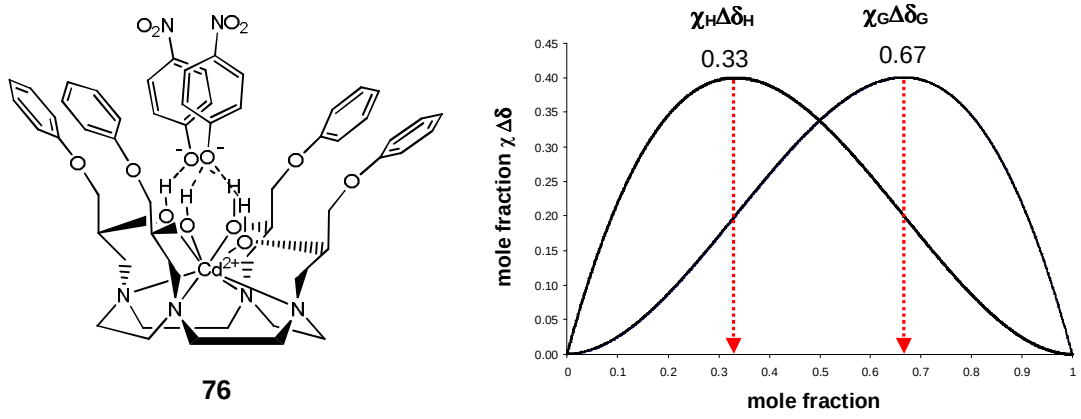

Figure 3.2 Representation of a Job's Plot produced from computer approximations of the Δδ values (**Equation 1.2** in **Appendix B**.) for 1:2 H:G stoichiometry giving the HG_2 complex ratio at χ_H = 0.33 and χ_G = 0.67. This simulation was obtained independent of *K* and only serves as an example of the expected shape for a system where two guest species are included in a host cavity.

3.2.3 Job's plots for host-guest complexes formed with [Cd(TracHP12)](ClO$_4$)$_2$, 49

Job's plots for [Cd(TracHP12)](ClO$_4$)$_2$, **49**, with various different aromatic anions *p*-nitrophenolate, *p*-nitrobenzoate, acetate, phenoxyacetate, D-histidinate and L-histidinate, were produced by maintaining, in an NMR tube, the total concentration of the two components at 12 μM in 700 μL of DMSO-d$_6$ and varying the moles of each constituent from 0 to 8.4 mmol to achieve mole fractions ranging from 0 to 1. Changes in the chemical shift of the guest resonances as the host-guest complex formed were monitored by ^{1}H NMR spectroscopy at 298 K. Each difference in the chemical shift of one particular resonance at the appropriate mole fraction was then multiplied by that mole fraction to obtain a value of $\chi_G\Delta\delta_G$ which was plotted against the mole fraction χ_G to give an inverted parabola. In all cases the maximum occurred at χ_G = 0.5. This is shown, for example, for the inclusion of phenoxyacetate in the cavity of [Cd(TracHP12)](ClO$_4$)$_2$, **49**, in **Figure 3.3** and for *p*-nitrophenolate in **Figure 3.4**.

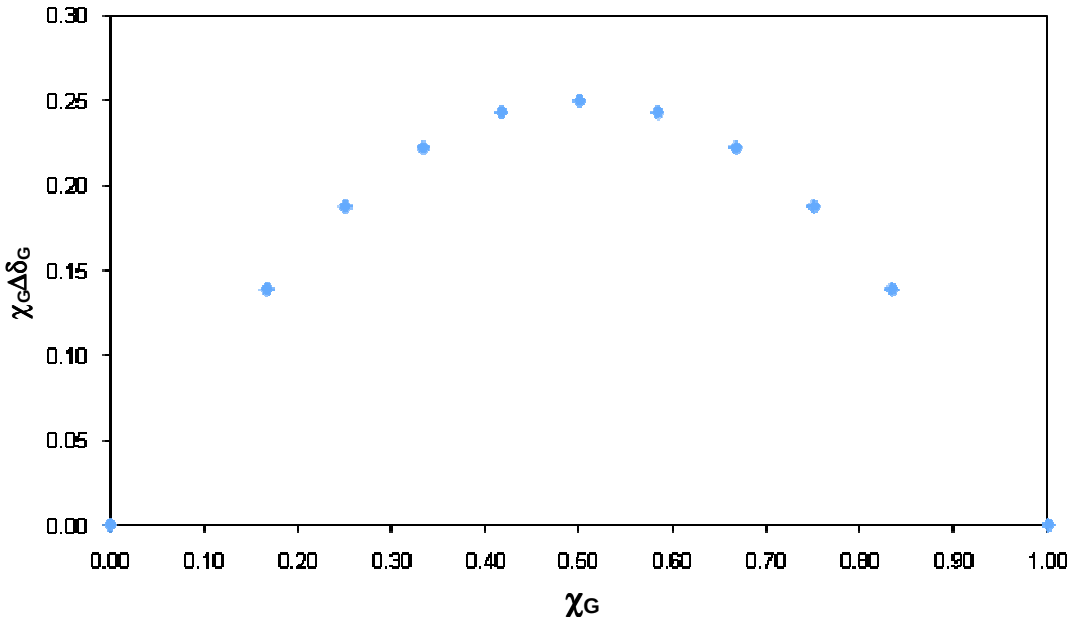

Figure 3.3 Job's Plot for phenoxyacetate inclusion in the cavity of [Cd(TracHP12)](ClO$_4$)$_2$, **49**, showing 1:1 composition.

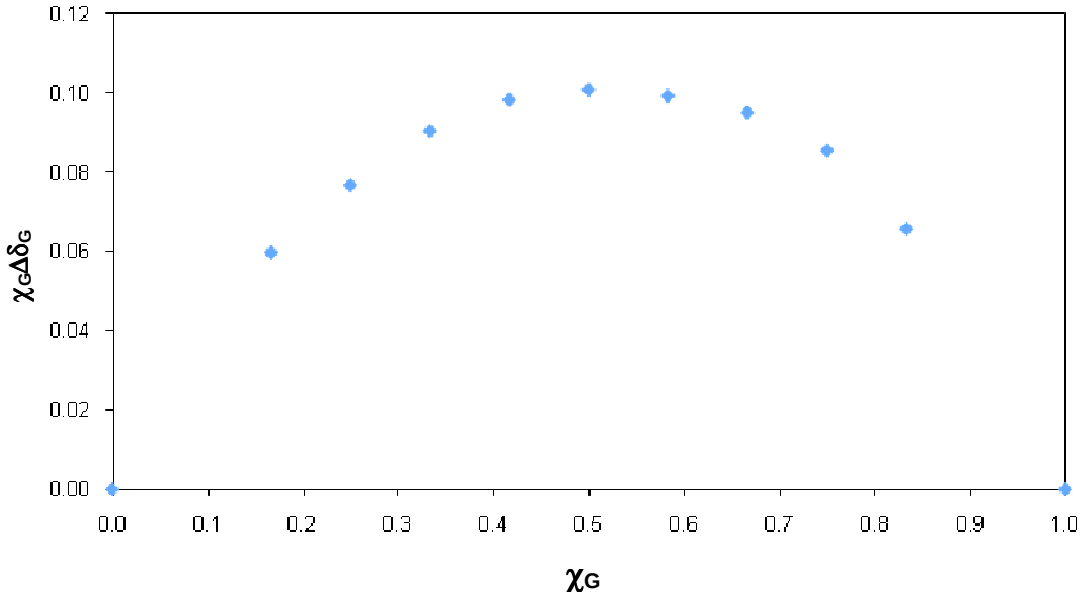

Figure 3.4 Job's Plot for *p*-nitrophenolate inclusion in the cavity of [Cd(TracHP12)]$(ClO_4)_2$, **49**, showing composition of between 1:1 and 1:2 for the complex defined by a slight asymmetry toward higher χ_G.

The barely discernible sharpening of the curve for phenoxyacetate inclusion compared to *p*-nitrophenolate inclusion suggests a higher binding constant. This was subsequently verified quantitatively, and is reported in **Section 3.2.5**.

At a glance the Job's plot for *p*-nitrophenolate appears to be symmetrical about χ_G = 0.5. However, careful inspection of the $\chi_G\Delta\delta_G$ values reveals that they are greater between χ_G = 0.5 and 1.0, compared to those between χ_G = 0 and 0.5. The appearance of this curve suggests a small contribution from a 1:2 H:G species to a solution that predominantly contains a 1:1 H:G species and is consistent with the 1:2 ratio of H:G found in the crystal structure of **76**, for which $K_2 << K_1$. No other anion of those investigated in this way showed evidence of 1:2 H:G association.

3.2.4 Strategy for obtaining guest molecule binding constant data

Prior to initiating guest binding constant determinations a selection of anionic guest species was required. These were chosen in consideration of previous guest inclusion

studies undertaken with the first generation of four armed cyclen derived receptor complexes, such as **26**. In that work the guests were mostly *p*-substituted aromatic ring molecules with C_2 symmetry, **Figure 3.5**, as their ^{1}H NMR spectra have an AA' BB' pattern of resonances whose chemical shifts are suitably removed from those of the host complex.

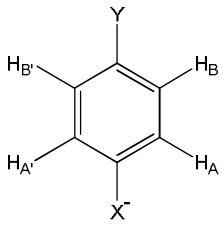

Figure 3.5 The generic structure of *p*-substituted aromatic anionic guest species containing an anionic substituent at position X with a different, non-ionic, substituent at Y.

In this work a typical pattern of chemical shift changes is seen in the inclusion of *p*-nitrophenolate into the cavity of the molecular receptor [Cd(TracHP12)](ClO$_4$)$_2$, **49**, in DMSO-d$_6$, **Figure 3.6**.

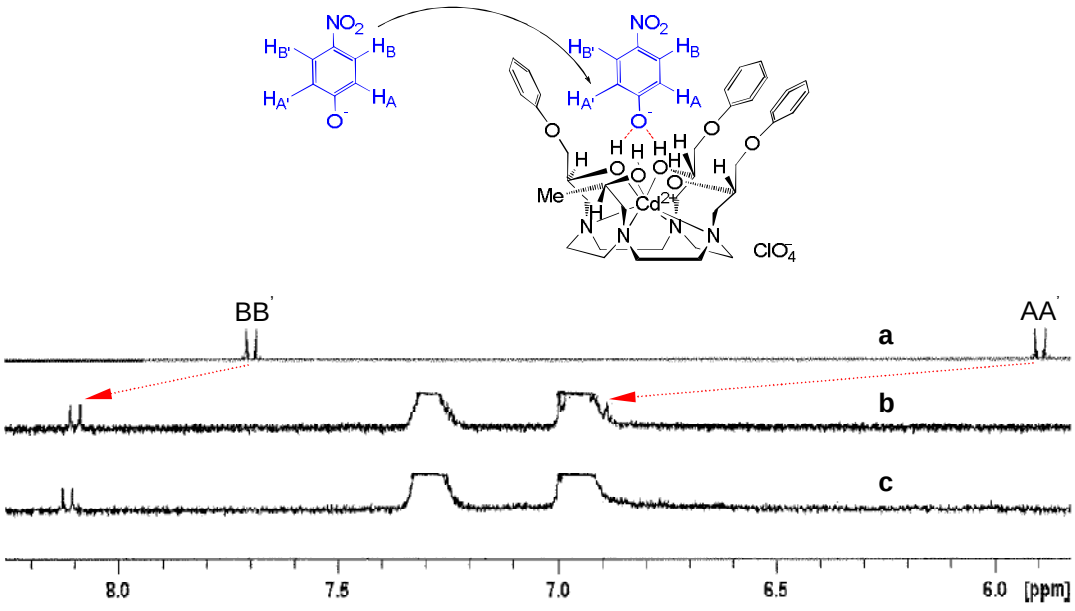

Figure 3.6 ^{1}H NMR spectra of (a), 10^{-3} mol dm^{-3} sodium *p*-nitrophenolate, (b), 10^{-3} mol dm^{-3} sodium *p*-nitrophenolate plus 5 x 10^{-3} mol dm^{-3} receptor **49**, and, (c), 10^{-3} mol dm^{-3} sodium *p*-nitrophenolate plus 10^{-2} mol dm^{-3} receptor **49**. All spectra were obtained in DMSO-d$_6$. Host resonances are truncated for clarity.

The downfield movement of the guest resonances can clearly be seen as the host complex is added. In earlier studies it was seen that the H_B protons show a smaller $\Delta\delta_{max.}$ than the H_A protons due to their increased distance from the phenolate binding site.[166, 186] This is also the case with the present system as the $\Delta\delta_{max.}$ for the H_B protons, *ca.* 0.41 ppm, is markedly less than that of the H_A protons, *ca.* 1.0 ppm.

However, the H_A proton resonances are only detectable up to a ratio of 5:1 H:G in the ^{1}H NMR spectra as they become obscured by the aromatic proton resonances of the host species beyond this point.

The changes in the chemical shift of the resonances for the H_B protons gave the titration curve shown in **Figure 3.7**, corresponding to a log*K* of 3.43 ±0.06.

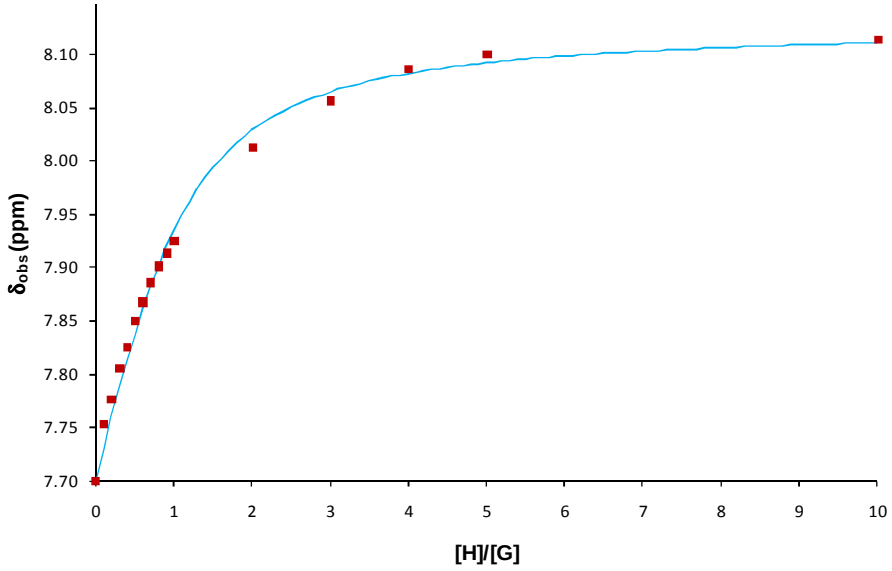

Figure 3.7 Titration curve displaying the change in chemical shift of the H_B protons of *p*-nitrophenolate with increasing ratio of [Cd(TracHP12)]$(ClO_4)_2$, **49**. The red squares represent experimental data points while the curve shows the theoretical δ values that best fit the calculated values of *K* and δ_{HG}.

A titration curve shown in **Figure 3.8** correlating with a log*K* of 3.47 ±0.04, was produced from the chemical shifts of the resonances of the H_A protons,.

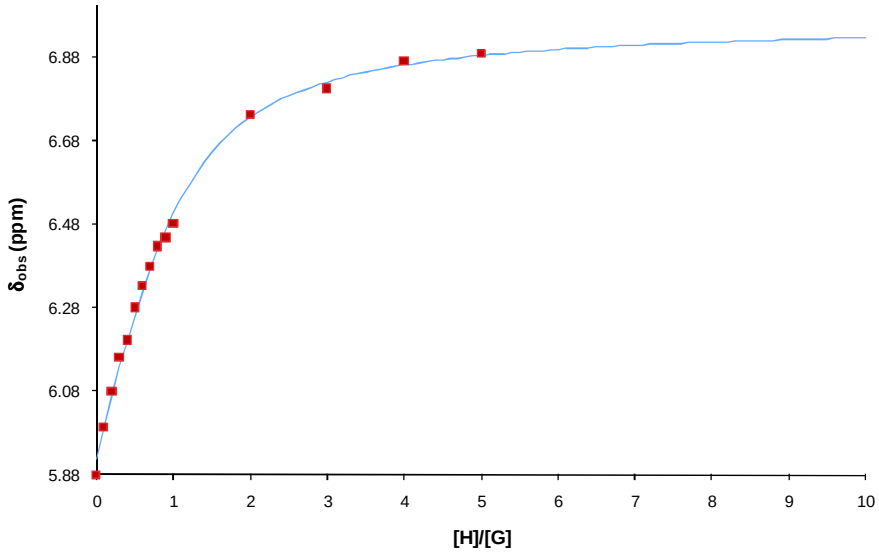

Figure 3.8 Titration curve displaying the change in chemical shift of the H_A protons of *p*-nitrophenolate with increasing ratio of [Cd(TracHP12)]$(ClO_4)_2$, **49**. The red squares represent experimental data points while the curve shows the theoretical δ values that best fit the calculated values of *K* and δ_{HG}.

The binding constant (*K*) values obtained from monitoring either the H_A or H_B doublets were of the same magnitude, allowing for experimental error, giving a mean value of log*K* = 3.45 ± 0.05 and showing the reproducibility of the method.

3.2.5 Binding constant studies of anionic aromatic guest species with [Cd(TracHP12)]$(ClO_4)_2$, 49

Binding constants for acetate, D-histidinate, L-histidinate, phenoxyacetate, and *p*-nitrobenzoate, with [Cd(TracHP12)]$(ClO_4)_2$, **49** were determined in the same way and are tabulated in **Table 3.1** alongside the values obtained for receptor **26**. Comparing the log*K* values of the host-guest complexes formed with $[Cd(TracHP12)]^{2+}$, **49**, with those formed with $[Cd((S)thphpc12]^{2+}$, **26**, it is seen that the value obtained for *p*-nitrophenolate with $[Cd(TracHP12)]^{2+}$, **49**, log*K* = 3.45 ±0.05, is smaller than the value obtained with $[Cd((S)thphpc12]^{2+}$, **26**, log*K* = 4.2 ± 0.2. This may be due to absence of the fourth aromatic moiety on the host pendant

arm framework. The relative magnitude of the other pairs of log*K* values shown in **Table 3.1** indicated a slight, but less significant, lowering of the guest binding constant upon loss of one aromatic moiety. Overall these measurements suggested that the loss of one aromatic ring through silica attachment, in the way proposed, would not be a serious impediment to anion binding.

Table 3.1 Binding constants (log*K*) for guest anion binding with Cd(II) coordinated receptor complexes, determined by ^{1}H NMR monitored titrations in DMSO-d_6 at 298 K.

	[Cd(TracHP12)]$^{2+}$, 49	**[Cd((*S*)thphpc12]$^{2+}$, 26[a]**	
Guest species	**log*K***	**log*K***	**pK_a[b]**
p-nitrophenolate	3.45 ± 0.05	4.2 ± 0.2	7.15
phenoxyacetate	4.5 ± 0.3	>4.5	3.17
p-nitrobenzoate	4.7 ± 0.3	4.5 ± 0.8	3.44
acetate	*c*	3.3 ± 0.2	4.76
D-histidinate[d]	3.37 ± 0.04	4.2 ± 0.2	1.82, 6.02[e], 9.17[f]
L-histidinate[d]	3.54 ± 0.09	4.2 ± 0.4	1.82, 6.0c[e], 9.17[f]

[a]Previous study conducted by Smith.[93, 94] [b]Data for the protonated species in H_2O acquired from NIST database.[200] [c]No chemical shift change. [d]Guest stock solution: 10% (v/v) D_2O in DMSO-d_6 conducted at 313 K [e]imidazole [f]NH_2.

3.2.6 ^{1}H NMR monitored titrations of amino acid anions with receptor [Cd(TracHP12)](ClO$_4$)$_2$, 49

The host-guest binding constants for both D- and L- histidinate with **49** were measured to ascertain whether or not the host would exhibit any level of enantioselectivity. The choice of D- and L-histidinate was derived from spectral studies of histidine indicating that at least the H_A proton (**Figure 3.9**) would be visible throughout the full range of the titration.[186] Thus, the H_A proton, which has its resonance furthest downfield, was used to derive the desired binding constants.

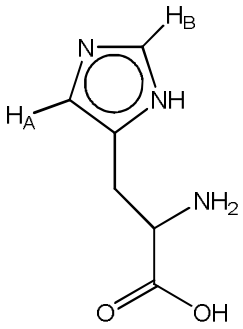

Figure 3.9 The structure of histidine showing the H_A and H_B protons the former of which was monitored in the ^1H NMR titration experiments.

The chemical shifts for the H_A proton resonances of the two enantiomers, when bound to the host were marginally different, with that of the L- enantiomer slightly further downfield than that of the D- enantiomer, **Figure 3.10**.

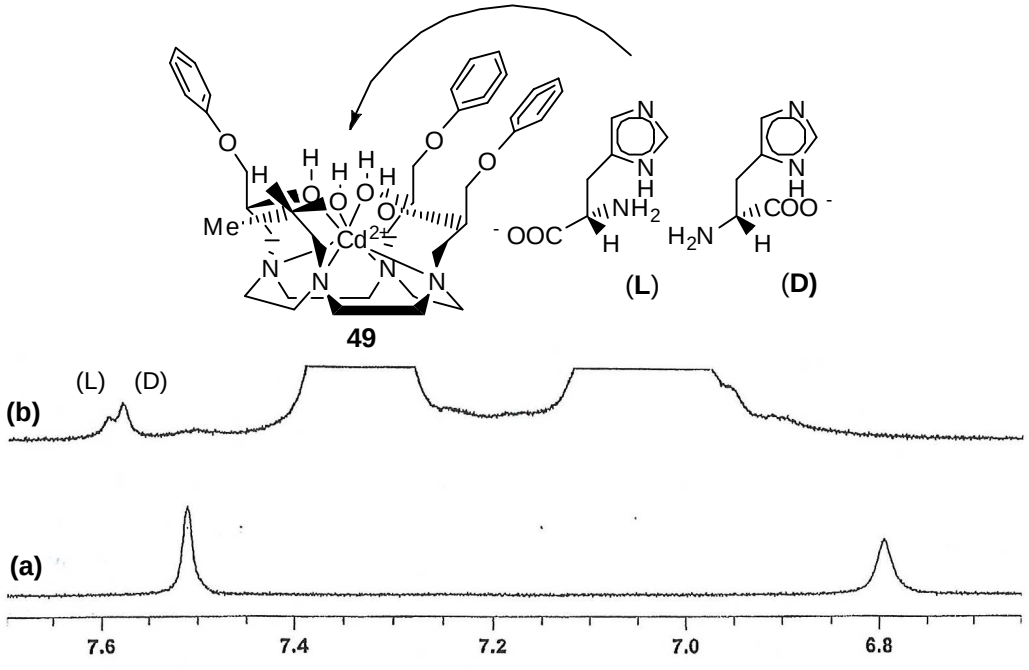

Figure 3.10 ^1H NMR spectra of (a) DL-sodium histidinate, **83**, and (b) 10:1 ratio of **49**:sodium DL-histidinate.

These chemical shift assignments were made using the chemical shift data obtained from the ^1H NMR monitored titration experiments of each enantiomer separately.

This phenomenon correlates well with the chemical shifts obtained with receptor **26**.[186] A difference from the studies of the complexation of both these histidinates with receptor **26**, is that with the latter the log*K* values for both complexes are of equal magnitude, log*K* (4.2 ± 0.2), whereas the log*K* values obtained for the complexes with receptor **49**, differ marginally, D-histidinate, log*K* (3.54 ± 0.09) and L-histidinate, log*K* (3.37 ± 0.04) . This indicates slight thermodynamic selectivity toward the D-enantiomer with receptor **49**. It is noteworthy that the H_A resonance for L-histidinate is broader than the one for D-histidinate showing that the less tightly bound guest is also more labile.

3.2.7 ^{1}H NMR titrations with hydroxy substituted benzoates

To ascertain whether hydroxy substitution on the aromatic rings of the guest species would affect the inclusion capabilities of [Cd(TracHP12)]$(ClO_4)_2$, **49**, a small group of hydroxy substituted benzoate guests was also studied. It is known that the formation of hydrogen bonds between the hydroxy hydrogen atoms of the host pendant-arms and the carboxylic oxygen atoms of the guest is the primary mode of binding experienced in these host-guest complexes. Therefore, this study was conducted to determine whether non-classical hydrogen bonding interactions between the guest hydroxy groups and the pendant arm aromatic moieties might be a factor in determining the magnitude of the binding strength of the guest molecule. This would be of interest since, a trend that showed binding constants with *o*-hydroxybenzoate > *m*-hydroxybenzoate > *p*-hydroxybenzoate was observed in related work by the Wainwright group using receptor **29** (page 98) in 20% aqueous dioxane.

A generic structure representing the sodium salt of a hydroxy substituted benzoate guest species is shown in **Figure 3.11**.

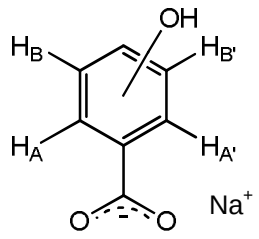

Figure 3.11 Generic structure depicting the sodium salt of a typical hydroxybenzoate guest species. H_A and H_B protons are shown for when the hydroxy group is in the *para* position.

This set of ^{1}H NMR titration experiments was conducted in DMSO-d_6 by a methodology identical to that specified in the preceding binding constant study. The ^{1}H NMR monitored titration experiments were run at a constant guest concentration of 10^{-3} M for benzoate, *p*-hydroxybenzoate, *o*-hydroxybenzoate, and 2,6-dihydroxybenzoate. This concentration was increased to 1.7 x 10^{-3} for *m*-hydroxybenzoate due to difficulty in monitoring the chemical shifts of the resonances for this guest species. Benzoate and all the hydroxybenzoate based guest species exhibited chemical shifts, $\Delta\delta_{max.,}$ of between 0.1 and 0.2 ppm and in all, excluding *p*-hydroxybenzoate, where the H_B protons were followed, the chemical shift monitored was from the resonance of the proton *para* to the carboxylate group. The chemical shifts for the resonance of this proton were always well removed from the host resonances.

Each transference of the hydroxy group from *para* to *ortho* was expected to bring the hydroxy group into a more favourable proximity and angular alignment for non-classical hydrogen bonding to the π-electron systems of the aromatic groups of the host pendant-arms. This is depicted in **Figure 3.12**. It is well known that the strength of hydrogen bonds is distance and angle dependent.[201] From the depiction of the host-guest complexes represented in **Figure 3.12**, which is based on X-ray determined structures, such as that in **Figure 1.10**, it is obvious that the potential for

non-classical hydrogen bonding is geometrically possible in **78** and **79**, but not in **77**.

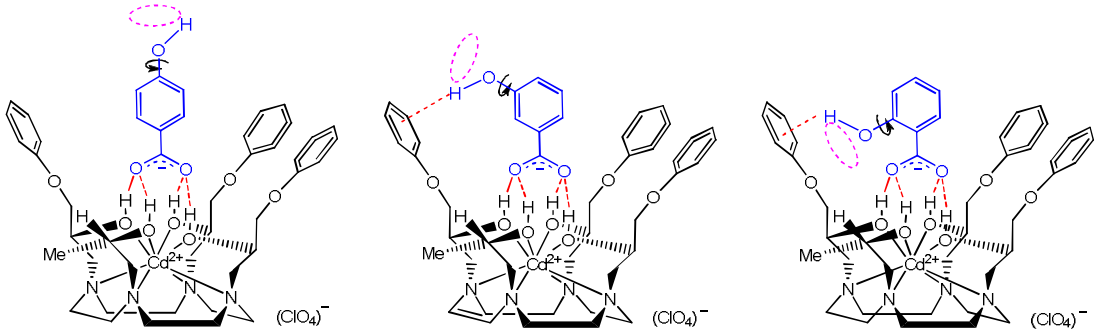

77 **78** **79**

Figure 3.12 Schematic representation of three hydroxybenzoate host-guest complexes showing the range of potential hydrogen bonding interactions between the hydroxy hydrogen atom of the guest and an aromatic group of receptor **49** The ellipse shows the path circumscribed by precession of the hydroxy hydrogen atom around the O-Ar bond.

Ab initio methods were used to model this phenomenon by Professor Sadegh Salehzadeh of Bu-Ali-Sina University with an *o*-hydroxybenzoate guest included in the cavity of receptor **29**.[129] The structure obtained displayed the potential for a hydroxy group in the *ortho* position to participate in hydrogen bonding with an aromatic group from the host pendant-arms.[129] This series of guests was also to be used for inclusion studies with the silica immobilised receptor **94** in aqueous conditions and this will be discussed in Chapter 6.

Prior to subjecting the hydroxybenzoate guests to ^{1}H NMR monitored titration in a search for enhanced binding strength attributable to non-classical hydrogen bonding a reference guest anion was needed. Sodium benzoate, shown in **Figure 3.13**, was chosen for this purpose.

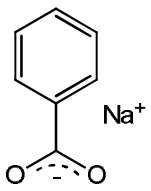

Figure 3.13 Structure of sodium benzoate.

An example of the titration curves obtained from the ^{1}H NMR monitored titration experiments with hydroxy substituted benzoate guest species is shown in titration curves A and B, for *o*-hydroxybenzoate and *p*-hydroxybenzoate, respectively, in **Figure 3.14**.

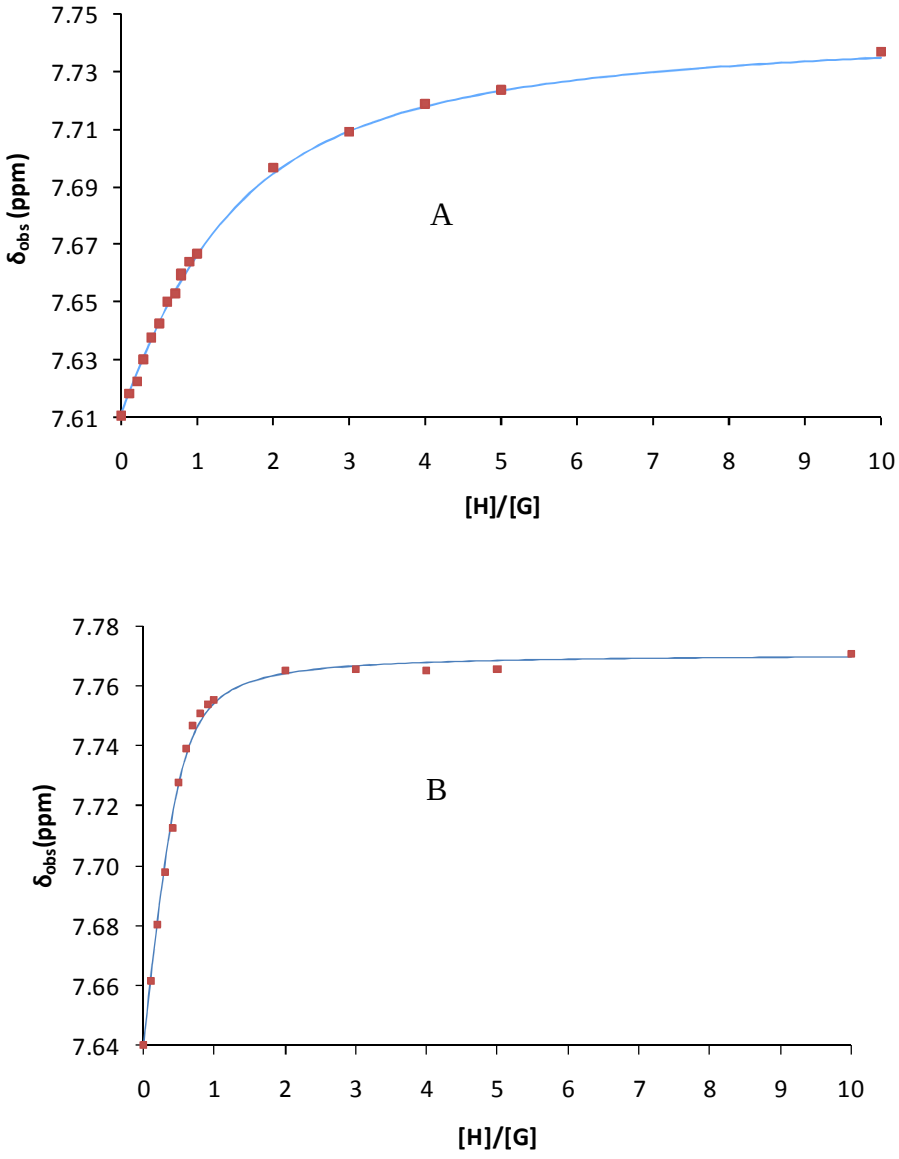

Figure 3.14 Examples of titration curves displaying, A, the change in chemical shift of the *para* proton of *o*-hydroxybenzoate and, B the H_B protons of *p*-hydroxybenzoate. Both titration curves were obtained at a constant guest concentration of 10^{-3} M, with increasing ratio (0-10 equivalents) of $[Cd(TracHP12)](ClO_4)_2$, **49**, in DMSO-d_6, The curves show the theoretical δ values that best fit the calculated values of *K* and δ_{HG}. The red square points show the experimentally obtained chemical shift values.

The full set of log*K* values obtained from inclusion studies with hydroxybenzoate guests and [Cd(TracHP12)]$(ClO_4)_2$, **49**, is shown in **Table 3.2**.

Table 3.2 Binding constants (log*K*) for guest anion binding of hydroxy substituted benzoates with [Cd(TracHP12)]$(ClO_4)_2$, **49**, determined by ^{1}H NMR monitored titrations in DMSO-d_6 with additional binding constants for benzoate and 2,6-dihydroxybenzoate determined in CD_3OD. Both sets of log*K* values were obtained at 298 K.

	[Cd(TracHP12)]$^{2+}$, 49		
Guest species	**logK^a**	**logK^b**	**p$K_a{}^c$**
benzoate[d]	4.11 ± 0.06	3.96 ± 0.09	4.19
p-hydroxybenzoate	4.09 ± 0.07	*e*	4.54
m-hydroxybenzoate	4.16 ± 0.09	*e*	4.30
o-hydroxybenzoate	3.08 ± 0.08	3.23 ± 0.03	2.97
2,6-dihydroxybenzoate	2.05 ± 0.03	*e*	1.05

[a]Acquired in DMSO-d_6 [b]Acquired in CD_3OD [c]Values obtained in H_2O from PHYSPROP database for their respective conjugate acids.[202] [d]Guest stock solution 10% (v/v) D_2O in DMSO-d_6. [e]Not attempted.

It is evident from the values that the trend of log*K* in which *o*-hydroxybenzoate > *m*-hydroxybenzoate > *p*-hydroxybenzoate is not seen here. Instead there is a clear relationship between the log*K* values and the basicity of the guest species whereby the more basic the guest species (indicated by higher pK_a) the higher the binding constant.

It is interesting to note that *o*-hydroxybenzoate and 2,6-dihydroxybenzoate both have significantly lower pK_as and log*K*s. This is explained by the fact that both species can engage in intramolecular hydrogen bonding not accessible to the *m*- and *p*-isomers. This internal hydrogen bonding is shown in **Figure 3.15**.

One consequence of this intramolecular hydrogen bonding is a lowering of the pK_a due to delocalisation of the negative charge on the carboxylate.[203, 204]

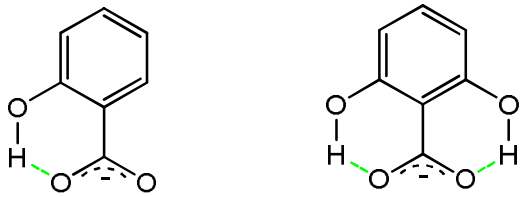

Figure 3.15 Representation of the intramolecular hydrogen bonded structures of *o*-hydroxybenzoate and 2,6-dihydroxybenzoate.

A second consequence is a weakening of the hydrogen bond acceptor capability of the carboxylate. For this reason the host-guest binding constants become appreciably lower in magnitude with *o*-hydroxybenzoate < *m*-hydroxybenzoate < *p*-hydroxybenzoate.

It appears from this study that binding strength with these types of guests may be dependent on the solvent in which guest inclusion occurs. Previous studies with receptor **29** were performed in 20% aqueous dioxane whereas this study with receptor **49** utilised DMSO-d_6 or CD_3OD as the solvent. Indications are that the hydrogen bond donor/acceptor abilities of the solvent have a significant bearing on the magnitude of the binding constants obtained. Further investigations of this and the turnaround in the present trend can be found in Chapter 6 where the silica bound host is used under aqueous conditions.

The data obtained from ^{1}H NMR monitored titration experiments with, $[Cd(TracHP12)](ClO_4)_2$, **49**, and a number of different anionic guest species demonstrate the suitability of a three-walled cavity for guest inclusion. From these results it can also be said that removal of one of the aromatic groups does not affect, to a great degree, the behaviour and efficacy of the binding cavity. Binding constants for inclusion of some of the guest species were lower, but not significantly reduced

such that they would indicate preclusion of molecular receptor precursor **46** and its derivatives **47** and **48** from acting as reasonable host species upon immobilisation on a silica surface.

CHAPTER FOUR

MODIFICATION OF THE SILICA SURFACE

CHAPTER 4 MODIFICATION OF THE SILICA SURFACE

4.1 Strategy for anchorage of tri-alkylated macrocycles to a solid inorganic support

The development of composite materials consisting of covalently bound inorganic-organic moieties has steered its focus toward silica as an anchorage point for the reasons given in the Introduction.

In this project the solid support used for anchoring the macrocyclic receptors was mainly chromatographic silica gel, with mesh size 70 - 230 and a surface area 300 m^2g^{-1}. In an endeavour to increase the surface loading of macrocyclic receptors two alternative forms of silica were also silanised with GPTS, **32**, and grafted with the macrocyclic receptor precursor, **46**: Amorphous silica gel with a smaller mesh size of 230 - 400, and therefore a larger surface area of 550 m^2g^{-1}; and, a structurally ordered mesoporous silica with a uniformly arranged hexagonal array of cylindrical mesopores, resembling a honeycomb network, known as MCM-41, with a surface area of about 1000 m^2g^{-1}.

Immobilisation of the receptor complexes used in this work on a silica surface requires covalent attachment of a linker molecule since bonding the bulky macrocycle directly to the silica surface will cause steric hindrances in the vicinity of the surface silanols.[136] This would restrict the effectiveness of the macrocyclic receptors in metal chelation and anionic guest inclusion.[136]

4.1.1 Strategy

Since it was now known from preliminary work that the trialkylated macrocyclic ligand **46** can easily be alkylated through reaction with an epoxide the strategy to be used to attach it to silica is shown in **Figure 4.1**. The advantage of this strategy is that Si-GPS, **33**, is a known material.

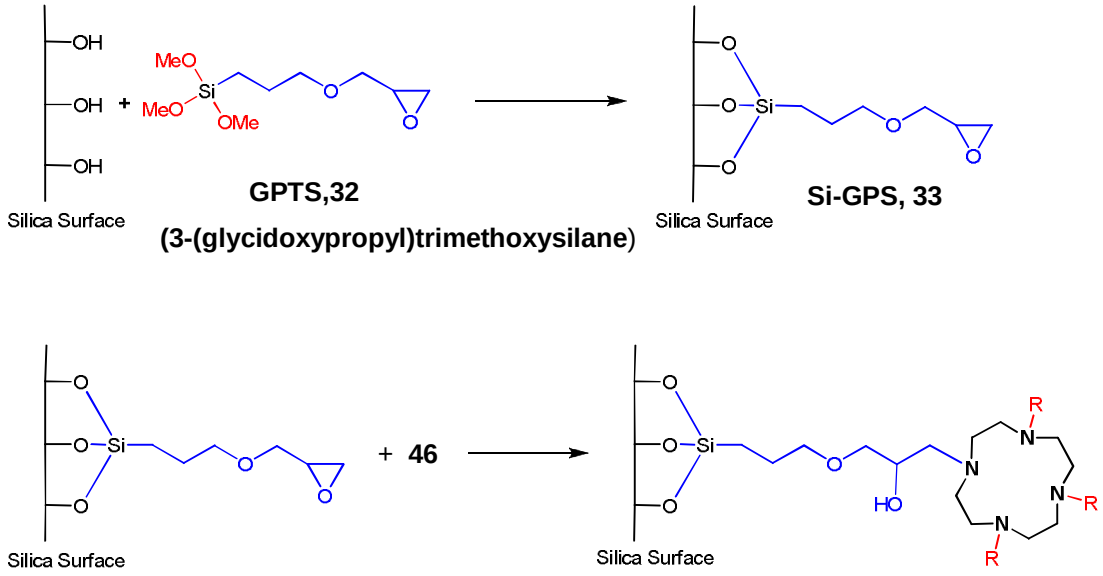

Figure 4.1 Diagram showing the strategy used for covalent attachment of a macrocyclic ligand to a silica surface via a glycidoxypropylsilane (GPS) linker.

4.1.2 Modification of the silica surface with an alkoxysilane linkage

The silanisation reaction employed to covalently bond the linker molecule onto the silica gel initiates hydrolysis of the methoxy groups followed by condensation of each with the release of a molecule of water, as shown in **Figure 4.2**.[205-207]

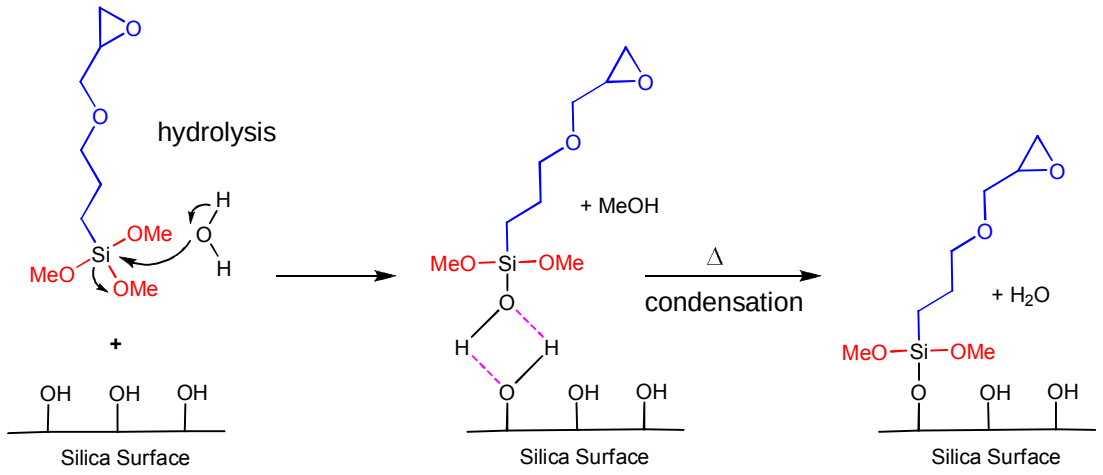

Figure 4.2 Schematic depiction of the mechanism for the silanisation reaction with 3-(gylcidoxypropyl)trimethoxysilane (GPTS, **32**) showing initial hydrolysis of the methoxy groups followed by a hydrogen bonded intermediate and condensation. Only one bond formation has been shown here for clarity.

Chemical modification of the silica surface with GPTS, **32**, was accomplished by treating dried chromatographic silica gel, 70 - 230 mesh, with an excess of racemic 3-(glycidoxypropyl)trimethoxysilane (GPTS), **32**, stirred in dry toluene at 90° C for 24 hours, **Scheme 4.1**.

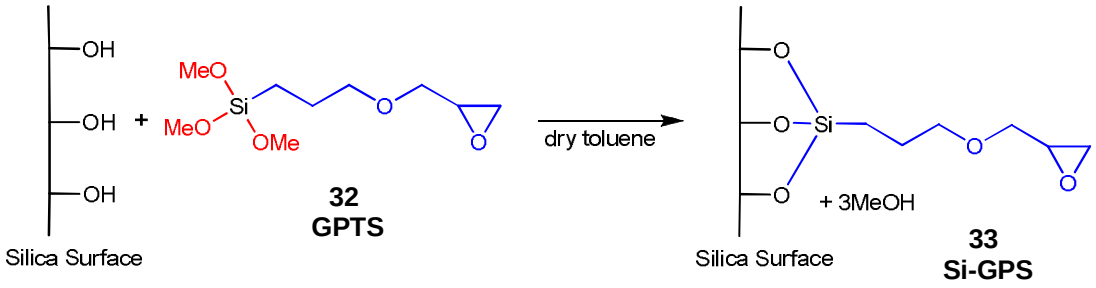

Scheme 4.1 Silanisation of silica surface with potentially cross-linking silane coupling agent, GPTS, **32**.

After filtration and washing with MeOH and toluene the silanised silica material was subjected to Soxhlet extraction in dry toluene for six hours to remove superfluous GPTS. The material was then dried *in vacuo* for two days and stored in a desiccator. The preparation of the silanised products, Si-GPS$^{230\text{-}400}$, **80**, and MCM-41-GPS, **81**, was performed in the same way.

A similar silica material Si-GPDMS, **83**, was also prepared by the previously described silanisation method for Si-GPS, **33**, **Scheme 4.2**.

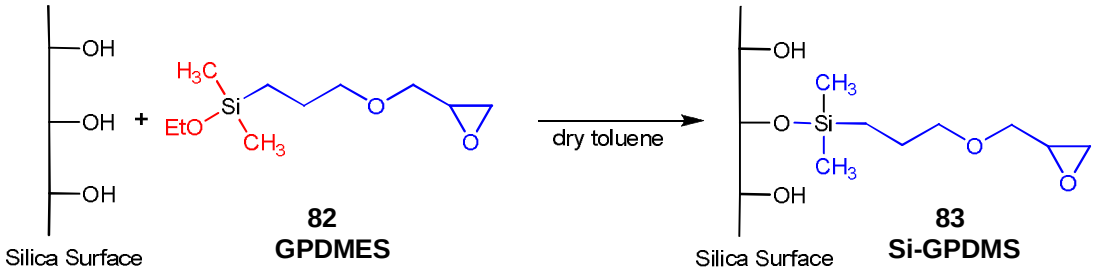

Scheme 4.2 Silanisation of silica surface with non-cross-linking silane coupling agent, GPDMES, **82**.

The alkoxysilane linker reactant GPTS, **32**, was replaced by racemic 3-

(glycidoxypropyl)dimethylethoxysilane (GPDMES), **82**, which has just a single hydrolysable group bonded to the silicon atom and, therefore, GPDMES, **82**, is unable to cross-link with itself to form a polymeric layer across the silica surface in the way shown in **Figure 4.3**.

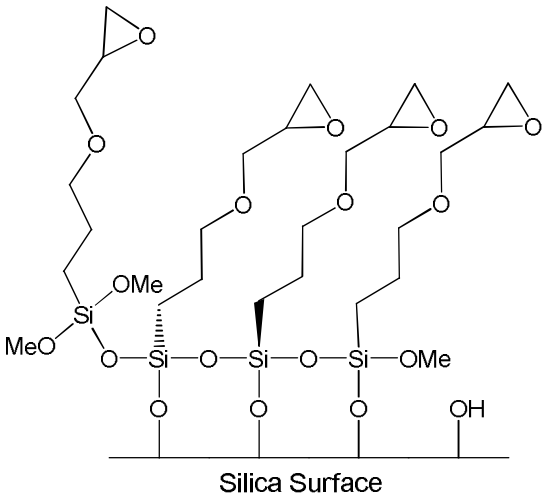

Figure 4.3 Representation of the ability of GPTS, **32**, to form oligomers and extend multidirectionally in a layer across the silica surface.

Si-GPDMS, **83**, was synthesised as it was thought that due to its inability to cross-link, silanisation of the silica surface would involve a single molecule of GPDMES, **82**, reacting with one silanol producing, in effect, a series of monolithic linker moieties randomly scattered over the silica surface, as opposed to a tegumental polymeric spread by GPTS, **32**. The difference between these two modes of binding to the silica surface is illustrated in **Figure 4.4**. It can be seen that GPTS, **32**, is able to form bonds in all directions and may even hang from GPS units already attached to the silica surface whereas GPDMES, **82**, is only able to bond to the silica surface. A comparison of the DRIFT spectra and the loading capacities for **33** and **83** would give an indication of the level and mode of coverage on the silica surface.

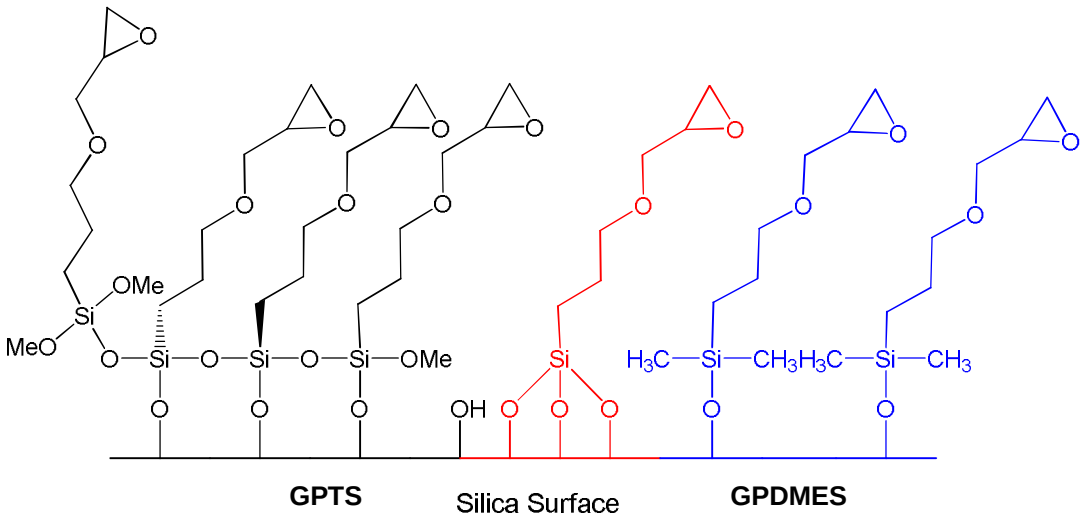

Figure 4.4 Schematic depiction of the difference in surface coverage by: GPTS, **32**, oligomeric and multidirectional (black) or monolithic (red); and, GPDMES, **82**, monolithic (blue).

4.1.3 Endcapping residual surface silanol groups

The process of functionalising the surface of silica gel does not necessarily consume all of the available surface silanol groups.[153] A proportion of these are unattainable due to accessibility restrictions originating from steric hindrances, for example, those that reside within pores in the silica gel. These residual silanol groups tend to be weakly acidic with a pK_a ~5, so there is the potential for them to undergo some cation exchange in solutions containing metal ions, **Equation 4.1**.

$$\mathrm{M}^{n+} + n(\mathrm{SiOH}) \rightleftharpoons \mathrm{M}(\mathrm{OSi}-)_n + n\mathrm{H}^+ \qquad \textbf{Equation 4.1}$$

Because of this it was considered desirable to chemically inactivate these residual silanol groups to prevent their complexation with metal ions when conducting metal uptake studies (Chapter 5) This is commonly known as endcapping.[153, 208]

The general procedure for endcapping is to silanise the silica gel surface, after derivatisation with the desired moiety, using trimethylchlorosilane (TMCS), **84**.

TMCS is a small molecule that can gain access where a larger molecule, such as GPTS, **32**, cannot.

Endcapping of the silanised silica material was effected by an adaptation of the methods used by Dudler,[153] and Silva,[209] whereby, Si-GPS, **33**, was treated with an excess of TMCS, **84**, in dry toluene and stirred under reflux for three hours with further stirring overnight at room temperature, **Scheme 4.4**.

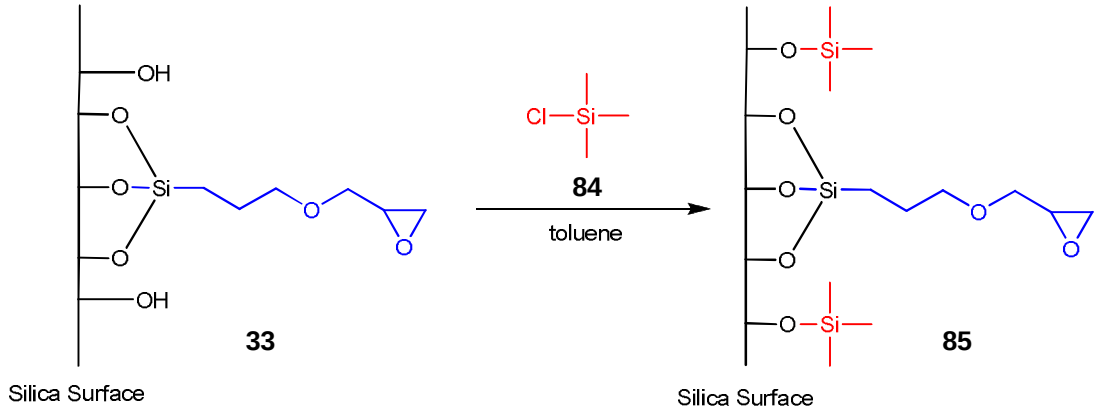

Scheme 4.4 Endcapping residual silanol groups of Si-GPS, **33**, with trimethylchlorosilane, **84**, (TMCS).

The endcapped silica material, Si-GPS-(TMS), **85**, was then filtered, washed with toluene to remove residual TMCS and water to remove the HCl produced during the reaction. This material was dried *in vacuo* and stored in a desiccator.

4.1.4 Preparation of the silica attached macrocyclic receptor ligands

The methods used for anchoring the three receptor precursor macrocycles to the silica attached linker were essentially identical with the only difference being the solvent. As the two pegylated pendant arm macrocycles **47** and **48** are not soluble in toluene the solvent was changed to acetonitrile. Loading capacity (to be discussed later) decreased when the reactions were performed in ethanol.

Synthesis of the silica attached receptor ligands proceeded by reacting the Si-

GPS, **33**, linker material with an excess of the macrocycle **46**, in dry toluene, or dry acetonitrile for **47** and **48**, for 2 days at 60° C followed by filtration and washing with toluene for **46**, or acetonitrile for **47**, and **48**, followed by Soxhlet extraction with methanol as shown in **Scheme 4.5**.

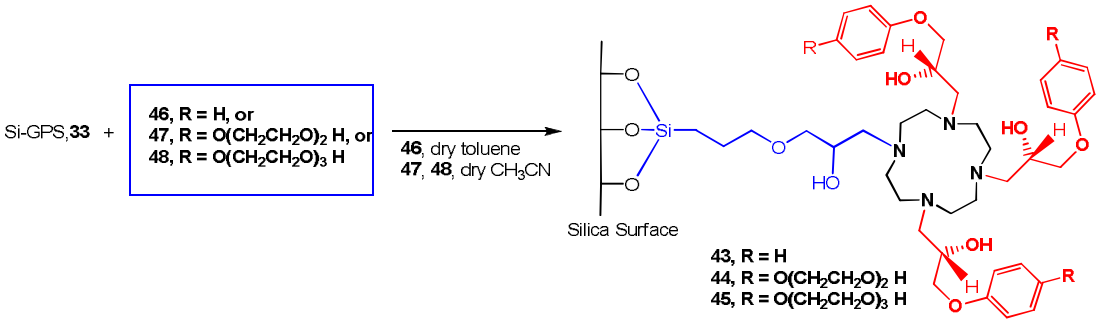

Scheme 4.5 Synthesis of the silica attached macrocyclic ligands, Si-GPS-Trac, **43**, Si-GPS-DiPTrac, **44**, and Si-GPS-TriPTrac, **45**.

The silica materials Si-GPS-Trac, **43**, Si-GPS-DiPTrac, **44**, and Si-GPS-TripPTrac, **45**, were dried *in vacuo* and kept in a desiccator. Synthesis of the immobilised macrocyclic adducts, Si-GPDMS-Trac, **86**, Si-GPS-Trac$^{230\text{-}400}$, **87**, and MCM-41-GPS-Trac, **88**, and endcapped receptor material Si-GPS-Trac(EC), **89**, followed procedures identical with those used for the preparation of Si-GPS-Trac, **43**. The synthesis of the endcapped material is depicted in **Scheme 4.6**.

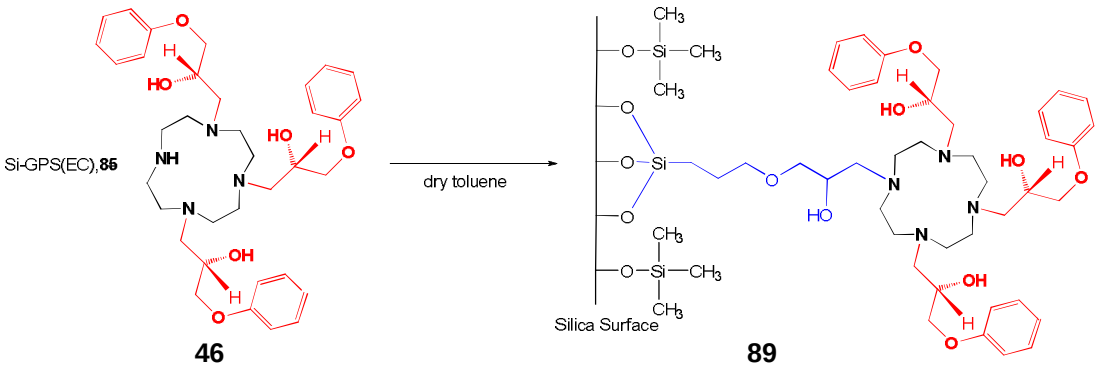

Figure 4.6 Synthesis of the endcapped silica immobilised macrocyclic receptor ligand, **89**.

4.2 Characterisation of modified silica materials

4.2.1 Techniques used for characterisation of silica materials

Characterisation of the silica based materials was performed by established literature methods utilising ^{13}C Cross Polarisation Magic Angle Spinning Nuclear Magnetic Resonance (^{13}C CPMAS NMR) and Diffuse Reflectance Infrared Fourier Transform (DRIFT) infrared spectroscopy.[207, 209, 210]

Loading capacities for all the prepared silica materials were determined by microanalytical calculation of the carbon content for the linker materials; and both the carbon and nitrogen content for silica immobilised macrocyclic materials.[153, 211] Thermal decomposition of the materials at 800^{o} C was also employed to establish the extent of functionalisation on the silica surface.[212]

4.2.2 Diffuse Reflectance Infrared Fourier Transform spectroscopy

Diffuse Reflectance Infrared Fourier Transform (DRIFT) is an effective spectroscopic technique for qualitative analysis of surface species on solid materials for which normal infrared spectra may be difficult to acquire.[213-215] For this reason, DRIFT spectroscopy was used as a qualitative tool to assess the changes to the surface of dried silica gel as stepwise modifications were chemically imparted. These spectral frequency changes are manifest in the DRIFT spectral traces displayed in, **Figure 4.5**, demonstrating the transition from pure silica gel, through attachment of the GPS linker, to attachment of a macrocyclic species to the linker.

The expected absorption frequencies for the dried silica gel, Trace A, are visible with an additional band at 3739 cm^{-1} for the $\nu_{(OH)}$ frequency of isolated silanol groups freed of hydrogen bonding by the removal of physisorbed water from the surface by thermal pre-treatment.[216-219]

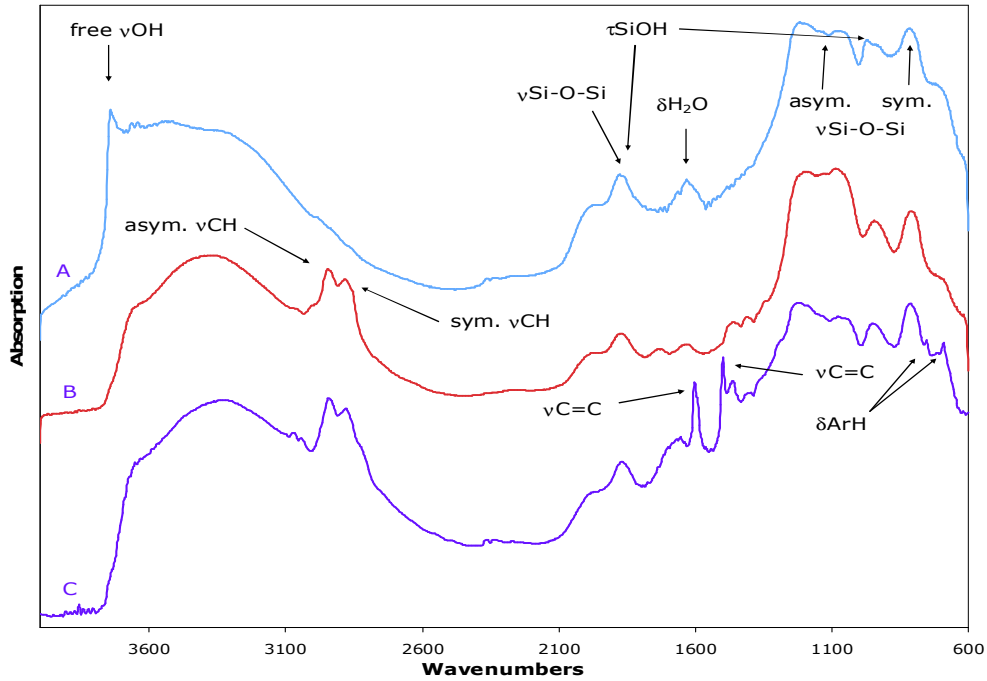

Figure 4.5 DRIFT spectra showing the progressive modification of a silica surface. A, Dried silica gel; B, after silanisation with linker species, GPTS, **32**; C, after covalently bonding Trac, **46** to the linker.

Following chemical treatment with GPTS, **32**, Trace B confirms that modification of the silica surface has occurred as evidenced by the significant decrease in the intensity of the band at 3739 cm^{-1} and the appearance of two bands for asymmetric and symmetric $\nu_{(C-H)}$ from the $Si(CH_2)_3$ carbon chain of GPS at 2944 cm^{-1} and 2879 cm^{-1}, respectively.[216, 220] An increase in the intensity of the asymmetric and symmetric frequencies for the siloxane $\nu_{(Si-O-Si)}$ between 1072 and 1192 cm^{-1} suggests that the GPS linker has formed a multi-directional polymeric network across the silica surface with intermittent attachment to the surface rather than a large number of monolithic, three bond, siloxane-bonded, monomeric alkoxysilane entities as stylised in **Figure 4.4**.[207, 219, 221] Further evidence for this phenomenon comes from the DRIFT spectra shown in **Figure 4.6**, for Si-GPDMS, **83**. In trace A, for Si-GPDMS, **83**, the asymmetric $\nu_{(Si-O-Si)}$ band at 1089 cm^{-1} shows a single broad band, which broadens into two bands at 1169 and 1057 cm^{-1}, in trace B,

for Si-GPS, **33**. The symmetric $\nu_{(Si\text{-}O\text{-}Si)}$ band at 950 cm^{-1} (Trace A) becomes more prominent, at 935 cm^{-1}, for Si-GPS, **33**, in Trace B.[219, 221-223]

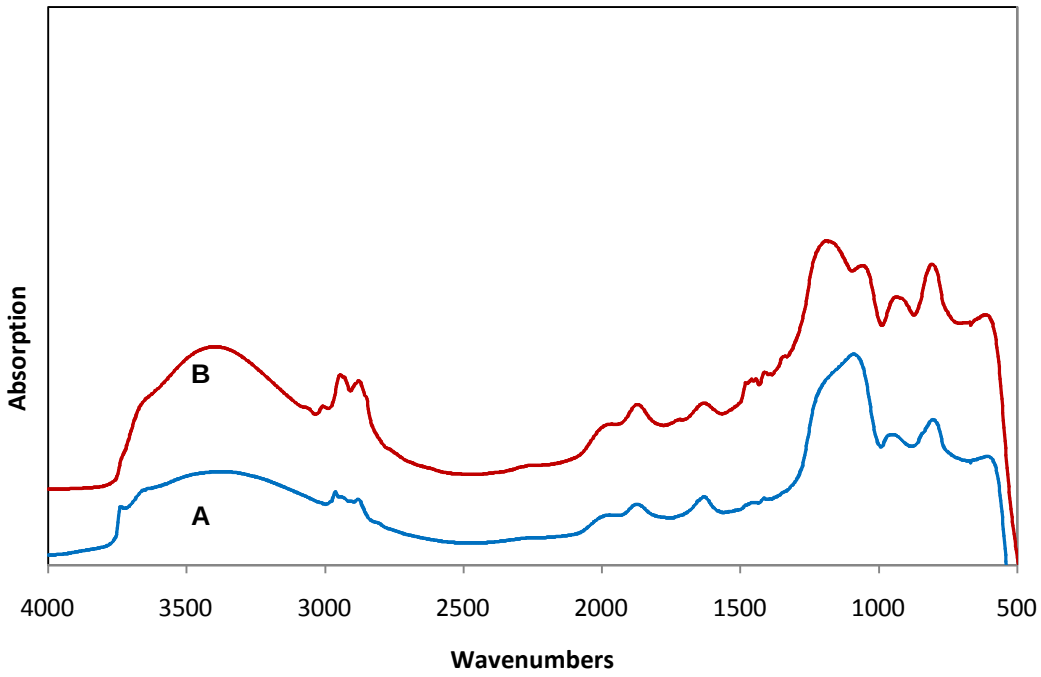

Figure 4.6 DRIFT spectra of A, Si-GPDMS, **83**, and B, Si-GPS, **33**.

The DRIFT spectrum for Si-GPS-Trac, **43,** Trace C in **Figure 4.5**, indicates the presence of the macrocycle with bands at 752 cm^{-1} and 690 cm^{-1}, which are the Ar-H out-of-plane bending frequencies and two bands at frequencies of 1602 cm^{-1} and 1497 cm^{-1} for $\nu_{(C=C)}$ in the pendant aromatic groups of the immobilised macrocycle.

The DRIFT spectra for the silica-based MCM-41 and 230 - 400 mesh silica materials are basically identical to the spectra for the 70 - 230 mesh silica materials. An obvious difference, however, is in the band at 3745 cm^{-1} for dried MCM-41, **Figure 4.7**, which is of notably higher intensity and decidedly sharper, indicating a greater density of silanol moieties on its surface. This increase suggests that the thermal preparation of MCM-41 *i.e.*, calcination at 550° C, has, in addition to freeing the surface of physisorbed water, eliminated chemisorbed water hydrogen bonded to

the surface silanol groups.[224, 225]

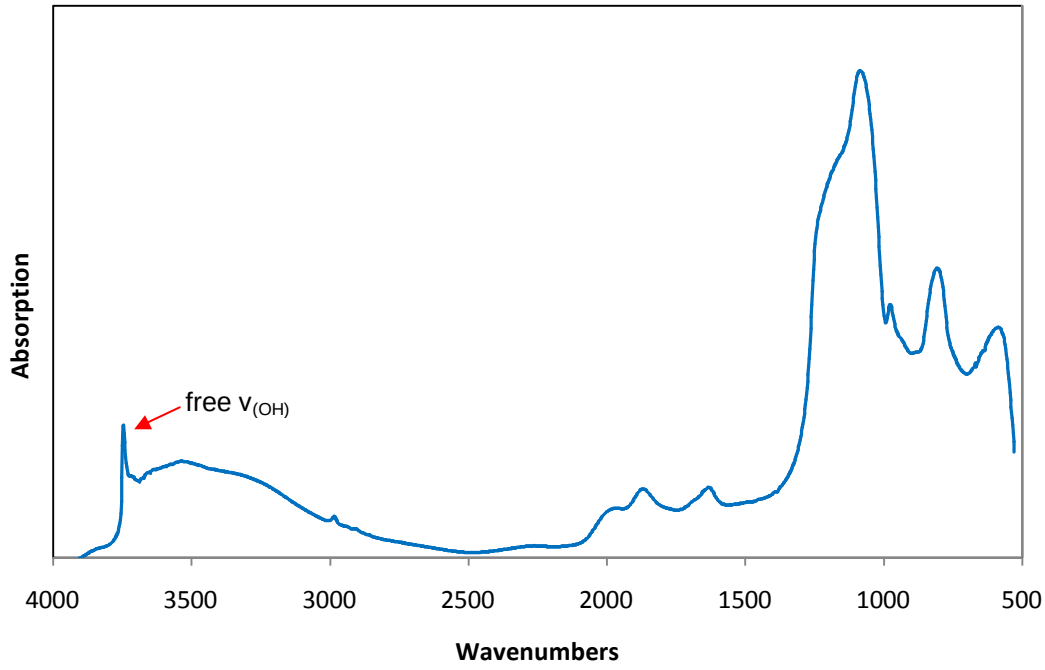

Figure 4.7 DRIFT spectrum of silica-based material MCM-41.

DRIFT spectra for both the silica immobilised, pegylated, molecular receptor ligands Si-GPS-DiPTrac, **44** (**Figure 4.8**), and Si-GPS-TriPTrac, **45**, exhibit two bands at 2981 cm^{-1} and 2889 cm^{-1} These bands are in the region associated with asymmetric and symmetric $\nu_{(C\text{-}H)}$ and can be ascribed to the methylene groups of the organolinker moiety, the pendant arm and the dendritic glycol ether. Other than this slight increase there doesn't appear to be a great deal of difference between the spectra for the materials with pegylated macrocycles and the material with the non-pegylated macrocycle. However, it can be accepted that owing to the appearance of $\nu_{(C=C)}$ bands for the macrocycle, which has broadened and lessened in intensity at 1600 cm^{-1} and increased considerably in intensity at 1509 and 1459 cm^{-1} that these silica materials do in fact contain receptor ligands comprising dendritic ethereal chains appended to the aromatic rings of the pendant arms. The out-of-plane Ar-H

bands for *para* substituted aromatic rings expected between 860 and 800 cm^{-1} are not adequately resolved due to masking by the broad symmetric $\nu_{(Si\text{-}O\text{-}Si)}$ band at ~850 - 750 cm^{-1}.

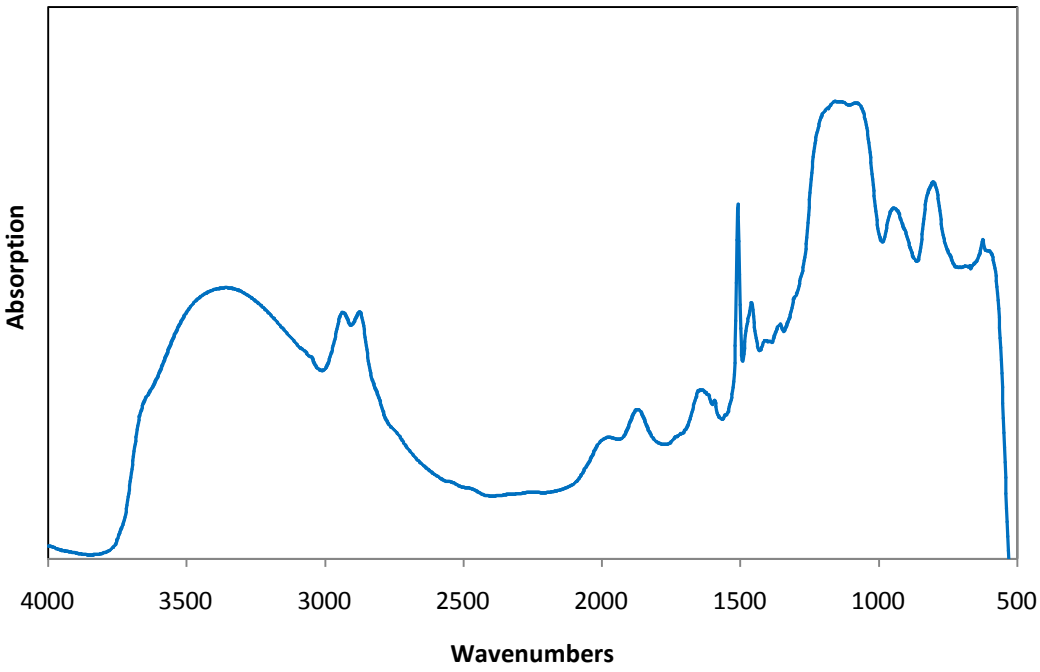

Figure 4.8 DRIFT spectrum of Si-GPS-DiPTrac, **44**.

4.2.3 Solid State Nuclear Magnetic Resonance

The obvious difficulty in attempting to characterise the silica attached adducts with solution based NMR techniques was circumvented by utilising solid state NMR methodology. Initially ^{13}C spectra were obtained with Cross polarisation and Magic Angle Spinning for Si-GPS, **33**, and Si-GPS-Trac, **43**, to ascertain whether the desired synthetic objective was realised, **Figure 4.9**.

Spectrum A for Si-GPS, **33**, correlates suitably with literature values for GPTS, **32**, and similar organolinker modified silica gel.[219] It is clearly evident from the chemical shifts exhibited in the spectrum for, Si-GPS, **33**, that the linker species is present and by inference, attached to the silica surface. In addition to the linker

resonances, the spectrum for Si-GPS-Trac, **43**, shows four resonances for the carbon atoms of the aromatic groups of the immobilised macrocyclic receptor at 159.7, 129.4, 120.1 and 114.8 ppm and enhanced intensity in the aliphatic region between 50 and 70 ppm where the methylene and methine carbon atom resonances are known to arise in solution spectra of the model receptor ligand, **51**.

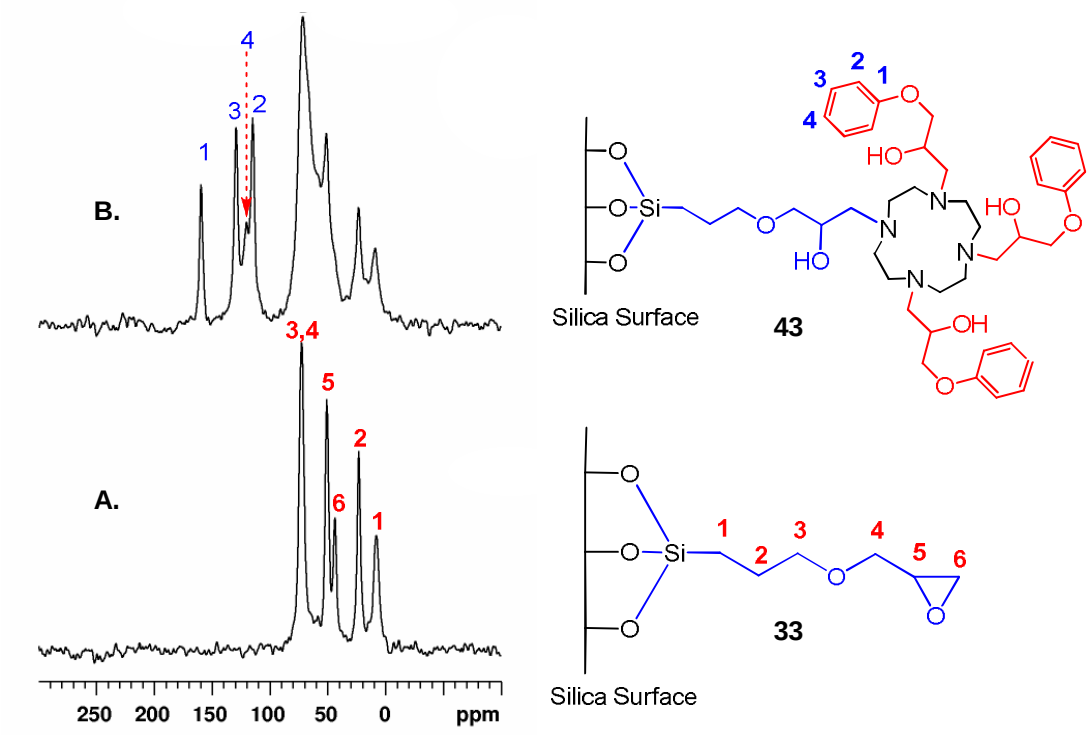

Figure 4.9 Solid State, ^{13}C CPMAS NMR, spectra for, A, Si-GPS, **33**; and, B, Si-GPS-Trac, **43**.

4.2.4 Loading level: Microanalysis and Thermal Combustion of the materials

The primary technique used to obtain the loading of either the linker or the macrocyclic receptor ligands on the silica was microanalysis to obtain the percentage carbon or nitrogen content of the material. Thermal decomposition was also used with some of the silica-based materials to verify the microanalytical results. Microanalysis of the dried silica materials, SiO_2 and MCM-41 showed some residual carbon, which was taken into account when calculating the loading for the various

materials in mmol of the attached species per gram of material. Thermal studies also revealed that the materials contained 4% physisorbed water, which was also taken into account when processing the data from thermal combustion experiments.

4.2.5 Loading level: Linker materials

Comparison of the loading level of the two linker species Si-GPS, **33**, and, Si-GPDMS, **83**, illustrates the correlation between the loading capacity and the difference in the mode of attachment of each of the parent linker compounds, GPTS, **32**, and GPDMES, **82**. It is assumed that the number of silanol centres available to each of these species is similar; therefore, if the potential for polymerisation is excluded, it could be argued that as the GPTS, **32**, species has three groups able to react with the silica surface, its coverage would be one third that of GPDMES, **83**, which has only one group able to link with the silica surface. However, this outcome, is not evident from the microanalytical data. In fact Si-GPS, **33**, exhibits a surface coverage approximately three times more than Si-GPDMS, **83**, **Table 4.1**. This result must be due to the tendency of GPTS, **32**, to form a polymeric layer on the silica as shown in **Figure 4.4**.

Surface loading of GPS decreases slightly on the smaller mesh 230 - 400 silica gel, $Si^{230\text{-}400}$-GPS, **80**, due to inconsistency with respect to the distribution and character of the surface silanol groups. Most of the increase in surface area of the 230 - 400 mesh compared to 70 - 230 mesh silica gel is accommodated within the pores. The surface coverage of linker molecules polymerised across the surface cannot access the silanol groups in the pores. Thus, the GPTS, **32**, molecule may be too large to take advantage of the higher surface area of the 230 - 400 mesh because it cannot react with the internal surface silanol groups. However, the coverage of GPS linker groups on the MCM-41 material, MCM-41-GPS, **81**, shows a marked

increase in surface coverage from the other forms of silica-based materials used. This is indicative of the significant increase in the isolated silanol population as observed in the DRIFT spectra, for this material, shown in **Figure 4.7**.

Table 4.1 Comparison of the loading of the linker species, GPTS, **32**, on various forms of silica with the non-cross-linking species GPDMES, **83**. Also showing residual carbon present in the dried silica materials, SiO_2 and MCM-41.

Si-Material	Microanalysis %[a]		Loading		
	C	H	Micro[b] mmol g^{-1}	Thermal[b] wt %[b]	Thermal[b] mmol g^{-1}
$SiO_2^{70\text{-}230}$	0.25	0.92	--	--	--
$SiO_2^{230\text{-}400}$	0.20	1.30	--	--	--
MCM-41	0.01	1.33	--	--	--
$Si^{70\text{-}230}$-GPS, **33**	7.64	1.43	1.10	11.98	1.04
Si-GPDMS, **83**	3.39	2.26	0.35	5.25	0.42
$Si^{230\text{-}400}$-GPS, **80**	6.34	1.36	0.88	*c*	*c*
MCM-41-GPS, **81**	12.23	2.17	1.70	*c*	*c*

[a]Error = ± 0.3%; [b]Error = ± 10%; [c]Not attempted.

4.2.6 Loading level: Macrocyclic receptor ligand materials

Loading levels for the immobilised macrocycles are limited by the level of coverage of the linker molecules. Some linker molecules could be situated within the pores of the silica, whereas, others could reside beneath an oligomeric layer and consequently be inaccessible to the macrocycle. The significance in the linker's mode of coverage becomes apparent in the degree of grafting of the macrocycle to the silica attached linker achieved, since covalent attachment can only occur to linker molecules that are available for reaction.

The loading capacities for the macrocycle immobilised on amorphous silica materials, Si^{70-230}-GPS-Trac, **43**, and $Si^{230-400}$-GPS-Trac, **87**, as calculated from the carbon and nitrogen content obtained from microanalysis data indicate that within experimental error they are of similar magnitude, **Table 4.2**.

Table 4.2 The loading capacity of the macrocyclic receptor ligands immobilised on various types of linker modified silica materials.

Si-Material	Microanalysis %[a]			Loading[b]		
	C	H	N	Micro mmol g^{-1}	Thermal wt %	Thermal mmol g^{-1}
Si^{70-230} -GPS-Trac, **43**	18.09	2.67	1.75	0.31	24.03	0.33
Si-GPDMS-Trac, **86**	10.37	2.05	0.85	0.15	*c*	*c*
$Si^{230-400}$-GPS-Trac, **87**	17.44	2.57	1.52	0.27	*c*	*c*
MCM-41-GPS-Trac, **88**	18.05	2.74	1.60	0.22	*c*	*c*
Si-GPS-DiPTrac, **44**	14.89	2.47	0.93	0.17	16.59	0.18
Si-GPS-TriPTrac, **45**	11.85	2.25	0.54	0.10	12.63	0.12

[a]Error = ± 0.3%; [b] ±10% ; [c]Not attempted.

As expected the loading of macrocycle on the non-crosslinked linker material, **86**, is reduced markedly due to the lower number of available linker moieties. The mesoporous silica material, MCM-41-GPS-Trac, **88**, also displays a reduction in loading of the macrocycle, demonstrating the proposition that it is not only the degree of surface coverage with linker molecules that dictates the extent of bound macrocyclic receptor ligands, but the number of these linker molecules that are accessible for reaction.

This proposition also holds true with the two hydroxy terminated poly ether (HTPE) appended silica materials, Si-GPS-DiPTrac, **44**, and, Si-GPS-TriPTrac, **45**

and, more so due to the larger size of these molecules. However, it cannot be argued that the reduction in macrocycle loading for these materials is controlled solely by the accessibility of linker molecules. These two materials contain macrocyclic receptor ligands that are inherently larger at their periphery and with the dynamic nature of the HTPE appendages there could be an amplification in steric crowding in the vicinity of the parent nucleophilic centres. These two unfavourable conditions would in combination contribute to the lower degree of macrocycle loading observed with the HTPE appended silica materials.

CHAPTER FIVE

METAL ION UPTAKE STUDIES WITH SILICA IMMOBILISED RECEPTOR LIGANDS

CHAPTER 5 METAL ION UPTAKE STUDIES WITH SILICA IMMOBILISED MOLECULAR RECEPTOR LIGANDS

5.1 Metal(II) ion uptake studies with Si-GPS-Trac, 43

Having successfully prepared the silica immobilised molecular receptor ligands metal ion uptake studies with Si-GPS-Trac, **43**, were conducted to examine the level and rate of metal ion uptake of this material for a select group of divalent metal ions, Cd(II), Zn(II), Cu(II), Pb(II), and Ca(II). This immobilised macrocyclic ligand was expected to possess similar if not identical metal uptake properties to the model **49** and the first generation receptors, such as, **26**, but this needed to be verified.

A deviation from the attachment of four enantiomerically pure pendant arms is that the GPTS linker precursor is racemic. So, the stereochemistry around the stereogenic carbon atom associated with the linker arm could be either *R* or *S* giving rise to two diastereomeric forms of the immobilised macrocycle: *SSSS* and *SSSR*. It seemed remotely possible that the *SSSR* diastereomer could produce something other than the usual eight coordinate receptor complexes previously observed with Cd(II) and Pb(II) using homochiral ligands of this type. This is because of the possibility of conformer C, shown in **Figure 5.1**, forming, whereby the uniform spiralling direction of the (*S*)-pendant arms may be opposed by the (*R*)-pendant arm.

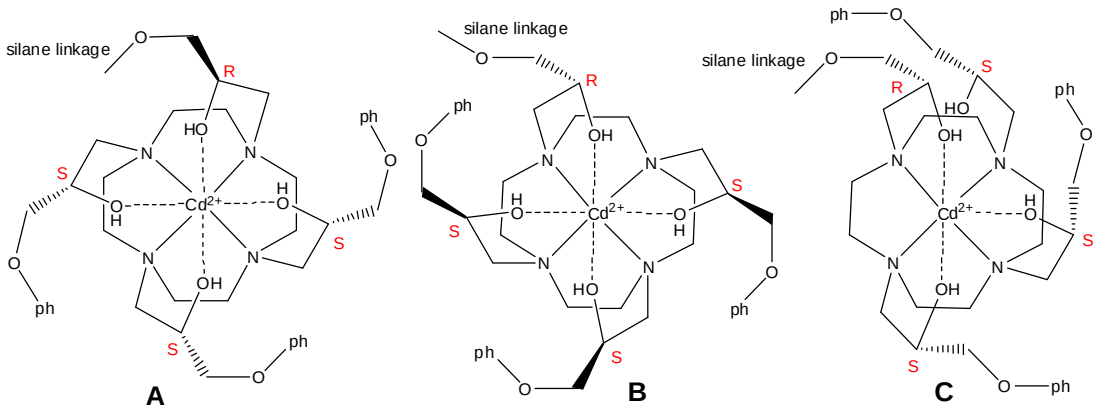

Figure 5.1 Representation of some of the possible coordinative bonding arrangements with the *SSSR* enantiomeric form of the silica immobilised receptor material, **43**.

Conformer C had never been observed in studies using homochiral ligands of this type, but the situation with non-homochiral ligands was unknown.[226]

Furthermore, this study would give an indication of any selectivity towards particular metal(II) ions. Finally, as each macrocyclic terminus is theoretically expected to coordinate to one metal(II) ion, then the number of moles of these ions taken up should equate to the number of moles of macrocycles immobilised on the mass of functionalised silica gel provided. The results obtained from these metal uptake studies could then be compared with the loading capacity from microanalysis and thermal combustion data to verify the number of available macrocyclic receptor ligands per unit mass of material. This series of experiments was also undertaken to determine whether the time provided for metal uptake would affect the metal loading capacity of the receptor material.

Other silica based materials: silica gel, Si-GPS, **33**, Si-GPS(endcapped), **85**, and, Si-GPS-Trac (endcapped), **89**, were also subjected to metal(II) ion uptake experiments to determine whether the free linker molecules and silanol groups, both free and endcapped, had an effect on the uptake capacity observed in the experiments with Si-GPSTrac, **43**.

5.1.1 Strategy for metal(II) ion uptake with Si-GPS-Trac, 43

Metal loading experiments were conducted by the batch uptake method, with five replicates undertaken to check reproducibility. These were performed by shaking 10 cm^3 of an aqueous solution, at pH ~5 (HEPES) containing the appropriate metal(II) nitrate (2×10^{-2} - 5×10^{-2} mol dm^3) with 100 mg of the silica based material for between 15 minutes and 18 hours as shown for Si-GPS-Trac, **43**, in **Scheme 5.1**.

At the end of the shaking time the silica material was recovered by filtration and the filtrate and washings collected in a volumetric flask.

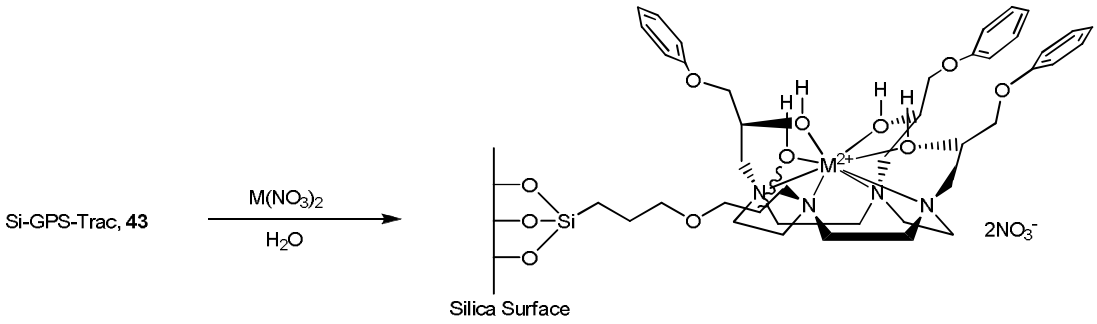

Scheme 5.1 Metal(II) ion coordination with Si-GPS-Trac, **43**.

The filtrate was then analysed by atomic absorption spectroscopy to obtain the equilibrium metal ion concentration. Metal ion uptake was then determined by the difference between the initial and equilibrium concentrations of the divalent metal ions. Percent metal uptake and metal loading capacity over time are shown in **Figure 5.2** for up to 3 hours as beyond this the uptake level does not change.

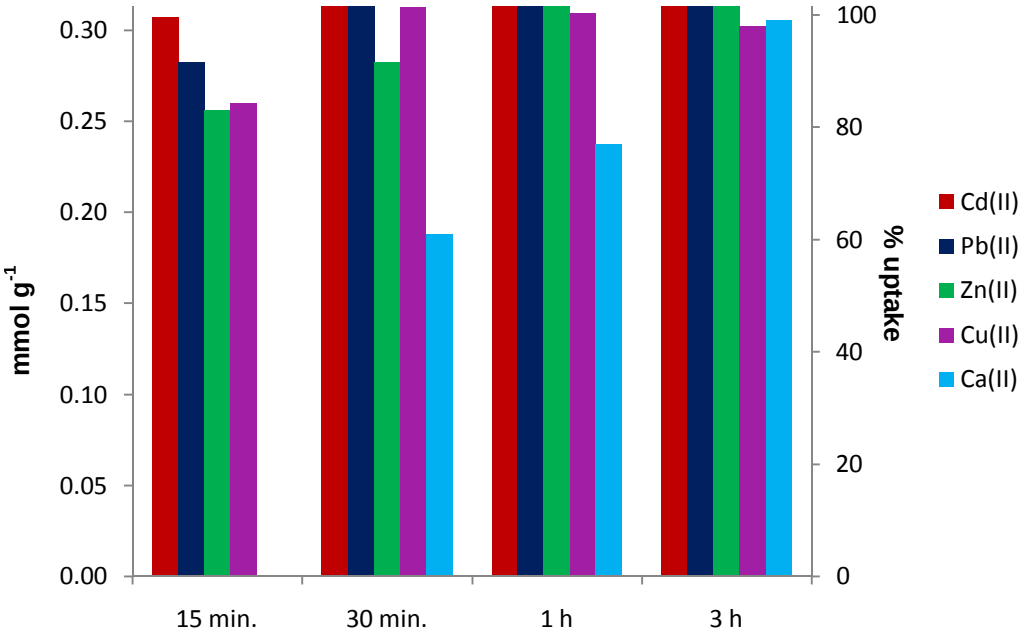

Figure 5.2 Metal uptake from t = 0 to t = 3 hours with Cd(II), Pb(II), Zn(II), Cu(II), and Ca(II) and receptor ligand, **43**, conducted in aqueous conditions at pH ~5 in HEPES buffer and T = 298 K.

It can be seen from the percent values in **Figure 5.2** that uptake of the metal(II)

ions by Si-GPS-Trac, **43** is in most cases rapid, for example, Cd(II) occupies 99% of the available macrocyclic coordination sites after 15 minutes. This translates to 0.31 mmol Cd(II) ions per gram of the silica immobilised macrocycles which, itself has a measured loading of 0.31 mmol of macrocycle moieties per gram of the silica immobilised material, **Table 4.2**. Loading of the metal(II) ions with Si-GPS-Trac, **43**, after 15 and 30 minutes of the uptake time are shown in **Table 5.1**.

Table 5.1 Percent uptake and loading capacity of Cd(II), Pb(II), Zn(II), Cu(II) and Ca(II) ions with Si-GPS-Trac, **43**, at t = 15 min. and t = 30 min.

	15 min.		30 min.	
	% Uptake[a]	mmol g^{-1}[b]	% Uptake[a]	mmol g^{-1}[b]
Cd(II)	99	0.31	101	0.32
Pb(II)	91	0.29	101	0.32
Zn(II)	83	0.26	91	0.29
Cu(II)	84	0.26	101	0.32
Ca(II)	0	0.00	60	0.19

[a]Error = ±3% [b]Error = ±10%

It can be seen from the above table that within 30 minutes the uptake of Cd(II), Pb(II) (eight coordinate) and Cu(II) (five or six coordinate) with Si-GPS-Trac, **43**, has reached maximum capacity. However, Zn(II) (five or six coordinate) takes an hour to attain maximum capacity whereas Ca(II) (eight coordinate) coordinates poorly after 15 minutes and takes three hours to reach full capacity.

5.1.2 Metal uptake studies with other related silica based materials

After establishing that the time needed to ensure full loading capacity with metal(II) ions it was of interest to ascertain whether precursor materials or residual silanol groups on the silica surface were also involved with metal complexation and should be taken into account. Therefore, dried silica gel, SiO_2; silica gel modified with GPS

linker material, Si-GPS, **33**; endcapped Si-GPS(EC), **85**; Si-GPS, Trac, **43** and, endcapped Si-GPS-Trac(EC), **89**, were studied. A 100 mg sample of each of these materials was treated with a solution of each of the divalent metal ions by the batch method described in **section 5.1.1** and, shaken for the times mentioned. The results for this series of experiments are shown in **Figure 5.3**.

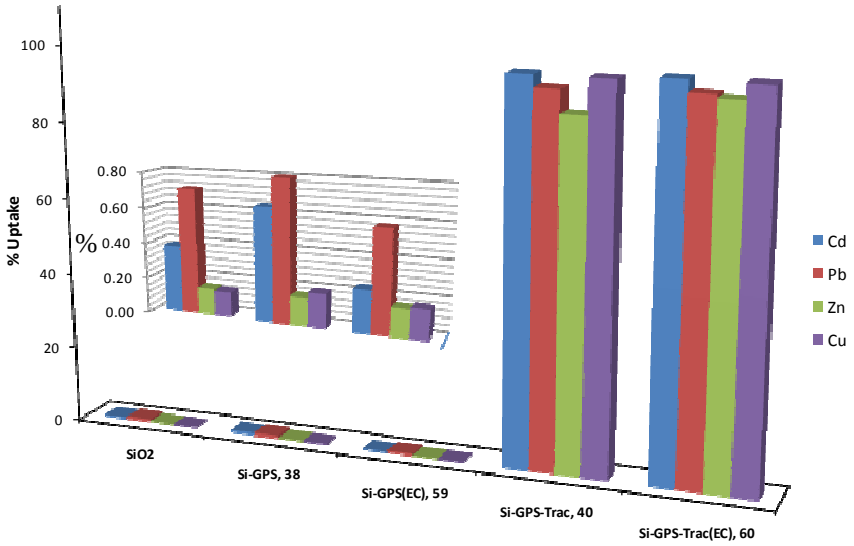

Figure 5.3 Percent uptake after 1 hour from experiments conducted with the divalent metal ions Cd(II), Pb(II), Zn(II) and Cu(II) utilising various silica based materials. Uptake of metal(II) ions with SiO_2, Si-GPS, **33**, and Si-GPS(EC), **85**, is reported as the percentage by weight of the metal in the material. Uptake with Si-GPS-Trac, **43**, and Si-GPS-Trac(EC), **89**, is reported as the percentage of the theoretical uptake based on the calculated macrocycle loading.

As expected, dried silica gel shows very little ability to complex with the metal(II) ions, which demonstrates that the silanol groups on its surface are not effective in coordinating with these divalent metal ions under the experimental conditions. After modification of the silica surface with GPTS the uptake of metal ions increases slightly showing that the glycidyl moieties have a slight, but very weak ability to coordinate with these divalent metal ions. After endcapping of this material a slight reduction in the percent uptake occurs with Cd(II), Cu(II) and

Zn(II); with Pb(II) showing a lesser decrease. The observed reduction in metal uptake was expected and is indicative of the purpose of the endcapping treatment. However, these uptake values, regardless of increase or decrease with variation of the functional groups on the silica surface, are small demonstrating that the non-macrocyclic ligand component of the material does not significantly contribute to the overall uptake of metal(II) ions. This is supported by the experiments conducted with Si-GPS-Trac, **43**, and endcapped Si-GPS-Trac(EC), **89**, where inactivation of the silanol groups with TMCS, **84**, appears to make little difference to the percent uptake of the metal ions.

Due to this it was decided to proceed with guest molecule inclusion studies with Si-GPS-[Cd(Trac)]$(ClO_4)_2$, **94**, and dispense with endcapping as it did not appear to make any significant difference to the coordination of the metal(II) ions. It is clear from **Figure 5.3** that these metal uptake experiments revealed no particular thermodynamic selectivity towards any of the particular metal(II) ions that were investigated.

From the results obtained with the metal uptake studies it was decided that the receptor functionalised material Si-GPS-Trac, **43**, and its HTPE derivatives, **44**, and **45**, could be activated by metal coordination using $Cd(ClO_4)_2 \bullet 6(H_2O)$ as, in the previous work, perchlorate anions have been shown to be easy to replace by the inclusion of an anionic guest species.

Preparation of the cadmium(II) complexed materials was completed by stirring a suspension of Si-GPS-Trac, **43**, or Si-GPS-DiPTrac, **44**, or Si-GPS-TriPTrac, **45**, in an aqueous solution containing an excess of cadmium perchlorate hexahydrate for two hours at room temperature as shown in **Scheme 5.2**.[94] The suspension was then filtered and washed with copious amounts of de-ionised water to yield Si-GPS-

[Cd(Trac)]$(ClO_4)_2$, **94**, or Si-GPS-[Cd(DiPTrac)]$(ClO_4)_2$, **95** or Si-GPS-[Cd(TriPTrac)]$(ClO_4)_2$, **96**.

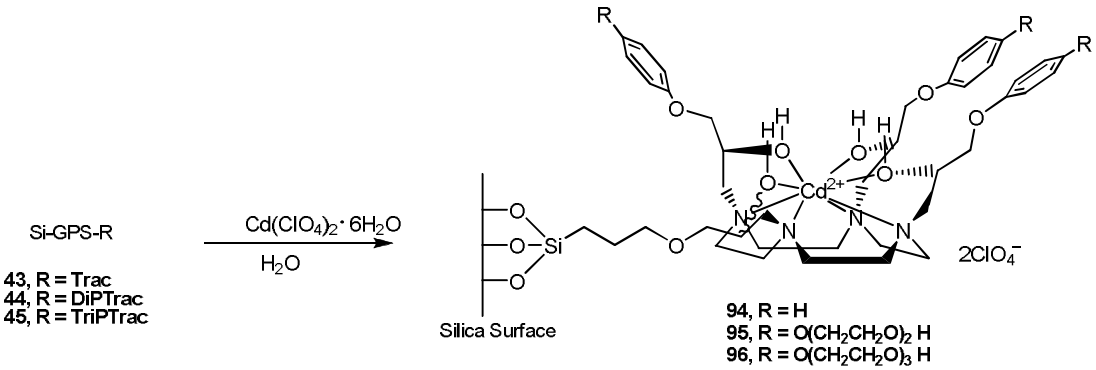

Scheme 5.2 Complexation of silica immobilised receptor ligands with cadmium perchlorate hexahydrate.

CHAPTER SIX

GUEST MOLECULE INCLUSION STUDIES WITH SILICA IMMOBILISED RECEPTORS

CHAPTER 6 GUEST MOLECULE INCLUSION STUDIES WITH SILICA IMMOBILISED RECEPTORS

6.1 Guest Inclusion with silica immobilised receptor complexes: Background

Studies with molecular receptor model **49** in DMSO-d_6, have demonstrated the suitability of a three-walled binding cavity for guest molecule inclusion and prompted the present investigation with silica bound receptor complexes. As the preliminary studies were conducted in an organic solvent, it was expected that the current investigation, which would be conducted in the more interesting aqueous environment, might provide some contrasting results regarding binding behaviour between host and guest in this medium.

As host-guest binding constants for the silica immobilised receptors could not be determined by conventional methods due to the difficulty in organising conditions, such that, an equilibrium is established between bound and unbound guest; provisional binding strength was established by evaluating the percent of guest species removed from the initial solution after contact with the receptor. Percent inclusion of guest species was determined by UV-Vis spectroscopy and calculated by the equation

$$\%\ \text{inclusion} = \left[\frac{n_i - n_e}{mL}\right] 100$$

where n_i is the number of mmol of guest species in the initial solution, n_e is the number of mmol in the solution at equilibrium, m the mass of the silica material (g) and L the loading of macrocycles on the silica material (mmol g^{-1}) to yield % inclusion of the respective guest species.

6.1.1 Strategy for guest molecule inclusion with silica immobilised hosts

Guest inclusion with silica immobilised host materials was effected by the treatment

of 100 mg of the host material, Si-GPS[Cd(Trac)]$(ClO_4)_2$, **94**, Si-GPS-[Cd(DiPTrac)] $(ClO_4)_2$, **95**, or Si-GPS-[Cd(TriPTrac)]$(ClO_4)_2$, **96**, with 10 cm^3 of an aqueous solution containing a *ca.* 50% excess of the sodium salt of the appropriate guest species at a concentration of 5 x 10^{-3} mol dm^{-3} at pH 7 in 0.01 mol dm^{-3} HEPES buffer. HEPES buffer was brought to pH 7 from its native pH of ~5.3 by the addition of 1 M NaOH. All phenolate inclusion was conducted in an unbuffered 10% DMSO/acetonitrile mixture to avoid protonation of the oxoanion moiety. The host/guest suspension was stirred for one hour at 298 K after which the solid phase was isolated by filtering the aqueous phase into a 250 ml volumetric flask and washing it with ample amounts of de-ionised water. Percent guest inclusion was then established by calculation of guest species remaining in the filtrate using the method described. An example of the general host-guest complexation reaction with silica immobilised receptors is shown in **Scheme 6.1**.

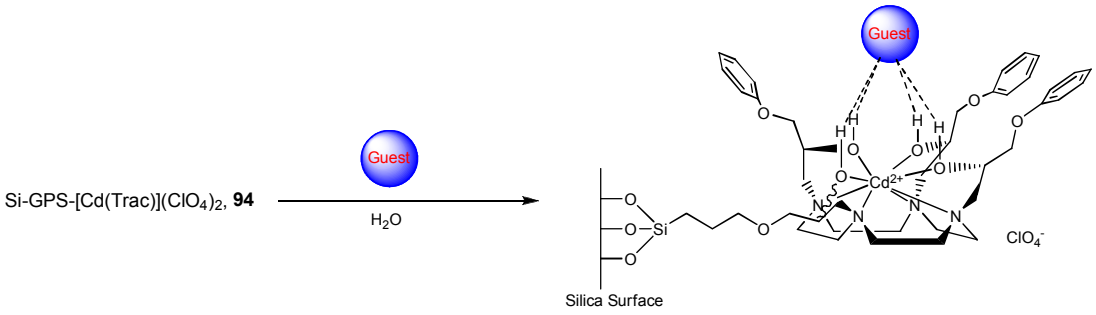

Scheme 6.1 General procedure for guest inclusion with silica immobilised receptor complexes, depicted here with four hydrogen bonds to the host binding pocket.

6.1.2 Guest molecule inclusion with Si-GPS-[Cd(Trac)]$^{2+}$, 94

To enable comparisons with binding studies conducted with model receptor **49** it was decided that the initial series of inclusion experiments with the silica immobilised receptors would involve the same set of guest species *p*-nitrophenolate (in 10% DMSO v/v in acetonitrile), acetate, *p*-nitrobenzoate, phenoxyacetate, L-histidinate

and D-histidinate. Guest inclusion with an additional two amino acid guests D- and L-phenylalanate was also attempted. It was of interest to observe whether the percent inclusion values obtained for this set of guest species would mirror their respective binding constants as determined in DMSO-d_6 with receptor **49**. The results for guest inclusion studies with this series of guests and silica bound receptor **94** are tabulated in **Table 6.1**.

Table 6.1 Percent guest inclusion of with Si-GPS-$[Cd(Trac)]^{2+}$, **94**, conducted in aqueous solution with a guest concentration of 5 x 10^{-3} mol dm^{-3} at pH 7 in 0.01 mol dm^{-3} HEPES buffer compared with log*K* determined for $[Cd(TracHP12)]^{2+}$, **49**, by ^{1}H NMR monitored titration in DMSO-d_6.

	Si-GPS-$[Cd(Trac)]^{2+}$, 94	$[Cd(TracHP12)]^{2+}$, 49	
Guest Species	**% Inclusion**[a]	**log*K***[b]	**pK_a**[c]
p-nitrophenolate	72[d]	3.45 ± 0.05	7.15
acetate	7	*e*	4.96
p-nitrobenzoate	16	4.7 ± 0.3	3.44
phenoxyacetate	27	4.5 ± 0.3	3.17
L-phenylalanate	23	*f*	2.20[g]
D-phenylalanate	24	*f*	2.20[g]
L-histidinate	35	3.37 ± 0.04	1.82[g]
D-histidinate	35	3.54 ± 0.09	1.82[g]

[a]Error = ± 3%. [b]Determined by ^{1}H NMR monitored titration in DMSO-d_6. [c]Data for the protonated species in H_2O acquired from NIST database. [d]Guest stock solution unbuffered 10% v/v DMSO in acetonitrile. [e]No change in chemical shift. [f]Not attempted. [g]COOH.

With these guest species the only good correlation between receptor **94** and receptor **49** is with *p*-nitrophenolate. In this case, according to **Figure A.1** in Appendix A, the observation of 72 ±3% inclusion at a 50% excess of the guest over host approximately correlates with a log*K* value of 3.45 ±0.05. However, as the *p*-

nitrophenolate inclusion experiment was conducted in a DMSO/acetonitrile mixture to maintain the anionic character of this guest species, the observed result, is not altogether surprising and is not comparable with those found for the other anions in **Table 6.1** where uptake was performed in aqueous conditions.

The other guest species, which all have a carboxylate hydrogen bond acceptor group, display a trend where the less basic species are more highly included. This is a reversal of the binding constant trend obtained with model receptor **49** in DMSO-d_6 where the binding strength increased with increasing basicity, in conformity with the expected strength of hydrogen bonding interactions between the guest species and the base of the host binding pocket. The low uptake of acetate, which lacks an aromatic group, suggests that an aromatic moiety in the structure of the guest contributes to molecular recognition of guest molecules.

6.1.3 Inclusion of hydroxybenzoate guest species with silica immobilised receptors

A series of hydroxy substituted guest molecules was also subjected to guest inclusion with receptor **94** in an aqueous environment in conditions identical with those for the previous set of guest species. The data are tabulated in **Table 6.2**. It can be seen that percent inclusion for hydroxybenzoate guest species in aqueous conditions demonstrates a reversal of the trend *o*-hydroxybenzoate < *m*-hydroxybenzoate < *p*-hydroxybenzoate observed for this series of guest molecules with receptor **49** in DMSO-d_6 (Chapter 3). However, the percent inclusion values obtained in aqueous conditions with receptor **94** mirror the log*K* values acquired with receptor **29** from fluorescence monitored titration experiments in 20% aqueous dioxane. Thus it appears that by switching from DMSO to aqueous conditions one can reverse the trend in binding constants.

Table 6.2 Percent inclusion data for hydroxybenzoate guest species with Si-GPS-[Cd(Trac)]$(ClO_4)_2$, **94**, conducted in aqueous media with a guest concentration of 5 x 10^{-3} mol dm^{-3} at pH 7 in 0.01 mol dm^{-3} HEPES buffer at 298 K and, log*K* values for [Cd((*S*)-athppc)]$(ClO_4)_2$, **29**, in 20% aqueous dioxane and model receptor [Cd(TracHP12)]$(ClO_4)_2$, **49**, in DMSO-d_6 also at 298 K.

	Receptor 94	Receptor 29	Receptor 49	
Guest species	**% Inclusion**[a]	**log*K***[b]	**log*K***[c]	**pK_a**[d]
benzoate	30	2.3 ± 0.1	4.11 ± 0.06	4.19
p-hydroxybenzoate	32	4.5 ± 0.3	4.09 ± 0.07	4.54
m-hydroxybenzoate	48	5.3 ± 0.5	4.16 ± 0.09	4.30
o-hydroxybenzoate	81	7.1 ± 0.5	3.08 ± 0.08	2.97
2,6-dihydroxybenzoate	95	7.5 ± 0.9	2.05 ± 0.03	1.05

[a]Conducted in aqueous solution. [b]Obtained by fluorescence monitored titrations in 20% aqueous dioxane. [c]Conducted in DMSO-d_6. [d]Values obtained in H_2O from PHYSPROP database for their respective conjugate acids.[202]

Rationalisation of the trend in DMSO-d_6 with receptor **49** was explained by the inability of three guest species, benzoate, *p*-hydroxybenzoate and *m*-hydroxybenzoate to participate in intramolecular hydrogen bonding and, therefore, in DMSO-d_6 they exhibited significantly larger binding constants than *o*-hydroxybenzoate and 2,6-dihydroxybenzoate, which are both known to form strong hydrogen bonds between their phenolic and carboxylate groups in that medium.[227, 228] The trend observed in aqueous conditions with receptor **94** appears to result from weaker intramolecular hydrogen bonds within these two *ortho*-substituted guest molecules due to competition with water molecules. Weakening intramolecular hydrogen bonding within these molecules strengthens the O-H···O hydrogen bonding and also allows for non-classical hydrogen bonding interactions to occur between the guest hydroxy groups and aromatic π-systems of the host pendant arms as shown in **Figure 6.1**.

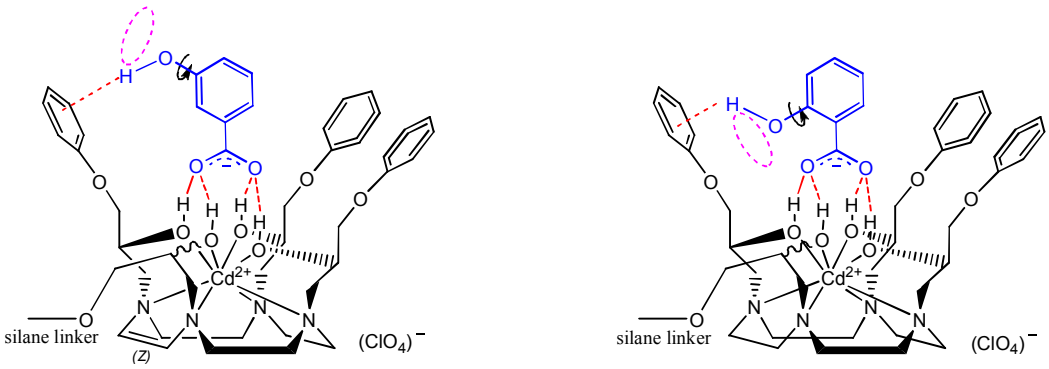

97 **98**

Figure 6.1 Potential non-classical hydrogen bonding interactions with the pendant arms of receptor material **94** when the guest hydroxy groups are in the *meta* or *ortho* positions. The ellipse shows the path circumscribed by precession of the hydroxy hydrogen atom around the O-Ar bond.

Therefore, retention of these guest species within the host cavity is strengthened by summing classical hydrogen bonding between the host hydroxy groups and guest carboxylate moiety and the previously mentioned non classical hydrogen bonds with host aromatic moieties. As this additive effect is potentially only viable in *m*-hydroxybenzoate, *o*-hydroxybenzoate and 2,6-dihydroxybenzoate it is not surprising that as the hydroxy group is moved into positions where interactions with the host π system are more favourable there is a corresponding increase in binding strength.

Of the three guest molecules potentially able to hydrogen bond with the host's aromatic rings the hydroxy hydrogen atom of *m*-hydroxybenzoate satisfies the criteria for hydrogen bonding over only part of its range of movement prescribed by rotation along the axis of the O-Ar bond, whereas, re-positioning the hydroxy moiety into an *ortho* position fulfils the criteria irrespective of rotation around the aromatic carbon to oxygen bond. This justifies the difference in percent inclusion and log*K* values obtained for *m*-hydroxybenzoate compared to the values obtained for *o*-hydroxybenzoate and 2,6-dihydroxybenzoate with receptors **94** and **29**. Moreover, judging by the increase in binding strength for 2,6-dihydroxybenzoate, which

contains two hydroxy groups in the *ortho* position, it would appear that more than one such non-classical hydrogen bond is possible.

As the relative magnitude of the binding constants, obtained in DMSO-d_6, for the hydroxybenzoate guests is the inverse of those obtained in 20% aqueous dioxane,[129, 166] and suggested by percent inclusion values obtained in H_2O with the silica bound macrocyclic receptor **94**, ^{1}H NMR monitored titration experiments were also conducted with receptor **49** in CD_3OD. This is a solvent with hydrogen bond acceptor and donor properties more closely related to those of H_2O. It was anticipated that in CD_3OD the same trend as seen in 20% aqueous dioxane with receptor **29** might be observed. However, as may be seen in **Table 3.2** this was not the case. It would appear that the presence of water is an essential criterion for the trend observed with receptors **29** and **94** to occur.

A speculative explanation for this phenomenon can be extracted from the crystal structure of an *o*-hydroxybenzoate guest included in the cavity of Δ-[Cd(*S*-thpc12)]$(ClO_4)_2$·0.5H_2O as shown in **Figure 6.2**.[97]

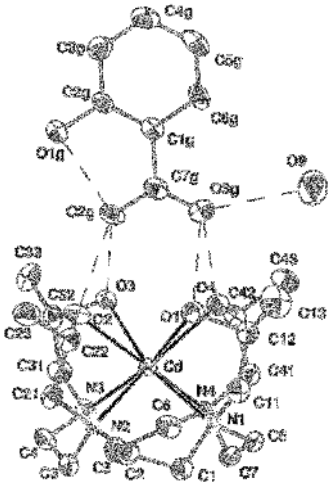

Figure 6.2 Crystal structure showing the interaction of an intramolecularly H-bonded *o*-hydroxybenzoate guest H-bonded to hydroxyl groups of Δ-[Cd(*S*-thpc12)]$(ClO_4)_2$·0.5H_2O. H-bonds are in dashed lines. H atoms and perchlorate are omitted for clarity. O9 is the water molecule atom.[97]

It can be seen here that a water molecule is hydrogen bonded to the carboxylate oxygen atom of the *o*-hydroxybenzoate guest. This suggests that in aqueous conditions with receptors **29** and **94** there exists in a similar way the potential for H_2O molecules to mediate hydrogen bond bridges between the guest hydroxy groups and the host aromatic rings, as shown in **Figure 6.3 (a)** and **(b)**. If, for instance, water molecules were to form a hydrogen bond bridging network within the host cavity as shown by **(a)** and **(b)**, the observed increase in binding strength for *ortho* substituted hydroxybenzoates in water could be explained.[229]

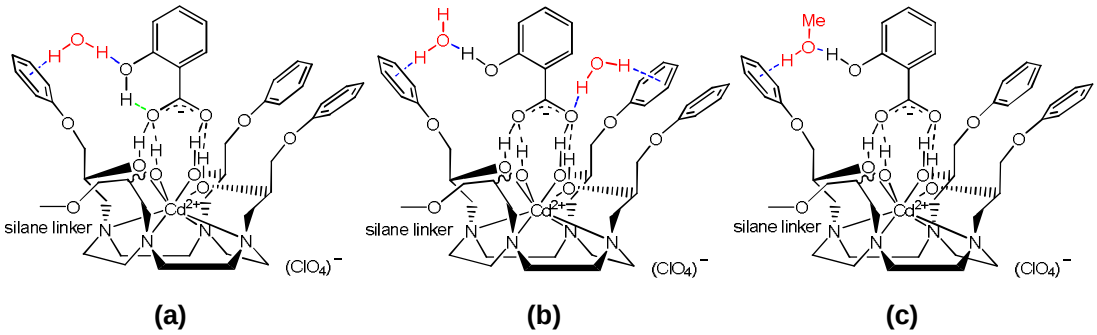

Figure 6.3 Representation of potential hydrogen bonding schemes that may be contributing to the difference in guest selectivity experienced in H_2O as opposed to DMSO and MeOH.

Water molecules, having two hydrogen bond donor atoms, are able to form hydrogen bond bridges from guest carboxylate oxygens and hydroxy hydrogens whereas, methanol is only able to bridge to an aromatic ring from guest hydroxy hydrogen atoms (**Figure 6.3 (c)**) over a more limited distance, making it a less effective mediator.

To verify whether the trend observed in aqueous conditions was linked to non-classical hydrogen bonding a series of test experiments was conducted with receptor **94** using a similar set of guest molecules, but eliminating the potential for non-classical hydrogen bonding interactions by replacing the hydroxy group with a

methoxy group, as portrayed by the generic example in **Figure 6.4**.

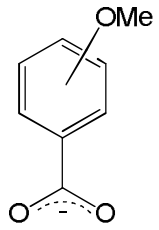

Figure 6.4 A generic example of a methoxy substituted benzoate guest molecule.

The guest species chosen for this study were *p*-methoxybenzoate, *m*-methoxybenzoate, *o*-methoxybenzoate and 2,6-dimethoxybenzoate. The results from this study are tabulated in **Table 6.3**.

Table 6.3 Comparison of inclusion data for hydroxybenzoate and methoxybenzoate guest species with Si-GPS-[Cd(Trac)]$(ClO_4)_2$, **94**, in aqueous solution with a guest concentration of 5 x 10^{-3} mol dm^{-3} at pH 7 in 0.01 mol dm^{-3} HEPES buffer at 298 K.

Guest Species	%	pK_a[a]	Guest Species	%	pK_a[a]
p-hydroxybenzoate	32	4.54	*p*-methoxybenzoate	60	4.47
m-hydroxybenzoate	48	4.30	*m*-methoxybenzoate	55	4.09
o-hydroxybenzoate	81	2.97	*o*-methoxybenzoate	29	3.90
2,6-dihydroxybenzoate	95	1.05	2,6-dimethoxybenzoate	23	3.44

[a]Values obtained in H_2O from PHYSPROP database for their respective conjugate acids.[202]

It would be expected that without the influence of non-classical hydrogen bonding that the more basic methoxybenzoate species would exhibit stronger binding capacities. This is the case with the methoxybenzoate guests, giving a data set that is a virtual mirror image of that observed for hydroxybenzoate inclusion in DMSO-d_6 with receptor **49** and, a reversal of the trend observed with receptor **94** in aqueous conditions with the same set of hydroxybenzoate guest molecules. Comparing

percent inclusion with the pK_a values for each set of benzoate guest molecules it is clear that the hydroxy groups are having some effect on the binding mode in aqueous conditions. This inclusion study with methoxybenzoate guests, which was conducted under identical conditions to the previous study with hydroxybenzoate guests, demonstrates the proposition that non-classical hydrogen bonding interactions contribute to host-guest binding strength only in the presence of water.

Another question that could be asked with regard to the studies with hydroxybenzoate and methoxybenzoate guests is why *p*-methoxybenzoate uptake is *ca.* double that of *p*-hydroxybenzoate. Obviously, there is something other than hydrogen bonding contributing to the increase in percent inclusion for *p*-methoxybenzoate as their pK_a values are similar. The discrepancy observed could be the result of a hydrophobic effect driving the *p*-methoxybenzoate molecule into the cavity of receptor **94**, and away from the aqueous surroundings, as its methoxy group is less hydrophilic than the hydroxy group of *p*-hydroxybenzoate. Conversely, the hydroxy group of *p*-hydroxybenzoate could be drawing it out of the cavity of receptor **94** by a hydrophilic effect. A lesser rendering of these hydrophobic and hydrophilic effects could describe the decrease in difference between percent inclusion values of *m*-methoxybenzoate and *m*-hydroxybenzoate since the substituents on these molecules are in the neighbourhood of the boundary dividing the interior and exterior regions of the host cavity.

Hydroxybenzoate guest species with various other substitution patterns were also used in these inclusion studies to see if any variation in the location of the hydroxy substituent would affect binding with receptor **94**. The guest molecules chosen were 2,5-dihydroxybenzoate, 3,5-dihydroxybenzoate, 2,4,6-trihydroxybenzoate and 3,4,5-trihydroxybenzoate (gallate). **Table 6.4** displays the percent inclusion values for

these guest molecules with receptor **94**.

Table 6.4 Percent guest inclusion of different hydroxybenzoate guest species with Si-GPS-[Cd (Trac)]$(ClO_4)_2$, **94,** in aqueous solution with a guest concentration of 5 x 10^{-3} mol dm^{-3} at pH 7 in 0.01 mol dm^{-3} HEPES buffer at 298 K.

Guest Species	% Inclusion	pK_a [a]
2,4,6-trihydroxybenzoate	94	1.68
2,5-dihydroxybenzoate	82	2.95
3,5-dihydroxybenzoate	50	4.04
3,4,5-trihydroxybenzoate	73	4.41

[a]Values obtained in H_2O from PHYSPROP database for their respective conjugate acids.[202]

High inclusion values for 2,5-dihydroxybenzoate and 2,4,6-trihydroxybenzoate further demonstrate that having hydroxy groups in the *ortho* position increases binding strength through hydrogen bonding interactions with the host pendant arms. The relatively high inclusion value for 3,4,5-trihydroxybenzoate is a little surprising in that this guest molecule not only lacks a hydroxy group in the *ortho* position, but in that both of the *meta* hydroxy groups are not equally available for hydrogen bonding due to one being intramolecularly hydrogen bonded with the *para* hydroxy group. This effectively leaves only one hydroxy group to form a hydrogen bond with the host aromatic group. Some compensation by stronger bonding through the benzoate moiety due to its higher basicity (pK_a = 4.41) is suggested.

6.1.4 Guest inclusion with immobilised hydroxy terminated polyether (HTPE) receptors

Due to the organic nature and hence low wettability in water of the receptor component of Si-GPS-[Cd(Trac)]$(ClO_4)_2$, **94**, it was thought that a receptor moiety with hydrophilic groups attached to its pendant arm framework would provide better

contact with an aqueous environment and therefore water soluble guest species. This would, in essence, endow the receptor part of the material with a greater degree of wettability enabling the inclusion process to occur in a single phase. Accordingly, guest inclusion studies were performed with two silica immobilised receptor materials Si-GPS-[Cd(DiPTrac)]$(ClO_4)_2$, **95**, and Si-GPS-[Cd(TriPTrac)]$(ClO_4)_2$, **96**, appended with hydroxy terminated polyether (HTPE) moieties at the periphery of each receptor's cavity. Both materials were expected to possess a level of wettability through increased hydrogen bonding between their ethereal and hydroxy oxygens and water molecules. Solubility of the silica free materials was evaluated by suspending 50 mg of each of the precursor macrocyclic compounds DiPTrac, **47**, and TriPTrac, **48**, in 1 cm^{-3} of water and gradually adding a small amount of water to each over time until it was completely dissolved. Solubility in water at 298 K obtained for these compounds was 0.007 mol L^{-1} for **47** and, 0.032 mol L^{-1} for **48**. These values are significant in the context of Trac, **46**, which has essentially zero solubility in water. Furthermore, when water is added to either of materials **95** or **96** the resultant suspension is visibly different than that for **94**. A perceivable translucence with the appearance of the material blending with the aqueous environment gives the impression that these materials are more wettable. The results from the study of the uptake of hydroxybenzoate guests with Si-GPS-[Cd(DiPTrac)]$(ClO_4)_2$, **95**, and Si-GPS-[Cd(TriPTrac)]$(ClO_4)_2$, **96**, are given in **Table 6.5**. The percent inclusion values for *p*-hydroxybenzoate and *m*-hydroxybenzoate for all three materials do not vary greatly. For *o*-hydroxybenzoate and 2,6-dihydroxybenzoate the immobilised HTPE materials show very different percent inclusion values. Si-GPS-[Cd(DiPTrac)]$(ClO_4)_2$, **95**, exhibits similar binding to Si-GPS-[Cd(Trac)]$(ClO_4)_2$, **94**, but Si-GPS-[Cd(TriPTrac)]$(ClO_4)_2$, **96**, includes

only about half of that taken up by the two former materials.

Table 6.5 Guest inclusion data for hydroxybenzoate guest species with receptor complexes Si-GPS-[Cd(Trac)]$(ClO_4)_2$, **94**, Si-GPS-[Cd(DiPTrac)]$(ClO_4)_2$, **95**, and Si-GPS-[Cd(TriPTrac)]$(ClO_4)_2$, **96**, conducted in aqueous media at pH 7 in 0.01 mol dm^{-3} HEPES buffer at 298 K.

	Percent Guest Inclusion			
	Silica Immobilised Receptors			
Guest Species	**Trac, 94**	**DiPTrac, 95**	**TriPTrac, 96**	**pK_a[a]**
benzoate	30	*b*	*b*	4.19
p-hydroxybenzoate	32	50	31	4.54
m-hydroxybenzoate	48	45	30	4.30
o-hydroxybenzoate	81	76	45	2.97
2,6-dihydroxybenzoate	95	92	46	1.05

[a]Values obtained in H_2O from PHYSPROP database for their respective conjugate acids.[202]

[b]Not attempted.

Lowering of the percent inclusion values seen for Si-GPS-[Cd(TriPTrac)]$(ClO_4)_2$, **96**, could be related to the HTPE chain length of this material. Whereas Si-GPS-[Cd(DiPTrac)]$(ClO_4)_2$, **95**, has two ethoxy moieties between its aromatic and hydroxy groups, Si-GPS-[Cd(TriPTrac)]$(ClO_4)_2$, **96**, has three. The extra length in the HTPE chain could result in orientation of the chain into the host cavity resulting in hydrogen bonding with the hydroxy groups at its base or even with each other. This would effectively create a barrier at the opening to the cavity as well as an obstruction of the host hydroxy groups making them sterically unavailable to guest molecules. This is shown in **Figure 6.5**. On the other hand the polyether chain of Si-GPS-[Cd(DiPTrac)]$(ClO_4)_2$, **95**, may be too short to interact with the binding cavity and hence the percent inclusion values for this material mirror values for receptor **94**.

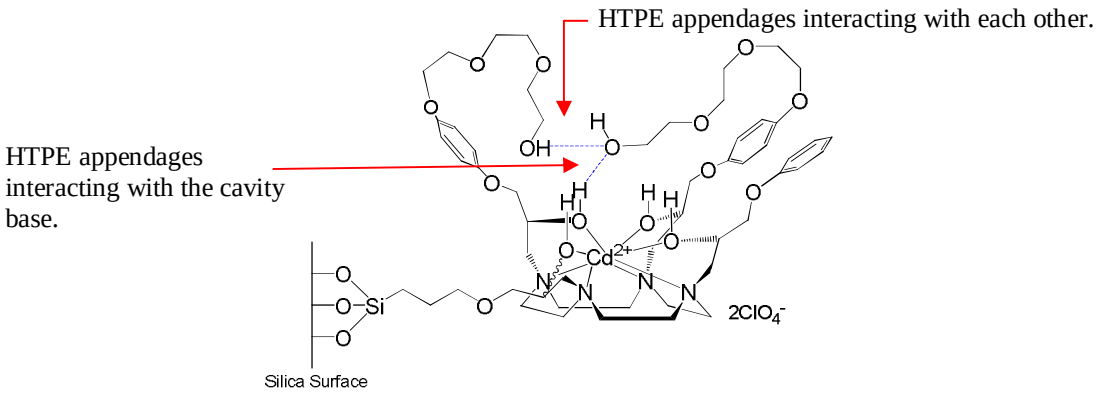

Figure 6.5 Diagrammatic depiction of the possible orientation of HTPE appendages on the pendant arms of immobilised receptor Si-GPS-[Cd(TriPTrac)$(ClO_4)_2$, **96**.

6.1.5 Guest inclusion with aminobenzoates

A further study was conducted to ascertain whether other guest molecules substituted with hydrogen bond donor groups would display a similar trend to that of the hydroxybenzoate guest species in aqueous conditions. The guest molecules chosen to test this proposition were a set of amino substituted benzoates: *p*-aminobenzoate, *m*-aminobenzoate and *o*-aminobenzoate. It was thought that these guest molecules may mimic with N-H···π the hydrogen bonding interactions postulated for hydroxybenzoate guests in identical conditions. To check the validity of this proposition guest inclusion of a series of similarly substituted nitrobenzoate guest molecules: *p*-nitrobenzoate, *m*-nitrobenzoate and *o*-nitrobenzoate were also investigated. The structures of these guests are depicted in **Figure 6.6**.

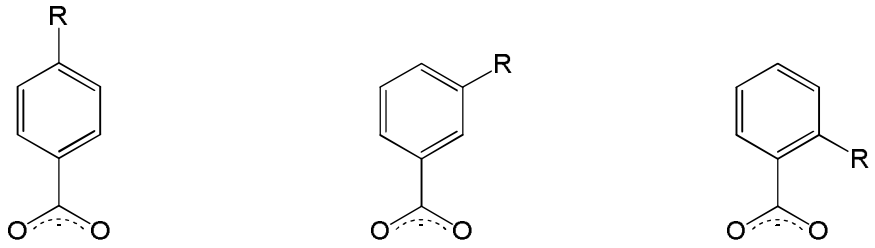

R = NH_2 or NO_2

Figure 6.6 Illustration of the structure of *para*, *meta* and *ortho* substituted-aminobenzoate and nitrobenzoate guest species.

Percent inclusion values for these two sets of guest molecules are tabulated in **Table 6.6**. The expected trend with aminobenzoate guest species was partially observed with a lower percent value (22%, pK_a 2.38) for *p*-aminobenzoate than for *o*-aminobenzoate (43%, pK_a 2.14).

Table 6.6 Percent guest inclusion of aminobenzoate and nitrobenzoate guest species with Si-GPS-[Cd(Trac)]$(ClO_4)_2$, **94**, in aqueous solution with a guest concentration of 5 x 10^{-3} mol dm^{-3} at pH 7 in 0.01 mol dm^{-3} HEPES buffer at 298 K.

Guest Species	%	pK_a[a]	Guest Species	%	pK_a[a]
p-aminobenzoate	22	2.38	*p*-nitrobenzoate	16	3.44
m-aminobenzoate	12	3.07	*m*-nitrobenzoate	23	3.46
o-aminobenzoate	43	2.14	*o*-nitrobenzoate	12	2.47

[a]Values obtained in H_2O from PHYSPROP database for their respective conjugate acids.[202]

These values demonstrate an increase in binding for *o*-aminobenzoate, 43%, compared with of *p*-aminobenzoate, 22%, despite the lower basicity of the former. This suggests that a degree of non-classical hydrogen bonding with the host pendant arms is contributing to the higher value for *o*-aminobenzoate. However, inclusion with *m*-aminobenzoate appears to oppose this suggestion with a value of 12%. Considering that *m*-aminobenzoate has the highest pK_a (3.07) of the aminobenzoates its percent inclusion value is anomalously low.

Inclusion with nitrobenzoate guest species conforms with binding as predicted by the basicity of the guest molecule. The guest with the highest pK_a (3.46), *m*-nitrobenzoate, also shows the highest inclusion value (23%) with *p*-nitrobenzoate next with 16% followed by *o*-nitrobenzoate (12%). These percent inclusion values demonstrate that nitro substituents do not significantly assist in binding of guest species. Amino substituents are somewhat helpful, but not as effective as hydroxy substituents.

6.1.6 Guest inclusion studies with guest species containing different substituents

To check whether variation of substituents in the *para* position would affect binding values a series of different benzoate guests was also subjected to guest inclusion experiments with Si-GPS-[Cd(Trac)]$(ClO_4)_2$, **94**. The guest molecules used were *p*-methylbenzoate, *p*-fluorobenzoate, *p*-chlorobenzoate and *p*-formylbenzoate.

Also a set of hydroxybenzoates with the phenolic hydroxy group deprotonated in addition to the carboxy group were used in these experiments to see if endowing a guest molecule with more than one oxoanion would have an influence on binding strength. The guests for these experiments were *p*-carboxyphenolate and *m*-carboxyphenolate. Preparation of *p*-carboxyphenolate and *m*-carboxyphenolate was by treatment of their conjugate acids with NaOH while maintaining the solution above pH 12. This series of experiments was conducted at pH 12 using 0.02 mol dm^3 CAPS buffer.

Furthermore to ascertain whether π-π interactions between guest and host species would also increase binding, two π enriched guest molecules: 1-naphthoate and 2-naphthoate were also used in guest inclusion experiments. The rationale was that either guest π-π interactions (edge to face or face to face) directly with the host or π···H-O-H···π H_2O bridged hydrogen bonding would contribute to the overall binding in the host-guest complexes formed. **Table 6.7** shows the percent inclusion values for these sets of experiments.

It appears from the percent inclusion values attained for series 1 that the character of the substituent in this case does not alter these values significantly as they tend to agree with the binding values expected with respect to the basicity of the guest species.

Table 6.7 Percent guest inclusion of different guest species with Si-GPS-[Cd(Trac)]$(ClO_4)_2$, **94**, in aqueous solution with a guest concentration of 5 x 10^{-3} mol dm^{-3} at 298 K. These experiments were performed at pH 12 in 0.02 mol dm^{-3} CAPS buffer for *p*-, and *m*-carboxyphenolate and at pH 7 in 0.01 mol dm^{-3} HEPES buffer for the other guest species.

Series	Guest Species	%	pK_{aCOOH}[a]	pK_{aOH}
1	*p*-methylbenzoate	43	4.37	
	p-fluorobenzoate	33	4.14	
	p-chlorobenzoate	38	3.98	
	p-formylbenzoate	19	3.77	
2	*p*-carboxyphenolate	4	4.54	9.32[b]
	m-carboxyphenolate	2	4.30	9.92[b]
3	1-naphthoate	76	3.60	
	2-naphthoate	98	4.17	

[a]Values obtained in H_2O from PHYSPROP database for their respective conjugate acids.[202]
[b]IUPAC.[230]

Series 2 guest species show little binding with the host. This could be attributed to increased aqueous solubility of these dianionic guest molecules. They are potentially able to bind at either of their anionic ends with the binding pocket leaving the other anionic moiety projecting into the aqueous phase. They are more hydrophilic than their monoanionic parent compounds and will, therefore, prefer to remain surrounded by water rather than bind within the host cavity which is essentially hydrophobic.

The percent inclusion values for series 3 guest species show a significant increase in host-guest complex formation with 2-naphthoate attaining a value (98%) near that of the strongest binding hydroxybenzoates. As these guest molecules do not possess a hydrogen bond donating atom within their framework, the higher percent values cannot be attributed solely to their basicity as evidenced by their pK_a values 1-

naphthoate (pK_a = 3.60) and 2-naphthoate (pK_a = 4.17). This has been corroborated previously by guest inclusion studies with hydroxybenzoate guest species where benzoate (pK_a =4.19) and *p*-hydroxybenzoate (pK_a =4.54) both show modest percent inclusion values although their pK_a values are high. So, some other factor must be responsible for augmenting their binding values. For instance, the contribution of π electrons from the adjoining aromatic ring increases the potential for forming hydrogen bond bridges between the guest and host aromatic groups.[231-233] There is also the possibility of hydrophobic effects and π-π interactions between guest and host species if the respective aromatic groups come within bonding distance of one another. Summation of these modes of binding appears to be reflected in increased percent inclusion values for 1-naphthoate and 2-naphthoate with the difference resulting from one being more basic than the other. It is known from crystal structures of Na_4[calix[4]arene sulfonate]•13.5H_2O that water molecules are able to bridge, through hydrogen bonding, between two aromatic π-acceptor groups.[231] Indications of how these bridging π···H-O-H···π hydrogen bonding interactions might occur between a naphthoate guest and the host species are given in **Figure 6.5**.

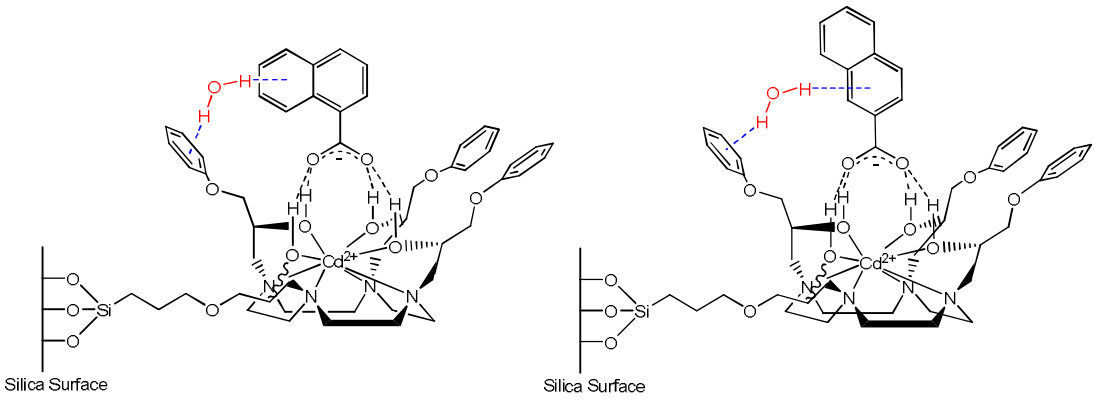

Figure 6.5 Representation of the possible hydrogen bonding interactions enhancing the binding between naphthoate guests and Si-GPS-[Cd(Trac)]$(ClO_4)_2$, **94**.

6.1.7 Guest inclusion studies with precursor silica materials

There exists the possibility that the silica surface or the silane linker may adsorb guest molecules. Therefore, to determine whether percent inclusion values obtained from guest inclusion experiments are correspondingly enhanced, both pristine SiO_2 and Si-GPS, **33**, were treated with guest anions using some of the guest species used in the previous studies with Si-GPS-[Cd(Trac)]$(ClO_4)_2$, **94**. Neither SiO_2 nor Si-GPS, **33**, showed any significant uptake of any of the guest molecules tested. For both materials the uptake of any guest species was less than 3%.

Inclusion was also attempted with hydroxybenzoate guest species using cadmium-free ligand materials Si-GPS-Trac, **43**, and Si-GPS-TriPTrac, **45**, to determine their binding capability. The observed percent uptake for these materials was considerably reduced to values of between 10 and 20% indicating that metal-ion complexation is a necessary feature for activation of these receptor materials to enable guest inclusion.

6.1.8 Characterisation of the silica immobilised host-guest complexes

Solid materials that are not readily solubilised, without disturbance of their composition, present difficulties in their characterisation. These problems can be overcome by subjecting these materials to analytical methods that are non-intrusive and yet provide useful information about the material. One such technique is solid state NMR, in particular ^{13}C CPMAS NMR. It is a very effective method for determining structure within solid materials. As the host-guest complexes formed in the preceding work are immobilised on a silica surface their characterisation was achieved in this way.

A sample size of ~150 mg of the silica immobilised host-guest material was tamped into a 4 mm zirconium oxide rotor stoppered with a Kel-F end-cap. The

spectrum for the material was then attained at a spin rate of 5 kHz with a recycle delay time of 4 s utilising TOSS (TOtal Suppression of Spinning Sidebands) software to eliminate the appearance of spinning side-bands. Solution ^{13}C NMR spectra (proton decoupled) were also obtained in DMSO-d_6 for the guest species to allow chemical shift assignment of their resonances, for example, as shown in **Figure 6.6** for 2,6-dihydroxybenzoic acid and 2,6-dihydroxybenzoate.

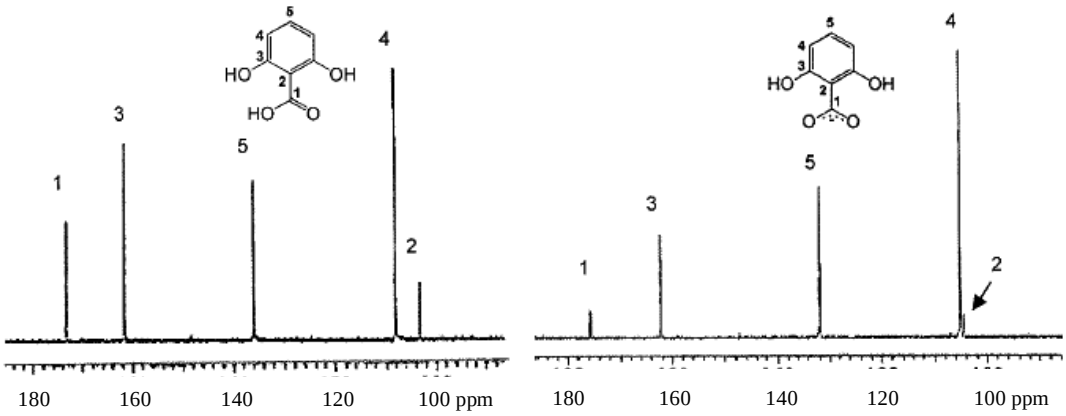

Figure 6.6 Solution $^{13}C\{^1H\}$ NMR spectra of (A) 2,6-dihydroxybenzoic acid and (B) sodium 2,6-dihydroxybenzoate obtained in DMSO-d_6.

Both of the above spectra show sharp singlet resonances for each of the five inequivalent carbon atoms present in 2,6-dihydroxybenzoic acid and 2,6-dihydroxybenzoate. However, the ^{13}C spectra seen in solution do not mirror those seen in the ^{13}C solid state NMR, as evidenced by the spectra obtained for 2,6-dihydroxybenzoic acid and sodium 2,6-dihydroxybenzoate, depicted in **Figure 6.7**.

Spectra A and B for 2,6-dihydroxybenzoic acid and sodium 2,6-dihydroxybenzoate show line broadening with extra resonances for C3 and C4 in 2,6-dihydroxybenzoic acid, and C3, C4 and C5 in sodium 2,6-dihydroxybenzoate.

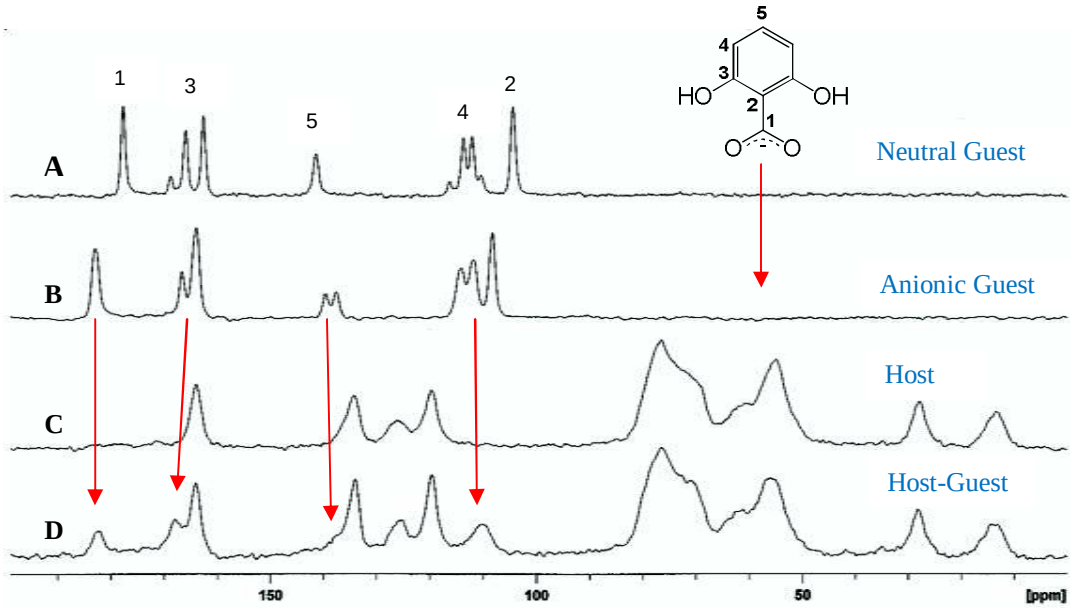

Figure 6.7 ^{13}C CPMAS NMR spectra for (A) 2,6-dihydroxybenzoic acid (B) sodium 2,6-dihydroxybenzoate, (C) Si-GPS-[Cd(Trac)]$(ClO_4)_2$ and (D) Si-GPS-[Cd(Trac)(2,6-dihydroxybenzoate)](ClO_4). All spectra are shown with line broadening.

This arises because hydroxybenzoates are able to hydrogen bond across their carboxy as well as their hydroxy termini, both intramolecularly and intermolecularly, which will give rise to a number of conformationally different molecules in the solid state.[234-236] Thus the extra bands observed in the solid state are due to the differences in sample dynamics between the two methods. In solution, anisotropic NMR interactions are averaged to zero to give the observed chemical shifts as sharp isotropic signals.[237, 238] In the solid, state, however, the molecules are virtually static and because of this anisotropic or orientation-dependent interactions can be observed.[237, 238] Furthermore, polymorphism within the powder structure puts some of the carbon atoms into different environments and, as solid state NMR can distinguish these different molecular conformations in addition to configurational dissimilarities in a segment of a molecule the spectra obtained display a more complex pattern for some resonances.[239, 240]

In examining spectrum D for evidence of the inclusion of 2,6-dihydroxybenzoate

it should be borne in mind that previous comparisons of solution ^{13}C NMR arising from guest anions and host guest complexes of this type have always revealed almost negligible chemical shift perturbation for the host carbon atom resonances, but usually some quite significant perturbation to the chemical shift values of the guest resonances. Proceeding on this basis it is then reasonable to postulate that the new resonance in spectrum D (compared to C) at 182.2 ppm is from C1 of the guest (183.0 ppm in B), the new resonance at 167.9 ppm is from C3 (166.7 ppm in B), the new shoulder at 138.0 ppm is from C5 (139.7 ppm in B) and the new broad resonance at 110.2 is from a merging of C4 and C2 (113.0 and 108.3 ppm in B). Thus there seems little doubt that not only is 2,6-dihydroxybenzoate present in the sample used to produce spectrum D, but that the altered chemical shift values for the guest indicate a more intimate association than just a physical mixture of the two species.

The preceding spectra are for a host-guest combination where the very highest uptake of the guest occurred (95%) so examination of the solid state NMR spectra from a lower percentage uptake combination is also illustrative as a basis for comparison. The guest species, *m*-methoxybenzoate, with 55% inclusion in Si-GPS-[Cd(Trac)]$(ClO_4)_2$, **94**, was chosen for this purpose. The acquired spectra are depicted in **Figure 6.8**.

Spectrum A, for *m*-methoxybenzoate, shows splitting of all of the single resonances found in the solution spectrum. This spectrum when viewed in combination with spectrum B does display evidence for inclusion of *m*-methoxybenzoate in Si-GPS-[Cd(Trac)]$(ClO_4)_2$, **94**, as depicted in spectrum C, with some bands for this guest molecule clearly visible, particularly C1 which moves from 183.0 ppm in A to 184.1 ppm in C.

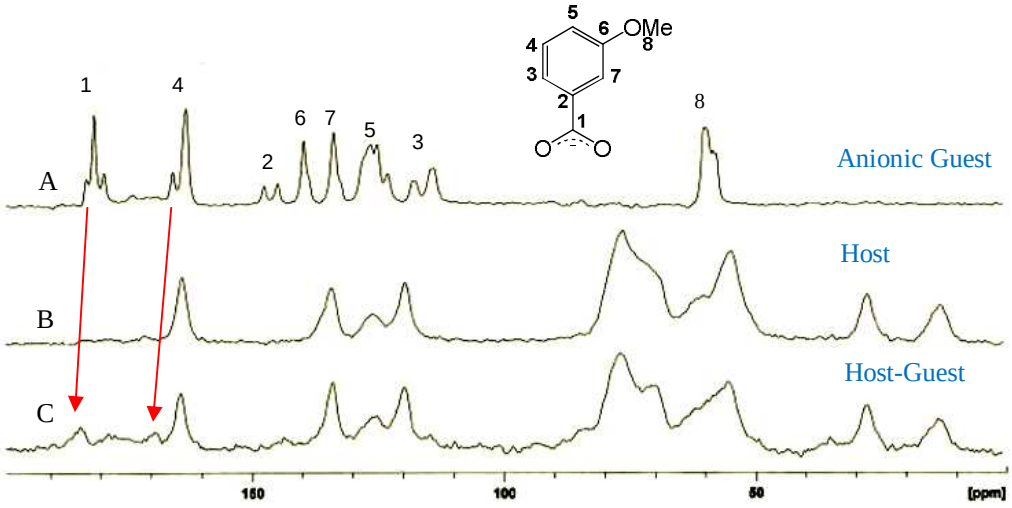

Figure 6.8 ^{13}C CP MAS NMR spectra for (A) sodium *m*-methoxybenzoate, (B) Si-GPS-[Cd(Trac)]$(ClO_4)_2$ and (C) Si-GPS-[Cd(Trac)(*m*-methoxybenzoate)](ClO_4). All spectra are shown with line broadening.

However, overall the comparison is not as convincing as that seen in **Figure 6.7** and this is completely in line with uptake of *m*-methoxybenzoate by **94** being measured as 55% instead of 96%. Resonances from carbon atoms C2 to C7 in spectrum C are either superimposed or appear only with a barely discernible signal to noise ratio.

To confirm that high percent inclusion materials would display bands for host material with included guest species another high inclusion material, sodium 2, 4, 6-trihydroxybenzoate, 94%, was analysed. The relevant spectra for this material are displayed in **Figure 6.9**.

As sodium 2, 4, 6-trihydroxybenzoate is a high binding guest its spectral bands are quite prominent in spectrum C for the host-guest material. The band for the carboxylate carbon C1 is clearly visible at 183.0 ppm. A large band for the *ipso* carbon C2 in spectrum A at 101.7 ppm is distinguishable, but broadened and much smaller at 100.2 ppm in spectrum C. Additional bands between 150.0 ppm and 169.0 ppm for C3, C4 and C5 are shifted downfield in spectrum C.

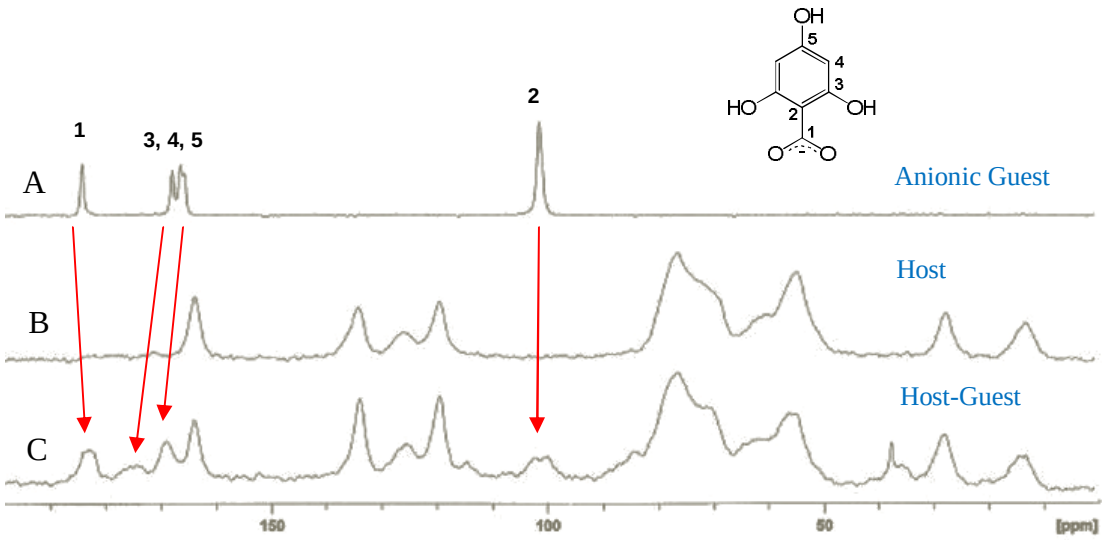

Figure 6.9 ^{13}C CP MAS NMR spectra for (A) sodium 2,4,6-trihydroxyoxybenzoate, (B) Si-GPS-[Cd(Trac)]$(ClO_4)_2$ and (C) Si-GPS-[Cd(Trac)(2,4,6-trihydroxybenzoate)](ClO_4). All spectra are shown with line broadening.

These spectra are indicative of inclusion of the guest species in Si-GPS-[Cd(Trac)]$(ClO_4)_2$, **94**, and confirm the UV-Vis analytical uptake measurement.

Host-guest inclusion complexes formed with Si-GPS-[Cd(Trac)]$(ClO_4)_2$, **94**, that had percent inclusion values lower than 50% do not display any visible evidence of host-guest complex formation in solid state NMR spectra. It appears that the concentration of the guest species relative to the host material is too low for the solid state NMR method to detect it once uptake diminishes below this level. Also, inclusion spectra for some guest species, such as *p*-nitrophenolate (73%), with high percent inclusion, did not display discernible resonances as they were masked by the host signals. Further sets of ^{13}C CPMAS spectra for high guest uptake host-guest combinations are provided in **Appendix C**.

6.2 The model receptor complex revisited: Determination of binding constants in the presence of water

To confirm the proposition that the presence of water in the system would enhance the binding strength of hydroxybenzoate guests with *ortho*, and to a lesser

extent, *meta*-positioned hydroxy groups it was decided to revisit ^{1}H NMR monitored titration experiments with the receptor model [Cd(TracHP12)]$(ClO_4)_2$, **49**, this time in 20% aqueous acetonitrile buffered at pH 7. The guest molecules used for this series of binding constant studies were benzoate, *p*-hydroxybenzoate, *m*-hydroxybenzoate, *o*-hydroxybenzoate and 2,6-dihydroxybenzoate. This was done in an attempt to mirror previous studies utilising 20% aqueous dioxane with receptor **29**.[129] The method used to obtain the binding constants was the same as for ^{1}H NMR monitored titrations in DMSO-d_6. A diversion from the previous study with **49** in DMSO-d_6 was that with 2,6-dihydroxybenzoate the H_B protons were followed rather than the *para* proton as it was masked by the host resonances when in 20% D_2O/CD_3CN buffered at pH 7. The results of these experiments are shown in **Table 6.8**.

Table 6.8 Inclusion of hydroxybenzoate guest species with [Cd(TracHP12)]$(ClO_4)_2$, **49**, in 20% D_2O/CD_3CN solution with a guest concentration of 10^{-3} mol dm^{-3} at pH 7 in 0.01 mol dm^{-3} HEPES buffer at 298 K, compared with inclusion for previously used systems.

	Solvent Conditions					
	DMSO	CD_3OD	H_2O[a]	20% H_2O/dioxane[b]	20% D_2O/CD_3CN	
	Host Species					
Guest Species	49	49	94	29	49	pK_a[c]
benzoate	4.11 ±0.06	3.96 ±0.09	30	2.3 ±0.1	3.10 ±0.08	4.19
p-OH	4.09 ±0.07	*d*	32	4.5 ±0.3	3.18 ±0.28	4.54
m-OH	4.16 ±0.09	*d*	48	5.3 ±0.5	3.49 ±0.17	4.30
o-OH	3.08 ±0.08	3.23 ±0.03	81	7.1 ±0.5	3.70 ±0.15	2.97
2,6-diOH	2.05 ±0.03	*d*	95	7.5 ±0.9	4.64 ±0.36	1.05

[a]Percent uptake. [b]Obtained by fluorescence studies.[129] [c]Values obtained from PHYSPROP database for their respective conjugate acids.[202] [d]Not attempted.

The log*K* values obtained for this study demonstrate that addition of water to the system does reverse the trend from *p*-hydroxybenzoate > *m*-hydroxybenzoate > *o*-hydroxybenzoate found in DMSO-d_6 to *o*-hydroxybenzoate > *m*-hydroxybenzoate > *p*-hydroxybenzoate. This is markedly apparent for 2,6-dihydroxybenzoate where the log*K* value increases from 2.05 in DMSO-d_6 by *ca*. three orders of magnitude to 4.64 in 20% aqueous acetonitrile. The log*K* values obtained correlate well with those obtained for receptor **29** by fluorescence monitored titration.[129] Therefore, the ordering of the percent guest uptakes measured in water with immobilised receptor **94** is consistent with the findings for these types of receptors. The reversal of the trend shows that regulation of the system is dependent on specific solvent effects, in this case, most likely, the ability of water molecules to mediate hydrogen bonding between the guest hydroxy groups and the host aromatic rings. Examples of ^{1}H NMR monitored titration curves obtained in this series of experiments are shown for *m*-hydroxybenzoate in **Figure 6.10** and 2,6-dihydroxybenzoate in **Figure 6.11**.

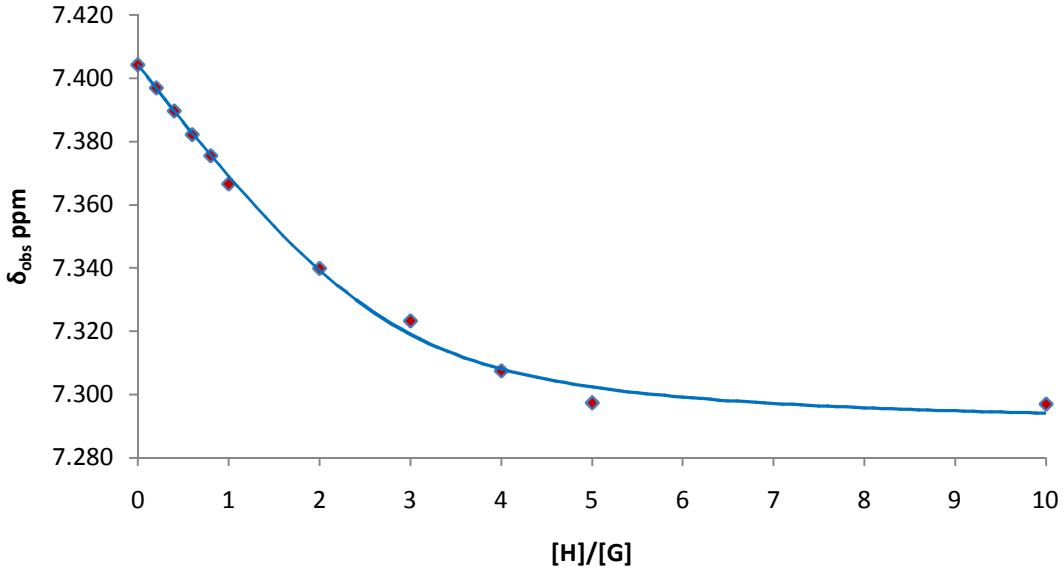

Figure 6.10 Example of ^{1}H NMR monitored titration curve for *m*-hydroxybenzoate with $[Cd(TracHP12)]^{2+}$, **49**, in 20% D_2O/CD_3CN buffered at pH 7 with HEPES buffer, showing the downward arc due to the upfield perturbation in the chemical shift of the *p*-proton.

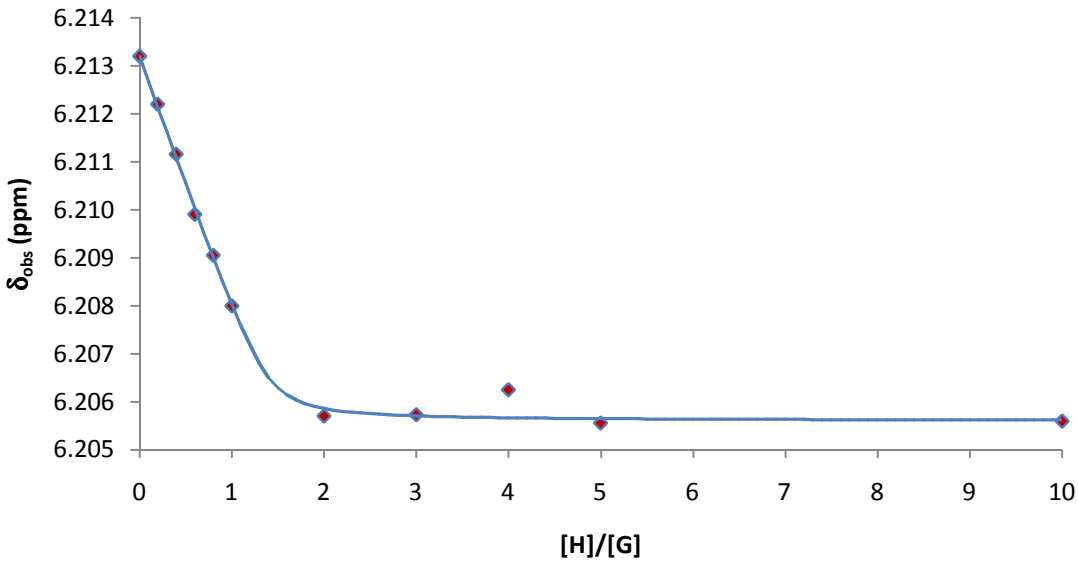

Figure 6.11 Example of ^{1}H NMR monitored titration curve for 2,6-dihydroxybenzoate with $[Cd(TracHP12)]^{2+}$, **49**, in 20% D_2O/CD_3CN buffered at pH 7 with HEPES buffer, showing the downward arc due to the upfield perturbation in the chemical shift of the H_B protons.

CHAPTER SEVEN

EXPERIMENTAL

CHAPTER 7 EXPERIMENTAL

7.1 General Experimental

All reactions were performed under an atmosphere of nitrogen unless specified otherwise. Solvents were purified by using known literature methods.[241] Cyclen in 98% purity was purchased from Strem Chemicals, U.S.A. and was used without further purification. Silica gel 60 (70 - 230 mesh) was purchased from Merck. The methods detailed by Zubrick were used for purifications utilising silica chromatography.[242] Stationary phase packing was purchased from Merck as silica gel 60 (230 - 400 mesh). Monitoring of silica chromatography progress was performed by thin layer chromatography (tlc) using Merck No. 5554 aluminium backed silica gel 60 PF_{254} plates.

7.2 Physical methods

Microanalyses were carried out at the University of Otago, New Zealand. ^{1}H and ^{13}C NMR spectra were obtained using one of the following spectrometers: Varian Oxford 200, Varian Gemini 300 or Bruker 400 Avance. ^{1}H spectra were collected at an operating frequency of 199.985, 300.075 or 400.13 MHz, respectively. The ^{13}C spectra were recorded at 50.291, 75.462 or 100.61 MHz, respectively. Referencing of the ^{13}C NMR chemical shifts was in relation to the central resonance of the multiplets of the solvents used: δ 77.00 for $CDCl_3$, δ 39.52 for DMSO-d_6, 118.10 for CD_3CN and δ 49.00 for CD_3OD. ^{13}C NMR spectra obtained in D_2O were referenced by the addition of 1,4-dioxane (δ 67.19). ^{1}H NMR chemical shifts were referenced to the central resonance of the residual solvent peak: δ 7.26 for $CDCl_3$, δ 2.50 for DMSO-d_6, δ 1.94 for CD_3CN and δ 3.31 for CD_3OD. Optical rotation was measured at 298 K with a PolAAr polarimeter. Molar conductivity measurements (Λ) utilised

10^{-3} mol dm^{-3} solutions in anhydrous DMF at ambient temperature with a Model Aqua-C Conductivity-TDS-Temp. Meter. Thermal combustion determination of loading capacity was conducted in 15 cm^3 porcelain crucibles at 1073 K in a C Muffle Furnace manufactured by H. B. Selby and Co. Pty. Ltd.

7.3 Host-Guest binding constant measurements

All guest species were used as their sodium salts, which were prepared by treatment of aqueous or ethanolic solutions of their conjugate acids with NaOH until the pH of the solution was at least two pH units above the pK_a of either their carboxy or hydroxy moiety. The salt was then isolated either by filtration or removal of the solvent *in vacuo* and recrystallisation of the residue from ethanol or methanol.

NMR monitored titration experiments, conducted at 298 K except where otherwise noted in the text, were used where the standard procedure required preparation of individual samples containing guest or host and guest in 0.7 cm^3 DMSO-d_6 in 5 x 180 mm NMR tubes. Samples for NMR titrations were added to the NMR tubes with Gilson Pipetman micropipettes (2 - 20 µl, 20 - 100 µl, 100 - 200 µl and 200 - 1000 µl). Concentration of the guest species in each tube was kept constant at 1 mM while varying the host for each sample from 0 mM to 10 mM. The samples in each tube were prepared by addition of 50µl of guest from a 14 mM stock solution made up in DMSO-d_6. A host stock solution of 14 mM was prepared from which aliquots of between 5 and 500 µl were added to each sample to give host:guest ratios between 0.1 and 10 in a total of 15 increments. Host-guest binding constants in CD_3OD and 20% D_2O in CD_3CN buffered at pH 7 with HEPES buffer were obtained by the same method.

IGOR data analysis software was used to process the chemical shift data to obtain

binding constants (log*K* values) and generate best-fit theoretical titration curves using a non-linear regression procedure written by Dr. A. K. W. Stephens of Flinders University, Adelaide, South Australia.[243]

7.4 Metal ion uptake determined by Atomic absorption spectroscopy

Metal ion uptake was determined by atomic absorption spectroscopy with a GBC 901 Atomic Absorption Spectrophotometer. Calibration curves were constructed for each of the divalent metal ions Cd(II), Pb(II), Zn(II), Cu(II) and Ca(II). A 100 mg sample of the silica-based material was then stirred at 298 K with 10 cm^3 of an aqueous solution (2 x 10^{-2} - 5 x 10^{-2} mol dm^{-3}) of the appropriate metal ion at pH ~5 in HEPES buffer from 15 min. to 18 hours, for uptake over time, and for 1 hour for general uptake. The silica-based material was then separated by filtration into a volumetric flask, washed thoroughly, and the percent uptake of the metal ions was determined by the difference between the initial concentration and the equilibrium concentration in the filtrate.

7.5 Solid state guest molecule uptake measured by Ultraviolet-Visible spectroscopy

Measurement of UV-Visible spectra were performed with a Varian Cary 50 SCAN UV-Visible spectrophotometer utilising 1.0 cm path length quartz cuvettes over a wavelength of 200 - 500 nm at 0.15 nm intervals, with a scan rate of 50 nm per minute and a slit width of 5.0 nm. Concentrations of guest solutions were 5 x 10^{-3} mol dm^{-3} in de-ionised water that was maintained at pH 7 with 0.01 mol dm^{-3} HEPES buffer for benzoates, and in 10% DMSO in acetonitrile (v/v) for phenolates. For carboxyphenolates 0.02 mol dm^{-3} 3-(cyclohexylamino)propane sulfonic acid (CAPS) buffer was used (pH 12). All spectra were obtained using baseline corrections with a

blank containing the relevant solvent and buffer species. The guest solutions used were prepared immediately before use and were equilibrated at 298 K.

Prior to performing each guest inclusion experiment, a calibration curve was constructed for the appropriate guest species. The general method for guest inclusion experiments was to stir 10 cm^3 of the guest species at a concentration of 5 x 10^{-3} mol dm^{-3} in de-ionised water with 100 mg of the cadmium(II) complexed silica-based receptor material for 1 hour. The solid material was then isolated by filtration into a volumetric flask and washed with copious amounts of de-ionised water. Percent inclusion was determined by the difference between the initial concentration of the guest species and the concentration at equilibrium in the filtrate. For phenolates the procedure was identical apart from the solvent which was 10% DMSO in acetonitrile (v/v).

7.6 Diffuse reflectance infrared Fourier transform (DRIFT) spectroscopy

The silica-based materials were characterised by DRIFT spectroscopy as a finely ground KBr mixture in aluminium sample cups on either a Biorad FTS 40 A Infrared Spectrometer fitted with a Spectra-Tech 30-034 DRIFT accessory with an MCT detector or a Nicolet Nexus 8700 FTIR Spectrophotometer fitted with a Smart Collector DRIFT accessory.

7.7 Solid State ^{13}C CPMAS NMR

Solid state nuclear magnetic resonance (^{13}C CPMAS NMR) spectra for the linker attached and the combined receptor-linker attached silica materials were recorded at an operating frequency of 50.318 MHz on a Varian Unity 200 spectrometer using a Doty high speed probe in an open ended 7 mm zirconium oxide rotor with Kel-F endcaps. The samples were spun at 5 kHz with a contact time of 1 ms and a recycle

delay time of 4 s. ^{13}C CPMAS NMR spectra for the host-guest complexes were recorded on a Bruker 400 Avance spectrometer at an operating frequency of 100.61 MHz with TOSS (TOtal Suppression of Spinning Side-bands) software in a 4 mm zirconium oxide rotor with a Kel-F end-cap. The sample was spun at 5 kHz and a contact time of 1 ms with a recycle delay time of 4 s.

7.8 Synthesis of the pendant arm epoxides

(*2S*)-(+)-3-phenoxy-1,2-epoxypropane, 56

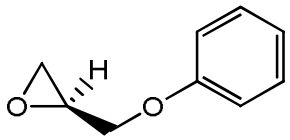

56

The procedure described by Smith,[94] was used to synthesise this compound. To a suspension of sodium hydride, (95%, 1.5 g, 62.50 mmol), in dry DMF (15 cm^3) a solution of phenol, **57**, (4.63 g, 49.20 mmol), dissolved in dry DMF (10 cm^3) was added dropwise and stirred at ambient temperature for 1 h. A solution of (*2S*)-(+)-glycidyl tosylate, **58** (9.12 g, 40.00 mmol), dissolved in dry DMF (15 cm^3) was added and the mixture was stirred at ambient temperature for 20 h. The progress of the reaction was monitored by tlc on silica (10% hexane/DCM). The reaction was quenched with NH_4Cl (10 cm^3), diluted with de-ionised water (1 x 150 cm^3) and extracted with ether (5 x 150 cm^3). The combined ether extracts were washed with ice-cold NaOH (0.1 M, 4 x 100 cm^3, de-ionised water (1 x 200 cm^3), brine (1 x 100 cm^3), dried over Na_2SO_4 and concentrated *in vacuo* to yield a pale yellow oil. Purification by column chromatography over silica (eluent 10% hexane/DCM rf: 0.37) afforded **56** as a clear oil: yield 4.5 g, 75%. ^1H NMR ($CDCl_3$): δ 7.34-7.29 (2

H, m, Ar-*H*); 7.02-6.93 (3 H, m, Ar-*H*); 4.22 (1 H, dd, *J* = 3.08, 11.04 Hz, -*H*CH-); 3.92 (1 H, dd, *J* = 5.8, 11.04 Hz, -HC*H*-); 3.36-3.33 (1 H, m, -C*H*O-); 2.88 (1 H, dd, *J* = 4.16, 4.96 Hz, -HC*H*O-); 2.74 (1 H, dd, *J* = 2.68, 4.98 Hz, -*H*CHO-). ^{13}C NMR ($CDCl_3$): δ 158.34 (1 C, Ar, *ipso*); 129.35 (2 C, Ar, *meta*); 121.04 (1 C, Ar, *para*); 114.47 (2 C, Ar, *ortho*); 68.52 (1 C, -*C*H_2-); 49.96 (1 C, -*C*HO-); 44.46 (1 C, -*C*H_2O-).

2-[(2-hydroxyethoxy)ethoxy]-toluene-4-sulfonate, 64

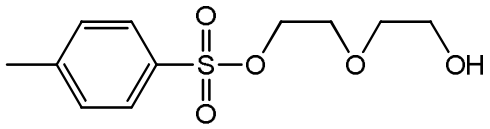

64

Preparation of the title compound was from a method adapted from Ameijde *et al*.[174] Triethylamine, (2.70 g, 26.4 mmol), was added to a stirred solution of di-ethylene glycol (digol), **61**, (5.59 g, 52.70 mmol), dissolved in 50 cm^3 dichloromethane. The solution was stirred for 15 mins at room temperature after which time tosyl chloride, **63**, (3.01 g, 15.80 mmol), was added in a single measure and stirred at 0^o C for 2 hours and thence stirred for 15 hours at room temperature. The solution was then washed with $KHSO_4$, (1M, 3 x 100 cm^3), and 5% $NaHCO_3$, (1 x 100 cm^3), and dried over Na_2SO_4. Purification of the product was achieved by column chromatography over silica (eluent 40% EtOAc/DCM, rf: 0.22), and concentrated *in vacuo* to yield **64** as a colourless oil, 3.33 g, 81%.^{1}H NMR ($CDCl_3$): δ 7.80 (2 H, d *J* = 8.0 Hz); 7.35 (2 H, d, *J* = 8.0 Hz); 4.20-4.17 (2 H, m, -OCH_2-); 3.70-3.65 (4 H, m, -OCH_2-); 3.54-3.51 (2 H, m, -OCH_2-); 2.44 (3 H, s, -CH_3); 2.14 (1 H, s, OH). ^{13}C NMR ($CDCl_3$): δ 144.69 (1 C, Ar, *para*); 132.45 (1 C, Ar, i*pso*); 129.56 (2 C, Ar, *meta*); 127.52 (2 C, Ar, *ortho*); 72.17 (1 C, -*C*H_2-CH_2OH); 69.06 (1

C, -*C*H_2- CH_2OSO_2); 68.11 (1 C, -*C*H_2-OSO_2); 61.08 (1 C, *C*H_2-OH); 21.21 (1 C, -*C*H_3).

1-[2-(2-hydroxyethoxy)ethoxy]-4-benzyloxybenzene•0.5H_2, 66

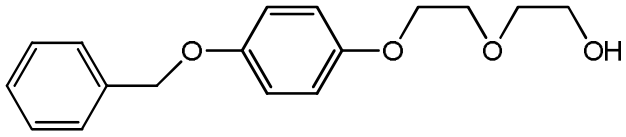

66

The named compound was synthesised by a procedure modified from Amabilino and co-workers.[244] A solution of 4-(benzyloxy)phenol, **68**, (2.34 g, 11.70 mmol), dissolved in anhydrous DMF (10 cm^3) was added slowly over 10 min. to a stirring suspension of finely ground anhydrous K_2CO_3, (4.04 g, 29.30 mmol), in anhydrous DMF (5 cm^3). The mixture was stirred at 80^o C for 1 h in an atmosphere of nitrogen. A solution of the tosylate **64** (3.10 g, 11.90 mmol), dissolved in dry DMF (10 cm^3) was then added dropwise and stirred for 4 days at 80^o C. The mixture was diluted with water, (1 x 200 cm^3), and extracted with CH_2Cl_2, (5 x 100 cm^3). The CH_2Cl_2 extracts were washed with $KHSO_4$, (1M, 3 x 100 cm^3), brine, (3 x 100 cm^3), and water, (3 x 100 cm^3), and dried over $MgSO_4$.The solvent was removed *in vacuo* to yield a brown oil which was purified by column chromatography over silica (eluent 40% EtOAc/DCM, rf: 0.35), and concentrated *in vacuo* to obtain **66** as an off-white oil which solidified overnight into a white waxy solid, (2.6 g, 76%). ^{1}H NMR ($CDCl_3$): δ 7.38-7.30 (5 H, m,, Bn-*H*); 6.92-6.85 (4 H, m, Ar-*H*); 5.01 (2 H, s, Bn-C*H*$_2$-); 4.10-3.84 (2 H, m, -OC*H*$_2$); 3.78-3.76 (2H, m, -OC*H*$_2$); 3.76-3.66 (4 H, m, -OC*H*$_2$); 2.10 (1 H, br s, -OH). ^{13}C NMR ($CDCl_3$): δ 153.19 (1 C, Ar, *para*); 152.94 (1 C, Ar, *ipso*); 137.18 (1 C, Bn, ipso);128.48 (2 C, Bn, *meta*); 127.83 (1 C, Bn,

para); 127.41 (2 C, Bn, *ortho*); 115.80 (2 C, Ar, *ortho*); 115.59 (2 C, Ar, *meta*); 72.52 (1 C, -*C*H_2-OAr); 70.60 (2 C, -*C*H_2-Bn); 69.72 (1 C, -*C*H_2-CH_2-OAr); 68.03 (1 C, -*C*H_2-OAr); 61.71 (1 C, -*C*H_2-OH). (Found C, 70.54; H, 7.56. $C_{17}H_{20}O_4$•0.5H_2 requires C, 70.57; H, 7.32%).

1-[2-(2-hydroxyethoxy)ethoxy]-4-hydroxybenzene, 69

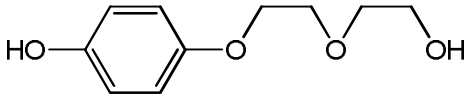

69

A solution of **66** (2.5 g, 8.67 mmol), dissolved in anhydrous DCM (25 cm^3) was added to a suspension of Pd/C, (10%, 0.30 g), in anhydrous MeOH (25 cm^3) and stirred at ambient temperature under an atmosphere of H_2 gas for 2 days. The catalyst was removed by filtration through celite. The solvent was removed *in vacuo* to yield **69** as a brown oil in quantitative yield. ^{1}H NMR ($CD_3OD/CDCl_3$): δ6.68-6.61 (4 H, m, Ar-*H*); 4.06 (2 H, br s, 2 x -OH); 3.95-3.93 (2 H, m, -OCH_2); 3.70-3.67 (2 H, m, -OCH_2); 3.62-3.59 (2 H, m -OCH_2); 3.53-3.50 (2 H, m, -OCH_2). ^{13}C NMR ($CD_3OD/CDCl_3$): δ151.42 (1 C, Ar, *para*); 150.56 (1 C, Ar, *ipso*); 115.32 (2 C, Ar, *meta*); 115.31 (2 C, Ar, *ortho*); 72.10 (1 C, -*C*H_2-CH_2OH); 69.12 (1 C, -*C*H_2-CH_2OAr); 68.11 (1 C, -*C*H_2-OAr); 61.08 (1C, -*C*H_2-OH).

(*2S*)-(+)-3-(phenoxy-4-[2-(2-hydroxyethoxy)ethoxy]-1,2-epoxypropane, 59

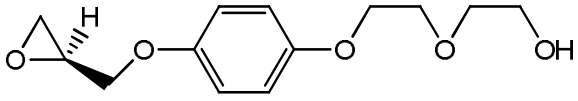

59

A solution of **69** (2.00 g, 10.1 mmol), was added slowly over 20 min. to a stirring suspension of anhydrous K_2CO_3, (3.5 g, 25.3 mmol), in anhydrous DMF (10 cm^3). The mixture was stirred at 50^o C for 2 h. (*2S*)-(+)-glycidyl tosylate, **58**, (2.30 g, 10.0 mmol), dissolved in anhydrous DMF (10 cm^3) was then added dropwise and the mixture was stirred at 50^o C for 4 days. The reaction was quenched with saturated NH_4Cl, (1 x 10 cm^3), and then diluted with water, (1 x 200 cm^3). The product was extracted with CH_2Cl_2, (4 x 150 cm^3). The organic extracts were then washed with brine, (2 x 100 cm^3), and water, (1 x 100 cm^3), concentrated *in vacuo* and purified by column chromatography over silica (eluent 40% EtOAc/DCM, rf: 0.20). The pure product was concentrated *in vacuo* to yield **59**, 1.73 g, 68%, as a pale yellow oil. ^{1}H NMR ($CDCl_3$): δ6.81 (4 H, s, Ar-*H*); 4.13 (1 H, dd, *J* = 3.0, 11.5 Hz, -*H*CH-); 4.05-4.02 (2 H, m, -OC*H*$_2$-); 3.84 (1 H, dd, *J* = 5.7, 11.5 Hz, -HC*H*O-); 3.80-3.77 (2 H, m, -OC*H*$_2$-); 3.70 (2 H, br s, -OC*H*$_2$-); 3.62-3.60 (2 H, m, -OC*H*$_2$-); 3.29 (1 H, m, -C*H*O-); 2.90 (1H, br s, -O*H*); 2.85 (1 H, t, *J* = 4.5 Hz, -HC*H*O-); 2.70 (1 H, dd, *J* = 2.7, 4.8)-*H*CHO-). ^{13}C NMR ($CDCl_3$): δ153.04 (1 C, Ar, *ipso*); 152.75 (1 C, Ar, *para*); 115.52 (2 C, Ar, *meta*); 115.47 (2 C, Ar, *ortho*); 72.48 (1 C, -*C*H$_2$- *C*H$_2$OH); 69.55 (1C, -*C*H$_2$-CH-); 69.29 (1 C, -*C*H$_2$-CH$_2$OAr); 67.87 (1 C, -*C*H$_2$-OAr-); 61.53 (1 C, -*C*H$_2$-OH); 50.09 (1 C, -*C*H-); 44.48 (1 C, -*C*H$_2$-OCH-). $[\alpha]^{25}_D$ = +4.21^o (c 2.19, MeOH)

[2-(2-(2-hydroxyethoxy)ethoxy)ethoxy]-toluene-4-sulfonate, 65

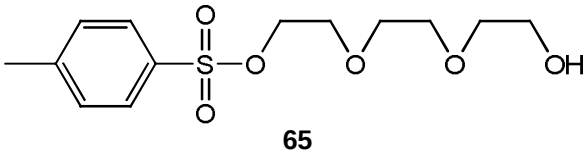

65

The preparation of this compound was from triethylene glycol (trigol) **62** (6.7 g, 44.91 mmol), triethylamine (2.3 g, 22.45 mmol) and tosyl chloride, **63**, (2.6 g, 13.47 mmol), by the same procedure as for **64** (rf: 0.19)**.** The product **65** was gained as a colourless oil, 3.12 g, 76%. ^{1}H NMR ($CDCl_3$): δ 7.75 (2 H, d, *J* = 8.4 Hz, Ar-H; 7.29 (2 H, d, *J* = 8.4 Hz, Ar-H); 4.13-4.10 (2 H, m, -OC*H*$_2$-); 3.67-3.64 (4 H, -OC*H*$_2$-); 3.56-3.50 (6 H, m, -OC*H*$_2$-); 2.60 (1 H, s, -O*H*); 2.40 (3 H, s, -C*H*$_3$). ^{13}C NMR ($CDCl_3$): δ 144.87 (1 C, Ar, *para*); 132.77 (1 C, Ar, i*pso*); 129.80 (2 C, Ar, *meta*); 127.89 (2 C, Ar, *ortho*); 72.33 (1 C, *C*H$_2$-CH$_2$OH; 70.68 (1 C, *C*H$_2$-OCH$_2$CH$_2$OH); 70.14 (1 C, -*C*H$_2$-OCH$_2$CH$_2$OSO2); 69.11 (1 C, -*C*H$_2$-CH$_2$OSO$_2$; 68.62 (1 C, *C*H$_2$-OSO$_2$); 61.63 (1 C, *C*H$_2$-OH); 21.58 (1 C, -*C*H$_3$).

1-[2-(2-(2-hydroxyethoxy)ethoxy)ethoxy]-4-benzyloxybenzene, 67

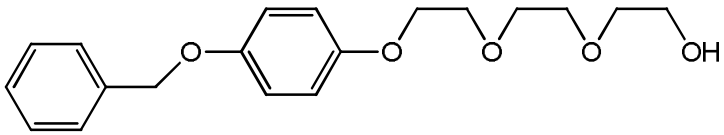

67

Preparation of this compound was by a method analogous to that used for the preparation of **66** from 4-(benzyloxy)phenol, **68** (3.25 g, 16.23 mmol), K_2CO_3, (5.6 g, 40.60 mmol), and **65** (5.01 g, 16.45 mmol)**,** (rf: 0.18)**,** to obtain **67** as an off-white oil which solidified overnight into a white, waxy solid (4.6 g, 85%). ^{1}H NMR ($CDCl_3$): δ 7.44-7.31 (5 H, m, Bn-*H*); 6.92-6.84 (4 H, m, Ar-*H*); 5.01 (2 H, s, Bn-C*H*$_2$-); 4.10-4.07 (2 H, m, -OC*H*$_2$-); 3.86-3.82 (2 H, m, -OC*H*$_2$-); 3.75-3.70 (6H, m, -OC*H*$_2$-); 3.63-3.60 (2 H, m, -OC*H*$_2$-); 2.52 (1 H, br s, OH). ^{13}C NMR ($CDCl_3$): δ 153.12 (1 C, Ar, *para*); 153.01 (1 C, Ar, *ipso*); 137.21 (1 C, Bn, *ipso*); 128.46 (2 C,

Bn, *meta*); 127.79 (1 C, Bn, *para*); 127.39 (2 C, Bn, *ortho*); 115.75 (2 C, Ar, *ortho*); 115.57 (2 C, Ar, *meta*); 72.43 (1 C, -*C*H_2-CH_2OH); 70.72 (1 C, -*C*H_2OCH_2CH_2OH; 70.59 (1 C, -CH_2-Bn); 70.32 (1 C, -*C*H_2OCH_2CH_2OAr); 69.79 (1 C, -*C*H_2-CH_2OAr); 67.97 (1 C, -*C*H_2-OAr, 61.69 (1 C, -*C*H_2-OH). (Found C, 68.60; H, 7.24. $C_{19}H_{24}O_5$ requires C, 68.66; H, 7.28%).

1-[2-(2-(2-hydroxyethoxy)ethoxy)ethoxy]-4-hydroxybenzene, 70

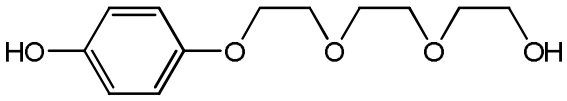

70

Deprotection of this compound was analogous to the preparation of **69** using **67** (3.6 g, 10.83 mmol), and Pd/C, (10%, 0.40 g), to obtain **70** as a brown oil in quantitative yield. ^{1}H NMR ($CD_3OD/CDCl_3$): δ6.70-6.64 (4 H, m, Ar-*H*); 4.68 (2 H, br s, 2 x -O*H*); 3.95-3.93 (2 H, m, -OC*H*$_2$-); 3.75-3.72 (2 H, m, -OC*H*$_2$-); 3.69-3.64 (4 H, m, -OC*H*$_2$-); 3.62-3.60 (2 H, m, -OC*H*$_2$-); 3.55 (2 H, m, -OC*H*$_2$-) ^{13}C NMR ($CD_3OD/CDCl_3$),: δ 152.37 (1 C, Ar, *para*); 150.14 (1 C, Ar, *ipso*); 116.07 (2 C, Ar *meta*); 115.66 (2 C, Ar, *ortho*); 72.50 (1 C, -*C*H_2-CH_2OH); 70.73 (1 C, -*C*H_2-OCH_2CH_2OH); 70.21 (1 C, -*C*H_2-CH_2CH_2OAr; 69.88 (1 C, *C*H_2-CH_2OAr; 67.85 (1 C, -*C*H_2-OAr; 61.68 (1 C, -*C*H_2-OH).

(*2S*)-(+)-3-(phenoxy-4-[2-(2-(2-hydroxyethoxy)ethoxy)ethoxy]-1,2-epoxypropane, 60

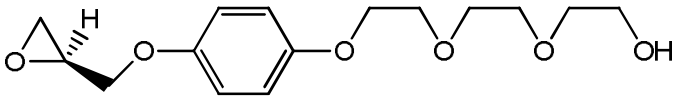

60

The preparation of this compound was by the same method as for **59** using **70** (4.21 g, 17.40 mmol), K_2CO_3, (6.01 g, 43.5 mmol), and (*2S*)-(+)-glycidyl tosylate, **58**, (3.97 g, 17.39 mmol), to yield **60** as a pale yellow oil, 3.71 g, 74%, rf: 0.21. ^{1}H NMR ($CDCl_3$): δ 6.82 (4 H, s, Ar-*H*); 4.14 (1 H, dd, *J* = 3.2, 11.04 Hz, -*H*CH-); 4.06-4.04 (2 H, m, -OC*H*$_2$-); 3.86 (1 H, dd, *J* = 5.7, 11.04 Hz, -HC*H*); 3.82-3.79 (2 H, m, -OC*H*$_2$-); 3.71-3.64 (6 H, m, -OC*H*$_2$-); 3.59-3.57 (2 H, m, -OC*H*$_2$-); 3.32-3.28 (1 H, m, -C*H*-O-); 2.87 (1 H, t, *J* = 4.48 Hz, -HC*H*-O-); 2.71 (1 H, dd, *J* = 2.68, 4.91 Hz, -*H*CHO-); 2.15 (1 H, br s, O*H*). ^{13}C NMR ($CDCl_3$): δ 153.15 (1 C, Ar, *ipso*); 152.75 (1 C, Ar, *para*); 115.53 (2 C, Ar, *meta*); 115.48 (2 C, Ar, *ortho*); 72.39 (1 C, *C*H$_2$-CH$_2$OH; 70.66 (1 C, -*C*H$_2$-OCH$_2$CH$_2$OH); 70.24 (1 C, -*C*H$_2$-OCH$_2$CH$_2$OAr); 69.71 (1 C, -*C*H$_2$CH-); 69.35 (1 C, -*C*H$_2$-CH$_2$OAr); 67.87 (1 C, -*C*H$_2$-OAr); 61.61 (1 C, -*C*H$_2$-OH); 50.14 (1 C, -*C*H-); 44.56 (1 C, -*C*H$_2$-OCH$_2$-).$[\alpha]^{25}_D$ = +2.35^o (c 2.13, MeOH).

7.9 Synthesis of the mono-protected cyclen synthon

1,4,7-triformyl 1,4,7,10-tetraazacyclododecane, 52

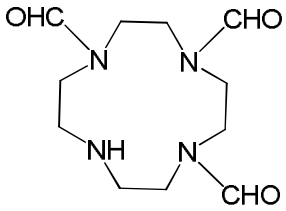

52

This compound was synthesised by a method previously established by Boldrini,[131] and modified by Yoo.[109] To a stirred solution of cyclen, **21**, (1.0 g 5.80 mmol), in anhydrous ethanol (30 cm^3), chloral hydrate, (3.84 g, 23.20 mmol), was

added in a single portion. The mixture was stirred at 60^{o} C for 4 h under a dry nitrogen atmosphere, concentrated *in vacuo* to complete dryness and subsequently held under vacuum (0.75 mmHg) for 2 days to yield **52** as a clear, resinous, oil 1.46 g, quantitative. ^{1}H NMR ($CDCl_3$): δ8.30-7.82 (3H, br, *H*C=O), 3.90-2.65 (17H, br, cyclen). ^{13}C ($CDCl_3$): δ164.01-162.89 (3C, -*C*HO), 53.10-40.00 (8C, cyclen -*C*H_2).

1,4,7-triformyl-10-(benzyloxycarbonyl)-1,4,7,10-tetraazacyclododecane, 53

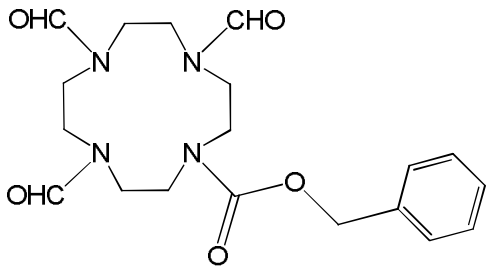

53

The synthesis of **53** was effected by applying a method reported by Yoo.[109] To a solution of **52** (682 mg, 2.7 mmol, pH 9) dissolved in de-ionised water, benzyl chloroformate, **54**, (710 mg, 4.15 mmol), was added and the mixture was stirred for 1 h at ambient temperature, after which the pH was adjusted from 4 to 10 with saturated Na_2CO_3 solution. Benzyl chloroformate, **54**, (710 mg, 4.15 mmol), was added and the mixture was stirred for 1 h at ambient temperature, after which the pH was adjusted from 6 to 10 with saturated Na_2CO_3 solution. Benzyl chloroformate, **54**, (710 mg, 4.15 mmol) was again added and the mixture was stirred overnight at ambient temperature under a nitrogen atmosphere. The product was extracted with dichloromethane, (5 x 20 cm^3), and the combined organic layers were washed with saturated $NaHCO_3$ (1 x 10 cm^3), dried over $MgSO_4$ and concentrated *in vacuo* to obtain crude **53** as a yellow oil, 583 mg which was used in the triformyl deprotection step without further purification.

For the purpose of spectral characterisation crude **53** was purified by refrigeration in ether for 7 days after which time a white solid precipitated. The white solid was filtered under nitrogen and washed with copious quantities of ether to give **53** as a fine extremely hygroscopic white powder in 92% yield. ^{13}C NMR ($CDCl_3$): δ166.10 (1 C, C=O); 165.25 (1 C, C=O); 163.76 (1 C, C=O); 163.76 (1 C, C=O); 162.97 (1 C, Bn); 157.54 (1 C, Bn); 135.87 (2 C, Bn); 129.15 - 128.71 (2 C, Bn); 67.86 - 67.67 (1 C, Bn-*C*H_2); 52.56-43.29 (8 C, cyclen -*C*H_2).

1-(benzyloxycarbonyl)-1,4,7,10-tetraazadodecane•3HCl•1.5H_2O, 55

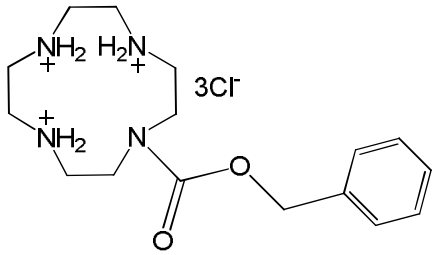

55

A solution of **53** (504 mg, 1.38 mmol), dissolved in HCl, (1M, 35 cm^3, 35 mmol), was stirred a 50^o C for 5 h after which the solvent was removed completely *in vacuo* at 60^o C to yield an off-white solid. The crude product was suspended in ethanol (20 cm^3), refluxed for 1 h, cooled to room temperature, filtered and dried in air to yield **55**: 1st crop 64 mg, 12%. Excess ether was added to the filtrate to assess the cloudiness of the solution and the white precipitate filtered and washed with ether (1 x 5 cm^3) and dried in air to yield **55**: 2nd crop 450 mg 84%. Both crops exhibited equal purity and were combined for an overall yield of, 514 mg, 96%. (Found C, 43.22; H, 7.45; N, 12.50. $C_{16}H_{29}Cl_3N_4O_2$•1.5H_2O requires C, 43.40; H, 7.28; N, 12.65%). ^{1}H NMR (D_2O/1,4-dioxane): δ7.45 (5 H, br s, Bn-*H*); 5.21 (2 H, br s, Bn-C*H*$_2$); 3.72 (4 H, br s, cyclenC*H*$_2$); 3.20 (12 H, br s, cyclenC*H*$_2$). ^{13}C NMR (D_2O/1,4-

dioxane): δ 158.67 (1 C, *C*=O); 135.87 (1 C, Bn, *ipso*); 129.10 (1 C, Bn, *para*); 129.01 (2 C, Bn, *meta*); 128.59 (2 C, Bn, *ortho*); 68.82 (1 C, Bn-*C*H_2); 46.73 (2 C, cyclen -*C*H_2); 45.34 (2 C, cyclen -*C*H_2); 44.81 (2 C, cyclen -*C*H_2); 42.97 (2 C, cyclen -*C*H_2).

1-(benzyloxycarbonyl)-1,4,7,10-tetraazacyclododecane, 50

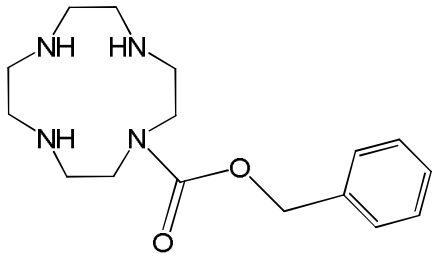

50

Chilled NaOH was added, dropwise, to a stirred solution of **55** (514 mg 1.24 mmol), dissolved in milliQ water (5 cm^3) raising the pH to 13. The solution was stirred for 2 h at room temperature and extracted with $CHCl_3$, (4 x 20 cm^3). The combined organic extracts were washed with chilled NaOH, (1.25 M, (1 x 10 cm^3), $NaHCO_3$, (1 x 5 cm^3), brine, (1 x 5 cm^3), dried over Na_2SO_4, filtered and concentrated *in vacuo* to give the free base **50** as a yellow oil in 98% yield. ^{1}H NMR ($CDCl_3$): δ 7.34 (5 H, br s, Bn); 5.08 (2 H, s, -C*H*$_2$-Bn); 3.61-3.56 (4 H, br m, cyclenC*H*$_2$); 3.31 (3 H, -N*H*-); 3.14 - 3.08 (12 H, ^{13}C NMR ($CDCl_3$): δ156.90 (1 C, C=O); 136.50 (1 C, Bn, *ipso*); 128.24 (1 C, Bn, *para*); 128.05 (2 C, Bn, *meta*); 127.77 (2 C, Bn, *ortho*); 66.93 (1 C, Bn-*C*H_2); 48.91 (2 C, cyclen -*C*H_2); 48.64 (2 C, cyclen -*C*H_2); 47.69 (2 C, cyclen -*C*H_2); 46.03 (2 C, cyclen -*C*H_2).

7.10 Synthesis of macrocyclic receptor ligands

1-(benzyloxycarbonyl)-4,7,10-*tris*-((*S*)-2-hydroxy-3-phenoxypropyl)-1,4,7,10-tetraazacyclododecane, 71

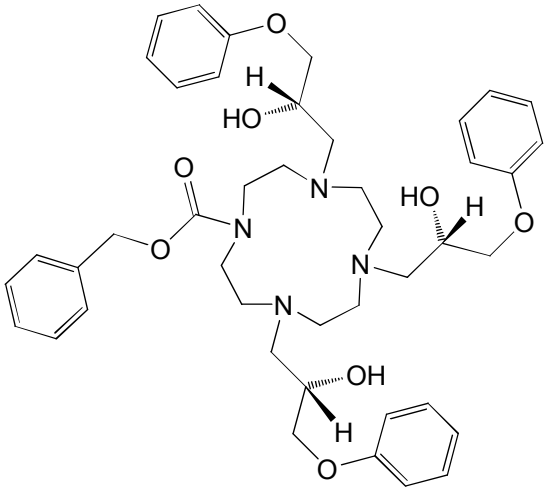

71

This compound was synthesised by an established method modified from Smith.[94] A solution of **56** (638 mg, 4.25 mmol), in anhydrous ethanol (10 cm^3) was added drop-wise to a refluxing solution of **50** (424 mg, 1.40 mmol), dissolved in anhydrous ethanol (10 cm^3). The reaction was monitored for the disappearance of the starting epoxide by TLC on silica (eluent 10% hexane/DCM rf: 0.39) for the disappearance of **56**, 10 days. Evaporation of the solvent *in vacuo* gave **71** as a viscous yellow oil; yield 1.0 g, quantitative. ^{13}C NMR ($CDCl_3$): δ 158.48 (3 C, Ph, *ipso*); 156.35 (1 C, *C*=O); 136.45 (1 C, Bn, *ipso*); 129.28 (6 C, Ph); 129.25 (1 C, Bn); 128.34 (2 C, Bn); 127.88 (2 C, Bn); 120.72 (3 C, Ph); 114.38 (6 C, Ph); 69.62 (2 C, O*C*H_2); 68.82 (1 C, O*C*H_2); 67.10 (1 C, O*C*H_2Bn); 66.70 (2 C, *C*H); 65.93 (1 C, *C*H); 59.10 (2 C, *C*H_2N); 57.89 (1 C, *C*H_2N); 54.06 (2 C, cyclen -*C*H_2); 53.31 (2 C, cyclen -*C*H_2); 50.40 (2 C, cyclen -*C*H_2); 47.42 (2 C, cyclen -*C*H_2).

1-(benzyloxycarbonyl)-4,7,10-*tris*-((*S*)-2-hydroxy-3-phenoxypropyl)-1,4,7,10-tetraazacyclododecane•3HCl, 90

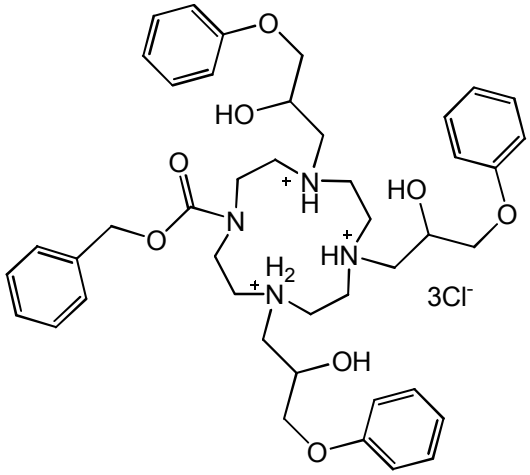

90

To a solution of **71** (796 mg, 1.05 mmol), dissolved in dry EtOH (5 cm^3) and stirred at 0^o C was added 36% HCl, (10 cm^3, 116.50 mmol). The mixture was stirred for 2 h, after which the solvent was removed *in vacuo*. The white solid obtained was redissolved in EtOH and precipitated with Et_2O filtered, and washed with ice-cold EtOH (5 cm^3) and Et_2O (5 cm^3) to yield **90** as a white solid, 840 mg, 92%. ^{13}C NMR (CD_3OD): δ159.90 (1 C, *C*=O); 159.63 (3 C, Ph, *ipso*); 136.7 (1 C, Bn, *ipso*); 130.57 (6 C, Ph); 129.91 (1 C, Bn); 129.70 (4 C, Bn); 122.30 (2 C, Ph); 122.17 (1 C, Ph); 115.70 (6 C, Ph); 70.98 (3 C, O*C*H_2); 70.01 (1 C, -*C*H_2Bn); 67.90 (1 C, *C*H); 65.95 (2 C, *C*H); 58.1 (1 C, *C*H_2N); 57.80 (2 C, *C*H_2N); 53.69 (2 C, cyclen -*C*H_2); 52.10 (2 C, cyclen -*C*H_2); 50.80 (2 C, cyclen -*C*H_2); 46.01 (2 C, cyclen -*C*H_2). (Found C, 59.52; H, 6.98; N, 6.30. $C_{43}H_{60}Cl_3N_4O_8$ requires C, 59.55; H, 6.97; N, 6.46%).

1,4,7-*tris*-((*S*)-2-hydroxy-3-phenoxypropyl)-1,4,7,10-tetraazacyclododecane, 46

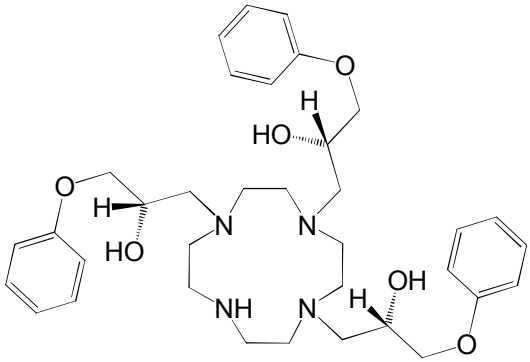

46

To a stirred suspension of Pd/C catalyst, (10%, 500 mg), in absolute ethanol (10 cm^3), a solution of **71** (523 mg, 0.69 mmol) dissolved in absolute ethanol (5 cm^3) was added. The mixture was stirred for 5 min. and then cyclohexene, **74**, (283 mg, 3.45 mmol), was added. The mixture was stirred under gentle reflux for 5 h, cooled to room temperature and filtered through a small celite column and washed with absolute ethanol (5 cm^3). The product was concentrated *in vacuo* to give **46** as a brown viscous oil, yield 426 mg, quantitative. ^{13}C NMR ($CDCl_3$): δ158.70 (2 C, Ar, *ipso*); 158.62 (1 C, Ar, *ipso*); 129.31 (4 C, Ar); 129.28 (2 C, Ar); 120.73 (2 C, Ar); 120.64 (1 C, Ar); 114.63 (4 C, Ar); 114.45 (2 C, Ar); 69.88 (2 C, O*C*H_2); 69.23 (1 C, O*C*H_2); 65.45 (2 C, *C*H); 65.24 (1 C, *C*H); 58.60 (2 C, *C*H_2N); 58.24 (1 C, *C*H_2N); 51.33 (2 C, cyclen -*C*H_2); 49.79 (2 C, cyclen -*C*H_2); (2 C, cyclen -*C*H_2); 44.33 (2 C, cyclen -*C*H_2).

1,4,7-*tris*-((*S*)-2-hydroxy-3-phenoxypropyl)-1,4,7,10-tetraazacyclododecane•4HCl, 91

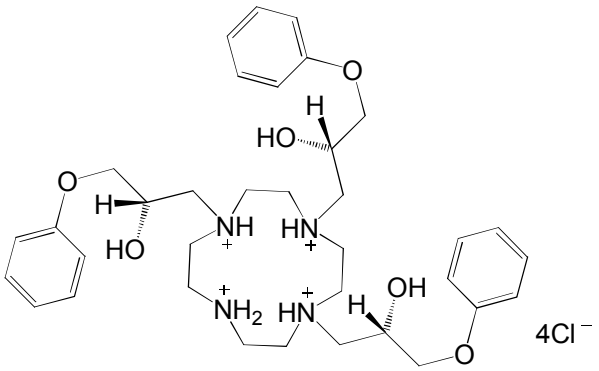

91

A solution of **46** (400 mg, 0.64 mmol), in ice-cold dry EtOH (5 cm^3) was treated dropwise with 37% HCl, (10 cm^3, 121.00 mmol), over 10 min. and then stirred for a further 2 h. The resultant mixture was then concentrated *in vacuo* and redissolved in MeOH (0.5 cm^3), precipitated and then triturated with of Et_2O to give an off-white solid, which was filtered, washed with Et_2O (10 cm^3) and dried under reduced pressure, to yield **91** 426 mg, 86%. ^{13}C NMR (CD_3OD): δ 159.95 (2 C, Ar, *ipso*); 159.73 (1 C, Ar, *ipso*); 130.56 (6 C, Ar); 122.33 (2 C, Ar); 122.11 (1 C, Ar); 115.68 (6 C, Ar); 71.20 (2 C, O*C*H_2); 70.85 (1 C, O*C*H_2); 67.44 (1 C, *C*H); 65.67 (2 C, *C*H); 58.37 (1 C, *C*H_2N); 57.80 (2C, *C*H_2N); 52.20 (2 C, cyclen -*C*H_2); 51.89 (2 C, cyclen -*C*H_2); 44.20 (2 C, cyclen -*C*H_2); 43.74 (2 C, cyclen -*C*H_2). (Found C, 54.54; H, 6.88; N, 7.57 $C_{35}H_{54}Cl_4N_4O_6$ requires C, 54.69; H, 7.08; N, 7.29%).

1-(benzyloxycarbonyl)-4,7,10-*tris*(*S*)-2-hydroxy-3-[4-((2-(2-hydroxyethoxy)ethoxy)phenoxypropyl]-1,4,7,10-tetraazacyclododecane, 72

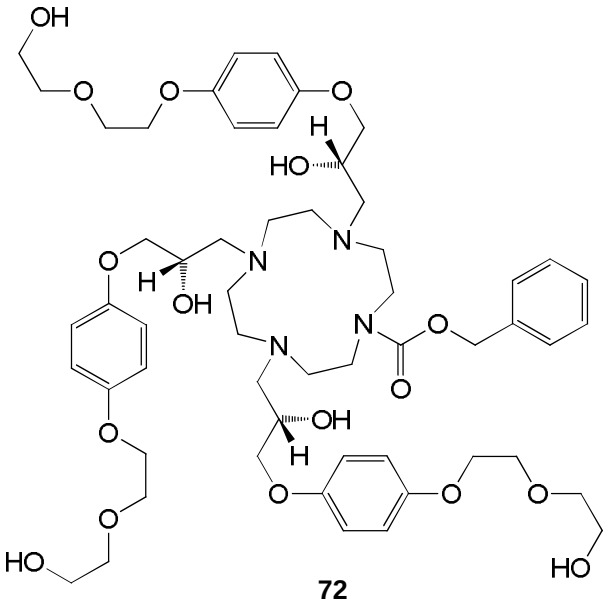

72

Synthesis of this compound was by a method analogous to that used for the preparation of **71** using **50** (415 mg, 1.35 mmol) and **59** (1.04 g, 4.08 mmol), to give **72** as a thick brown oil, 1.44 g, in quantitative yield. ^{13}C NMR ($CDCl_3$): δ 156.26 (1 C, *C*=O); 152.95 (3 C, Ph, *ipso*); 152.77 (3 C, Ph, *para*); 136.54 (1 C, Bn, *ipso*); 128.29 (1 C, Bn); 127.80 (1 C, Bn); 127.77 (1 C, Bn); 127.70 (2 C, Bn); 115.40 (6 C, Ph); 115.33 (6 C, Ph); 72.46 (3 C, -*C*H_2 HTPE); 71.23 (1C, -O*C*H_2); 70.42 (1C, -O*C*H_2); 70.30 (1C, -O*C*H_2); 69.47 (3 C, -*C*H_2 HTPE); 67.86 (3 C, -*C*H_2 HTPE); 66.93 (2 C, -*C*H); 66.72 (1 C, -*C*H); 65.98 (1 C, -*C*H_2, Bn); 61.28 (3 C, -*C*H_2 HTPE); 59.15 (3 C, -*C*H_2N); 52.76 (2 C, cyclen -*C*H_2); 50.05(2 C, cyclen -*C*H_2); 47.50 (2 C, cyclen -*C*H_2); 44.43 (2 C, cyclen -*C*H_2).

1,4,7-*tris*(*S*)-2-hydroxy-3-[4-((2-(2-hydroxyethoxy)ethoxy)phenoxypropyl]-1,4,7,10-tetraazacyclododecane, 47

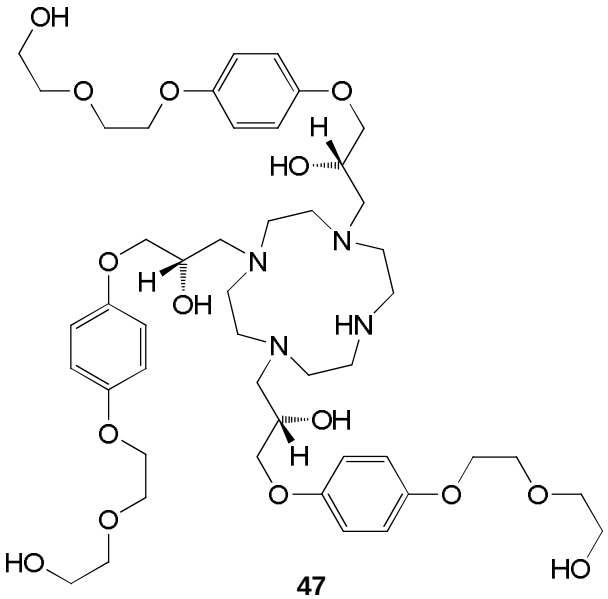

47

Synthesis of this compound was by a method analogous to that used for the preparation of **46** using **72** (396 mg, 0.37 mmol), and, cyclohexene, **74**, (158 mg, 1.92 mmol), to give **47** as a thick brown oil, 345 mg, in quantitative yield. δ 153.35 (3 C, Ph, *ipso*); 153.19 (3 C, Ph, *para*); 115.85 (12 C, Ph); 72.93 (3 C, -*C*H_2 HTPE); 71.67 (1C, -O*C*H_2); 71.13 (2C, -O*C*H_2); 69.92 (3 C, -*C*H_2 HTPE); 68.30 (3 C, -*C*H_2 HTPE); 67.11 (3 C, -*C*H); 61.66 (3 C, -*C*H_2 HTPE); 59.10 (3 C, -*C*H_2N); 52.50 (2 C, cyclen -*C*H_2); 51.80 (2 C, cyclen -*C*H_2); 50.20 (2 C, cyclen -*C*H_2); 44.20 (2 C, cyclen -*C*H_2).

1-(benzyloxycarbonyl)-4,7,10-*tris*(*S*)-2-hydroxy-3-[4-(2-(2-(2-hydroxyethoxy)-ethoxy)ethoxy)phenoxypropyl]-1,4,7,10-tetraazacyclododecane, 73

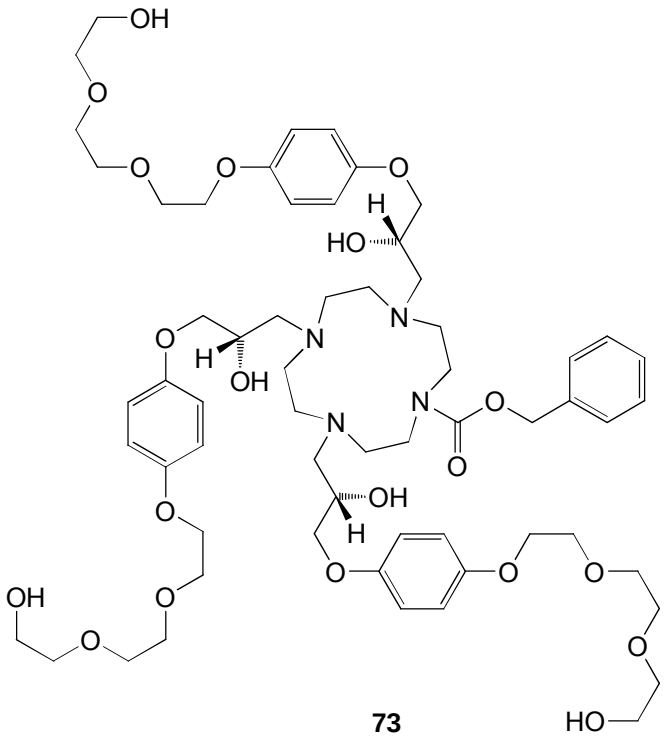

73

Synthesis of this compound was by a method analogous to that used for the preparation of **71** using **50** (503 mg, 1.64 mmol), and **60** (1.50 g, 4.94 mmol), to give **73** as a thick brown oil, 1.93 g, in quantitative yield. ^{13}C NMR ($CDCl_3$): δ 156.18 (1 C, *C*=O); 152.89 (3 C, Ph, *ipso*); 152.74 (3 C, Ph, *para*); 136.49 (1 C, Bn, *ipso*); 128.26 (1 C, Bn); 127.75 (4 C, Bn); 115.37 (6 C, Ph); 115.27 (6 C, Ph); 72.34 (3 C, -O*C*H_2 HTPE); 70.47 (3 C, -O*C*H_2 HTPE); 70.31 (1 C, Bn, -*C*H_2); 70.03 (3 C, -O*C*H_2 HTPE); 69.53 (3 C, -O*C*H_2 HTPE); 67.76 (3 C, -O*C*H_2 HTPE); 66.91 (2 C, O*C*H_2); 66.80 (1 C -O*C*H_2) 66.02 (3 C, -*C*H); 61.33 (3 C, -O*C*H_2 HTPE); 59.08 (2 C, -N*C*H_2); 58.00 (1 C, -N*C*H_2); 53.61 (2 C, cyclen *C*H_2); 52.68 (2 C, cyclen *C*H_2); 50.61 (2 C, cyclen *C*H_2); 47.47 (2 C, cyclen*C*H_2).

1,4,7-*tris*(*S*)-2-hydroxy-3-[4-(2-(2-(2-hydroxyethoxy)ethoxy)-ethoxy)phenoxypropyl]-1,4,7,10-tetraazacyclododecane, 48

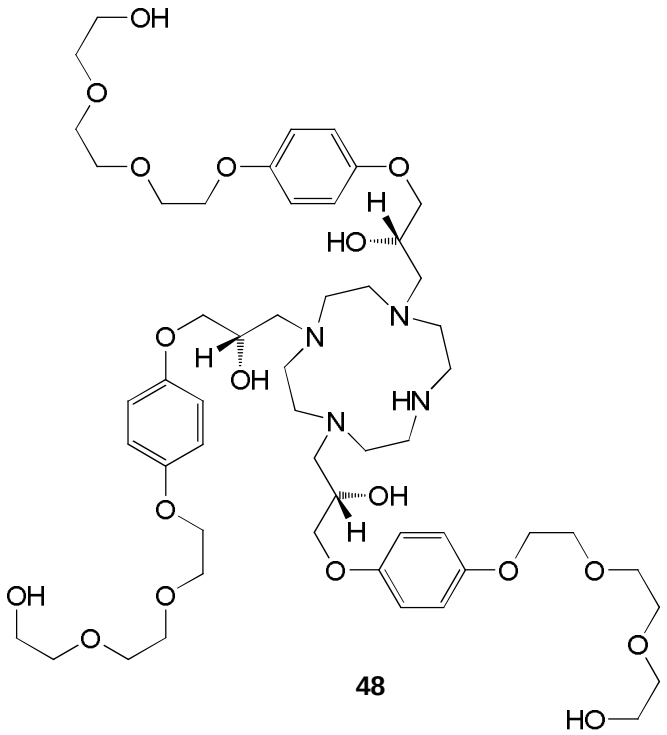

48

Synthesis of this compound was by a method analogous to that used for the preparation of **46** using **73** (457 mg, 0.39 mmol), and, cyclohexene, **74**, (183 mg, 2.22 mmol), to give **48** as a thick brown oil, 415 mg, in quantitative yield. ^{13}C NMR (CD_3CN): δ 153.15 (1 C, Ph, *ipso*); 153.090 (1 C, Ph, *ipso*); 153.05 (1 C, Ph, *ipso*); 152.98 (1 C, Ph, *para*); 152.91 (1 C, Ph, *para*); 152.85 (1 C, Ph, *para*); 115.63 (2 C, Ph); 115.59 (4 C, Ph); 115.48 (6 C, Ph); 72.54 (2 C, -O*C*H_2 HTPE); 72.51 (1 C, -O*C*H_2 HTPE); 70.72 (2 C, -O*C*H_2 HTPE); 70.70 (1 C, -O*C*H_2 HTPE); 69.78 (3 C, -O*C*H_2 HTPE); 67.96 (3 C, -O*C*H_2 HTPE) 61.56 (2 C, -O*C*H_2 HTPE); 61.50 (1 C, -O*C*H_2 HTPE); 71.27 (2 C, -O*C*H_2); 70.27 (2 C, -O*C*H_2); 69.66 (2 C, -*C*H); 69.42 (1 C, -*C*H); 59.00 (2 C, -N*C*H_2); 58.45 (1 C, -N*C*H_2); 50.1 (4 C, cyclen -*C*H_2); 44.05 (4 C, cyclen -*C*H_2).

1-(2-hydroxypropyl)-4,7,10-*tris*-((*S*)-2-hydroxy-3-phenoxypropyl)-1,4,7,10-tetraazacyclododecane, 51

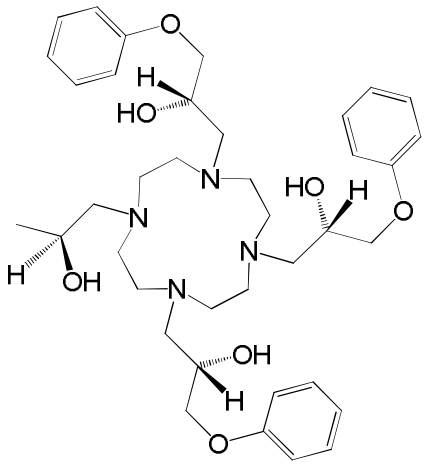

51

To a pressure vessel containing a solution of **46** (600 mg, 0.963 mmol) in dry CH_3CN (1 cm^3) and LiBr (262 mg, 0.302 mmol), (*S*)-(-)-propylene oxide, **75**, (0.088 g, 1.51 mmol) was added. The mixture was stirred at 80^oC for 3 days. The reaction was then diluted with 20 cm^3 of de-ionised water and extracted with $CHCl_3$ (3 x 10 cm^3). The extracts were dried over $MgSO_4$ and then concentrated *in vacuo* to yield, **51**, as a brown oil, 630 mg, 96%. ^1H NMR ($CDCl_3$): δ 7.3 (6 H, m, Ar*H*); 6.9 (9 H, m, Ar*H*); 4.8 - 2.8 (37 H br m, -C*H*$_2$, -O*H* & -C*H*); 1.3 (3 H, br s, (-C*H*$_3$). ^{13}C NMR (CD_3Cl_3): δ 158.35 (2 C, Ar, *ipso*); 158.32 (1 C, Ar, *ipso*); 129.25 (6 C, Ar); 120.92 (2 C, Ar); 120.73 (1 C, Ar) 114.57 (2 C, Ar); 114.49 (2 C, Ar); 114.39 (2 C, Ar); 70.13 (1 C, O*C*H$_2$); 70.04 (2 C, O*C*H$_2$); 67.84 (1 C, *C*H); 65.89 (1 C, *C*H); 65.67 (1 C, *C*H); 65.34 (1C, *C*H); 63.26 (1 C, -*C*H$_2$N) 58.04 (1 C, *C*H$_2$N); 56.92 (2 C, *C*H$_2$N); 52.33 (2 C, cyclen *C*H$_2$); 51.04 (2 C, cyclen *C*H$_2$); 50.36 (2 C, cyclen *C*H$_2$); 49.71 (2 C, cyclen *C*H$_2$); 21.87 (1 C, -*C*H$_3$).

1-(2-hydroxypropyl)-4,7,10-*tris*-((*S*)-2-hydroxy-3-phenoxypropyl)-1,4,7,10-tetraazacyclododecane•4HCl•1.5H_2O, 92

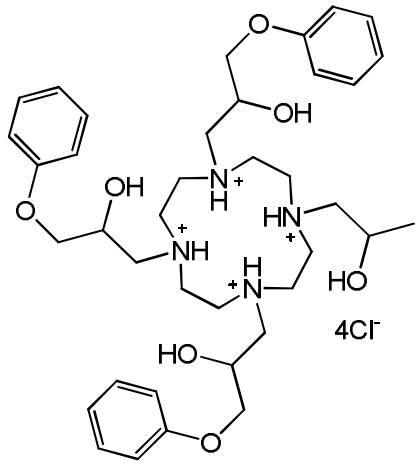

92

The preparation of the title compound was by a procedure identical to that for **91**, but using **51** (534 mg, 0.79 mmol) to give **92** as an off-white powder, 583 mg, 89%. (Found C, 53.46, H, 7.23; N, 6.57 $C_{38}H_{60}Cl_4N_4O_7$•1.5H_2O requires C, 53.46; H, 7.44; N, 6.56%). ^{1}H NMR (CD_3OD): δ 7.3 (6 H, m, Ar*H*); 6.9 (9 H, m Ar*H*); 4.8 - 2.8 (41 H br m, -C*H*$_2$, -N*H*, -O*H* & -C*H*); 1.3 (3 H, br s, (-C*H*$_3$). ^{13}C NMR (CD_3OD): 159.83 (1 C, Ar, *ipso*); 159.76 (1 C, Ar, *ipso*); 159.68 (1 C, Ar, *ipso*); 130.53 (6 C, Ar); 122.30 (2 C, Ar); 122.18 (1 C, Ar) 115.72 (4 C, Ar); 115.66 (2 C, Ar); 70.93 (1 C, -O*C*H$_2$); 70.85 (2 C, -O*C*H$_2$); 66.67 (1 C, -*C*H); 66.35 (1 C, -*C*H); 66.19 (1 C, -*C*H); 65.59 (1 C, -*C*H); 64.83 (1 C,-N*C*H$_2$); 58.18 (1 C, -N*C*H$_2$); 57.64 (2 C, -N*C*H$_2$); 52.20-51.15 (4C, cyclen -*C*H$_2$); 51.00 -50.00 (4C, cyclen -*C*H$_2$); 22.10 (1 C, -*C*H$_3$).

[Cd(1-(2-hydroxypropyl)-4,7,10-*tris*-((*S*)-2-hydroxy-3-phenoxypropyl)-1,4,7,10-tetraazacyclododecane)]$(ClO_4)_2$•0.5H_2O, 49

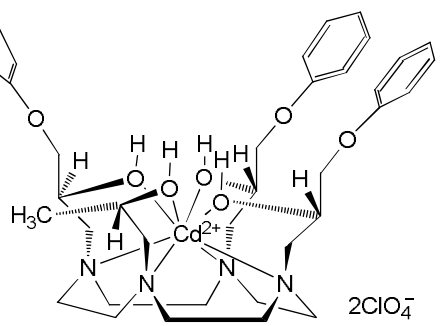

49

To a refluxing solution of **51** (248 mg, 0.36 mmol) in dry ethanol (10 cm^3), cadmium perchlorate hexahydrate (168 mg, 0.40 mmol) dissolved in dry ethanol (5 cm^3) was added dropwise over 5 min. A white precipitate formed and redissolved immediately. The reaction was heated at reflux temperature for a further 1 h and then cooled to room temperature. The solvent was removed *in vacuo* resulting in a viscous light brown oil which was dissolved in minimal MeOH then precipitated and triturated with diethyl ether to yield **49** as an off-white powder that was dried under reduced pressure, 281 mg, 79%. Λ_M = 128 Ω^{-1} cm^2 mol^{-1} (1 x 10^{-3}). (Found C, 45.62; H, 5.54; N, 5.42 $C_{38}H_{56}CdCl_2N_4O_{15}$•0.5$H_2O$ requires C, 45.59; H, 5.74; N, 5.60%). ^{13}C NMR (CD_3OD): 159.92 (1 C, Ar, *ipso*); 159.86 (1 C, Ar, *ipso*); 159.79 (1 C, Ar, *ipso*); 130.67 (2 C, Ar); 130.63 (2 C, Ar); 130.56 (2 C, Ar); 122.40 (3 C, Ar); 115.81 (2 C, Ar); 115.74 (2 C, Ar); 115.66 (2 C, Ar); 70.66 (1 C, -O*C*H_2); 70.42 (1 C, -O*C*H_2); 70.04 (1 C, -O*C*H_2); 66.65 (2 C, -*C*H); 66.50 (1 C, -*C*H); 65.79 (1 C, -*C*H); 63.26 (1 C,-N*C*H_2); 56.24 (2 C, -N*C*H_2); 56.15 (1 C, -N*C*H_2); 54.56 (2C, cyclen -*C*H_2); 53.05 (2C, cyclen -*C*H_2); 51.53 (2C, cyclen -*C*H_2); 50.49 (2C, cyclen -*C*H_2); 22.13 (1 C, -*C*H_3).

7.11 Preparation of the silica materials

Si-(GPS), 33

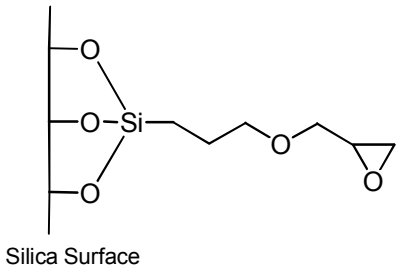

33

To a stirred suspension of silica gel (2.2 g; Merck 70-230 mesh; preheated at 120^{o} C, at, 0.75 mm Hg for 24 h) in dry toluene (50 cm^{3}), 3-(glycidoxypropyl)trimethoxysilane, **32** (2.08 g, 8.8 mmol) was added. The mixture was stirred at 90^{o} C for 24 h, cooled to room temperature, filtered and washed with dry toluene (100 cm^{3}) and absolute methanol (100 cm^{3}). The resulting white powder, **33**, was then subjected to Soxhlet extraction with dry toluene (80 cm^{3}) for 6 h, air dried and stored under vacuum. Microanalysis gave 7.64% C and 1.43% H corresponding to a loading of 1.1 mmol g^{-1} material. IR (KBr, DRIFT): $\nu_{(C-H)}$ 2944 cm^{-1}, 2879 cm^{-1}; asym. $\nu_{(Si-O-Si)}$ 1192cm^{-1}, 1072 cm^{-1}; sym. $\nu_{(Si-O-Si)}$ 950 cm^{-1}, 807 cm^{-1}.

Si-GPS(230-400), 80

The preparation of this material was analogous to, **33**, using silica gel (1.0 g, Merck 60 230-400 mesh) and 3-(glycidoxypropyl)trimethoxysilane, **32** (950 mg, 4.0 mmol). Microanalysis gave 6.34% C and 1.36% H corresponding to a loading of 0.88 mmol g^{-1} of material.

Si-GPS-Trac, 43

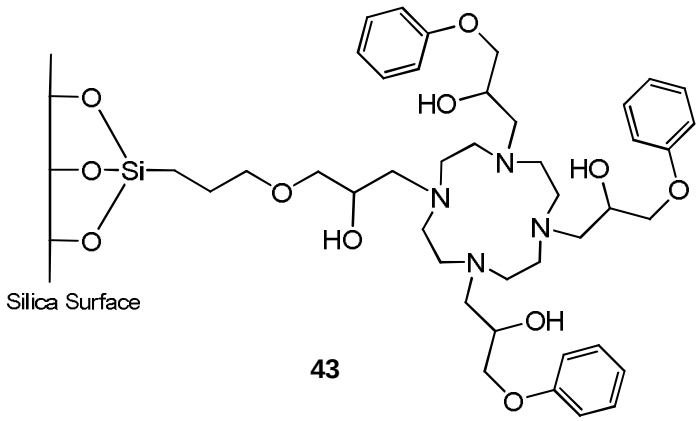

43

To a stirred suspension of **33** (1.5 g, 1.1 mmol GPS g^{-1} material) in dry toluene (40 cm^3) a solution of **46** (2.57 g, 4.13 mmol) dissolved in dry toluene (10 cm^3) was added and the mixture was stirred at 60^o C for 2 days. The suspension was filtered, washed with dry toluene and subjected to Soxhlet extraction with MeOH for 4 h to obtain **43** as a light brown powdered material. Residual **46** was recovered by evaporating the washing and Soxhlet solvents. Microanalysis gave 18.09% C, 2.67% H and 1.75% N corresponding to a loading of 0.31 mmol g^{-1} material. IR (KBr, DRIFT): $\nu_{(C-H)}$ 2942 cm^{-1}, 2875 cm^{-1}; $\nu_{(C=C)}$ 1602 cm^{-1}, 1497 cm^{-1}; $\nu_{(Ar-H)}$ 752 cm^{-1}, 690 cm^{-1}.

Si-GPS (endcapped), 85

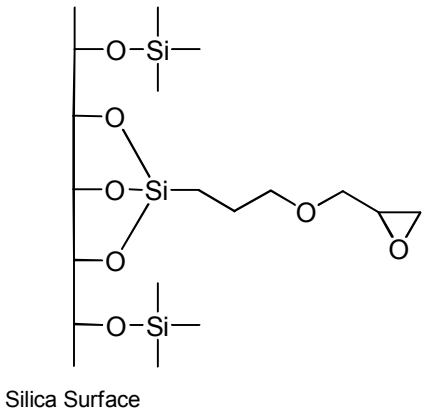

85

To a suspension of **33** (1.48 g, 1.1 mmol g^{-1}) in dry toluene (20 cm^3) trimethylchlorosilane (TMCS), **84** (5.92 g, 54.5 mmol) was added and the mixture was heated at reflux temperature for 3 h. After cooling the suspension it was stirred at ambient temperature overnight. The solid was then filtered and washed with toluene (100 cm^3) and de-ionised water (200 cm^3). The resultant solid **85** was then dried under vacuum for 24 h and stored in a desiccator.

Si-GPS-Trac(endcapped), 89

Preparation of this material was by the same method as used for **43**, but using **85** (1.3 g) and **46** (2.23 g, 3.58 mmol).

Si-GPS-Trac(230-400), 87

This material was prepared by an analogous method to, **33**, but using **80** (1.0 g, 0.88 $mmol^{-1}$) and **46** (1.4 g, 2.2 mmol). Microanalysis gave 17.44% C, 2.57% H and 1.52% N corresponding to a loading of 0.27 mmol g^{-1} of material.

Si-GPDMS 83

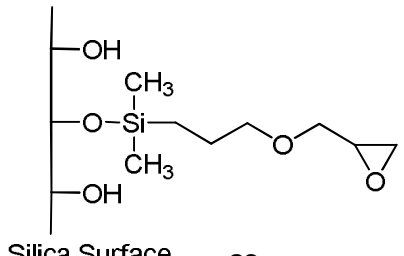

83

This material was prepared by a procedure analogous to that used for **33** with

silica gel (1.5 g; Merck 60 70 - 230 mesh and 3-(glycidoxypropyl)dimethylethoxysilane (GPDMES), **82** (1.3 g, 6.0 mmol). Microanalysis gave 3.39% C and 2.26% H corresponding to a loading of 0.35 mmol g^{-1} of material.

Si-GPDMS-Trac, 86

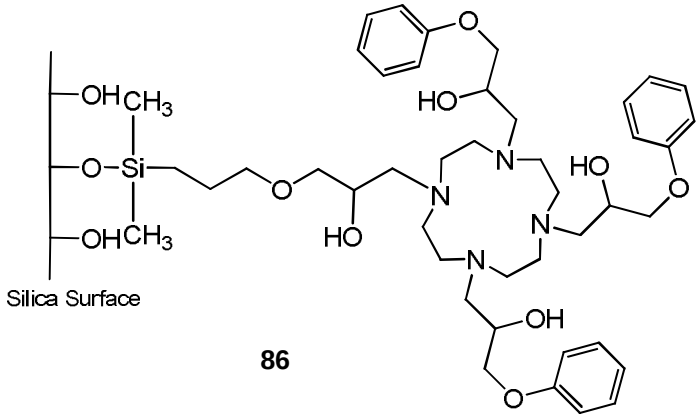

86

The preparation of the title material was by the method employed for the synthesis of, **43**, but using **83** (1.5 g, 0.35 mmol g^{-1}) and **46** (1.3 g, 2.1 mmol). Microanalysis gave 10.37% C, 2.05% H and 0.85% N corresponding to a loading of 0.15 mmol g^{-1} of material.

MCM-41, 93

This material was prepared by adapting a method reported by Beck.[245] To a stirred suspension of sodium silicate (9.0 cm^3, Na_2O: 8.55%, SiO_2: 27.45%) diluted with de-ionised water (28 cm^3) was added H_2SO_4 (0.4 cm^3, 98%) and allowed to continue stirring at room temperature for 30 minutes, after which time a solution of cetyltrimethylammonium bromide (CTAB) (10 g, 27.44 mmol) in de-ionised water (28 cm^3) stirred at 75^o C was added with rapid stirring forming a thick white suspension that was stirred for a further 5 minutes. The contents were then diluted with de-ionised water (10 cm^3 and allowed to stir overnight at 75^o C forming a white

gel-like suspension that was cooled to room temperature, filtered and washed with copious amounts of de-ionised water to obtain a translucent gel-like substance that turned white and solidified on drying in air. The white solid was then calcined at 550^{o} C for 5 h giving a hard white, chalk-like solid that was readily ground.

MCM-41-GPS, 81

Synthesis of this material was by a method analogous to the method used for **33** but using **93** (1.6 g) and 3-(glycidoxypropyl)trimethoxysilane, **32** (1.5 g, 6.4 mmol). Microanalysis gave 12.23% C and 2.17% H corresponding to a loading of 1.7 mmol g^{-1} of material.

MCM-41-GPS-Trac, 88

This material was synthesised by a method analogous to that used for the synthesis of receptor material **43** but using **81** (1.2 g, 1.7 mmol g^{-1}) and **46** (3.17 g, 5.1 mmol). Microanalysis gave 18.05% C, 2.74% H and 1.60% N corresponding to a loading of 0.22 mmol g^{-1} of material.

Si-GPS-DiPTrac, 44

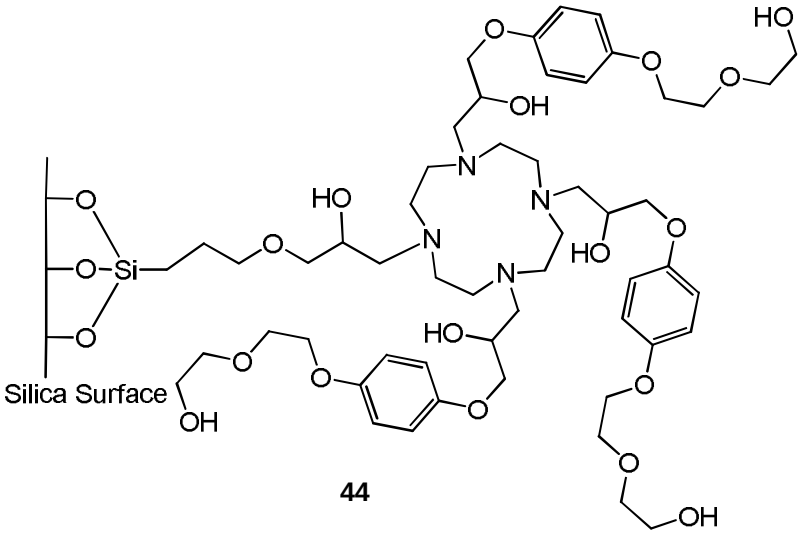

44

To a stirred suspension of **33** (2.0 g, 1.1 mmol g^{-1}) in dry acetonitrile (30 cm^3) a solution of **47** (6.2 g, 6.6 mmol) dissolved in dry acetonitrile (5 cm^3) was added and the mixture was stirred at 60^o C for 3 days. The suspension was filtered, washed with dry acetonitrile and subjected to Soxhlet extraction with MeOH for 4 h to obtain **44** as a light brown powder. Microanalysis gave 14.89% C, 2.47% H and 0.93% N corresponding to a loading of 0.17 mmol g^{-1} of material. IR (KBr, DRIFT): $\nu_{(C-H)}$ 2981 cm^{-1}, 2888 cm^{-1}; $\nu_{(C=C)}$ 1509 cm^{-1}, 1458 cm^{-1}; $\nu_{(Si-O-Si)}$ 955 cm^{-1}, 794 cm^{-1}.

Si-GPS-Tri-Trac, 45

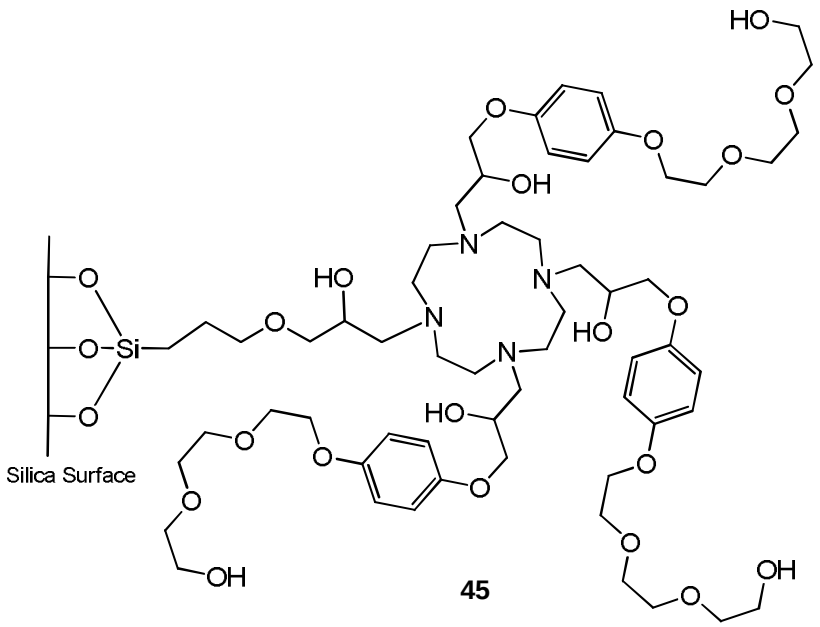

45

The title compound was prepared by the same method used for, **44** but using. **33** (2.0 g, 1.1 mmol g^{-1}) and **48** (7.04 g, 6.6 mmol). Microanalysis gave 11.85% C, 2.25% H and 0.54% N corresponding to a loading of 0.10 mmol g^{-1} of material. IR (KBr, DRIFT): $\nu_{(C-H)}$ 2981 cm^{-1}, 2888 cm^{-1}; $\nu_{(C=C)}$ 1508 cm^{-1}, 1457 cm^{-1}; $\nu_{(Si-O-Si)}$ 953 cm^{-1}, 796 cm^{-1}.

Appendix A

APPENDIX A BINDING CONSTANT DETERMINATION PROCEDURES

A.1. Outline of the theory used in determination of binding constants using 1H NMR titration experiments.[186]

To obtain the binding constants, *K*, for the host-guest combinations that have been reported the chemical shift data obtained in the ^{1}H NMR titration experiments outlined in **Chapter 3** were subjected to a non-linear least squares curve fitting analysis. This was achieved using a procedure written by Dr. A. K. W. Stephens of the Flinders University of South Australia, utilising the Igor data analysis software.[186]

The binding constant *K*, which is sought, pertains to the following equilibrium:

$$\mathbf{H + G} \underset{}{\overset{K}{\rightleftharpoons}} \mathbf{HG} \qquad \textbf{(1.1)}$$

where $K = \mathbf{HG / H \times G}$

H is the free binary receptor complex (host) concentration, and **G** is the free guest concentration. **HG** is the concentration of the ternary (host-guest) complex.

The total amount of host present ($\mathbf{H_T}$) is given by the formula:

$$\mathbf{H_T = HG + H} \qquad \textbf{(1.2)},$$

Likewise, $\mathbf{G_T}$ is the total concentration of guest present in solution, and corresponds to:

$$\mathbf{G_T = HG + G} \qquad \textbf{(1.3)},$$

Therefore, equation (1.1) can be rewritten using equations 1.2 and 1.3 as:

$$K = \frac{\mathbf{G_T - G}}{\mathbf{(H_T - G_T + G) \times G}} \qquad \textbf{(1.4)}$$

Rearranging equation 1.4 gives equation 1.5:

$$K\mathbf{G}^2 + \mathbf{G}(K\mathbf{H_T} - K\mathbf{G_T} + 1) - \mathbf{G_T} = 0 \qquad \textbf{(1.5)},$$

which can be solved to give the concentration of G by using equation 1.6:

$$\mathbf{G} = \frac{-b \pm \sqrt{b^2 - 4ac}}{2a} \qquad \textbf{(1.6)},$$

where $a = K$
$b = KH_T - KG_T + 1$
$c = -G_T$

Equation 1.5 can be related to the observed ^{1}H NMR guest chemical shifts through the use of equation 1.7:

$$\delta_{calc} = \delta_G\chi_G + \delta_{HG}\chi_{HG} \qquad \textbf{(1.7)},$$

where: $\chi_G = G/G_T$, mole fraction of unbound guest
χ_{HG} = mole fraction of bound guest = $1 - \chi_G$
δ_G = chemical shift of unbound guest
δ_{HG} = chemical shift of bound guest

An estimate of G at each H_T value is obtained by the computer subjecting a trial value of *K* and known values of H_T and G_T to equation 1.6. Equation 1.7 then allows the determination of preliminary values for δ_{calc}, at each H_T, for a trial value of δ_{HG}. The computer program then iteratively varies *K* and δ_{HG}, until the best match of δ_{calc} at each H_T with δ_{obs} at that H_T is obtained.

Several sample titration curves are shown in Figure A.1. These simulations show the variation in guest chemical shift (δ_{obs}) for illustrative values of the binding constant (log*K*), and indicate the difference in the shape of these curves as the binding constant varies. A chemical shift difference of 1.0 ppm between bound and complexed guest is assumed, and the guest concentration is set at 1×10^{-3} mol dm^{-3}, which was the concentration used in the experimental work described in this thesis.

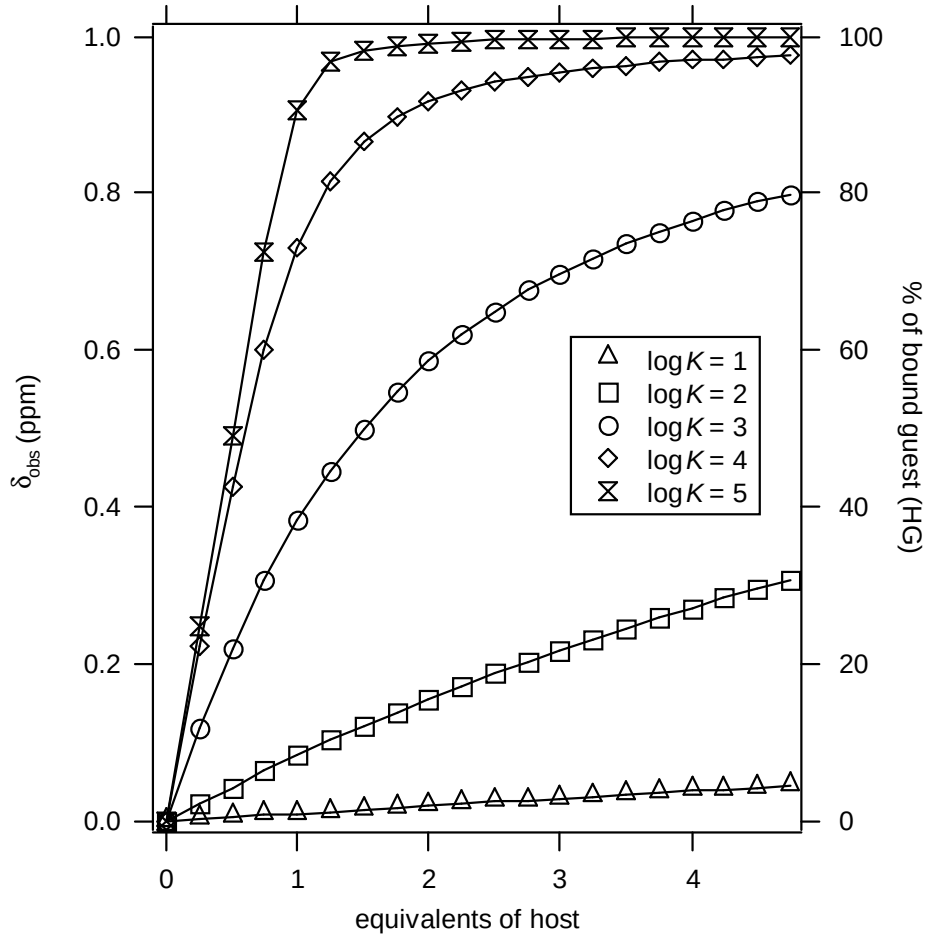

Figure A.1: Titration curve simulations for different log*K* values at an assumed guest concentration of 1 x 10^{-3} mol dm^{-3} and a chemical shift difference of 1.0 ppm between free and bound guest. The typical titration points correspond to the guest chemical shift (left Y-axis) at each host concentration. The curves represent the changing percentage of bound guest (HG) (right Y-axis) as a function of increasing host concentration.

Appendix B

APPENDIX B DETERMINATION OF STOICHIOMETRY BY THE METHOD OF CONTINUOUS VARIATION

The method of continuous variation (or isomolar solutions) is also known as Job's method as it was first suggested by P. Job in 1928.[165, 246] It is popularly employed to determine the stoichiometry of a system containing two species that are likely to interact with one another to form a complex comprised of both species at equilibrium, for example.

$$H_n + G_m \rightleftharpoons H_nG_m$$

The general procedure for the method of continuous variations requires the preparation of a series of solutions in which the total molar concentration $H_n + G_m$ is kept constant while the ratio (χ) H_n:G_m is varied incrementally such that a fixed volume is maintained. A range of molar concentrations is established so that

$$0 \leq G_m/(H_n + G_m) \leq 1$$

A measurable quantity such as the change in chemical shift $\Delta\delta$ of one of the constituent species is monitored and plotted in the normalised form $\chi\Delta\delta$ as a function of the χ of that species to give a curve that is commonly known as a Job's Plot, **Figure B.1**.[195, 197, 198]

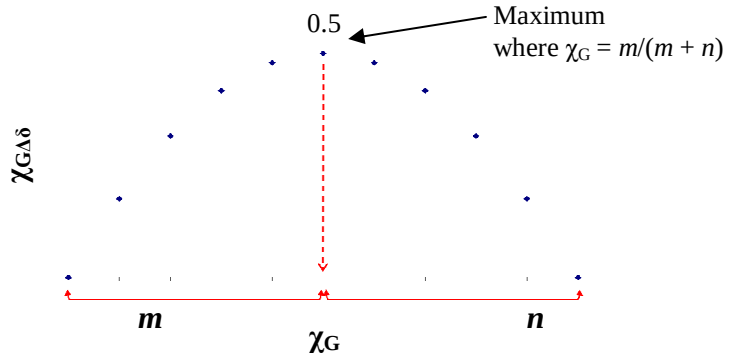

Figure B.1 Job's Plot showing the correlation between the stoichiometry of the host-guest complex H_nG_m formed and the molar fraction χ of one of the constituent species, in this case the guest, G.[195, 198]

The stoichiometry of the product H_nG_m has a maximum where the *x*-coordinate, in this case χ_G equals

$$\chi_G = \frac{m}{m+n}$$

If the complex forms predominantly in a 1:1 H:G ratio the value at the maximum will be 0.5 where $m = n = 1$. For a 1:2 H:G complex where $m = 2$ and $n = 1$ the value at the maximum reaches 0.67 or 0.33 depending on which species is monitored, **Figure B.3**.[197, 237] This method is generally used where only a single complex is formed as the calculations required are more complex using multi-equilibria equations.

The following equations were used to generate simulated curves for 1:1 and 1:2 H:G complex formation. **Equation 1.1** was used to generate a simulated curve for a 1:1 H:G complex shown as **Figure B.2** below [196]:

$$\chi_G \Delta\delta_G = \frac{\Delta\delta_{HG}}{2Kc_T}\left(Kc_T + 1 - \sqrt{(Kc_T + 1)^2 - 4K_a^2 c_T^2 \chi_G(1 - \chi_G)}\right) \quad \textbf{(1.1)},$$

where $\Delta\delta_{HG}$ is the limit where G = H for a 1:1 complex equalling 1 ppm in this case, *K* is the association constant and c_T is the total concentration. This equation also applies for $\chi_H \Delta\delta_H$.

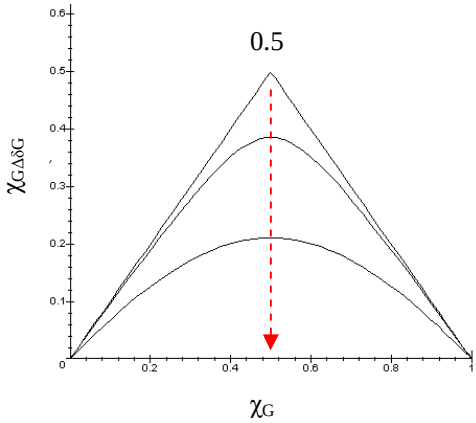

Figure B.2 Simulated Job's Plot for 1:1 stoichiometry generated with Maple V,[199] from **Equation 1.1**. The data plotted in this figure is for a model system where $\Delta\delta_{HG}$ = 1.0 ppm and $\Delta\delta_{HGmax}$ = 0.5 ppm, with *K* ranging from (a), 3 x 10^2 M^{-1} through (b), 3 x 10^3 M^{-1} to (c), 10^6 M^{-1}.

Equation 1.2 was adapted from Likassar[247] and used to generate a simulated curve for a 1:2 H:G complex:

$$\chi_G\Delta\delta = y_{max}(m+n)\chi_G - (n+m)^m(m+n)(1-\chi_G) - (1-y)^n \qquad \textbf{(1.2)},$$

where y_{max} = 0.1 and the correction factor y = 2.77784 x 10^{-5}. The curve produced with this equation, **Figure B.3** originates from computer approximations of y_{max} and y and serves only as an example of the curve expected for 1:2 H:G complex formation.

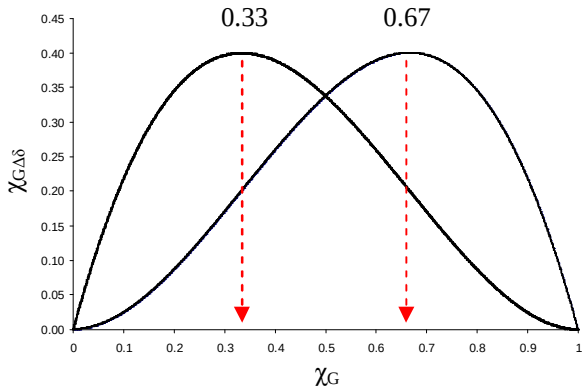

Figure B.3 Representation of a Job's Plot produced from computer approximations of the Δδ values generated from **Equation 1.2** for 1:2 H:G stoichiometry giving the HG_2 complex ratio at χ_H = 0.33 and χ_G = 0.67. This simulation was obtained independent of *K*.

APPENDIX C

^{13}C CPMAS NMR SPECTRA OF SOME HIGH UPTAKE HOST-GUEST COMPLEXES

Si-GPS-[Cd(Trac)(1-naphthoate)](ClO$_4$)

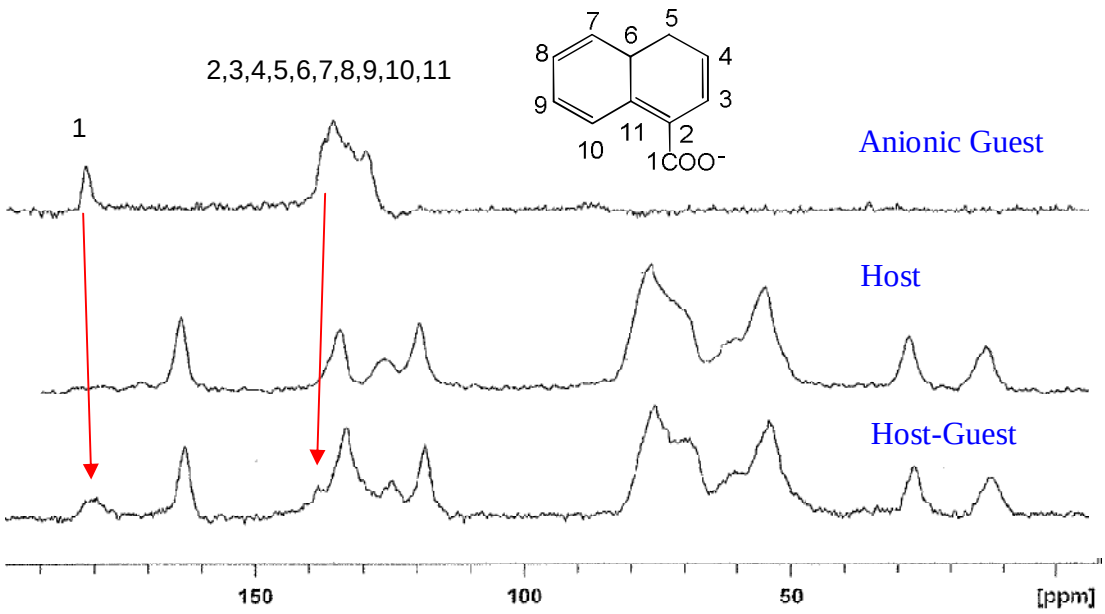

Si-GPS-[Cd(Trac)(2-naphthoate)](ClO$_4$)

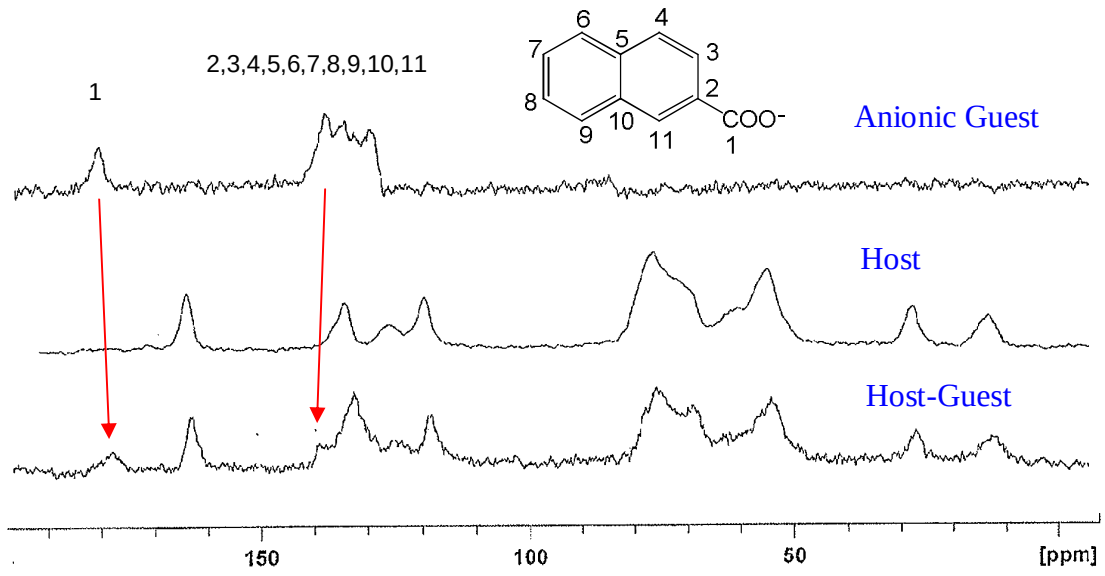

Si-GPS-[Cd(Trac)(*o*-hydroxybenzoate)](ClO_4)

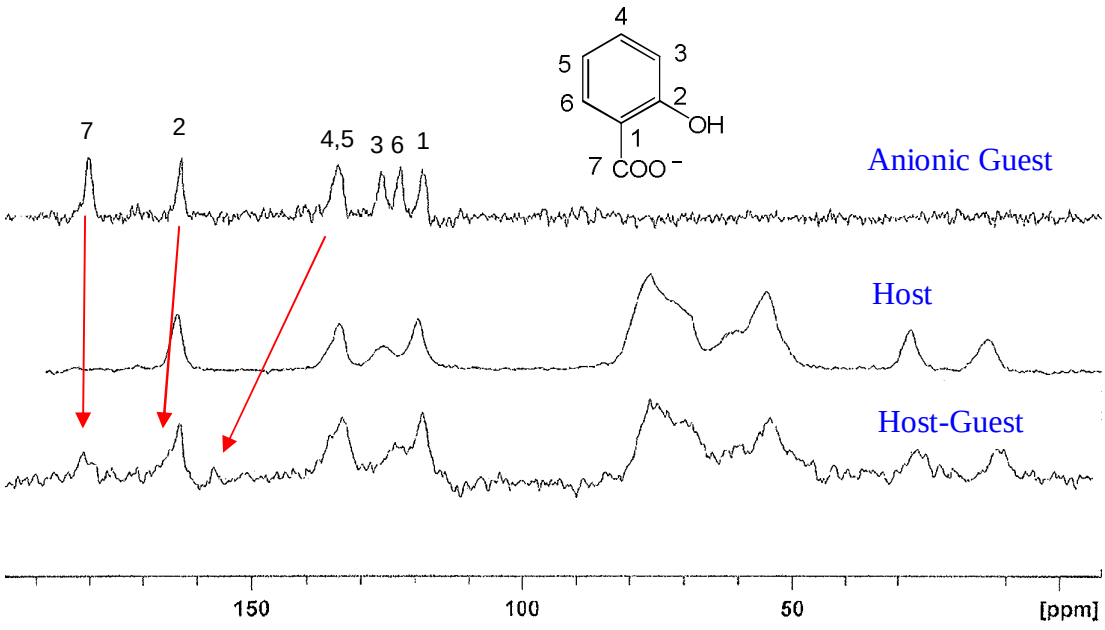

Si-GPS-[Cd(Trac)(3,4,5-trihydroxybenzoate)](ClO_4)

OH groups on either C4 or C6 could be hydrogen bonded to OH group on C5 ∴ 4 and 6 in the guest spectrum could be interchanged.

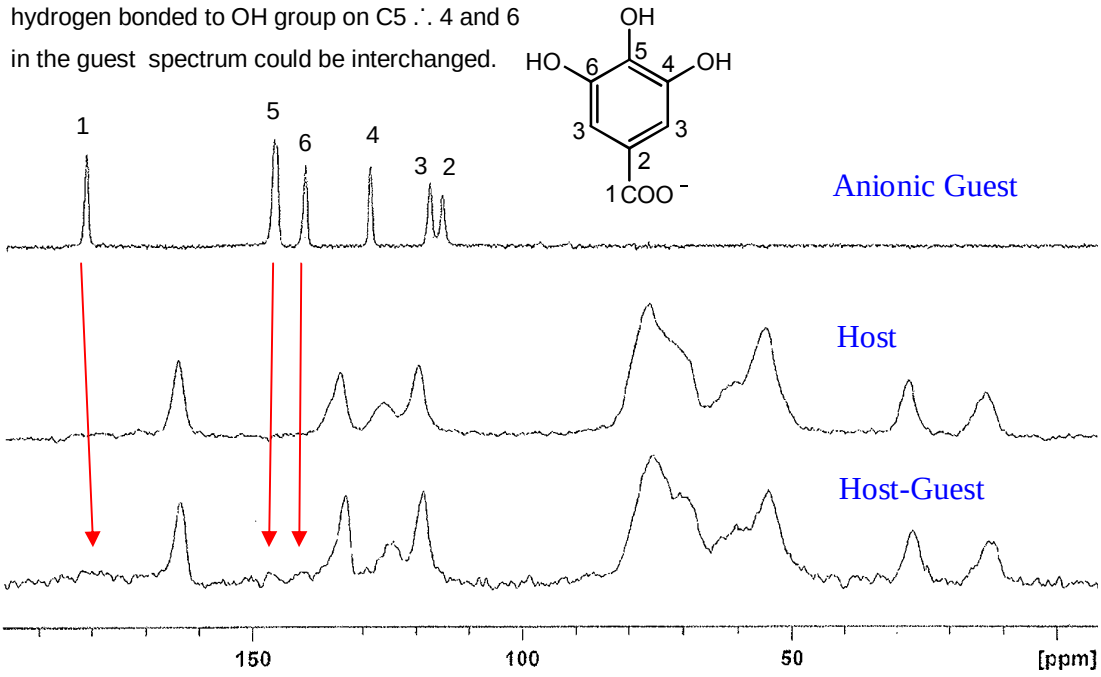

Si-GPS-[Cd(Trac)(2,5-diydroxybenzoate)](ClO$_4$)

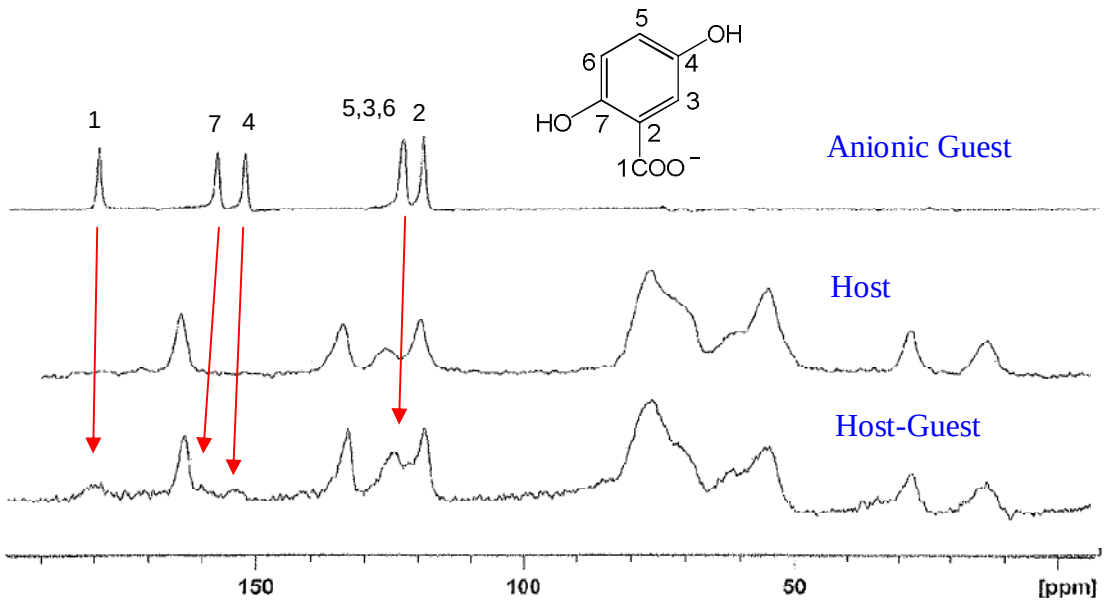

Si-GPS-[Cd(DiPTrac)(2,6-dihdroxybenzoate)](ClO$_4$)

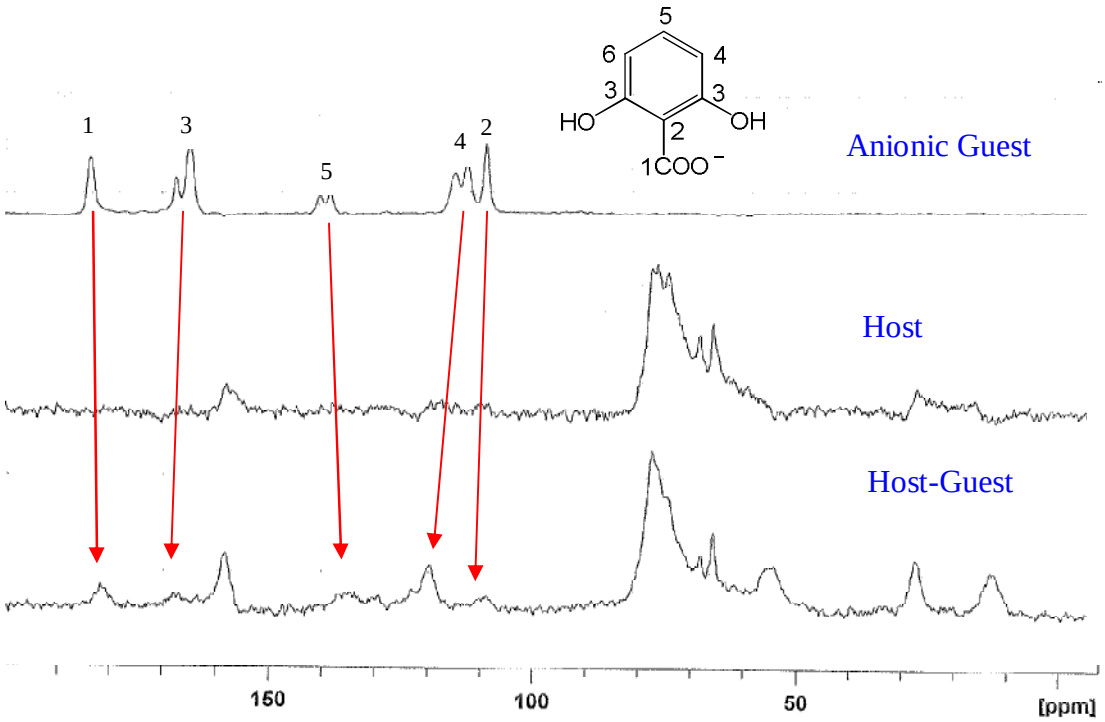

Si-GPS-[Cd(DiPTrac)(*o*-hydroxybenzoate)](ClO_4)

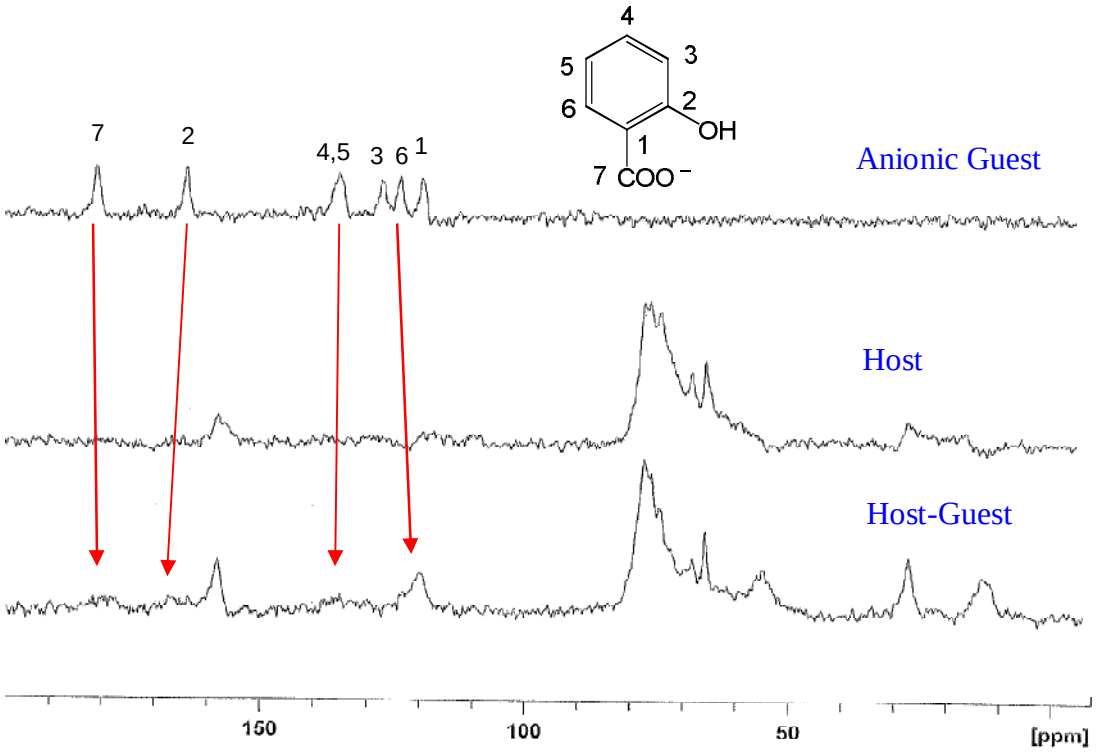

REFERENCES

REFERENCES

1. D. J. Cram and J. M. Cram, *Science*, 1974, **183**, 803-809.

2. M. Albrecht, *Naturwissenschaften*, 2007, **94**, 951-966.

3. G. R. Desiraju, *Nature*, 2001, **412**, 397-400.

4. D. N. Reinhoudt and M. Crego-Calama, *Science*, 2002, **295**, 2403-2407.

5. J. L. Sessler, P. A. Gale and W. S. Cho, *Anion Receptor Chemistry*, Royal Society of Chemistry, Cambridge, 2006.

6. A. J. Wilson, *Annu. Rep. Prog. Chem. Sect. B*, 2007, **103**, 174-192.

7. J. W. Steed and J. L. Atwood, *Supramolecular Chemistry*, Wiley, Chichester, 2000.

8. J-M. Lehn, *Angew. Chem. Int. Ed. Engl.*, 1988, **27**, 89-112.

9. J-M. Lehn, *Pure Appl. Chem.*, 1994, **66**, 1961-1966.

10. S. Kubik, C. Reyheller and S. Stuwe, *J. Inclusion Phenom. Mol. Recognit. Chem.*, 2005, **52**, 137-187.

11. K. Bowman-James, *Acc. Chem. Res.*, 2005, **38**, 671-678.

12. W. T. S. Huck, L. J. Prins, R. H. Fokkens, N. M. M. Nibbering, F. C. J. M. van Veggel and D. N. Reinhoudt, *J. Am. Chem. Soc.*, 1998, **120**, 6240-6246.

13. K. Fujimoto, T. Miyata and Y. Aoyama, *J. Am. Chem. Soc.*, 2000, **122**, 3558-3559.

14. R. E. Babine and S. L. Bender, *Chem. Rev.*, 1997, **97**, 1359-1472.

15. D. Tzalis and Y. Tor, *Tetrahedron Lett.*, 1996, **37**, 8293-8296.

16. I. A. Banerjee, L. Yu and H. Matsui, *J. Am. Chem. Soc.*, 2003, **125**, 9542-9543.

17. P. J. Worsfold, *Pure Appl. Chem.*, 1995, **67**, 597-600.

18. S. W. Park, S. Y. Choi, K. H. Chung, S. I. Hong and S. W. Kim, *Biochem. Eng. J.*, 2005, **11**, 87-93.

19. F. Svec, *Electrophoresis*, 2006, **27**, 947-961.

20. I. Bhushan, R. Parshad, G. N. Qazi, G. Ingavle, T. M. Jamalpure, C. R. Rajan, S. Ponrathnam and V. K. Gupta, *J. Bioact. Compat. Polym.*, 2007, **22**, 174-194.

21. P. Bernfeld and J. Wan, *Science*, 1963, **142**, 678-679.

22. T. H. Yang, *Recent Patents on Materials Science*, 2008, **1**, 29-40.

23. G. V. Oshovsky, D. N. Reinhoudt and W. Verboom, *Angew. Chem. Int. Ed. Engl.*, 2007, **46**, 2366-2393.

24. J. J. Lavigne and E. V. Anslyn, *Angew. Chem. Int. Ed. Engl.*, 2001, **40**, 3118-3130.

25. R. A. Samant, V. S. Ijeri and A. K. Srivastava, *J. Chem. Eng. Data*, 2003, **48**, 203-207.

26. M. Vincenti, *J. Mass Spectrom.*, 1995, **30**, 925-939.

27. D. L. Caulder and K. N. Raymond, *Acc. Chem. Res.*, 1999, **32**, 975-982.

28. E. C. Constable, *Angew. Chem. Int. Ed. Engl.*, 1991, **30**, 1450-1451.

29. K. Muller-Dethlefs and P. Hobza, *Chem. Rev.*, 2000, **100**, 143-168.

30. P. T. Corbett, J. Leclaire, L. Vial, K. R. West, J. L. Weiter, J. K. M. Sanders and S. Otto, *Chem. Rev.*, 2006, **106**, 3652-3711.

31. T. Zielinski, M. Kedziorek and J. Jurczak, *Chem. Eur. J.*, 2008, **14**, 838-846.

32. F. P. Schmidtchen, *Coord. Chem. Rev.*, 2006, **250**, 2918-2928.

33. M. D. Lankshear and P. D. Beer, *Coord. Chem. Rev.*, 2006, **250**, 3142-3160.

34. D. J. Cram, *Science*, 1988, **240**, 760-767.

35. D. J. Cram and J. M. Cram, *Acc. Chem. Res.*, 1978, **11**, 8-14.

36. P. D. Beer and P. A. Gale, *Angew. Chem. Int. Ed. Engl.*, 2001, **40**, 486-516.

37. F. Arnaud-Neu, S. Barboso, F. Berny, A. Casnati, N. Muzet, A. Pinalli, R. Ungaro, M. J. Schwing-Weill and G. Wipff, *J. Chem. Soc., Perkin Trans. 2*, 1999, 1727-1738.

38. F. Arnaud-Neu, Z. Asfari, B. Souley, P. Thuery and M. Nierlich, *J. Chem. Soc., Perkin Trans. 2*, 2000, 495-499.

39. R. Carrillo, V. S. Martín, M. López and T. Martín, *Tetrahedron*, 2005, **61**, 8177-8191.

40. H. Hai, M. Linjing, H. Jiaqi and C. Jin-Pei, *J. Org. Chem.*, 2003, **68**, 7605-7611.

41. N. Branda, R. Wyler and J. Rebek, *Science*, 1994, **263**, 1267-1268.

42. A. P. Davis and R. S.Wareham, *Angew. Chem. Int. Ed. Engl.*, 1998, **37**, 2270-2273.

43. K. M. Bhattarai, A. P. Davis, J. J. Perry, C. J. Walter, S. Menzer and D. J. Williams, *J. Org. Chem.*, 1997, **62**, 8463-8473.

44. H. S. Park, Q. Lin and A. D. Hamilton, *J. Am. Chem. Soc.*, 1999, **121**, 8-13.

45. J. Huuskanen, J. E. H. Buston, N. D. Scotchmer and H. L. Anderson, *New J. Chem.*, 1999, **23**, 1245-1252.

46. P. V. Bernhardt and E. J. Hayes, *Inorg. Chem.*, 2003, **42**, 1371-1377.

47. E. Garrier, S. Le Gac and I. Jabin, *Tetrahedron: Asymmetry*, 2005, **16**, 3767-3771.

48. F. P. Schmidtchen and M. Berger, *Chem. Rev.*, 1997, **97**, 1609-1646.

49. J. P. Clare, A. J. Ayling, J. B. Joos, A. L. Sisson, G. Magro, M. N. Perez-Payan, T. N. Lambert, R. Shukla, B. D. Smith and A. P. Davis, *J. Am. Chem. Soc.*, 2005, **127**, 10739-10746.

50. M. M. G. Antonisse and D. N. Reinhoudt, *Chem. Commun.*, 1998, 443-448.

51. B. L. Schottel, H. T. Chifotides and K. R. Dunbar, *Chem. Soc. Rev.*, 2008, **37**, 68-83.

52. P. Blondeau, M. Segura, R. Perez-Fernandez and J. de Mendoza, *Chem. Soc. Rev.*, 2007, **36**, 198-210.

53. P. A. Gale, S. E. Garcia-Garrido and J. Garric, *Chem. Soc. Rev.*, 2008, **37**, 151-190.

54. B. Dietrich, *Pure Appl. Chem.*, 1993, **65**, 1457-1464.

55. J. Kielland, *J. Am. Chem. Soc.*, 1937, **59**, 1675-1678.

56. C. H. Park and H. E. Simmons, *J. Am. Chem. Soc.*, 1968, **90**, 2431-2432.

57. K. W. Piepgrass, J. H. Davis, M. Sabat and R. N. Grimes, *J. Am. Chem. Soc.*, 1991, **113**, 680-681.

58. P. Schiessl and F. P. Schmidtchen, *J. Org. Chem.*, 1994, **59**, 509-511.

59. A. Bianchi, K. Bowman-James and E. Garcia-Espana, eds., *Supramolecular Chemistry of Anions*, Wiley VCH, New York, 1997.

60. A. Villiers, *Compt. Rend.*, 1891, **112**, 536-538.

61. J. Szejtli, *Chem. Rev.*, 1998, **98**, 1743-1753.

62. L. F. Lindoy and I. M. Atkinson, *Self-Assembly in Supramolecular Systems*, Royal Society of Chemistry, Cambridge, 2000.

63. D. T. Pham, P. Clements, C. J. Easton and S. F. Lincoln, *Tetrahedron: Asymmetry*, 2008, **19**, 167-175.

64. Y. L. Zhao, H. Y. Zhang, M. Wang, H. M. Yu, H. Yang and Y. Liu, *J. Org. Chem.*, 2006, **71**, 6010-6019.

65. K. Kano, Takenoshita and T. Ogawa, *Chem. Lett.*, 1982, 321-324.

66. Y. Fu, L. Liu and Q. X. Guo, *J. Inclusion Phenom. Mol. Recognit. Chem.*, 2002, **43**, 223-229.

67. Z. J. Tan, X. X. Zhu and G. R. Brown, *Langmuir*, 1994, **10**, 1034-1039.

68. R. J. Bergeron, M. A. Channing, G. J. Gibeily and D. M. Pillor, *J. Am. Chem. Soc.*, 1977, **99**, 5146-5151.

69. R. J. Bergeron, M. A. Channing and K. A. McGovern, *J. Am. Chem. Soc.*, 1978, **100**, 2878-2883.

70. A. Buvari-Barcza, E. Rak and A. Meszaros, *J. Inclusion Phenom. Mol. Recognit. Chem.*, 1998, **32**, 453-459.

71. D. M. Davies and J. R. Savage, *J. Chem. Soc., Perkin Trans. 2*, 1994, 1525-1529.

72. J. Vicens and V. Bohmer, eds., *Calixarenes: A Versatile Class of Macrocyclic Compounds*, Kluwer Academic Publishers, Dordrecht, 1991.

73. G. McMahon, S. O'Malley and K. Nolan, *Arkivoc*, 2003, **vii**, 23-31.

74. C. D. Gutsche, *Calixarenes*, Royal Society of Chemistry, Cambridge, 1989.

75. H. Goldmann, W. Vogt, E. Paulus and V. Bohmer, *J. Am. Chem. Soc.*, 1988, **110**, 6811-6817.

76. A. Ikeda and S. Shinkai, *Chem. Rev.*, 1997, **97**, 1713-1734.

77. G. D. Andreetti, R. Ungaro and A. Pochini, *J. Chem. Soc., Chem. Commun.*, 1979, 1005.

78. S. G. Bott, A. W. Coleman and J. L. Atwood, *J. Am. Chem. Soc.*, 1986, **108**, 1709-1710.

79. F. Sansone, L. Baldini, A. Casnati, M. Lazzarotto, F. Ugozzoli and R. Ungaro, *Proc. Natl. Acad. Sci. USA*, 2002, **99**, 4842-4847.

80. K. Kavallieratos, C. M. Bertao and R. H. Crabtree, *J. Org. Chem.*, 1999, **64**, 1675-1683.

81. P. A. Gale, ed., *The Encyclopaedia of Supramolecular Chemistry*, Dekker, New York, 2004.

82. S. I. Kondo, Y. Hiraoka, N. Kurumatani and Y. Yano, *Chem. Commun.*, 2005, 1720-1722.

83. M. A. Hossain, S. O. Kang, D. Powell and K. Bowman-James, *Inorg. Chem.*, 2003, **42**, 1397-1399.

84. T. Zielinski and J. J. P. Dydio, *Tetrahedron*, 2008, **64**, 568-574.

85. F. Troisi, A. Russo, C. Gaeta, G. Bifulco and P. Neri, *Tetrahedron Lett.*, 2007, **48**, 7986-7989.

86. S. J. Brooks, S. E. Garcia-Garrido, M. E. Light, P. A. Cole and P. A. Gale, *Chem. Eur. J.*, 2007, **13**, 3320-3329.

87. R. Martinez-Manez and F. Sancenon, *Chem. Rev.*, 2003, **103**, 4419-4476.

88. H. J. Kim, S. K. Kim, J. Y. Lee and J. S. Kim, *J. Org. Chem.*, 2006, **71**, 6611-6614.

89. P. S. Vermersch, D. D. Lemon, J. J. G. Tesmer and F. A Quiocho, *Biochemistry*, 1991, **30**, 6861-6866.

90. D. K. Smith, *Org. Biomol. Chem.*, 2003, **1**, 3874-3877.

91. S. Ghosh, A. R. Choudhury, T. N. G. Row and U. Maitra, *Org. Lett.*, 2005, **7**, 1441-1444.

92. M. Staffilani, K. S. B.Hancock, J. W. Steed, K. T. Holman, J. L. Atwood, R. K. Juneja and R. S. Burkhalter, *J. Am. Chem. Soc.*, 1997, **119**, 6324-6335.

93. C. B. Smith, A. K. W. Stephens, K. S. Wallwork, S. F. Lincoln, M. R. Taylor and K. P. Wainwright, *Inorg. Chem.*, 2002, **41**, 1093-1100.

94. C. B. Smith, K. S. Wallwork, J. M. Weeks, M. A. Buntine, S. F. Lincoln, M. R. Taylor and K. P. Wainwright, *Inorg. Chem.*, 1999, **38**, 4986-4992.

95. C. B. Smith, M. A. Buntine, S. F. Lincoln and K.P. Wainwright, *Dalton Trans.*, 2003, 3028-3033.

96. C. B. Smith, M. A. Buntine, S. F. Lincoln, M. R. Taylor and K. P. Wainwright, *Aust. J. Chem.*, 2006, **59**, 123-128.

97. C. B. Smith, S. F. Lincoln, M. R. Taylor and K. P. Wainwright, *Acta Crystallogr.*, 2002, **E58**, m33-m35.

98. P. J. Davies, S. F. Lincoln, C. B. Smith, M. R. Taylor, K. P. Wainwright and K. S. Wallwork, *Acta Crystallogr., Sect C: Cryst. Struct. Commun.*, 2000, **C56**, 28-30.

99. R. D. Hancock, *Chem. Rev.*, 1989, **89**, 1875-1914.

100. R. D. Hancock, M. S. Shaikjee, S. M. Dobson and J. C. A. Boeyens, *Inorg. Chim. Acta*, 1988, **154**, 229-238.

101. M. Subat, K. Woinaroschy, C. Gerstl, B. Sarkar, W. Kaim and B. Koenig, *Inorg. Chem.*, 2008, **47**, 4661-4668.

102. A. S. Delephine, R. Tripier and H. Handel, *Org. Biomol. Chem.*, 2008, **6**, 1743-1750.

103. A. de Castries, A. Escande, H. Fensterbank, E. Magnier, J. Marrot and C. Larpent, *Tetrahedron*, 2007, **63**, 10330-10336.

104. P. S. K. Chia, A. Ekstrom, I. Liepa, L. F. Lindoy, M. McPartlin, S. V. Smith and P. A. Tasker, *Aust. J. Chem.*, 1991, **44**, 737-746.

105. K. E. Borbas and J. I. Bruce, *Org. Biomol. Chem.*, 2007, **5**, 2274-2282.

106. A. Uchida, A. Komori and S. Watanabe, *Acta Crystallogr., Sect E: Struct. Rep.*, 2007, **E63**, o648-o649.

107. C. D. Edlin, S. Faulkner, D. Parker, M. P. Wilkinson, M. Woods, J. Lin, E. Lasri, F. Neth and M. Port, *New J. Chem.*, 1998, **22**, 1359-1364.

108. C. Li and W. T. Wong, *Tetrahedron Lett.*, 2002, **43**, 3217-3220.

109. J. Yoo, D. E. Reichert and M. J. Welch, *Chem. Commun.*, 2003, 766-767.

110. P. V. Bernhardt and G. A. Lawrence, *Coord. Chem. Rev.*, 1990, **104**, 297-343.

111. R. Delgado, V. Felix, M. P. L. Lima and D. W. Price, *Dalton Trans.*, 2007, 2734-2745.

112. J. Van Alphen, *Recl.: J. R. Neth. Chem. Soc.*, 1936, **55**, 835-840.

113. J. Van Alphen, *Recl.: J. R. Neth. Chem. Soc.*, 1937, **56**, 343-350.

114. E. Maimon, I. Zilbermann, H. Cohen, D. Kost, R. van Eldrick and D. Meystein, *Eur. J. Inorg. Chem.*, 2005, 4997-5004.

115. H. Stetter and W. Frank, *Angew. Chem. Int. Ed. Engl.*, 1976, **15**, 686-686.

116. H. Kubo, T. N. Player, S. Shinoda, H. Tsukube, H. Nariai and T. Takeuchi, *Anal. Chim. Acta*, 2003, **504**, 137-140.

117. P. Caravan, J. J. Ellison, T. J. McMurry and R. B. Lauffer, *Chem. Rev.*, 1999, **99**, 2293-2352.

118. D. D. Dischino, E. J. Delaney, J. E. Emswiler, G. T. Gaughan, J. S. Prasad, K. Srivastava and M. F. Tweedle, *Inorg. Chem.*, 1991, **30**, 1265-1269.

119. E. Kimura and E. Kikuta, *J. Biol. Inorg. Chem.*, 2000, **5**, 139-155.

120. E. Kimura and T. Koike, *Chem. Commun.*, 1998, 1495-1500.

121. C. Waengler, B. Waengler, M. Eisenhut, U. Haberkorn and W. Mier, *Bioorg. Med. Chem.*, 2008, **16**, 2606-2616.

122. H. Maumela, R. D. Hancock, L. Carlton, J. H. Reibenspies and K. P. Wainwright, *J. Am. Chem. Soc.*, 1995, **117**, 6698-6707.

123. R. D. Hancock, J. H. Reibenspies and H. Maumela, *Inorg. Chem.*, 2004, **43**, 2981-2987.

124. K. P. Wainwright, *Adv. Inorg. Chem.*, 2001, **52**, 293-333.

125. E. Kimura, Y. Kodama, T. Koike and M. Shiro, *J. Am. Chem. Soc.*, 1995, **117**, 8304-8311.

126. S. L. Whitbread, P. Valente, M. A. Buntine, P. Clement, S. F. Lincoln and K. P. Wainwright, *J. Am. Chem. Soc.*, 1998, **120**, 2862-2869.

127. S. L. Whitbread, P. Valente, M. A. Buntine, P. Clement, S. F. Lincoln and K. P. Wainwright, *J. Am. Chem. Soc.*, 1998, **120**, 11212-11212.

128. A. Damsyik, S. F. Lincoln and K. P. Wainwright, *Inorg. Chem.*, 2006, **45**, 9834-9842.

129. A. J. Bradbury, S. F. Lincoln and K. P. Wainwright, *New J. Chem.*, 2008.

130. M. Di Vaira, F. Mani, N. Nardi, P. Stoppioni and A. Vacca, *J. Chem. Soc., Dalton Trans.*, 1996, 2679-2684.

131. V. Boldrini, G. B. Giovenzana, R. Pagliarin, G. Palmisano and M. Sisti, *Tetrahedron Lett.*, 2000, **41**, 6527-6530.

132. F. Barbette, F. Rascalou, H. Chollett, J. L. Babouhot, F. Denat and R. Guilard, *Anal. Chim. Acta*, 2004, **502**, 179-187.

133. P. K. Jal, R. K. Dutta, M. Sudarshan, A. Saha, S. N. Bhattacharyya, S. N. Chintalapudi and B. K. Mishra, *Talanta*, 2001, **55**, 233-240.

134. R. K. Dey, U. Jha, A. C. Singh, S. Samal and A. R. Ray, *Anal. Sci.*, 2006, **22**, 1105-1110.

135. N. L. Dias Filho, Y. Gushikem, W. L. Polito, J. C. Moreira and E. O. Ewrin, *Talanta*, 1995, **42**, 1625-1630.

136. P. K. Jal, S. Patel and B. K. Mishra, *Talanta*, 2004, **62**, 1005-1028.

137. P. Qiaosheng, S. Qiaoyu, H. Zhide and S. Zhixing, *Analyst*, 1998, **123**, 239-243.

138. J. S. Kim, S. Chah and J. Yi, *Korean J. Chem. Eng.*, 2000, **17**, 118-121.

139. A. T. Yordanov and D. M. Roundhill, *Coord. Chem. Rev.*, 1998, **170**, 93-124.

140. W. Szczepaniak and A. Szymanski, *Acta Chromatogr.*, 1993, **2**, 7-20.

141. M. E. Mahmoud, *Anal. Chim. Acta*, 1999, **398**, 297-304.

142. M. M. A. Akl, I. M. M. Kenawy and R. R. Lasheen, *Microchem. J.*, 2004, **78**, 143-156.

143. T. Meyer, S. Spange, S. Hesse, C. Jager and C. Bellman, *Macromol. Chem. Phys.*, 2003, **204**, 725-732.

144. X. Huang, X. Chang, Q. He, Y. Cui, Y. Zhai and N. Jiang, *J. Hazard. Mater.*, 2008, **157**, 154-160.

145. N. V. Deorkar and L. L. Tavlarides, *Ind. Eng. Chem. Res.*, 1997, **36**, 399-406.

146. R. S. Paredes, N. S. Valera and L. F. Lindoy, *Aust. J. Chem.*, 1986, **39**, 1071-1079.

147. F. Zipoli, D. Donadio and M. Bernasconi, *J. Phys.: Condens. Matter*, 2008, **20**, 224011/224011-224011/224016.

148. R. K. Iler, *The Chemistry of Silica: Solubility, Polymerisation, Colloid and Surface Properties, and Biochemistry*, John Wiley and Sons, New York, 1979.

149. J. Nawrocki, *J. Chromatogr. A*, 1997, **779**, 29-72.

150. M. E. Essington, *Soil and Water Chemistry: An Integrative Approach*, CRC Press, Routledge, U.S.A., 2003.

151. K. E. Bij, C. Horvath, W. R. Melander and A. Nahum, *J. Chromatogr.*, 1981, **203**, 65-84.

152. E. P. Plueddemann, *Silane Coupling Agents*, 2nd edn., Plenum Press, New York, 1991.

153. V. Dudler, L. F. Lindoy, D. Sallin and C. W. Schlaepfer, *Aust. J. Chem.*, 1987, **40**, 1557-1563.

154. T. N. T. Phan, M. Bacquet and M. Morcellet, *J. Inclusion Phenom. Mol. Recognit. Chem.*, 2000, **38**, 345-359.

155. K. Fujimura, T. Ueda and T. Ando, *Anal. Chem.*, 1983, **55**, 446-450.

156. A. Katz, P. Da Costa, A. C. P. Lam and J. M. Notestein, *Chem. Mater.*, 2002, **14**, 3364-3368.

157. V. Bohmer, *Angew. Chem.*, 1995, **107**, 785-817.

158. A. Ponchel, S. Abramson, J. Quartararo, D. Bormann, Y. Barbaux and E. Monflier, *Microporous Mesoporous Mater.*, 2004, **75**, 261-272.

159. C. K. Jue and P. N. Lipke, *J. Biochem. Biophys. Methods*, 1985, **11**, 109-115.

160. F. Cramer, W. Saenger and H. C. Spatz, *J. Am. Chem. Soc.*, 1967, **89**, 14-20.

161. R. J. Clarke, J. H. Coates and S. F. Lincoln, *Carbohydr. Res.*, 1984, **127**, 181-191.

162. C. S. Jeung, C. H. Kim, K. Min, S. W. Suh and J. Suh, *Bioorg. Med. Chem. Lett.*, 2001, **11**, 2401-2404.

163. T. Walenzyk and B. Koenig, *Inorg. Chim. Acta*, 2005, **358**, 2269-2274.

164. B. B. Jang, K. P. Lee, D. H. Min and J. Suh, *J. Am. Chem. Soc.*, 1998, **120**, 12008-12016.

165. K. Hirose, in *Analytical Methods in Supramolecular Chemistry*, , ed. C. A. Schally, Wiley-VCH, Weinheim, 2007, pp. 17-54.

166. A. J. Bradbury, PhD Thesis, Flinders University, 2007.

167. C. H. Manning, A. Skierawska, J. N. Marx and D. J. Bornhop, *Synth. Commun.*, 2003, **33**, 457-461.

168. J. M. Klunder, S. Y. Ko and K. B. Sharpless, *J. Org. Chem.*, 1986, **51**, 3710-3712.

169. J. M. Klunder, T. Onami and K. B. Sharpless, *J. Org. Chem.*, 1989, **54**, 1295-1304.

170. D. W. Branch, B. C. Wheeler, G. J. Brewer and D. E. Leckband, *Biomaterials*, 2001, **22**, 1035-1047.

171. R. Wang, Y. Zhang, G. Ma and Z. Su, *Colloids Surf. B*, 2006, **51**, 93-99.

172. L. J. Suggs, M. S. Shive, C. A. Garcia, J. M. Anderson and A. G. Mikos, *Biomed. Mater. Res.*, 1999, **46**, 22-32.

173. J. M. Harris, E. C. Struck, M. G. Case, M. S. Paley, M. Yalpini, J. M. Van Alstine and D. E. Brooks, *J. Polym. Sci.*, 1984, **22**, 341-352.

174. J. van Ameijde and R. M. J. Liskamp, *Org. Biolmol. Chem.*, 2003, **1**, 2661-2669.

175. D. B. Amabilino, P. R. Ashton, S. E. Boyd, M. Gomez-Lopez, W. Hayes and F. Stoddart, *J. Org. Chem.*, 1997, **62**, 3062-3075.

176. R. E. Parker and N.S. Isaacs, *Chem. Rev.*, 1959, **59**, 737-799.

177. Y. Pocker, B. P. Ronald and K. W. Anderson, *J. Am. Chem. Soc.*, 1988, **110**, 6492-6497.

178. W. F. Gilmore and H. A. McBride, *J. Pharm. Sci.*, 1974, **63**, 1087-1090.

179. C. Yuan, G. Wang and S. Chen, *Synthesis*, 1990, **6**, 522-524.

180. R. A. W. Johnstone and A. H. Wilby, *Chem. Rev.*, 1985, **85**, 129-170.

181. J. Huskens, D. A. Torres, Z. Kovacs, J. P. Andre, F. G. C. Carlos and A. D. Sherry, *Inorg. Chem.*, 1997, **36**, 1495-1503.

182. K. O. A. Chin, J. R. Morrow, C. H. Lake and M. R. Churchill, *Inorg. Chem.*, 1994, **33**, 656-664.

183. D. M. Corsi, H. van Bekkum and J. A. Peters, *Inorg. Chem.*, 2000, **39**, 4802-4808.

184. A. K. Chakraborti, A. Basak and V. Grover, *J. Org. Chem.*, 1999, **64**, 8014-8017.

185. A. K. Chakraborti, S. Rudrawar and A. Kondaskar, *Eur. J. Org. Chem.*, 2004, 3597-3600.

186. C. B. Smith, PhD Thesis, Flinders University, 2000.

187. D. P. Arnold and J. Blok, *Coord. Chem. Rev.*, 2004, **248**, 299-319.

188. L. Vaiana, C. Platas-Iglesias, D. Esteban-Gómez, F. Avecilla, A. de Blas and T. Rodríguez-Blas, *Eur. J. Inorg. Chem.*, 2007, **13**, 1874-1883.

189. W. J. Geary, *Coord. Chem. Rev.*, 1971, **7**, 81-122.

190. H. J. Kim, Y. H. Kim and J. I. Hong, *Tetrahedron Lett.*, 2001, **42**, 5049-5052.

191. I. Horman and B. Dreux, *Anal. Chem.*, 1983, **55**, 1219-1221.

192. K. K. Park, S. H. Kim and J. W. Park, *Bull. Korean Chem. Soc.*, 2004, **25**, 1635-1640.

193. Y. Cao, X. Xiao, R. Lu and Q. Guo, *J. Mol. Struct.*, 2003, **660**, 73-80.

194. A. Hazekamp and R. Verpoorte, *Eur.J. Pharm. Sci.*, 2006, **29**, 340-347.

195. L. Fielding, *Tetrahedron*, 2000, **56**, 6151-6170.

196. L. Sebo, PhD Thesis, Swiss Federal Institute of Technology, Zurich, 1999.

197. K. A. Connors, *Binding Constants*, John Wiley and Sons, New York, 1987.

198. K. Hirose, *J. Inclusion Phenom. Mol. Recognit. Chem.*, 2001, **39**, 193-209.

199. Waterloo Maple Inc., Maple V, Release 4, Student Power Edition, Brooks/Cole Publishing Co., Waterloo, Ontario, Canada, 1996.

200. A. E. Martell and R. M. Smith, National Institute of Science and Technology (NIST), Gaitherbury, MD, U.S.A, 2003.

201. G. A. Jeffrey, *An Introduction to Hydrogen Bonding*, Oxford University Press, New York, 1997.

202. P. Howard and W. Meylan, Physical Properties Database, Syracuse Research Corporation, Environmental Science Center, North Syracuse NY, 1999.

203. N. Papadopoulos and A. Avranas, *J. Solution Chem.*, 1991, **20**, 293-300.

204. W. A. Shapley, G. B. Bacskay and G. G. Warr, *J. Phys. Chem. B*, 1998, **102**, 1938-1944.

205. G. L. Witucki, *J. Coat. Technol.*, 1993, **65**, 57-60.

206. M. Farahani, W. E. Wallace, J. M. Antonucci and C. M. Guttman, *J. Appl. Polym. Sci.*, 2006, **99**, 1842-1847.

207. T. Horr and G. D. Reynolds, *J. Adhes. Sci. Technol.*, 1997, **11**, 995-1009.

208. D. L. Dugger, J. H. Stanton, R. N. Irby, R. L. McConnell, W. W. Cummings and R. W. Maatman, *J. Phys. Chem.*, 1964, **68**, 757-760.

209. C. R. Silva, I. C. S. F. Jardim and C. Airoldi, *J. Chromatogr. A*, 2001, **913**, 65-73.

210. E. Péré, H. Cardy, V. Latour and S. Lacombe, *J. Colloid Interface Sci.*, 2005, **281**, 410-416.

211. A. G. S. Prado and C. Airoldi, *J. Colloid Interface Sci.*, 2001, **236**, 161-165.

212. M. E. Mahmoud, M. M. El-Essawi, S. A. Kholeif and E. M. I. Fathalla, *Anal. Chim. Acta*, 2004, **525**, 123-132.

213. R. S. S. Murthy and D. E. Leyden, *Anal. Chem.*, 1986, **58**, 1228-1233.

214. E. Pere, H. Cardy, O. Cairon, M. Simon and S. Lacombe, *Vib. Spectrosc.*, 2001, **25**, 163-175.

215. J. Sirita, S. Phanichphant and F. C. Meunier, *Anal. Chem.*, 2007, **79**, 3912-3918.

216. S. P. Zhdanov, L. S. Kosheleva and T. I. Titova, *Langmuir*, 1987, **3**, 960-967.

217. F. Garbassi, L. Balducci, P. Chiurlo and L. Deiana, *Appl. Surf. Sci.*, 1995, **84**, 145-151.

218. M. C. Capel-Sanchez, L. Barrio, J. M. Campos-Martin and J. L. G. Fierro, *J. Colloid Interface Sci.*, 2004, **277**, 146-153.

219. E. F. Vansant, P. Van Der Voort and K. C. Vrancken, *Characterization and Chemical Modification of the Silica Surface*, Elsevier, Amsterdam, 1995.

220. K. G. Proctor, S. K. Ramirez, K. L. Williams, J. L. Huerta and J. J. Kirkland, *Special Publication - Royal Soc. Chem.*, 1996, **173**, 45-60.

221. J. Blumel, *J. Am. Chem. Soc.*, 1995, **117**, 2112-2113.

222. S. Ek, E. I. Iiskola, L. Niinisto, J. Vaittinen, T. T. Pakkanen, J. Keranen and A. Auroux, *Langmuir*, 2003, **19**, 10601-10609.

223. B. Lynch and J. D. Glennon, *Anal. Chem.*, 1997, **69**, 1756-1762.

224. L. T. Zhuralev, *Pure Appl. Chem.*, 1989, **61**, 1969-1976.

225. F. R. Steldt and P. G. Varlashkin, *Phys. Rev. B*, 1973, **7**, 3394-3396.

226. S. F. Lincoln, *Coord. Chem. Rev.*, 1997, **166**, 255-289.

227. S. O. Shan and D. Herschlag, *Proc. Natl. Acad. Sci. USA*, 1996, **93**, 14474-14479.

228. J. L. Cook, C. A. Hunter, C. M. R. Low, A. Perez-Velasco and J. G. Vinter, *Angew. Chem.*, 2007, **119**, 3780-3783.

229. A. Ben-Naim, *Biophys. Chem.*, 2002, **101-102**, 309-319.

230. L. H. J. Lajunen, R. Portanova, J. Piispanen and M. Tolazzi, *Pure and Appl. Chem.*, 1997, **69**, 329-381.

231. J. L. Atwood, F. Hamada, K. D. Robinson, G. W. Orr and R. L. Vincent, *Nature*, 1991, **349**, 683-684.

232. G. R. Desiraju and T. Steiner, *The Weak Hydrogen Bond In Structural Chemistry and Biology*, Oxford University Press, New York, 1999.

233. P. K. Bakshi, A. Linden, B. R. Vincent, S. P. Roe, D. Adhikesavalu, T. S. Cameron and O. Knop, *Can. J. Chem.*, 1994, **72**, 1273-1293.

234. P. W. Cains, *Chim. Oggi*, 2007, **25**, 10-12.

235. B. M. Kariuki, C. L. Bauer, K. D. M. Harris and S. J. Teat, *Angew. Chem. Int. Ed. Engl.*, 2000, **39**, 4485-4488.

236. C. Lopez, R. M. Claramount and J. Elguero, *Arkivoc*, 2008, **iv**, 33-46.

237. J. L. Atwood, J. E. D. Davies, D.D.MacNicol and F. Vogtle, eds., *Comprehensive Supramolecular Chemistry*, Elsevier Science Ltd, Oxford, 1996.

238. D. D. Laws, H. M. L. Bitter and A. Jerschow, *Angew. Chem. Int. Ed. Engl.*, 2002, **41**, 3096-3129.

239. K. Masuda, S.Tabata, H. Kono, Y. Sakata, T. Hayase, E. Yonemochi and K. Terada, *Int. J. Pharm.*, 2006, **318**, 146-153.

240. J. H. Yang, Y. Ho and D. L. M. Tzou, *Magn. Reson. Chem.*, 2007, **46**, 718-725.

241. D. D. Perrin and W. L. F. Armarego, *Purification of Laboratory Chemicals*, 3rd edn., Pergamon Press, Oxford, 1982.

242. J. Zubrick, *Organic Chem Lab Survival manual: a student's guide to techniques*, J. Wiley and Sons, New York, 1997.

243. Wavemetrics, Manual Revision 4/2005 5.04B ed., Wavemetrics Inc., Lake Oswego, OR, 2005.

244. D. B. Amabilino, P. L. Anelli, P. R. Ashton, G. R. Brown, E. Cordova, L. A. Godinez, W. Hayes, A. E. Kaifer, D. Philip, A. M. Z. Slavin, N. Spencer, J. F. Stoddart, M. S. Tolley and D. J. Williams, *J. Am. Chem. Soc.*, 1995, **117**, 11142-11170.

245. J. S. Beck, J. C. VartUli, W. J. Roth, M. E. Leonowicz, C. T. Kresge, K. D. Schmitt, C. T-W. Chu, D. H. Olson, E. W. Sheppard, S. B. McCullen, J. B. Higgins and J. L. Schlenker, *J. Am. Chem. Soc.*, 1992, **114**, 10834-10843.

246. V. M. S. Gil and N. C. Oliveira, *J. Chem. Educ.*, 1990, **67**, 473-478.

247. W. Likussar and D. F. Botz, *Anal. Chem.*, 1971, **43**, 1265-1272.